ANGLIA RUSKIN UNIVERSITY

FACULTY OF SCIENCE AND ENGINEERING

ANTIBODIES WITH SUPEROXIDE DISMUTASE ACTIVITY IN HEALTH AND DISEASES ASSOCIATED WITH OXIDATIVE STRESS

ASHLEY DAVID MAX CLARKE

A thesis in partial fulfilment of the requirements of
Anglia Ruskin University for the degree of
Doctor of Philosophy

This research programme was carried out in collaboration with
Cambridge University Hospitals NHS Foundation Trust

Submitted: 31st August 2021

Declaration

I declare that this PhD thesis is the result of my own work and includes nothing which is the outcome of work done in collaboration with another group or individual except where specifically indicated in the text. I have written this thesis entirely by myself and it has not been submitted for a degree or other qualification at Anglia Ruskin University or any other institution. I have read and adhered to the University's policy on plagiarism. All sources of information have been acknowledged, referenced, and clearly distinguished by quotation marks.

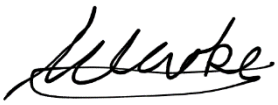

Ashley David Max Clarke
31st August 2021

Acknowledgements

The following thesis has been completed with the support and guidance of many people.

I would like to acknowledge the following people and express my gratitude and thanks for their valuable support, guidance and encouragement.

To the entire staff at the Core Biochemical Assay Laboratory, Cambridge, for their help and support throughout this process.

To Sam Virtue for his guidance in conducting western blotting and electrophoresis.

I would like to thank my university supervisor's Dr. Peter Coussons and Dr. Claire Pike for their support, advice, and most of all helping me to focus my ideas. I will never forget this process and I am forever thankful.

I would like to thank Dr. Philip Pugh for his guidance and technical support in performing multivariate analysis methods presented in Chapter 7.

I wish to give thanks to my work colleague and supervisor Mr Keith Burling. Keith always helped boost my morale, offered much technical advice when developing assays, aided in arranging course funding and always helped. Without him I would never have enrolled on this course.

A special thank you goes to my wife Eleanor for her support, love and encouragement.

I also dedicate this dissertation to my family who have always been willing to listen and offer constructive criticism. I will always appreciate all they have done, especially my younger sister Dr. Isobelle Clarke for talking through my ideas and proof reading some of my work.

Abstract

ANGLIA RUSKIN UNIVERSITY

FACULTY OF SCIENCE AND ENGINEERING

DOCTOR OF PHILOSOPHY

ANTIBODIES WITH SUPEROXIDE DISMUTASE ACTIVITY

IN HEALTH AND DISEASES ASSOCIATED WITH OXIDATIVE STRESS

ASHLEY DAVID MAX CLARKE

AUGUST 2021

It is not widely appreciated that antibodies of the immune system have structural homology with the enzyme antioxidant copper-zinc superoxide dismutase (CuZnSOD). Whilst enhanced superoxide dismutase activity of antibodies (AbSOD activity) has been detected at acidic pH (6.45) in atherosclerotic lesions, AbSOD activity has not been investigated in other disease states associated with oxidative stress and immune dysfunction. This research aimed to determine the effect of pH changes on AbSOD activity, and antioxidant and oxidative stress markers in different disease states.

Initial laboratory experiments investigated an antibody with reported AbSOD activity (HSA-9). Protein A agarose was used to purify the antibody, and electrophoresis and western blotting were performed. It was confirmed IgG-antibodies were the cause of superoxide dismutase activity (SOD activity) and CuZnSOD association was excluded. Additionally, a superoxide dismutase activity assay was optimised for the detection of AbSOD activity.

In an investigation of the pH dependency of CuZnSOD, and human and mouse IgG antibodies it was observed that CuZnSOD activity was independent of pH (5.5 – 8.0). AbSOD activity of IgG was optimal at acidic pH (5.5 – 6.5). Pro-oxidant activity of antibodies (AbPro activity) was detected upon prolonged exposure to superoxide, which was optimal at pH 7.5.

An exploratory observational study was performed on 59- patients compared to 19- ‘healthy’ controls. The pH dependency of AbSOD activity was investigated for antibodies isolated from the serum of patients with rheumatoid arthritis (RA), coeliac disease (CD), myocardial infarction (MI), breast cancer (BC), monoclonal gammopathy of unknown significance (MGUS) and myeloma (MM). Furthermore, patients’ serum catalase (ng/mL and U/mL), serum SOD (ng/mL and U/mL), and serum hydroperoxide (μmol H_2O_2 equivalents/L) were studied. Observed AbSOD activity was significantly increased in RA and MI at pH 5.5 and in myeloma between pH 6.0 – 7.4. Upon prolonged exposure to superoxide AbPro activity was decreased between pH 6.5 – 7.4 in myeloma.

In conclusion, this is the first report that AbSOD activity is increased at pH 5.5 in rheumatoid arthritis and myocardial infarction and is increased in myeloma between pH 6.0 – 7.4, compared to ‘healthy’ controls. AbSOD activity may confer antioxidant protection at sites of oxidative stress and inflammation, however more research into the pH dependency of peroxidases, and the potential of antibody-generated hydrogen peroxide in immune signalling is required. This research provides novel evidence that AbSOD activity may have a role in monoclonal gammopathies, autoimmune diseases and cardiovascular diseases.

Publications

Plans for journal publications

Antibodies with superoxide dismutase activity in multiple myeloma, rheumatoid arthritis, and myocardial infarction.

Cluster network analysis of SOD, CAT and AbSOD in diseases associated with oxidative stress and immune dysfunction.

Poster communications

Clarke, A., Coussons, P. and Pike, C., 2016. Do antibodies have antioxidant capabilities? Modelling inflammatory processes through acidic oxidative stress microenvironments. Poster presentation at: Tenth annual research student conference, Anglia Ruskin University, 17th June 2016, Chelmsford, Essex, England.

Clarke, A. and Coussons, P., 2017. Antibody SOD-like activity: The pH dependency of IgG and SOD. Poster presentation at: First FST/FMS research conference, 25th January 2017, Cambridge, England.

Clarke, A., Coussons, P. and Pike, C., 2017. Antibody superoxide dismutase-like activity: The pH dependency of immunoglobulin G and copper-zinc superoxide dismutase. Poster presentation at: FST 7th conference, Anglia Ruskin University, 10th May 2017, Cambridge, England.

Oral communications

Clarke, A., Coussons, P., Pike, C. and Burling, K. A., 2016. Do antibodies have antioxidant activity? Research seminar: Anglia Ruskin University, Cambridge, England, March 2016.

Clarke, A., Coussons, P., Pike, C. and Burling, K. A., 2020. Immunoglobulin and oxidant status; clinical associations with human disease states. Research seminar: Anglia Ruskin University – via MS Teams, March 2020.

Glossary of abbreviations

4-HNE	=	4-hydroxynonenal
Ab	=	Antibody
AbPro	=	Antibody pro-oxidant activity
AbSOD	=	Antibody superoxide dismutase activity
ACWOP	=	Antibody catalysed water oxidation pathway
AD	=	Autoimmune disease
ADP	=	Adenosine diphosphate
ALS	=	Amyotrophic lateral sclerosis
AMI	=	Acute myocardial infarction
ANOVA	=	Analysis of variance
AO	=	Antioxidants
ATP	=	Adenosine triphosphate
BC	=	Breast Cancer
BSA	=	Bovine serum albumin
CAT	=	Catalase
CD	=	Coeliac Disease
CSF	=	Cerebrospinal fluid
CuZnSOD	=	Copper-zinc superoxide dismutase
CVD	=	Cardiovascular disease
Da	=	Dalton
DDC	=	Diethyldithiocarbamic acid
DNA	=	Deoxyribonucleic acid
DS	=	Down syndrome
DTT	=	Dithiothreitol
ECL	=	Electrochemiluminescence
ECSOD	=	Extracellular superoxide dismutase
EDTA	=	Ethylenediaminetetraacetic acid
ELISA	=	Enzyme-linked immunoassay
ETC	=	Electron transport chain
Fab	=	Fragment antigen binding
Fc	=	Fragment crystallisable
Fe^{2+}	=	Ferrous ions
Fe^{3+}	=	Ferric ions
FLC	=	Free light chain
FTOA	=	Free radical theory of aging

Fv	=	Variable fragment
GPx	=	Glutathione peroxidases
H^+	=	Hydrogen ion
H_2O_2	=	Hydrogen peroxide
HCl	=	Hydrochloric acid
$HO_2^{\bullet}$	=	Hydroperoxyl radical
HRP	=	Horse radish peroxidase
Ig	=	Immunoglobulin
K_2HPO_4	=	Potassium phosphate dibasic
kDa	=	Kilodalton
KOH	=	Potassium hydroxide
LOOH	=	Lipid hydroperoxide
MDA	=	Malondialdehyde
MGUS	=	Monoclonal gammopathy of unknown significance
MI	=	Myocardial infarction
MM	=	Multiple myeloma
mM	=	Millimolar
MnSOD	=	Manganese superoxide dismutase
MPO	=	Myeloperoxidase
MS	=	Microsoft
MSD	=	Meso Scale Discovery
MW	=	Molecular weight
$NaCO_3$	=	Sodium carbonate
NADH	=	Reduced nicotinamide adenine dinucleotide
NaOH	=	Sodium hydroxide
ng/mL	=	Nanogram per millilitre
NK	=	Natural killer cell
nm	=	Nanometers
O_2	=	Oxygen
$O_2^{\bullet-}$	=	Superoxide radical
O_3	=	Ozone
OS	=	Oxidative stress
OS	=	Oxidative stress
PAGE	=	Polyacrylamide gel electrophoresis
PBS	=	Phosphate buffered saline
PCA	=	Principal component analysis
pH	=	Potential hydrogen

PMS	=	Phenazine methosulfate
PO	=	Pro-oxidants
PUFA	=	Polyunsaturated fatty acids
RA	=	Rheumatoid arthritis
RNS	=	Reactive nitrogen species
ROS	=	Reactive oxygen species
RS	=	Reactive species
$Ru(bpy)_3^{2+}$	=	Tris (2, 2'-bipyridine) ruthenium (II)
SDS	=	Sodium dodecyl sulphate
SOD	=	Superoxide dismutase
SOD1	=	Copper-zinc superoxide dismutase
SOD2	=	Manganese superoxide dismutase
SOD3	=	Extracellular superoxide dismutase
TAC	=	Total antioxidant capacity
TG2	=	Tissue transglutaminase 2
TPA	=	Tripropylamine
TPO	=	Thyroid peroxidase
XO	=	Xylenol orange
µg/mL	=	Microgram per millilitre
µL	=	Microlitre
µM	=	Micromolar

Table of contents

Table of figures

Table of tables

CHAPTER 1: Introduction

1.1 General introduction

Over 2.2 billion years ago, rising levels of diatomic oxygen (O_2) in the atmosphere led to the evolution of the first oxygen utilising eukaryotic organisms or aerobes (Halliwell and Gutteridge, 2015b). For these early organisms, oxygen was the most important chemical element to evolutionary success and provision of energy, but also posed its biggest threat, reactive oxygen species (ROS). Oxygen and ROS were cytotoxic, and organisms needed to adapt or evolve to survive. Eukaryotes emerged as they developed antioxidant defences; small molecules which could protect against oxygen toxicity. One of the first antioxidant defence molecules was an enzyme, superoxide dismutase (SOD) (Case, 2017). SOD may have formed a part of a defence system analogous to the first innate immune system, however defending organisms against the toxicity of oxygen (see section 1.5.4.1).

In 2017, of all cancer diagnoses in the UK 15.1 % (46,109) were breast cancer and 1.6 % (5,034) were multiple myeloma and malignant plasma cell neoplasms (Office for National Statistics, 2019). In 2018, four million people in the UK were living with an autoimmune condition, and ischaemic heart diseases were the second leading cause of mortality in the UK (Garcia, 2018; Office for National Statistics, 2020). All these diseases are associated with complex immune processes and a chemical process called oxidative stress (OS) (Halliwell and Gutteridge, 2015a).

In vivo, redox (reduction-oxidation) mechanisms are generally in a regulated balance between antioxidants (AO) and pro-oxidants (PO), when an imbalance occurs this results in OS. OS can cause oxidative damage to vital cellular components such as DNA, lipids, and proteins resulting in mutation, cellular destabilisation, and dysfunction. In some cancers such as multiple myeloma (MM), there is an increased proliferation of the antibody producing B-lymphocytes, and autoimmune diseases (ADs) are often characterised by presence of antibodies (Abs) directed towards host proteins (autoantibodies). Abs have a pivotal role in the immune system which makes them important targets and tools for diagnosis and therapies, in cancer and autoimmune diseases alike which are characterised by abnormal functioning of the immune system.

To reduce the risk of damage caused by OS, mammals have evolved several circulating proteins with enzymatic properties which directly neutralise free radicals (a type of pro-oxidant), the cause of OS. One important copper and zinc containing plasma protein, copper-zinc superoxide dismutase (CuZnSOD) confers protection against the potentially toxic oxygen free radical superoxide ($O_2^{-\bullet}$) by removing superoxide in a process called dismutation (Halliwell *et al.*, 1999).

It is not widely appreciated that antibody, or immunoglobulin (Ig) molecules, share structural homology with CuZnSOD (Richardson *et al.*, 1975). This intriguing observation led to the postulation antibodies may have antioxidant capabilities.

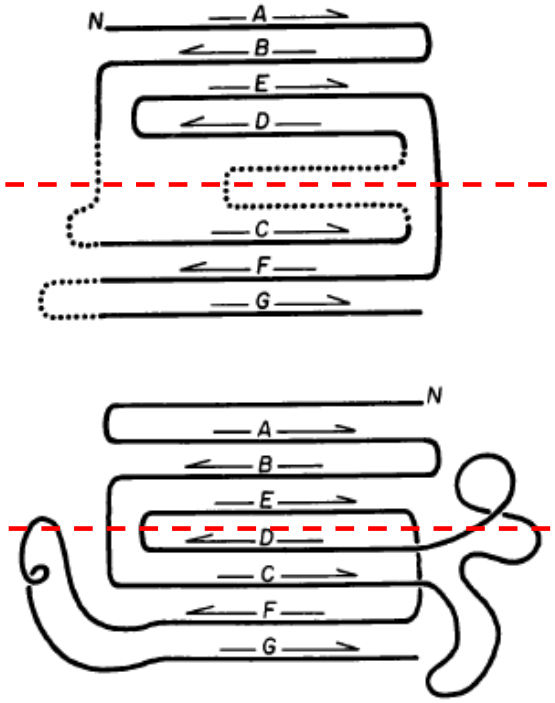

Figure 1.1: **The structural similarities between immunoglobulin variable domain and CuZnSOD subunit.**

Figure 1.1 schematic demonstrates the similar secondary protein structure between an immunoglobulin variable domain and a CuZnSOD subunit. Common to both proteins are seven beta pleated sheets (labelled A-G), which are all antiparallel except the first and last strands. These beta strands are divided into two layers (either side of the red dotted line) which curve to form a beta cylinder or barrel. The immunoglobulin variable domain has three additional loops between strands B and C, C and D, and F and G (denoted by black dotted lines), which are the hypervariable regions, vital parts of an antigen-binding site. Interestingly, the loops between C and D, and F and G in the CuZnSOD subunit form part of the copper

and zinc binding sites, integral for catalytical activity of the enzyme. The three dimensional or tertiary structure of the immunoglobulin variable domain and CuZnSOD are vital for the function of each protein alike. These similar structural and topological characteristics between these two proteins suggest the potential for a function relationship. Taken from Richardson *et al.*, 1975.

In 1996, Petyaev and Hunt elucidated the *in-vitro* ability of an antibody raised against the antigen albumin to elicit SOD enzymatic activity, localising activity to the antigen binding site. When compared to plasma SOD the SOD activity of antibodies was only significantly increased at pH 6.0 – 6.5 which is lower than that of plasma SOD (pH 7.4). This observation was hypothesised to reflect the lower pH values that accompany the inflammatory responses antibodies are directly involved in. In 1998, a subsequent study by Petyaev, Hunt, Mitchinson and Coussons further investigated CuZnSOD activity of antibodies purified from human arteries and atherosclerotic lesions (diseased vessels). By using a technique called immunoprecipitation (which binds and removes antibodies), it was demonstrated SOD activity in normal vascular tissue was predominantly due to CuZnSOD, but in lesion tissue was due to the accumulation of antibodies with SOD activity, so termed this activity ‘AbSOD’ activity.

1.2 Free radicals

1.2.1 What are free radicals and why are they significant?

A free radical has been defined as “any species capable of independent existence (hence the term ‘free’) that contains one or more unpaired electrons” (Halliwell and Gutteridge, 2015b). A chemical species with an unpaired electron configuration (one electron in the outer electron shell orbital) results in instability and usually makes a molecule or molecular fragment highly reactive. Consequently, free radicals will readily donate (oxidation) or accept (reduction) electrons to become stable, and for these reasons they are generally short-lived, lasting only a few milliseconds before they react with adjacent molecules. *In vivo*, the increased outer shell energy of free radicals can increase their reactivity with biomolecules such as lipids, proteins, and nucleic acids (Rahman, 2007).

The increased reactivity and continuous generation of free radicals, their precursors and derivatives *in vivo* explain why they play a pivotal role in physiological processes and human diseases. Physiologically, free radicals have been proven to function in immune defence, cellular signalling, and hormone synthesis (Steck and Grassl, 2014; Sies and Jones, 2020; Dupuy *et al.*, 1999). During antimicrobial defence free radicals and free radical intermediates are produced by NADPH oxidases (nicotinamide adenine dinucleotide phosphate oxidases), NOS (nitric oxide synthases), mitochondrial electron transport chain and MPO (myeloperoxidase) (Steck and Grassl, 2014). The free radicals and intermediates formed by these enzymes and in these processes target and damage DNA, proteins, and lipids. This leads to structural and functional impairment of the bacterial cell. On the other hand, if free radicals are not sequestered by antioxidants (see section 1.4), they may lead to disease by participating in the disruption of the normal functioning of host cellular processes and by damaging host cellular structures (Amici *et al.*, 1989; Kasai and Nishimura, 1984; Ylä-Herttuala *et al.*, 1989).

Many free radicals are reactive forms of oxygen or nitrogen, termed reactive oxygen species (ROS) and reactive nitrogen species (RNS) respectively, or reactive species (RS) collectively. The half-life of a RS is related to its stability and can be particularly variable. Those with the least stability have the fastest rate constants, such as the hydroxyl radical (•OH) and tend to react at the site of

generation, whereas those with greater stability have slower rate constants and can react at more distant sites (Sies, 1993).

1.2.2 Reactive oxygen and nitrogen species

The unique structure of oxygen (diatomic oxygen; O_2) means it has two unpaired electrons in its outer shell. The reduction of oxygen leads to the formation of different types of ROS.

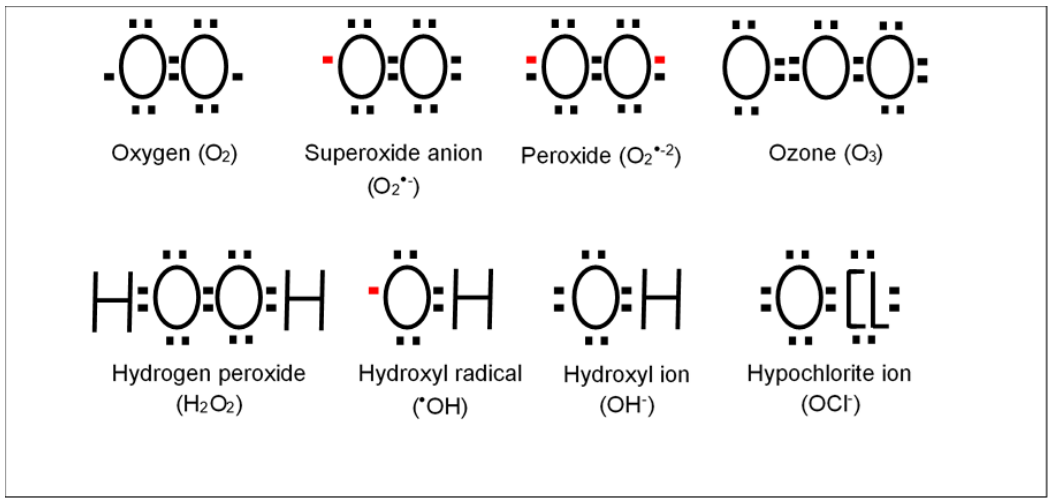

Figure 1.2: **Primary ROS.**
The diagrams show the Lewis structures of outer shell electronic configuration for common ROS. The red coloured electrons signify unpaired electrons and thus these molecules are radicals. Adapted from BioTek Instruments Inc. 2017.

ROS are reactive forms of oxygen, or oxygen containing oxidant molecules. They can be free radicals, such as superoxide anion radical ($O_2^{\bullet -}$), hydroxyl radical (OH•) and the peroxide radical ($O_2^{\bullet 2-}$), and non-radicals such as ozone (O_3), hydrogen peroxide (H_2O_2), singlet oxygen ($^1O_2$), hydroxyl ion (OH^-) and the hypochlorite ion (OCl^-) (Zorov, 2014). ROS have drawn greater research interest, but their role is still less understood than that of the RNS. RNS are reactive compounds of nitrogen and oxygen. They can be free radicals, such as nitric oxide (NO•) and nitrogen dioxide ($NO_2^{\bullet}$), and non-radicals such as peroxynitrite anion ($ONOO^-$) and dinitrogen trioxide (N_2O_3).

ROS and RNS are known collectively as reactive species, and some are more reactive than others. Those that are more reactive have shorter biological

half-lives, are localised to their site of formation, and can cause more damage to biomolecules. The term 'reactive' is not appropriate for all, as reactive species hydrogen peroxide (H_2O_2), Nitric oxide radical ($NO^{\bullet}$), and superoxide radical ($O_2^{\bullet-}$) react fast with few molecules, but hydroxyl radical ($OH^{\bullet}$) reacts fast with almost any molecule. Despite the reduced reactivity of some species, they may serve as precursors that are broken down spontaneously or by antioxidant enzymes to generate intermediates that react with other molecules such as oxygen, or to generate reactive species that are more reactive than themselves. The human body is estimated to generate 2 kg of ROS/year which equates to approximately 5 g of ROS/day (Halliwell, 1997).

1.2.2.1 Superoxide and hydroperoxyl radicals

Superoxide ($O_2^{\bullet-}$) is both a radical and an anion; radical denoted by a radical sign (•) and an anion by a negative charge (-1). Superoxide has two redox potentials, meaning it can function as a reductant ($E^{\circ\prime}$ (O_2 / $O_2^{\bullet-}$) = −330 mV) and an oxidant ($E^{\circ\prime}(O_2^{\bullet-}, 2H^+ / H_2O_2)$ = 940 mV) (Wardman, 1989).

$$O_2 + e^- \rightleftharpoons O_2^{\bullet-}$$

Figure 1.3: **Monovalent reduction of oxygen.**
The monovalent reduction of oxygen (O_2) leads to the generation of superoxide ($O_2^{\bullet-}$).

Superoxide is generated biologically as a biproduct of the mitochondrial electron transport chain, by nicotinamide adenine dinucleotide phosphate oxidase (NADPH oxidase) as part of immune defence of neutrophils to kill bacteria, in the catabolism of purines by xanthine oxidase (XO), and as a biological messenger (Handy and Loscalzo, 2012). Despite superoxide's status as a radical and its essential function in bacterial killing, it is relatively unreactive with biological molecules. The predominant damaging effects of superoxide are related to its role as a precursor to free radicals, ROS (e.g., Hydrogen peroxide; H_2O_2) and RNS (e.g., peroxynitrite; ONO_2^-) that have the potential to react with biological macromolecules such a lipids, proteins, and DNA (Lambeth, 2004).

Superoxide exists in equilibrium with its conjugate acid the hydroperoxyl radical (HOO•; HO_2) in aqueous solutions (Bielski, Cabelli and Arudi, 1985). The pKa of superoxide is 4.8, therefore the equilibrium is largely shifted towards the anionic form (superoxide; $O_2^{\bullet-}$) in human extracellular (pH 7.4) and intracellular (pH 7.0) fluids. A combination of superoxide's pKa and a half-life of an estimated 5 seconds at physiological pH (Marklund, 1976), means normally only a fraction of superoxide will transverse the cell membrane to the cytoplasm of cells and extracellular fluid (Auchère and Rusnak, 2002). However, during inflammatory states observed in disease pathologies local acidification (pH 6 – 7) may occur in the affected tissue such as in tumour microenvironments (Mazzio, Smith and Soliman, 2010), atherosclerotic lesions (Naghavi *et al.*, 2002), ischemic heart (Gebert, Benzing and Strohm, 1971; Garlick, Radda, Seeley, 1979) and rheumatic joints (Cummings and Nordby, 1966). The lowering of intracellular, extracellular and cell membrane pH significantly shifts the equilibrium of the protonated form hydroperoxyl and the anionic form superoxide to near equal proportions. This is significant as the hydroperoxyl radical is more reactive than superoxide and has increased membrane permeability due to its lack of charge (de Grey, 2002). Additionally, the pH near membranes may be more acidic, favouring the formation of hydroperoxyl radicals. Consequently, the higher concentrations present at the lower acidic pH associated with inflammation and near membranes causes the initiation of fatty acid peroxidation (Bielski, Arudi and Sutherland, 1983) which could cause lipid membrane damage.

Despite the few molecular targets of superoxide, it can damage proteins, specifically those with iron-sulphur (Fe-S) clusters. Iron-sulphur clusters are utilised as co-factors for redox centres in enzymes. In mammals, Aconitase an enzyme essential to the citric acid cycle can be inactivated by superoxide (Scandroglio *et al.*, 2014). Superoxide displaces iron from the catalytic centre, which can then participate in Fenton chemistry to generate hydroxyl radicals (HO•) and catalyse the Haber-Weiss reaction, both of which have significant roles in OS and can lead to oxidative damage.

There is much evidence relating superoxide to human diseases, such as cancer, rheumatoid arthritis and neurogenerative diseases (Hayyan *et al.*, 2016). In the process of redox homeostasis an antioxidant enzyme superoxide dismutase (SOD) maintains levels of superoxide in an optimum range; see section 1.5.

1.2.3 Formation and sources of reactive species

1.2.3.1 Mitochondria: a main source of superoxide

Mitochondria are membrane bound organelles located in the cytoplasm of nearly all eukaryotic cells whose primary function is to produce adenosine triphosphate (ATP) through cellular respiration. The main pathway of cellular respiration is the electron transport chain (ETC). The ETC utilises a series of inner mitochondrial membrane bound electron transporter proteins (complex I-IV) and cofactors (NADH and $FADH_2$) to donate and move electrons, that are accepted by oxygen. The movement of electrons causes a pumping of protons (H^+) from the mitochondrial matrix to the intermembrane space. The accumulation of H^+ ions that results, generates an electrochemical gradient between the intermembrane space and the matrix. To return to the matrix, H^+ ions move through ATP synthase (complex V), phosphorylating adenosine diphosphate (ADP) to ATP via a process called oxidative phosphorylation (Van der Bliek, Sedensky and Morgan, 2017). The electrons produced by the ETC and the H^+ ions reduce oxygen to form water. When this occurs inefficiently (i.e., $<4\ e^-$ and $<4H^+$) or when electrons leak out of the ETC, oxygen can be partially reduced resulting in production of superoxide (Chance, Sies and Boveris, 1979).

Reactive species can be formed endogenously and exogenously. Cellular respiration, the process by which cells produce energy from oxygen, is one of the endogenous processes for the formation of ROS. Electrons escape from the electron transport chain of the mitochondria to reduce oxygen to superoxide anion radicals.

1.2.3.2 Endogenous sources of reactive species

Approximately 90% of intracellular ROS is generated by mitochondria, the majority of this is superoxide with some hydrogen peroxide and a smaller amount of hydroxyl radical (Zhang *et al.*, 2019).

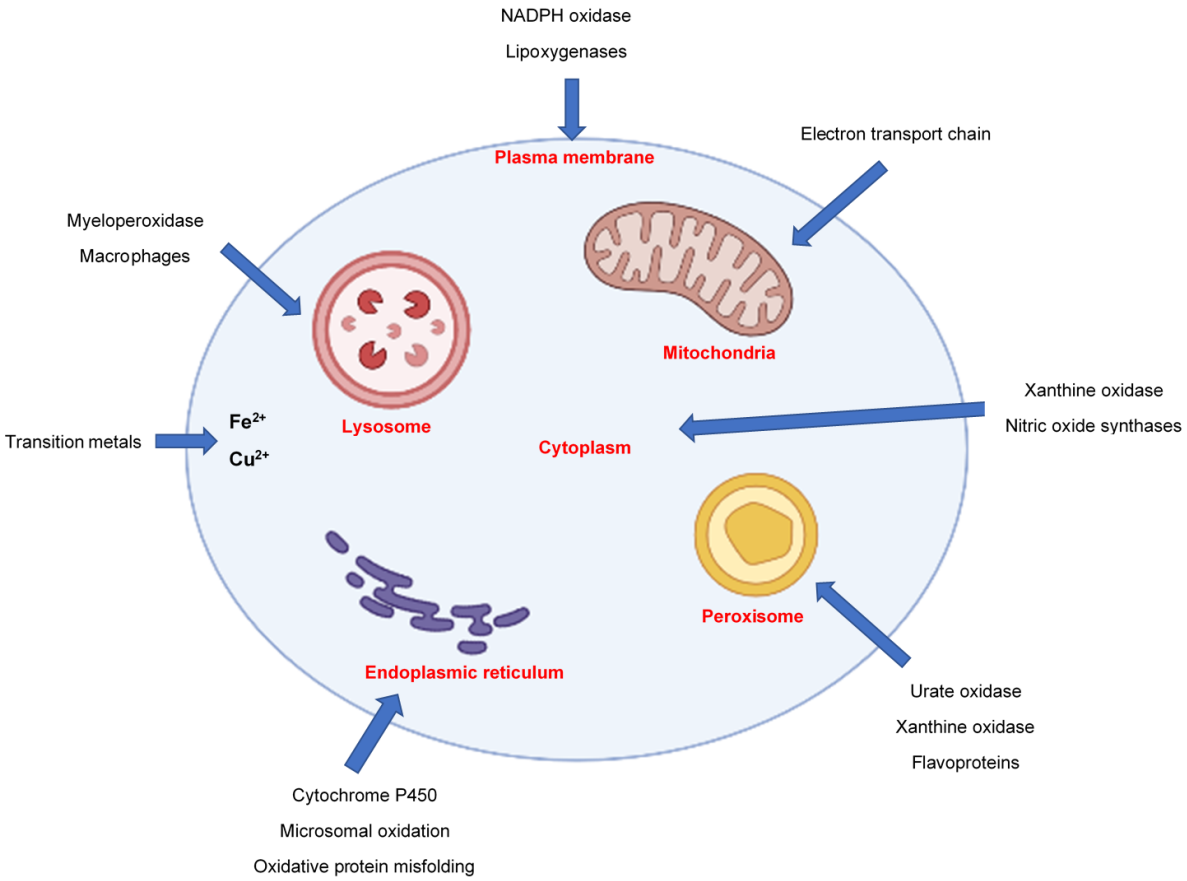

Figure 1.4: **Cellular sources of ROS / RNS.**
This image was created with BioRender.com (2020).

There are many sources of reactive species within cells. Organelles such as the mitochondria, endoplasmic reticulum, peroxisomes, and lysosomes are cellular machinery with high metabolic activity, that function to aid the cell throughout its life cycle. Vital chemical reactions for the formation and degradation of lipids, proteins, carbohydrates, and nucleic acids occur in cells. A variety of specialised enzymes and immune cells participate in these reactions; however, they can result in the formation of ROS and RNS, e.g., Fenton chemistry with transition metals. Consequently, cells have evolved enzymes and utilise vitamins as antioxidant defences to protect the cell. In circumstances, where there is overactive metabolic activity or metabolic dysfunction, the antioxidant defences are overwhelmed by RS, causing OS (see section 1.3).

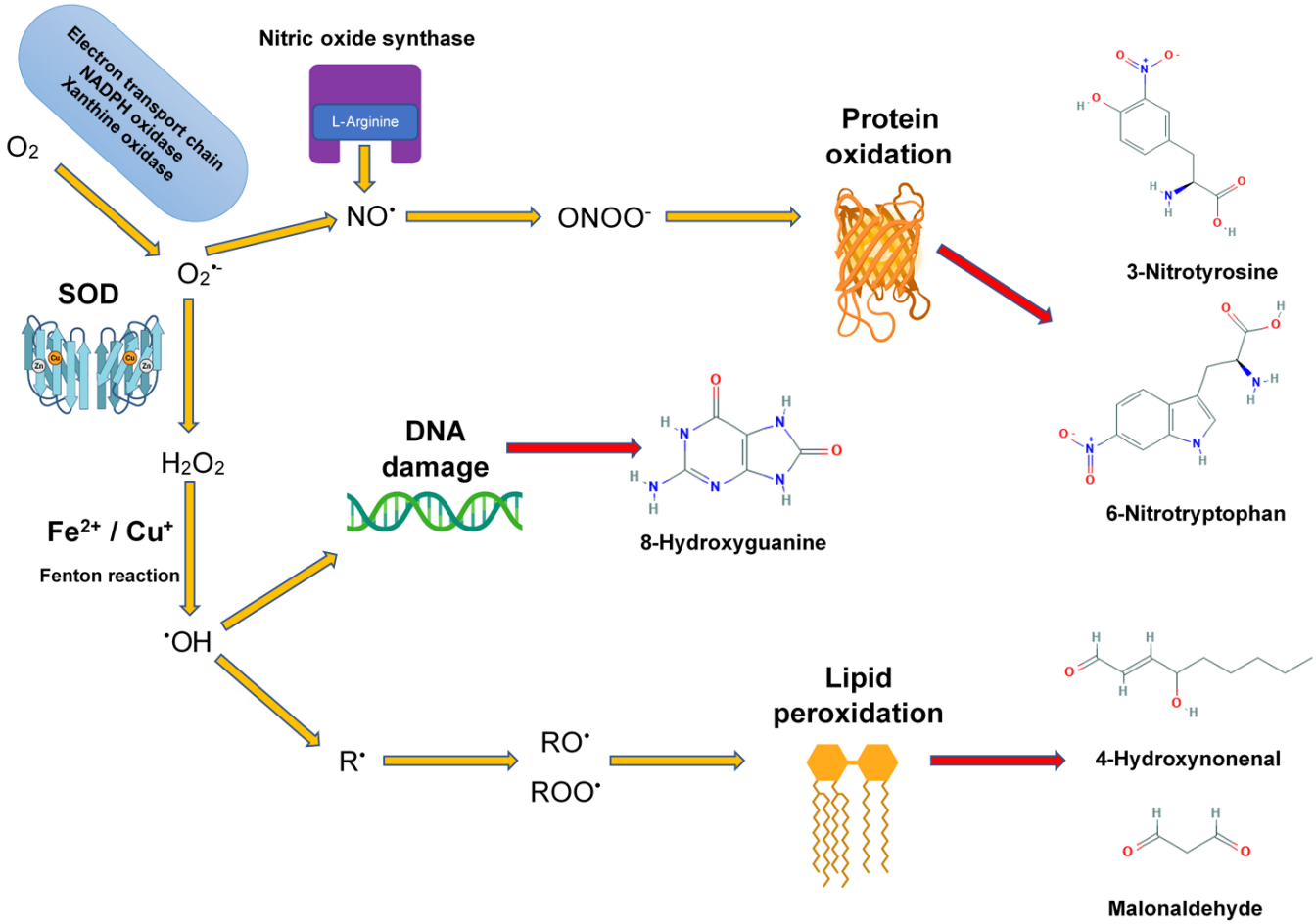

Figure 1.5: **Pathway of ROS and RNS formation and products of their reaction.** (Adapted from Poprac *et al.*, 2017). This image was created with BioRender.com (2020).

In vivo, the main sources of the superoxide radical other than the mitochondrial electron transport chain are plasma membrane bound and neutrophil NADPH oxidase and xanthine oxidase. The primary RNS is nitric oxide (NO•) which is enzymatically generated from the amino acid L-arginine by a family of enzymes called nitric oxide synthases (NOS e.g., endothelial NOS of the vascular endothelium). Other forms of RNS rely on the production of the ROS superoxide. The superoxide radical anion reacts with nitric oxide to form the peroxynitrite anion (ONOO-). Protein residues react with peroxynitrite resulting in oxidative modification and the formation of 6-nitro-tryptophan and 3-nitro-tyrosine.

The superoxide radical ($O_2^{\bullet-}$) is dismutated (enzymatically converted via disproportionation) to hydrogen peroxide (H_2O_2) and oxygen (O_2) by superoxide dismutase (SOD). Hydrogen peroxide can be decomposed to water (H_2O) and oxygen (O_2) by catalase and peroxidases such as glutathione peroxidase.

Alternatively, it is further decomposed to hydroxyl radical ions (OH•) via Fenton chemistry with catalytically active ferrous ions or cuprous ions. Hydroxyl radicals (OH•) can also be generated via the Haber-Weiss reaction between hydrogen peroxide (H_2O_2) and superoxide radicals ($O_2^{\bullet -}$). Hydroxyl ions react preferentially with DNA base guanine to form the oxidative DNA damage marker 8-hydroxyguanine (8-OHG) and can also react with lipids to form lipid radicals ($R^{\bullet}$). The lipid radicals react with oxygen forming lipid peroxyl ($ROO^{\bullet}$) or lipid alkoxyl ($RO^{\bullet}$) radicals, which along with unsaturated fatty acids can lead to lipid peroxides and markers of lipid peroxidation such as hydroperoxides, malondialdehyde (MDA) and hydroxynonenal (4-HNE).

1.2.3.3 Exogenous sources of reactive species

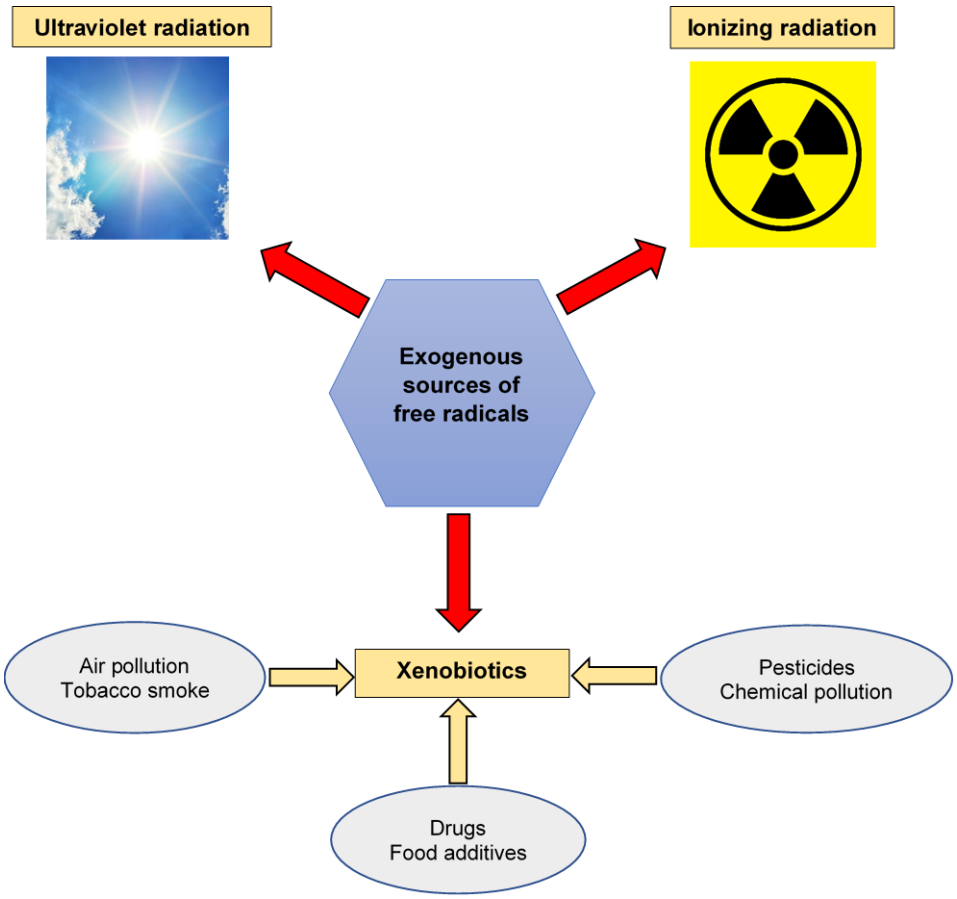

Figure 1.6: **Exogenous sources of ROS / RNS.**

Reactive species are generated from several exogenous sources including xenobiotics and radiation. RS and radicals can be formed when covalent bonds are broken (Halliwell and Gutteridge, 2015e). Ultraviolet (UV-light) and ionising

radiation (x-rays, γ-rays) can cause the formation of radicals and RS this way, which can cause cellular death, and DNA damage and gene mutation, which can lead to cancer (Riley, 1994).

Xenobiotics are chemicals found but not produced in organisms or the environment which access organisms through diet, air, drinking water, drug administration, and lifestyle choices (Patterson, Gonzaleza and Idle, 2010). They most recognisably include environmental pollutants and chemical substances, such as pesticides, carcinogens and hydrocarbons produced in industry, however, they also include some drugs and food additives. Cancer therapeutics such as cisplatin and adriamycin produce large quantities of ROS which results in DNA damage and the death of cancer cells via apoptosis (Krumova and Cosa, 2016). In a similar fashion, bactericidal antibiotics of the quinolone, β-lactam and aminoglycoside classes induce hydroxyl radical formation in *E. coli*, also leading to cell death (Kohanski *et al.*, 2007). The mechanism of action is proposed to be hyperactivation of the ETC, which produces excess superoxide, this is turn destabilises iron-sulphur clusters, releasing ferrous iron which participates in the Fenton reaction, forming hydroxyl radicals.

1.2.4 Free radicals in aging

Free radicals have received much media attention because of their potential link to various diseases and aging since the ‘free radical theory of aging’ was hypothesised in 1956 by Harman. According to the free radical theory of aging (FTOA), free radicals break down cellular constituents and connective tissue over time, causing increased production of free radicals and damage to cells that results in aging and diseases (such as cancer and neurodegenerative diseases like Alzheimer’s).

Harman modified his original theory in 1972 to incorporate the mitochondria as the main target of radical damage, termed ‘the mitochondrial theory of aging’. The current opinion of the theory suggests electrons escape from the mitochondrial electron-transport chain (process by which oxygen is utilised by cells to produce energy). These combine with oxygen to form ROS. The ROS damage biomolecules such as mitochondrial DNA causing mutation. The mutations in mitochondrial DNA result in dysfunctional mitochondria that generate a vicious cycle of increasing ROS and damage to biomolecules. This ultimately determines lifespan according to the mitochondrial theory of aging (Jang *et al.*, 2009).

In 2018, the population in the United Kingdom of people over 85 years was 1.6 million and this is expected to double over the next 25 years to 3 million (Office for National Statistics, 2019). As humans age, the increased generation of free radicals *in vivo* may be an important factor in the types of diseases which effect those populations. According to the FTOA, this suggests an increased likelihood of those populations experiencing diseases associated with OS.

Although free radicals (ROS and RNS) are a basic by-product of normal respiration, there have been various studies that have linked free radicals to disease (see section 1.8). Several studies and review articles (see section 1.2.5) have begun to challenge this concept and suggest the vital role of ROS and RNS as tools for signalling not only in disease but homeostasis or redox regulation.

1.2.5 Reactive species in physiology

1.2.5.1 Signalling

One of the primary roles of RS *in vivo* is signalling. The three main mechanisms in redox regulation are via:

1) H_2O_2 oxidation of protein thiol groups (Poole, 2015).

2) $O_2^{\bullet-}$ oxidation of Fe-S clusters (Scandroglio *et al.*, 2014).
   e.g., Aconitase in the citric acid cycle.

3) $ONOO^-$ nitration of tyrosine residues (Bartesaghi and Radi, 2018).
   e.g., Inactivation of manganese superoxide dismutase (SOD2) by tyrosine nitration (MacMillan-Crow *et al.*, 1996).

These modifications result in a change in function of the protein affected. For example, NRF2 (nuclear factor E2-related factor 2) a transcription factor, is under normal conditions (non-OS) bound by KEAP1 (Kelch like-ECH-associated protein 1). KEAP1 inhibits NRF2 by ubiquitination, marking it for degradation by the proteosome. The accompanying oxidation of cysteines (protein thiol) in KEAP-1 by hydrogen peroxide during OS, result in its inactivation, thus stabilising NRF2, allowing its translocation to the nucleus. In the nucleus, its role as a transcription factor results in the synthesis of antioxidants proteins in response to OS (Sies and Jones, 2020).

1.2.5.2 Immune response

An important role of RS is in the immune response. Phagocytic white blood cells – macrophages and neutrophils, migrate to the site of infection as part of the innate immune response. The inflammatory and bactericidal action of these phagocytes is associated with the oxidative or respiratory burst, whereby oxygen is converted into superoxide by NADPH (nicotinamide adenine dinucleotide phosphate) oxidase (Winterbourn, Kettle and Hampton, 2016). The superoxide then dismutates to hydrogen peroxide, which is then converted to the antimicrobial agent hypochlorous acid (HOCl) via myeloperoxidase (MPO), killing bacteria (Dahlgren and Karlsson, 1999). In chronic granulomatous disease, a genetic disorder characterised by caused by mutations in genes encoding for NADPH oxidase, reduced ROS are generated, which may result in increased susceptibility to infections (Marciano *et al.*, 2018).

RS (superoxide and hydrogen peroxide) can also mediate amplification of immune responses by lymphocytes. The activation of T-cells (T-lymphocytes) is enhanced by ROS, even after weak receptor stimulation by low concentrations of antigen (Dröge, 2002). Furthermore, physiological concentrations of hydrogen peroxide and superoxide induce interleukin-2 (IL-2) and IL-2 receptor (IL-2R) gene expression in antigenically stimulated T-cells (Los *et al.*, 1995).

1.2.5.3 Hormone synthesis

RS have a pivotal role in the synthesis of hormones and hormone-like compounds. During synthesis of thyroid hormones, dual oxidase (Duox) generates H_2O_2, which is utilised by thyroid peroxidase (TPO) to oxidise iodide, to covalently link oxidised iodine to tyrosine residues of thyroglobulin, and to couple the iodinated tyrosines to generate triiodothyronine (T_3) and thyroxine (T_4) (Song *et al.*, 2010).

Prostaglandins and leukotrienes are biologically active hormone-like molecules called eicosanoids that are present in many different tissues and their functions have been identified in blood clotting, vasodilation, inflammation and smooth muscle contraction (Ricciotti and FitzGerald, 2011). Prostaglandins and leukotrienes are derived from the oxidation of the polyunsaturated fatty acids, arachidonic acid present in cell membranes via two different pathways, cyclooxygenase (COX) and 5-lipoxygenase (5-LO) pathways, respectively.

1.2.5.4 Mitohormesis

It is generally accepted that increased levels of reactive species, such as superoxide and hydrogen peroxide, without antioxidant mediators, cause OS, but can also serve as redox switches in response to endogenous and exogenous derived stresses.

According to Harman's (1956) FTOA, the relationship between RS dose and mortality is linear, i.e., as RS increase so does the likelihood of mortality. The concept indicates that even small amounts of RS begin to increase mortality. Conversely, the concept of mitohormesis (mitochondrial hormesis – low dose stimulation) is non-linear, i.e., although high doses increase mortality, low doses of RS decrease mortality (Ristow and Zarse, 2010; Ristow and Schmeisser, 2014). The theory is priming of antioxidant defences with RS could be analogous to the immune system being 'trained' by a vaccine to respond to a virus or bacteria. The beneficial claims of increased longevity and health through adoption of regular exercise, calorie restrictive diets, intermittent fasting and consumption of dietary phytonutrients may function via the mitohormetic mechanism (Tapia, 2006).

A small study of 19 untrained and 20 pre-trained healthy young males, found exercise reduced insulin resistance and promoted endogenous antioxidant defense capacity. However, supplementation with antioxidants blocked the health-promoting effects of exercise (Ristow *et al.*, 2009). Conversely, a more recent systematic literature review (studies between June 2009 and September 2019) concluded that the elderly showed decreased muscle damage and improved response to exercise post- consumption of antioxidants and omega-3 PUFA's (Pastor and Tur, 2020). A possible explanation for these conflicting results could be explained by Radak *et al.* (2017). They hypothesised ROS generated in response to exercise causes an adaptive response which results in the beneficial effects of exercise (e.g., increased strength and improved efficiency) and this could be described by a bell-shaped curve. If antioxidant supplementation is delivered prior to the maximal adaptive response (plateau of the curve), antioxidants would depress the positive effects of exercise, whereas antioxidant supplementation post-maximal adaptive response, would improve performance, delay fatigue and improve recovery. They also postulated the greater an individual's level of fitness, the greater their tolerance to oxidative stress.

Ultimately, this highlights the importance of timing and individual capacity to oxidative stress and the complexities of antioxidant supplementation.

1.3 Oxidative stress

1.3.1 What is oxidative stress?

In redox homeostasis a “steady state” concentration of free radicals is maintained by the balance between rate of production and rate of removal by antioxidants. Different types of cells have different “steady states” determined by their cellular constituents and roles. When “steady state” diminishes and free radicals overwhelm antioxidant defences, cellular damage and dysfunction can occur (Schafer and Buettner, 2001).

According to Sies (1985), “Oxidative stress is a disturbance in the pro-oxidant – antioxidant balance in favour of the former”. Since its first use the term ‘oxidative stress’ (OS) has evolved and changed subtly over several decades. In 1991, Sies described OS as “a disturbance in the pro-oxidant-antioxidant balance in favour of the former, leading to potential damage”. The addition of the phrase “leading to potential damage” encompassed the main view of the time, that pro-oxidants (PO) were a necessary part of aerobic life, but when in excess of antioxidants (AO) could lead to pathophysiological processes. Over the next decade, many studies and reviews were conducted that complicated the concept of OS in the field. This was likely due to a lack of appreciation for the role of ROS and RNS in signalling and regulatory mechanisms *in vivo*. In 2004, Halliwell and Whiteman simplified the definition of OS as “a serious imbalance between production of reactive species and antioxidant defence”. A ‘serious imbalance’ was the prominent phrase Halliwell used to deter further researchers from interpreting the production of any reactive species without antioxidant defences as OS.

More recently, it has been acknowledged that terms such as OS and antioxidant have been used too loosely; it was therefore deemed necessary to standardise the vocabulary used in redox biology. A research group proposed the term OS should only be used to describe detrimental effects of an oxidative event (Sarsour *et al.*, 2014). Although differences in opinion still exist the primary consensus is that OS is “an imbalance between oxidants and antioxidants in favour of the oxidants, leading to a disruption of redox signalling and control and/or molecular damage”.

The concept of OS has continued to evolve, and it is now evident RS are “capable of exerting positive stress, eustress, as well as deleterious effects, distress” (Niki, 2016). Consequently, in this thesis the term ‘oxidative eustress’ will

be used to describe the physiological levels of RS and their positive effects relating to redox homeostasis, whereas 'OS' will only be used to describe the detrimental effects of redox imbalance; the molecular damage (damage to a biological molecule such as DNA, enzyme, protein or lipid that causes abnormal functioning of that molecule) and signalling disruption caused by an excess of oxidants, pro-oxidants, free radicals and reactive species in relation to dysfunctional or limited supply of antioxidants.

1.3.2 Oxidative damage on lipids

Oxidative damage occurs to lipids via a complex process known as lipid peroxidation which consists of three phases, initiation, propagation, and termination. Lipid peroxidation is destructive as it results in a decreased in membrane fluidity, permeability and inactivation of membrane bound receptors and proteins (Dinis, Almeida and Madeira, 1993), ultimately impairing membrane structure and function (Borchman *et al.*, 1992). Membrane lipids are susceptible to oxidation (Bast, 1993), especially polyunsaturated fatty acids (PUFAs), whose structure consists of double carbon bond (–C=C–) adjacent to methylene group (–CH2–), resulting in a weaker C–H bond.

The initiation phase occurs when a RS (e.g., $OH^{\bullet}$ or HO_2) abstracts a hydrogen atom from a methylene group or the RS is added to a membrane lipid, leaving or adding an unpaired electron at the central carbon, resulting in a lipid radical ($L^{\bullet;}$ –$C^{\bullet}$–H). The lipid radical stabilises through molecular rearrangement to form a conjugated diene. In the propagation phase, the unpaired electron at the carbon reacts with oxygen (O_2) to form a lipid peroxyl radical (LOO•), which abstracts another hydrogen atom from an adjacent membrane lipid in a further propagation reaction, resulting in a lipid hydroperoxide (LOOH) and an unpaired electron in the adjacent membrane lipid ($L^{\bullet;}$ –$C^{\bullet}$–H). A chain reaction will continue until the reaction is terminated by reaction of two peroxyl radicals or donation of a hydrogen atom by an antioxidant (Halliwell and Gutteridge, 2015a).

Lipid peroxidation results in a variety of breakdown products including the primary reaction product lipid hydroperoxides, and secondary products malonaldehyde (MDA) and 4-hydroxynonenal (4-HNE), which themselves can cause further damage to lipids, DNA, and proteins (Benedetti *et al.*, 1986;). In the case of 4-HNE, it will rapidly react with thiol groups and amino acids (cysteine, histidine, and lysine), and due to its lipophilicity will likely result in damage to membrane bound proteins (Schaur, 2003).

Measurement of breakdown products such as lipid peroxides enables the characterisation of OS *in vivo*. In a method comparison study of OS in Wistar rats (induced via an iron and manganese enriched diet), only quantitation of lipid peroxides in serum (compared to MDA, protein carbonyls and antioxidant capacity) were a useful predictor of intracellular OS (Argüelles *et al.*, 2004).

1.3.3 Oxidative damage on proteins

Protein oxidation is defined as “the covalent modification of a protein induced either directly by ROS or indirectly by reaction with secondary by-products of OS” (Shacter, 2000). Oxidative damage to proteins can have deleterious effects on their function and structure (receptors, enzymes, and transport proteins), and increase immunogenicity (Gerling, 2009). One study investigated the oxidation of the enzyme aconitase (functions in energy metabolism) in the mitochondrial matrix of flies, where increased levels of oxidation correlated to a reduction in enzyme activity (Yan, Levine and Sohal, 1997).

Direct reactions with RS (e.g., $OH\bullet$, $O_2^{\bullet-}$, H_2O_2 and $ONOO^-$) or indirect with oxidation end-products (e.g., in lipid peroxidation – MDA and 4-HNE) induce protein oxidation. For example, oxidation of thiol groups between the amino acid cysteine results in formation of disulphide bonds, disrupts folding and stability and thus protein structure, which is crucial to protein function (Halliwell and Gutteridge, 2015a). Oxidation of amino acid residues (lysine, arginine, and proline) leads to the formation of carbonyl derivatives. Protein oxidation can be detected through the protein carbonyl content assay (Levine *et al.*, 1994).

1.3.4 Oxidative damage on nucleic acids

ROS and RNS can damage nucleic acids and as deoxyribonucleic acid (DNA) and ribonucleic acid (RNA) are essentially templates that hold the genetic instructions for synthesis of proteins that are essential to life, oxidative damage to DNA can lead to changes in DNA that disrupt genome function and cause mutations (David, O'Shea and Kundu, 2007). The low oxidation potential of the DNA base guanine (G) makes it prone to oxidative attack, which results in generation of the measurable oxidised guanine marker, 8-hydroxyguanine (8-OHG) (Poetsch, 2020).

1.4 Antioxidants

1.4.1 What are antioxidants and why are they significant?

The term antioxidant (AO) was defined as “any substance that, when present at low concentrations compared with those of an oxidisable substrate, significantly delays or prevents oxidation of that substrate”. The term oxidisable substrate includes every organic and many inorganic molecules found *in vivo* (Halliwell and Gutteridge, 1995). Halliwell and Gutteridge found their definition was ‘imperfect’ and fell short of describing chaperones, repair systems, or inhibitors of RS generation as potential antioxidants. To include these potentials, they simplified the definition as “any substance that delays, prevents, or removes oxidative damage to a target molecule” (Halliwell and Gutteridge, 2015d, p. 77). Humans have evolved highly effective yet complex antioxidant defence systems to combat a constant onslaught of free radicals and reactive species generated both endogenously and exogenously.

The primary role of antioxidants is to neutralise the damaging effects of reactive species. This is achieved by the acceptance or donation of electrons (reduction and oxidation), eliminating unpaired electrons, and reducing overall reactivity. Antioxidants can react directly with free radicals and reactive species rendering them neutralised or terminated and may even become free radicals which are more stable, less reactive, and longer lived (Lü *et al.*, 2010). Some non-enzymatic antioxidants such as alpha tocopherol (biologically active form of vitamin E) have aromatic rings which can harbour delocalised unpaired electrons, effectively terminating free radical chain reactions (Debier and Larondelle, 2005).

1.4.2 Exogenous antioxidants

1.4.2.1 Vitamin C

Ascorbic acid (vitamin C) is an essential dietary micronutrient required for a variety of biological functions. It primarily functions as a cofactor for many enzymes, such as the prolyl and lysyl hydroxylases which are involved in collagen biosynthesis (Halliwell and Gutteridge, 2015c). A deficiency in vitamin C causes the disease scurvy. It is a water-soluble antioxidant that donates its electrons to compounds, such as ROS and RNS and their derivatives, preventing them being oxidised (Padayatty *et al.*, 2003). Vitamin C can protect against lipid peroxidation (section 1.3.2) and regenerate α-tocopherol (Bruno *et al.*, 2005).

1.4.2.2 Vitamin E

Vitamin E is a group of fat-soluble antioxidants (tocopherols and tocotrienols) that can inhibit lipid peroxidation by scavenging lipid peroxyl radicals (LOO•) via donation of a hydrogen atom from their hydroxyl group (Halliwell and Gutteridge, 2015c; Traber and Stevens, 2011). A study reported cigarette smokers supplemented with α-tocopherol had greater lipid peroxidation (measured by F2-isoprostane concentrations) and faster plasma α-tocopherol disappearance rates. Where participants were supplemented additionally with vitamin C the rate of plasma α-tocopherol disappearance reduced to that observed in non-smokers; they concluded that although vitamin E did not prevent radical formation, or oxidation of fatty acids, it did inhibit the lipid peroxidation chain reaction (Bruno *et al.*, 2005).

1.4.2.3 Vitamin A

Vitamin A is a group of fat-soluble antioxidants (retinol, retinal and pro-vitamin A carotenoids such as beta-carotene) that express their antioxidant activity in a variety of different ways, such as by scavenging singlet oxygen and peroxyl radicals (Palace *et al.*, 1999). From the 1980's to early 1990's, a clinical trial of the effects of α-tocopherol and β-carotene was conducted on 29,133 male smokers (age 50-69 years). The trial found an increase in the incidence of lung cancer in men that had received β-carotene; it was concluded supplementation with β-carotene may be harmful in smokers (Alpha-Tocopherol, Beta Carotene Cancer Prevention Study Group, 1994).

1.4.3 Endogenous antioxidants

1.4.3.1 Glutathione peroxidase

Glutathione peroxidases (GPx) are a family of enzymes that prevent the accumulation of hydrogen peroxide in a variety of different cells. The most abundant member of the family is GPx-1 (EC 1.11.1.9). The first characterisation of GPx-1 in 1957 discovered its essential role in protection of haemoglobin from oxidative damage (Mills, 1957). Selenium in the form of the amino acid selenocysteine is essential for the catalytic activity of GPx-1 (Flohe, Günzler and Schock, 1973).

1.4.3.2 Catalase

Catalase (CAT) was the first antioxidant enzyme to be discovered. Thénard (1811), discovered hydrogen peroxide and speculated that its tissue degradation was due to a 'special' substance activity. Later, Loew named this enzyme 'catalase', stating it converted hydrogen peroxide into water and oxygen (Loew, 1900). Catalase (EC 1.11.1.6) is a vital enzyme in the direct decomposition of hydrogen peroxide, consisting of four subunits, each containing haem (iron – Fe (III)) at its active site and one molecule of NADPH bound to it (Halliwell and Gutteridge, 2015d).

The deficiency of catalase (either acatalasemia or hypocatalasemia) is rare, but it is associated with type 1 and more commonly type 2 diabetes (Góth and Nagy, 2013). It has been reported that catalase enzyme activity is downregulated in cancer cell lines of human leukocytes and mammary epithelial cells compared to normal cells (Beck *et al.*, 2011; Glorieux *et al.*, 2016). The pH optimum of human catalase is between 6.8 – 7.5, outside this range the enzyme is denatured, and activity diminishes (Aebi, 1984).

1.4.3.3 Other endogenous AOs

The specific endogenous antioxidants such as CAT, SOD and GPx are generally in low concentration in extracellular fluids. ROS are constantly generated in extracellular fluids (by phagocytes, xanthine oxidase, etc.) and metal ions can participate in pro-oxidant reactions, therefore, several proteins function as antioxidants by scavenging ROS and sequestering metal ions. Proteins such as transferrin bind iron, and ceruloplasmin and albumin bind copper stopping

participation in Fenton chemistry (Halliwell and Gutteridge, 2015d). In Wilson's disease, copper is minimally incorporated in to ceruloplasmin, resulting in copper accumulation in the liver and other tissues such as the brain, eyes, kidneys, and joints (Tavill, 2014). This results in many different pathologies including liver failure, kidney injury and even liver cancer (Xu and Hajdu, 2008).

1.4.4 Antioxidant reports in the media

Since Harman's initial free radical theory of aging, like free radicals, antioxidants have received much media attention and endorsement from leading scientists (e.g., double Nobel prize winner Linus Pauling) for their reported potential health benefits, fuelling the modern antioxidant supplement industry. By the 1970's, the free radical theory of aging was built on by authors such as Richard Passwater who believed implementation of his 'supernutrition' plan (supplementation with vitamins, diet, and exercise), could reduce heart disease by 60-80% and cancer by 30-40% (Passwater, 1975). The 'antioxidant revolution' has yielded many claims of preventing diseases such as cancer, increasing energy, having 'de-toxifying' abilities, aiding weight-loss, protecting against pollutants, and smoking, and delaying aging, however many of these have not been substantiated in clinical trials.

1.4.4.1 Controversy in antioxidant supplementation

On the 18th of January 1996, a large-scale trial of supplementation with beta-carotene and retinyl palmitate (vitamin A) in men and women at risk of developing lung cancer (CARET intervention study) was halted 21 months prior to the study end date. Data emerged that there were 28% more lung cancers and 17% more deaths in the intervention group (Omenn *et al.*, 1996).

A meta-analysis published in the Lancet in 2004, of 14 randomised trials concluded there was no evidence antioxidant supplements prevented gastrointestinal cancers, and appeared to increase mortality (Bjelakovic *et al.*, 2004). Expanding on their findings, the group carried out a meta-analysis in collaboration with the Cochrane library, where they interrogated the data from 78 randomised trials with a total of 296,707 participants. The trials investigated the effects of antioxidant supplements including beta-carotene, vitamin A, C, E, and

selenium in a variety of diseases related to gastrointestinal, cardiovascular, neurological, endocrinological and rheumatic systems. No evidence was found that supported the use of antioxidants for the disease prevention and there was some indication that beta-carotene, vitamin A and E may increase mortality (Bjelakovic *et al.*, 2012).

Together these studies highlight the complexities in antioxidant supplementation and underline the potential benefits and harm antioxidants could have in disease management and prevention.

1.5 Superoxide dismutase

Superoxide dismutases (SODs) are metalloproteins which catalyse the disproportionation of superoxide radicals ($O_2^{-\cdot}$) to hydrogen peroxide (H_2O_2) and oxygen (O_2).

Figure 1.7: **The reaction of superoxide dismutase (SOD).**
This equation shows the disproportionation of superoxide anion radicals to form hydrogen peroxide and molecular oxygen via the dismutation reaction of superoxide dismutase (McCord and Fridovich, 1969).

This chemical reaction is required to reduce the potentially damaging chain reactions of superoxide radicals, which can act as precursors to OS. SODs are antioxidant enzymes that are part of the antioxidant defence system. There are three main types of SODs that are categorised based on cellular compartment localisation, metal enzymatic cofactor and protein folding.

1.5.1 SOD1

Mann and Keilin were the first to isolate copper containing proteins from bovine erythrocytes and liver tissue in 1938, terming the proteins respectively haemocuprein and hepatocuprein. In 1959, similar copper containing proteins were isolated from human erythrocytes, termed erythrocuprein and from human brains, termed cerebrocuprein (Markowitz, Cartwright and Wintrobe, 1959; Porter and Folch, 1957). In 1969, McCord and Fridovich published the first study to identify the enzymic activity of haemocuprein / erythrocuprein. The discovery that the protein catalysed the dismutation of superoxide radicals to produce H_2O_2 and O_2 prompted the apt renaming of the protein to superoxide dismutase.

In eukaryotes, CuZnSOD is predominantly isolated to the cytoplasm, nuclear compartments, and lysosomes (Crapo *et al.*, 1992). Several studies have measured CuZnSOD activity and protein concentration in blood serum and plasma (Gomez-Marcos *et al.*, 2016; Andrade *et al.*, 2000; Marklund, Holme and Hellner, 1982). The SOD1 gene is localised to region ‘q’ at position 22.11 of chromosome 21 in humans (Levanon *et al.*, 1985). Copper-zinc superoxide dismutase (CuZnSOD – EC 1.15.1.1), also known as SOD1, is a homodimer of two identical

non-covalently linked subunits (Briggs and Fee, 1978). In humans, each subunit of 15,936 Daltons (Da) is made up of 154 amino acids, plus one copper and one zinc ion which function in catalytic activity and stability (Uniprot, 23rd January 2007).

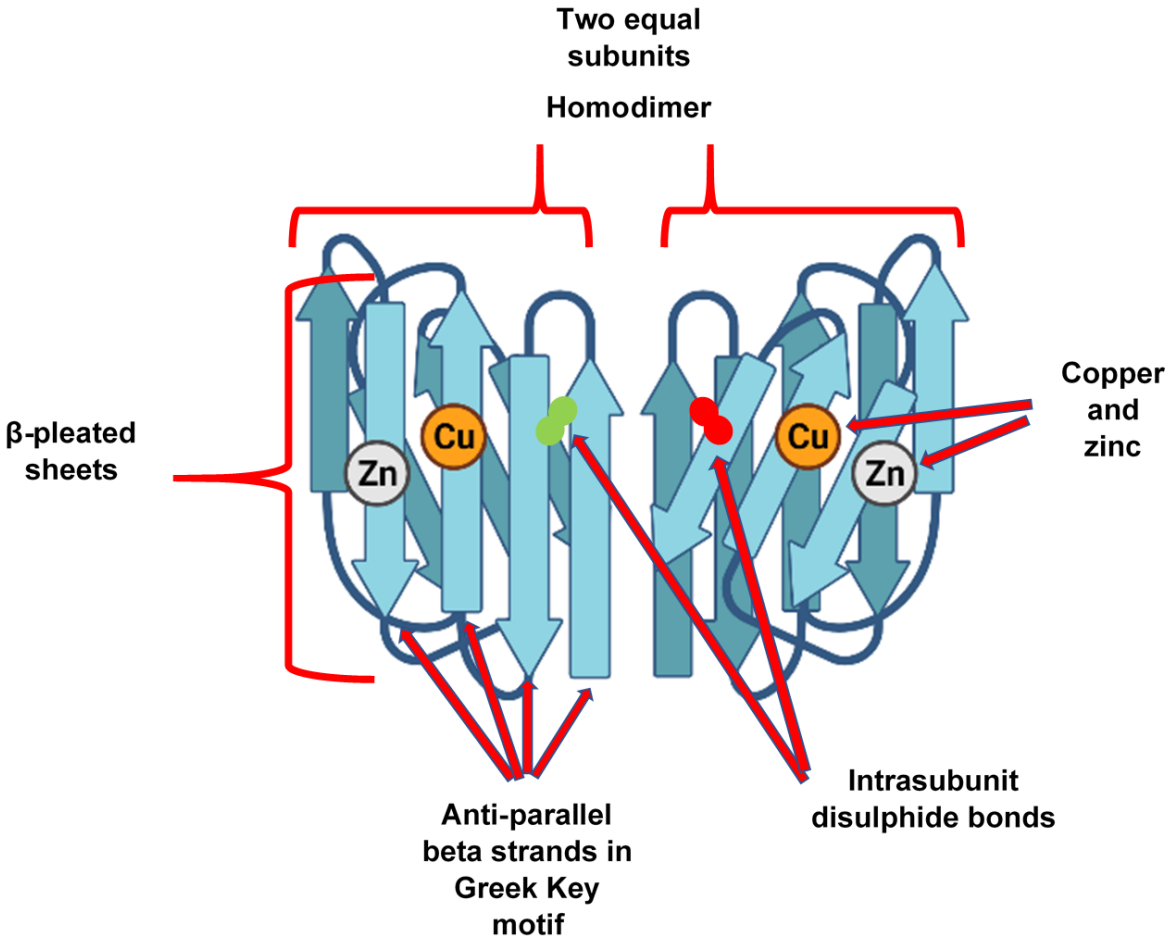

Figure 1.8: **Schematic presentation of SOD1 tertiary structure.**
This image was adapted from "Superoxide dismutase 1 (SOD1)", BioRender.com (2020). The subunits are made up of eight anti-parallel β-strands arranged in a Greek key motif forming a β-pleated sheet (Richardson, 1977). The core of each barrel is formed of tightly packed hydrophobic amino acids with leucine 'cork' residues filling each end of the sheet (Perry *et al.*, 2010). Two external loops function to stabilise the active site ("metal binding loop") and provide electrostatic guidance ("electrostatic loop") for the superoxide substrate to the copper ion (Getzoff, 1983). The active site of CuZnSOD is extremely specific as it can differentiate between oxygen and superoxide which have only one electron difference. Copper and zinc are vital for stability and their loss results in aggregation in disease models (see section 1.5.1.1).

1.5.2 SOD2

Manganese superoxide dismutase (MnSOD – SOD2) is a homotetramer of four subunits, each of which has a bound manganese ion. In humans, each of the individual subunits have a molecular weight of 24,750 Da and is made up of 222 amino acids (Uniprot, 20th December 2017). The SOD2 gene is localised to the 'q' region of chromosome 6 at position 25.3 in humans.

In eukaryotes the MnSOD is primarily a mitochondrial protein (Weisiger and Fridovich, 1973). Knock out SOD2 (-/-) mice, showed impairment of mitochondrial function that led to death within the first 10 days due to heart complications, metabolic acidosis, and accumulation of lipid in liver and skeletal muscle. It is hypothesised that SOD2 functions to protect mitochondrial enzymes from inactivation by superoxide radicals generated as a biproduct of the electron transport chain (Li *et al.*, 1995).

1.5.3 SOD3

Extracellular superoxide dismutase (ECSOD) is a homotetramer of four units, each of which has a bound copper and zinc ion. In humans, each individual subunit has a molecular weight 25,851 Da and is made up of 240 amino acids (Uniprot, 30th May 2006). The SOD3 gene is localised to the 'q' region of chromosome 4 at position 15.2 in humans.

SOD3 is present in extracellular fluids such as plasma, cerebrospinal fluid, seminal plasma, and lymph, however it is largely bound to heparan sulphate proteoglycans on cell surfaces, with particularly high concentrations on blood vessel walls and lungs (Antonyuk *et al.*, 2009).

1.5.4 Alternative roles of SOD1 in homeostasis

The homeostatic function of SOD1 is to catalyse the conversion of superoxide by dismutation to hydrogen peroxide and oxygen. There are two pathways for hydrogen peroxide – either participate in signalling or undergo decomposition by the enzyme catalase to produce water and oxygen. This has been the common view of SOD's primary purpose since discovery of its function by Fridovich and McCord in 1969. To summarise, SOD1 regulates the careful balance between superoxide and hydrogen peroxide signalling, whilst simultaneously

neutralising reactive oxygen species toxicity. As SOD1 reduces the damaging effects of the superoxide radicals it has functions in many processes. For example:

- It was observed, SOD1 played a role in the endometrium throughout the menstrual cycle and in early pregnancy where it may function to promote successful implantation and protect the embryo during development (Sugino *et al.*, 1996).
- It was reported, SOD1 plays a role in immune processes, modulating microbicidal activity. Inhibition of SOD1 decreased release of cytokines by activated macrophages (Marikovsky *et al.*, 2003).
- SOD1 -/- mice showed a 30% reduction in lifespan, which may be due to increased oxidative damage resulting in cellular senescence (Zhang *et al.*, 2017).
- In SOD1 -/- mice, age-related muscular atrophy was observed, where it was postulated redox signalling impairment was the primary cause, and not oxidative damage to the nerve (Sakellariou *et al.*, 2018).

1.5.4.1 SOD1 in the immune response

SOD1 does not defend the host against pathogens directly, however it protects the host against the potentially damaging effects of ROS generated during the inflammatory response. A type of phagocyte, called a macrophage, generates superoxide radicals, which either directly reacts with bacteria, or is spontaneously or catalytically converted to hydrogen peroxide. Superoxide radicals directly oxidise iron-sulphur (Fe-S) clusters in bacteria, resulting in the release of free iron (Scandroglio *et al.*, 2014). Free iron then participates in Fenton chemistry with hydrogen peroxide to yield hydroxyl radicals, which damages many biomolecules such as DNA, killing bacteria (Kohanski *et al.*, 2007).

SOD1 defends against ROS, more specifically superoxide radicals which are catalytically converted (dismutation) to hydrogen peroxide and oxygen. From an evolutionary perspective, SODs may have formed a protection system analogous to the first innate immune system, however defending host organisms against the toxicity of oxygen, not invading pathogens.

1.5.5 Genetic abnormalities and SOD1

1.5.5.1 Amyotrophic lateral sclerosis (ALS)

ALS, also known as motor neurone disease, is characterised by the gradual degeneration of motor neurons, the cells of the nervous system that carry neurotransmissions to muscles. Approximately 10% of ALS cases are categorised as familial and 90% are classified as sporadic. Mutations in the SOD1 gene account for around 12% of familial and approximately 1-2% of sporadic cases (Renton, Chiò and Traynor, 2014.). There is controversy surrounding the effects of mutations on function and activity of the SOD1 enzyme. There are numerous mutations which cause misfolding and aggregation of the SOD1 protein. These may result in either a gain of function, causing toxicity via increased dismutation and excessive hydrogen peroxide production, or a loss of function, causing decreased dismutation capacity, resulting in increased oxidative damage (Saccon *et al.*, 2013).

1.5.5.2 Trisomy 21

Down syndrome (DS), also known as trisomy 21, is a genetic condition caused by triplication of chromosome 21, which results in overexpression of the genes located on chromosome 21, including SOD1. It is hypothesised that increased expression of SOD1 results in increased hydrogen peroxide production which causes oxidative damage (Cowley *et al.*, 2017). A study of SOD1 levels in the brains of patients with DS showed SOD1 was increased (Gulesserian *et al.*, 2001). It is hypothesised that the accumulation of hydrogen peroxide associated with overexpression of SOD1 may be involved in the early onset of dementia and Alzheimer's disease (Gomez *et al.*, 2020).

1.6 Antibodies

1.6.1 What are antibodies and why are they significant?

In 1890, at the Koch's Institute in Berlin, Emil von Behring and Shibasaburo Kitasato were the first to discover antibodies (they termed anti-foreign bodies) through the neutralisation of the diphtheria and tetanus toxin using the serum of immunised animals. Antibodies, or immunoglobulins, are critical plasma glycoproteins of the adaptive immune system that recognise and bind immunogens and antigens (Liddell, 2005). Immunogens are any molecule that initiates an immune response whereas antigens bind to antibodies but do not always evoke an immune response. Immunogens and antigens can be categorised as pathogens, dysfunctional proteins, haptens and other foreign molecules. Binding of antibodies can neutralise immunogens by forming a physical barrier at a pathogens surface, blocking bacterial or viral proteins and polysaccharides. Upon binding, antibodies can also exert their effector functions, this marks immunogens for destruction by other immune cells (Delves *et al.*, 2017).

Antibodies are produced when an immunogen binds to an immunoglobulin displayed on the surface of a type of immune cell called a naïve or resting B lymphocyte. B lymphocytes develop in the bone marrow where they undergo V(D)J somatic recombination, a process whereby immunoglobulin variable (V), diversity (D) and joining (J) genes are rearranged to produce a diverse variety of antibody specificities (Hozumi and Tonegawa, 1976). In the bone marrow affinity maturation and B cell central tolerance also takes place, a process that selects only antibodies that react to 'non-self' immunogens. Binding of an immunogen stimulates the division and proliferation of mature B lymphocytes to secrete large amounts of immunoglobulins specific to the immunogen.

1.6.2 Structure of immunoglobulins

Immunoglobulin's (Ig) are categorised in to five different classes or isotypes IgA (α), IgD (δ), IgE (ε), IgG (γ), IgM (μ). These can also be split further into subclasses for example IgA is split into IgA_1 and IgA_2. Antibody monomers exist as four chains held together by covalent disulphide bonds (-S-S-), consisting of two light chains with a mass of approximately 25 kDa, which are associated only with the Fab region, and two heavy chains with a mass of approximately 55 kDa, which span the Fc and Fab regions. Heavy chains (α, δ, ε, γ and μ) determine the antibody

subclass or isotype (Zabriskie, 2009). The light chain consists of kappa (κ) or lambda (λ) chains. Antibodies have an N-terminus (amine group – NH_2) at Fab region and a C-terminus (carboxyl group – COOH) at the Fc region.

In IgG the Fab and Fc regions are linked together by a polypeptide chain called the hinge. IgG, IgE and IgD antibodies exist as monomers. On the other hand, IgA antibodies can exist as a monomer and dimer, and IgM can exist as monomers and pentamers.

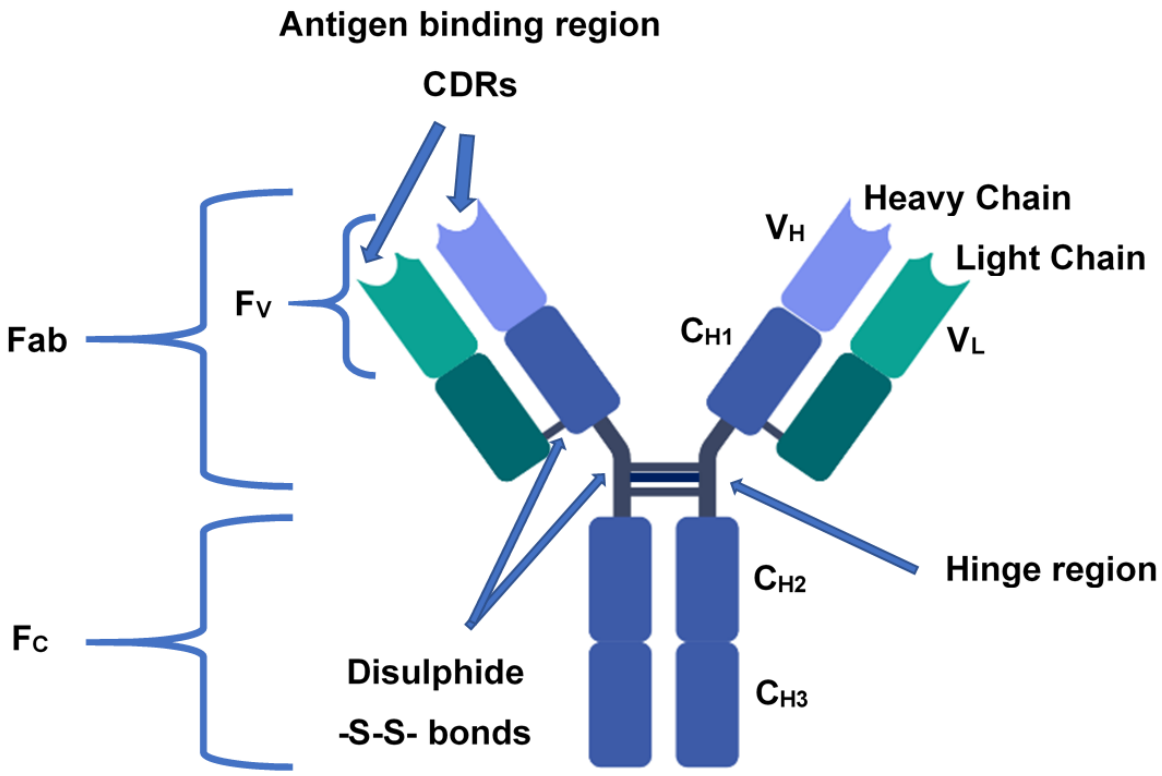

Figure 1.9: **The generic structure of immunoglobulin.**
This image was adapted from "Antibody IgG (with domains)", BioRender.com (2020). The structure of immunoglobulins (antibodies) consists of three units, the variable region, compromising two identical Fab (fragment antigen binding) regions that function in binding antigens, and a distinct third constant region, comprising the Fc (fragment crystallizable) region specific to the immunoglobulin subclass, which bind effector molecules to mediate and activate immune cell responses.

1.6.3 Immunoglobulin G

IgG has a molecular weight of approximately 150 kDa. It is the main immunoglobulin present in the blood, forming 15% of total serum protein concentrations and it has a half-life of approximately 21 days. IgG comprises five subclasses (IgG_1, IgG_{2a}, IgG_{2b}, IgG_3 and IgG_4) which differ in the length of their constant region of the heavy chain. There are several known functions of IgG that aid in the immune response (see Table 1.1)

Table 1.1: ***Known functions of IgG.***

Adapted from Schroeder and Cavacini (2010).

Function	**Description**
Opsonisation	Antibodies bind antigens on bacteria or viruses at their Fab region. The Fc region is then bound by immune cells which display Fc receptors such as macrophages, which then engulf and phagocytose the pathogen.
Agglutination	Agglutination occurs when IgG binds antigens, which then bind to each other to forming a precipitate. This is more easily detected by phagocytes.
Placental transfer	Unique to IgG is its ability only to cross the placenta, thus conferring passive immunity to the foetus.
Antibody-dependent cellular cytotoxicity (ADCC)	The Fab region of IgG will bind to tumour cells. This marks them for destruction by natural killer (NK) cells, which bind to Fc region and release cytotoxins.
Neutralisation	IgG can attach to the active site of toxins e.g., snake venom, rendering it inert. In viral infection, it will also bind to viral epitopes preventing viral absorption and release.
Activation of complement	IgG stimulates the activation of the complement cascade to signal phagocytes to assist the destruction of the infected cell. Complement also can aid antibodies in the direct killing of infected cells in the process of bacteriolysis.

1.6.4 Antibody-antigen interactions

The reactions between antigens and antibodies are dependent on weak non-covalent interactions which can combine to create stable complexes with strong avidity, however antibody-antigen binding is reversible.

Table 1.2: ***Known non-covalent interactions between antibody and antigen.*** Adapted from Morrison and Neuberger (2001).

Type of non-covalent interaction	Explanation
Hydrogen bonds	Where a hydrogen atom is shared between two electronegative atoms e.g., oxygen and nitrogen.
Hydrophobic interactions	Molecules are packed tightly in a space to avoid interactions with water.
Electrostatic forces	Molecules are attracted by their opposite charge.
Van der Waals forces	Fluctuations in the attraction or repulsion of electrons between two molecule results in a dipolarisation. This only occurs in close proximity.

The affinity between an antibody paratope and antigen epitope can be affected by temperature, pH and ionic strength of a solution or biological matrix because of their effects on the non-covalent interactions. Antibodies such as IgG can bind to antigens at single or dual epitopes (monovalent and bivalent binding). Antigens are also commonly multivalent, comprising multiple copies of the same epitope, or epitopes, that are recognised by multiple antibodies (Reverberi and Reverberi, 2007). Antibodies will often release their antigens on exposure to acidic pH, e.g., endosomes, they are then recycled into the extracellular space before they undergo lysosomal degradation (Klaus and Deshmukh, 2021).

1.6.5 Polyspecific antibodies

Antibodies are generally thought of as monospecific agents, specific to only one type of antigen / epitope (Landsteiner, 1947), however there is growing evidence of polyspecific antibodies – antibodies that bind a large repertoire of structurally unrelated proteins (Dimitrov, Pashov and Vassilev, 2012). It was reported polyspecificity can be induced by exposure to acidic pH (McMahon and O'Kennedy, 2000; Bouvet *et al.*, 2001). Additionally, increased recognition of bacterial antigens was observed when IgG was exposed to ROS-activated human neutrophils (Dimitrov *et al.*, 2006). Finally, it was also proven that antibodies gain polyspecificity upon exposure to inflammatory microenvironments (Mihaylova *et al.*, 2008).

1.6.6 Catalytic antibodies

The mechanisms and chemical similarities between antibody-antigen and enzyme-substrate interactions is noteworthy. Both antibodies and enzymes are very similar in that they have evolved to bind a large repertoire of ligands with high affinity and specificity (Yin and Schultz, 2005). The difference between the two is enzymes selectively bind and catalyse reactions of high-energy molecules, whereas antibodies bind molecules in their ground state.

In 1948, the first notion of catalytic antibodies was suggested by Linus Pauling after observing the similar features in the processes of transition state lowering in enzyme interactions and binding energies in antibody-immunogen complex reactions. Catalytic antibodies are antibodies that can catalyse chemical reactions, most commonly hydrolysis (Lacroix-Desmazes *et al.*, 2005).

There have been many naturally occurring catalytic antibodies described:

- In 1989, a study by Paul *et al.* described autoantibodies isolated from human sera that hydrolyzed vasoactive intestinal peptide (VIP).
- DNA-hydrolyzing activity was detected in the sera of patients with various autoimmune pathologies and was shown to be a property of autoantibodies (Shuster *et al.*, 1992).
- Peptide-methylcoumarinamide (peptide-MCA) hydrolyzing activity by polyclonal IgG was detected in healthy humans and significantly reduced in rheumatoid arthritis (Kalaga *et al.*, 1996).
- Peroxidase and superoxide dismutase activity of IgG was detected from the sera of healthy patients (Tolmacheva *et al.*, 2018).

1.7 Antibodies with superoxide dismutase-like activity

1.7.1 Structural similarity between SOD1 and IgG

In 1975, Richardson *et al.* characterised the structure of copper-zinc superoxide dismutase (CuZnSOD), and in 1976 compared the structure to immunoglobulin G (IgG). The three-dimensional or tertiary folding pattern of the proteins were studied using x-ray crystallography with analysis focussing on the immunoglobulin variable domain and the copper-zinc superoxide dismutase subunit. The group found “strikingly” similar tertiary structures between the protein units by superimposing alpha-carbon coordinates (locations of carbon atoms bonded to functional groups) and comparing a 3.0 Å resolution electron density map of bovine CuZnSOD (Richardson *et al.*, 1975) and a 3.1 Å resolution map of mouse myeloma protein McPC603 Fab fragment (Segal *et al.*, 1974). The typical immunoglobulin fold structure, as described in 1973 by Poljak *et al.*, was found to be present in CuZnSOD.

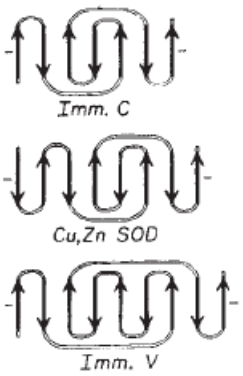

Figure 1.10: **β-sheet topology diagrams of IgG constant and variable regions, and CuZnSOD subunit.**
Each region has seven, eight and nine anti-parallel β-strands respectively. Taken from Richardson *et al.*, 1977.

1.7.2 Probability of similarity

Mathematical probability analysis of topology similarity was also completed. The purpose of this analysis was to estimate the likelihood of immunoglobulin variable domain and CuZnSOD subunit structures matching by chance in nature. Several assumptions of the structure were made when modelling the possible topologies, such as considering the structures of each protein as complete cylinders, factoring in and out 'cross' connections (connections by helixes or other stabilising connections such as disulphide bonds), and not allowing connecting chains to position inside the cylinder (an unfavourable topology for stability). The topological estimations were derived from the β-structures observed in previously characterised proteins which gave a body of evidence to create rules about common differences and similarities (conserved regions) between structures of proteins.

Analysis used empirical estimates (relative frequency of a folding event) on the superoxide dismutase subunit, one strand of beta pleated sheet at a time in sequence, considering external loop placement and the extra β-pleated sheet strand in the superoxide dismutase subunit. It was estimated the probability of topological similarity between the structure of the immunoglobulin variable domain and copper-zinc superoxide dismutase subunit occurred by chance would be approximately 1/2853. This observation showed it was very unlikely the three-dimensional structural similarities occurred only by chance.

1.7.3 Sequence homology

In 1974, Steinman *et al.* derived the complete amino acid sequence of bovine CuZnSOD, and Segal *et al.* the complete amino acid sequence of mouse immunoglobulin Fab fragment. The comparison of variable-length segments of amino acid sequences from the two proteins using computational amino acid sequence analysis located partially matching sequence segments but only slightly greater than random: 9% sequence identity (Martz and Francoeur, 2004).

1.7.4 Functional relationship between SOD1 and IgG

The combined investigations of β-sheet similarity, probability analysis of topology similarity and amino acid sequence homology, led to the postulation of an evolutionary and functional relationship between CuZnSOD and immunoglobulin.

Petyaev and Hunt conducted the first experiments investigating superoxide dismutase activity of antibodies (AbSOD activity) in 1996. Superoxide detection inhibition assays (xanthine oxidase-cytochrome C assay, NADH-PMS/NBT assay – please refer to section 1.8) were used to investigate SOD activity of CuZnSOD and IgG_1 (HSA-9) at pH 7.8. They found IgG_1 had an inhibitory effect on the detection of superoxide. They noted the NADH/PMS-NBT (nicotinamide adenine dinucleotide / phenazine methosulfate – nitroblue tetrazolium) assay compared to the other methods was more sensitive for IgG_1 (less antibody resulted in greater superoxide inhibition) and advantageous because it was functional at acidic and neutral pH.

1.7.5 Role of the antigen binding site in SOD activity

Petyaev and Hunt investigated the role of the antigen binding site in antibody SOD activity using the NADH/PMS-NBT assay. They concluded the SOD activity of murine antibody (NQ11.7.22 variable fragments (Fv) of antigen binding regions (Fab)) at concentration 10 μg/ml was comparable to that of human erythrocyte CuZnSOD at 0.1 μg/ml (Petyaev and Hunt, 1996). They then studied the contribution of certain amino acids to SOD activity of these Fv fragments using single point mutations. A change in a heavy chain tyrosine (vital for antigen binding) to phenylalanine at position 32, and a light chain histidine to leucine at position 27, both incurred a significant reduction in SOD activity. The heavy chain point mutation resulted in a 2.9 – 5.7-fold decrease in SOD activity when compared to the wild type Fv fragment.

These findings suggested SOD activity of antibodies was localised to the antigen binding site and amino acids involved centrally in antigen binding were required for a significant proportion of antibody SOD activity.

1.7.6 Significance of pH on SOD activity

In another experiment, Petyaev and Hunt (1996) investigated the effects of pH on SOD activity of Fv fragments. Extremes of acid and alkali, measured by the pH scale (potential of hydrogen), can cause proteins to denature (lose their structure). Hydrogen ions (H^+), which increase as the pH becomes more acidic, can disrupt and destabilise non-covalent interactions (see table 1.2), which are formed between amino acid residues that make up proteins and stabilise overall structure.

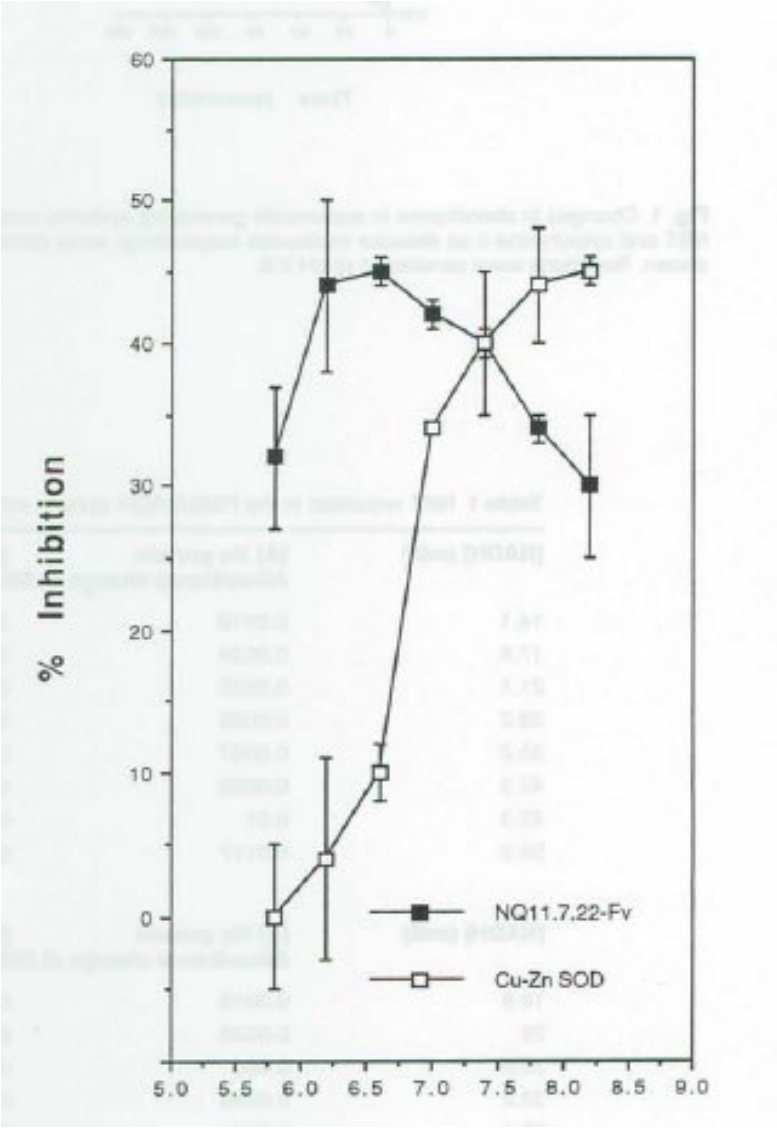

Figure 1.11: **The pH dependency of NQ11.7.22-Fv fragments and CuZnSOD.** The data was generated using the NADH/PMS-NBT assay, at 10µg/ml NQ11.7.22-Fv and 0.1µg/ml CuZnSOD (Petyaev and Hunt, 1996).

When comparing the pH profiles of CuZnSOD and NQ11.7.22-Fv, it was evident they expressed very different and almost opposite pH dependency. The optimum inhibition was achieved at approximately pH 6.25-6.50 for the Fv fragments and pH 7.80-8.25 for CuZnSOD. The Fv fragment appeared to maintain approximately 25-50% inhibition across the pH range however CuZnSOD had significantly reduced activity, over 90% reduction at acidic pH less than pH 6.5.

To appreciate the 'enzymic' efficiency the mass concentration and molar concentration need to be compared for these experiments. Considering the mass concentration of Fv at 10µg/ml to CuZnSOD at 0.1 µg/ml, the Fv fragments are present as 100 times more mass (10/0.1) than SOD, and for molar concentration over 130 times more molecules (Da = mg/mmol; mg/ml / mg/mmol = mmol/ml) to achieve the same effect. This is based on SOD of 32.5 kDa and Fv of 25 kDa.

Although the molar concentration and mass concentration of antibodies is greater than CuZnSOD this discovery is significant especially at acidic pH. Acidic pH is thought to be associated with inflammatory sites and LDL-oxidation in atherosclerotic lesions (Leake, 1997). The effects of pH are discussed in more detail in sections 4.1.1 and 5.1.1.

1.7.7 IgG enhances the production of hydrogen peroxide

NADH and PMS were used to generate superoxide, and the generation of hydrogen peroxide by IgG_1 (9.0 µg/ml) and human CuZnSOD (0.3 µg/ml) measured using the ferric-oxidation xylenol orange assay at pH 5.4, 6.8 and 7.8. At low pH hydrogen peroxide generation was increased with IgG_1 and decreased with CuZnSOD. IgG_1 yielded maximal hydrogen peroxide generation at pH 6.4. Both IgG_1 and CuZnSOD increased hydrogen peroxide formation at pH 7.8.

The discoveries of hydrogen peroxide formation and superoxide detection inhibition at acidic pH led to the postulation AbSOD activity could have a function *in vivo* in acidic pH environments (Petyaev and Hunt, 1996).

1.7.8 Antibodies from diseased arteries have SOD-like activity

A final published study by Petyaev, Hunt, Mitchinson and Coussons in 1998, investigated the SOD activity of tissue extracts from healthy human arteries and

atherosclerotic lesions (diseased vessels). In total, 19 patients aged 56-92 years were recruited, with specimens collected in matched pairs via human necroscopy.

PBS (phosphate-buffered saline) extracts of the lesions containing superoxide dismutase and antibodies were assayed for superoxide dismutase activity (SOD) using the xylenol orange hydrogen peroxide method at pH 6.45 and 7.81. The extracts of atherosclerotic tissue and lesion tissue were treated with diethyldithiocarbamic acid (DDC – binds Cu (II) ions inhibiting CuZnSOD activity) and staphylococcal protein A (protein A – binds and removes antibodies). Treatment of lesion tissue with protein A resulted in a 50% reduction in hydrogen peroxide formation at pH 7.81 and greater than 70% reduction at pH 6.45. The hydrogen peroxide formation was unchanged in healthy artery extracts treated with protein A suggesting the activity was attributable to antibodies in the lesion extracts. Treatment of both lesion and healthy artery extracts with DDC resulted in a decrease in hydrogen peroxide formation. This suggested antibodies with SOD activity (AbSOD) may be enhanced by copper ions.

1.7.9 Proposed mechanism of antibodies with superoxide dismutase activity

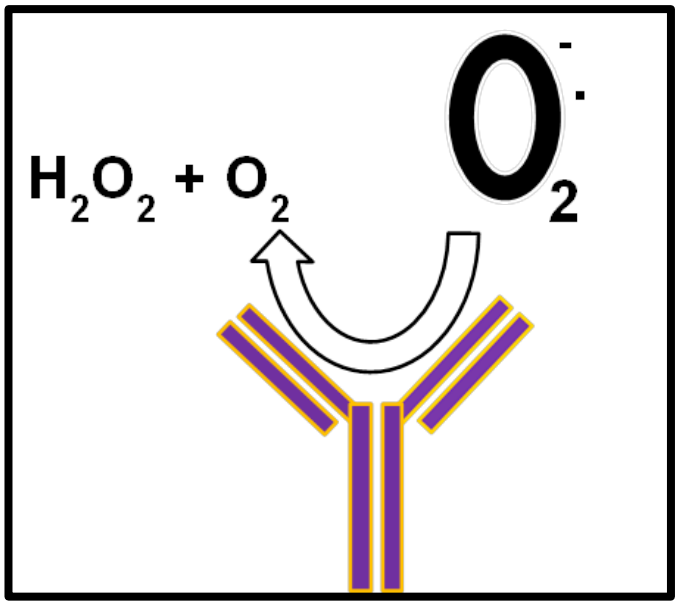

Figure 1.12: **Illustration of the mechanism of AbSOD activity**
(Based on current evidence). Antibody superoxide dismutase activity (AbSOD) is the ability of immunoglobulins to mimic superoxide dismutases, acting as catalysts to dismutate superoxide radicals into hydrogen peroxide and oxygen.

1.7.10 Supporting and alternative theories

1.7.10.1 Antibody catalysed water oxidation pathway (ACWOP)

In 2000, Wentworth *et al.* proposed antibodies produced ROS to aid in bacterial killing, where they reported hydrogen peroxide was generated by antibodies from singlet oxygen ($^1O_2$). The group later reported H_2O was required as an electron source (Wentworth *et al.*, 2001), naming this process the antibody-catalysed water oxidation pathway (ACWOP). In 2002, Wentworth *et al.* suggested hydrogen peroxide production alone was insufficient for bacterial killing – another molecule with a chemical signature like that of ozone (O_3) was detected.

Evidence for the generation of ozone was based on the reaction with indigo carmine to produce isatin sulfonic acid. A study examined the specificity of the indigo carmine method for ozone and observed superoxide converted indigo carmine to isatin sulfonic acid, in a reaction that was "completely inhibited by superoxide dismutase and unaffected by catalase" (Kettle, Clark and Winterbourn, 2004, p.18521). This meant the claims of ozone generation by the ACWOP were not substantiated using this probe. In 2003, an alternative probe for ozone was used to show antibody-coated neutrophils produced an oxidant with a chemical signature like ozone – it was hypothesised this may have a role in amplification of the inflammatory response (*Babior et al.*, 2003).

In a final review article of ACWOP in 2008, regarding the formation of ozone by IgG-coated polymorphonuclear leukocytes it was stated – "It should be noted that the evidence that ozone may be formed in phagocytes arises from indirect evidence using chemical probes. The case for ozone formation will be strengthened if and when it can be detected as directly as possible" (Wentworth and Witter, 2008, p.1851).

1.7.10.2 Evidence of dismutation by IgG and light chains

Since the late 1990's, where the dismutation of superoxide by variable fragments and whole IgG was detected, there have been numerous published articles that have added to the work by Petyaev and colleagues. There are several studies that have observed production of hydrogen peroxide by whole immunoglobulin molecules and immunoglobulin light chains. It has been proposed that Ig-light chain production of hydrogen peroxide promotes the production of MCP-1 (monocyte chemoattractant protein 1) to recruit monocytes such as

macrophages to sites of inflammation (Wang and Sanders, 2007; Basnayake *et al.*, 2010). In 2012, a study observed normal IgG decreased intracellular superoxide concentrations, which it was hypothesised led to decreased migration and cell permeability, and formation of stress fibres in human aortic epithelial cells isolated from a hypertensive patient (Wang, Wang and Sun, 2012). The most recent study of redox activity of antibodies observed increased IgG-dependent dismutation of IgG isolated from patients with multiple sclerosis compared to 'healthy' controls (Smirnova *et al.*, 2020).

Taken together, despite the differences in conclusions between these studies, they collectively support the notion that antibodies have a role to play in redox biology and signalling.

1.8 Immunoglobulins and oxidative stress in disease

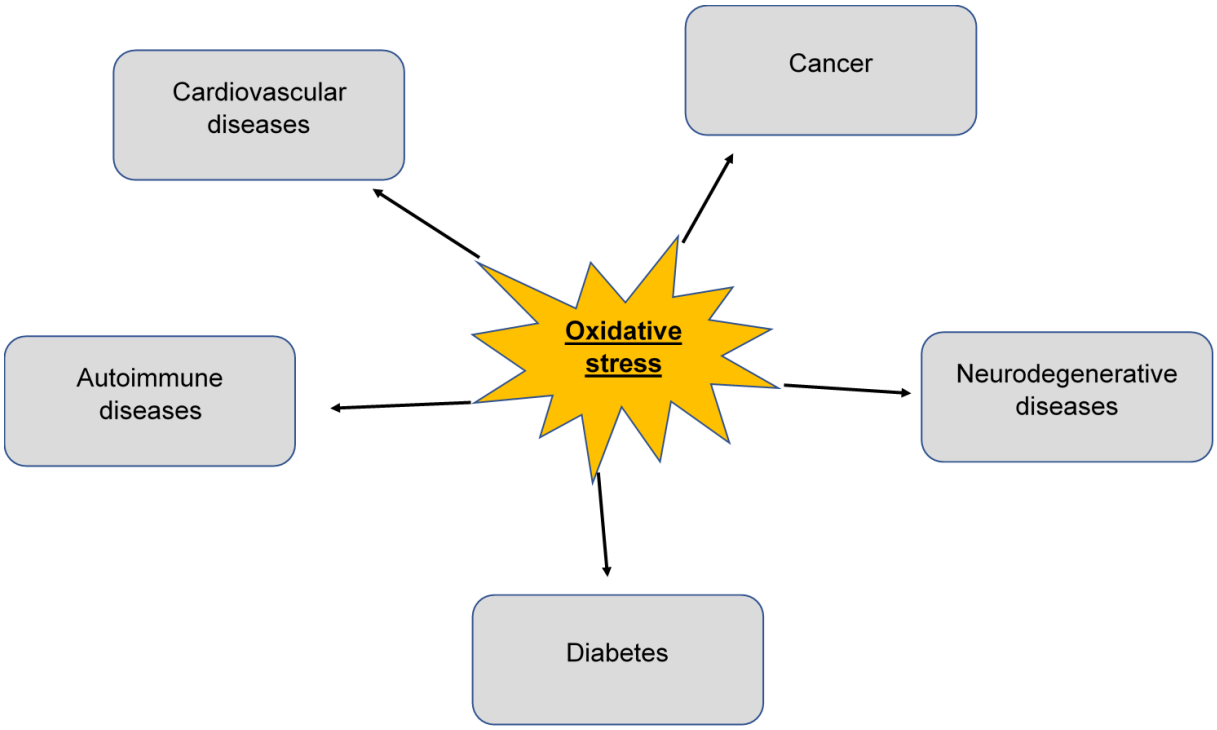

Figure 1.13: **OS-linked diseases.**

1.8.1 Rheumatoid arthritis (RA)

1.8.1.1 Characteristics and clinical significance

RA is a chronic autoimmune disease characterised by development of autoantibodies; the most referred one is rheumatoid factor, commonly of IgM, but sometimes IgG subclass which is directed to the Fc region of IgG. In RA, immune cells infiltrate the synovium of joints leading to acute inflammation which can transition to chronic, destructive synovitis (Weyand and Goronzy, 2021). Although RA is thought to be the result of diminishment of self-tolerance its exact cause is unknown.

1.8.1.2 OS in RA

In a study of 120- RA patients, observed a significant increase in lipid peroxidation, protein oxidation and DNA damage. A simultaneous decrease was seen in SOD and catalase activity. It was hypothesised that oxidative stress may contribute to the tissue damage observed in RA (Mateen *et al.*, 2016).

1.8.2 Coeliac disease (CD)

1.8.2.1 Characteristics and clinical significance of CD

Coeliac disease is a chronic autoimmune disease characterised by the development of autoantibodies against tissue transglutaminase 2 (TG2), that are understood to occur due to deamidation of gliadin by TG2 increasing its binding affinity for HLA-DQ2/DQ8 on antigen presenting cells. This is thought to initiate a cascade of events where deamidated gliadin is presented to T-cells and B-cells, which results in the release of cytokines and production of autoantibodies, leading to lymphocyte infiltration of the duodenal mucosa, that results in damage, presenting as deficiencies caused by malabsorption (Kivelä *et al.*, 2021).

1.8.2.2 OS in CD

A study of 54- patients with coeliac disease observed a significant increase in lipid peroxidation and protein oxidation, with a simultaneous decrease in total antioxidant capacity (TAC) and glutathione (GSH). A proportional increase in lipid peroxidation and decrease in TAC and GSH to the severity of duodenal atrophy was observed (Moretti *et al.*, 2018). This suggests oxidative stress and antioxidant defences play a major role in the progression and clinical features observed in CD.

1.8.3 Myocardial infarction (AMI)

1.8.3.1 Characteristics and clinical significance of AMI

Acute myocardial infarction (AMI), also known as a heart attack, is a condition characterised by partial or complete occlusion of the coronary artery, which causes restriction or stopping of blood (ischemia), and therefore oxygen, to the heart (White and Chew, 2008). The lack of oxygen causes a switch from aerobic to anaerobic metabolism, resulting in loss of myocyte contraction due to lactate accumulation, ATP depletion and sodium and calcium ion overload. As blood supply is restored (reperfusion), the electronic transport chain is re-initiated, generating ROS that cause lipid peroxidation and oxidative damage to DNA (Hashmi and Salam, 2015). Death of myocardial cells results in release of cardiac troponin, an important diagnostic biomarker for AMI.

1.8.3.2 RS and OS in AMI

In a study of 40- AMI patients and 40- ‘healthy controls, an increase in lipid peroxidation and protein oxidation was observed in the AMI group. Additionally, an increase in SOD and catalase, and decrease in vitamin E and C was reported. The increase in oxidative stress observed in AMI is thought to occur during reperfusion of ischaemic myocardium. It was hypothesised, the increase in SOD and catalase was indicative of compensatory mechanisms to prevent tissue damage caused by oxidative stress, or by mechanical tissue damage causing release of intracellular enzymes (Bagatini *et al.*, 2011).

1.8.4 Breast cancer (BC)

1.8.4.1 Characteristics and clinical significance of BC

Breast cancer is the group term for malignant tumours that occur in the breast tissue. As with other cancers, the cause of breast cancer is multifactorial, including both environmental and genetic factors. Factors such as damage to DNA or inheritance of genes such as BRCA1 and BRCA2 genes, increase the likelihood of developing breast cancer (Akram *et al.*, 2017).

1.8.4.2 OS in BC

In 2005, a study of 40- breast cancer patients observed enhanced lipid peroxidation, SOD and GPx and decreased CAT in tumour tissues compared to non-malignant tissues (Tas *et al.*, 2005). Another study in 2006 of 56- breast cancer patients showed serum lipid peroxidation was increased and TAC was significantly lower compared to controls. It was hypothesised oxidative stress may be related to breast cancer (Sener *et al.*, 2006).

1.8.5 Monoclonal gammopathies

1.8.5.1 Characteristics and clinical significance MM and MGUS

Monoclonal gammopathies, also known as paraproteinaemias, are a group of plasma cell disorders associated with monoclonal proliferation of plasma cells and production of monoclonal proteins (M-proteins) that are detectable by electrophoresis.

Monoclonal gammopathy of unknown significance (MGUS), as defined by the International Myeloma Working Group (2003), is characterised by a serum M-protein concentration of <30 g/L, with bone marrow clonal plasma cell infiltration <10% and absence of end-organ damage classified by normal serum calcium, no renal impairment, no anaemia, and no evidence of bone lesions (CRAB classification). MGUS is general thought to be asymptomatic.

Multiple myeloma (MM), is characterised by presence of a serum M-protein in the serum, bone marrow monoclonal plasma cells in the bone marrow ≥10% and/ or the presence of plasmacytoma, and myeloma-related organ damage classified by elevated calcium (corrected serum calcium >0.25 mmol/L above the upper limit of normal, or >2.75 mmol/L), renal insufficiency (serum creatinine >173 µmol/L), anaemia (haemoglobin 20 g/L below the lower limit of normal, or haemoglobin <100 g/L), and evidence of lytic bone lesions (International Myeloma Working Group, 2003). MM is often accompanied by frequent bacterial infections, blood hyper-viscosity and bone fractures.

1.8.5.2 OS in MGUS and multiple myeloma

In 2009, Sharma *et al.* observed the activity of SOD, GPx and CAT were significantly decreased compared to controls, along with vitamin C and E concentrations. Enhanced lipid peroxidation was evidenced by increased malondialdehyde (MDA) levels. Additionally, a study in 2012 by Gangemi *et al.* found serum levels of advanced oxidation protein products (AOPPs – evidence of albumin oxidation) and advanced glycation end products (evidence of protein and lipid glycation) were significantly increased in MM patients compared to controls and to MGUS subjects. Additionally, it was observed that AOPPs and AGEs were significantly higher in patients with bone lesions compared with those without lytic bone lesions (Gangemi *et al.*, 2012).

A literature search could not find any additional published data on antioxidant or oxidative stress markers in MGUS.

1.9 Probing antibodies with superoxide dismutase activity

The enzyme superoxide dismutase (SOD) catalyses the disproportionation of superoxide radicals ($O_2^{\bullet-}$) to hydrogen peroxide (H_2O_2) and oxygen (O_2) in a process called dismutation. Dismutation is the simultaneous oxidation and reduction of a chemical species (Halliwell and Gutteridge, 2015d).

Superoxide dismutase activity can be probed via two mechanisms, detection of the dismutation end-product hydrogen peroxide, or by competition between enzymatic dismutation of superoxide and reduction of a tetrazolium salt such as Nitroblue Tetrazolium (NBT) by superoxide to form formazan dyes (see Figure 1.13). Both method types require superoxide to be generated, which is achieved either enzymatically or non-enzymatically, providing a continuous flux of superoxide. A continuous flux of superoxide is essential due its relatively short half-life, which is estimated to be about 5 seconds at physiological pH (Marklund, 1976). Most commonly, assays rely on superoxide generated enzymatically via xanthine-xanthine oxidase or non-enzymatically via reduced nicotinamide adenine dinucleotide (β-NADH) and phenazine methosulphate (PMS).

Detection of superoxide is frequently achieved by the reduction of tetrazolium salts to yield formazan dyes. The formazan dyes absorb maximally at different wavelengths depending on the colour of the dye formed; nitroblue tetrazolium (NBT), so named as it yields a blue / purple product, absorbs at 560 nm. Superoxide dismutase assays are primarily performed at pH 7.8 due to the pH optimum of the xanthine oxidase used in these assays which is generally porcine liver or bovine milk derived.

A major advantage and reason why the NADH / PMS – NBT assay was selected for investigating the superoxide dismutase activity of antibodies instead of the xanthine / xanthine oxidase – NBT assay was its ability to be used at various pH levels. Superoxide can be generated via NADH / PMS at varying pH's, so enables the mimicking of pH environments reflective of those observed in inflammation and pathology *in vivo* (Petyaev and Hunt, 1996).

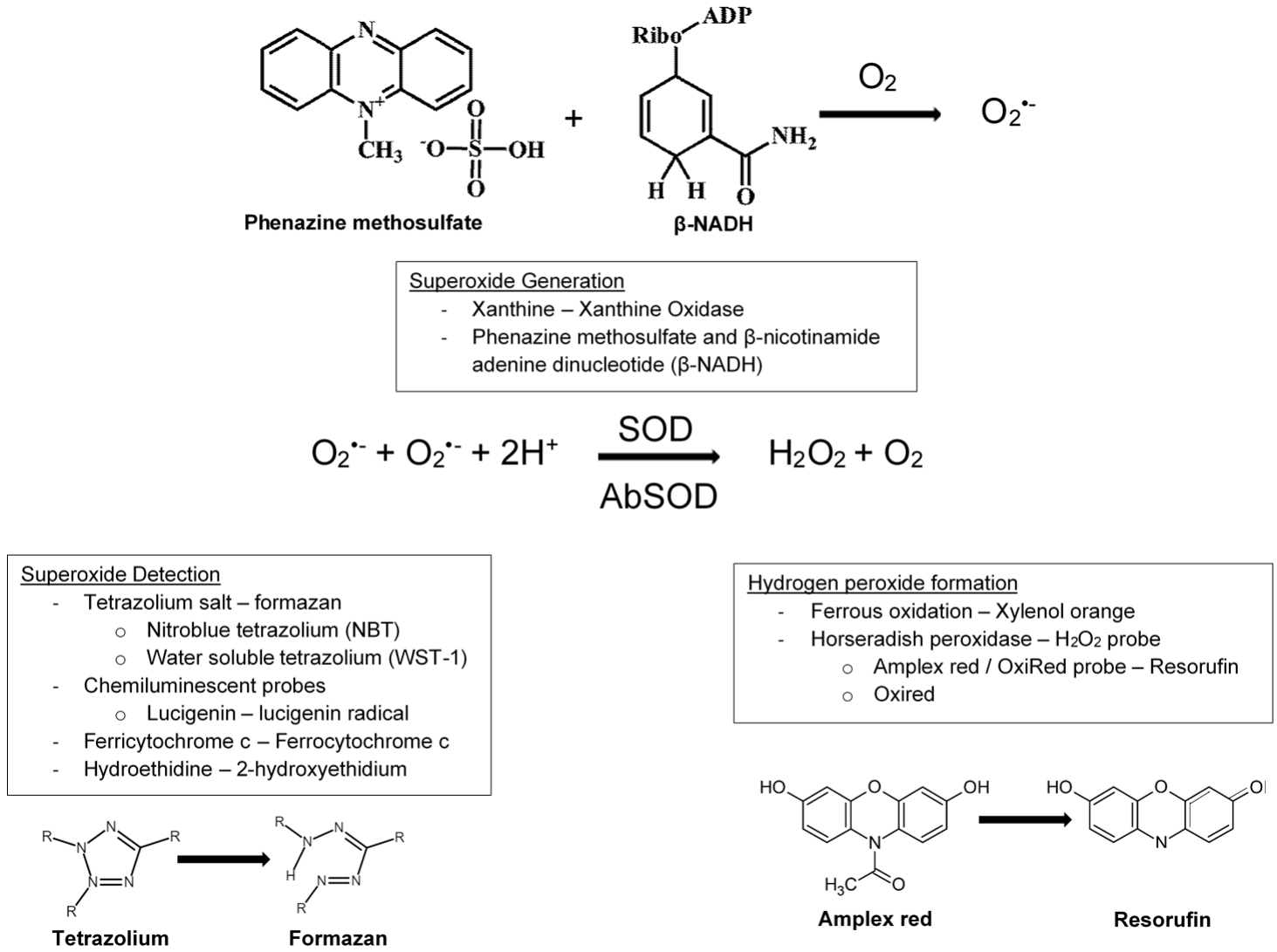

Figure 1.14: **Method review.**

The various main methods to generate superoxide are noted, with the chemical structure of PMS and NADH presented (Taken from Nimse and Pal, 2015). Superoxide is detected through the reduction of tetrazolium to formazan, e.g., NBT to formazan (blue coloured product). Other methods exist, however the combination of NADH-PMS/NBT can detect superoxide at varying pH's (Petyaev, 1996). SOD activity in inversely proportional to the colour formation. Previously, formation of hydrogen peroxide was utilised as a measure of SOD activity; amplex red to resorufin is the preferred method for detection of hydrogen peroxide. Chemical structures were created and found using chemspider.com.

1.10 Aims and objectives

The information described before this section indicates that antibodies of the immune system have a role to play in redox reactions *in vivo*, specifically in antioxidant protection in pathological and inflammatory environments. However, numerous questions about the function AbSOD activity may have across various oxidative stress-related pathologies remain. Whether the AbSOD activity of antibodies isolated from human serum in autoimmune disease, cardiovascular disease and cancer is affected by pH changes has yet to be investigated. Furthermore, whether these changes are significantly different compared to 'healthy' controls is yet to be examined in detail. A better understanding of the concentrations and activity of systemic antioxidants and oxidative stress markers (changes in serum CuZnSOD and catalase concentration and activity) would also provide insight into the overall redox status in these pathologies.

Table 1.3: ***Aims and hypotheses***

Aims	Key hypotheses
1) To study commercially available antibodies with superoxide dismutase activity.	The observed superoxide dismutase activity is caused by IgG and not associated host proteins.
1a) To confirm the presence of mouse IgG in commercially available IgG and investigate the level of protein contamination from antibody source.	Mouse IgG from ascites fluid is contaminated with host proteins with antioxidant potential and these are removed by purification with protein A agarose.
1b) To assess the constituent immunoglobulin subclasses or isotypes present in an antibody from mouse ascites fluid.	Mouse IgG_1 is the predominant isotype present in commercially available antibodies with superoxide dismutase activity.
2) To optimise an assay for the detection of superoxide dismutase activity of IgG	Modification of the concentration of the assay reactants could improve the sensitivity for detection of antibody superoxide dismutase activity.
2a) To develop a high-throughput 96-well micro-titre plate assay for the detection of antibody superoxide dismutase activity.	Miniaturisation of the NADH/PMS – NBT antibody superoxide dismutase-like activity assay could increase throughput, improve sensitivity, and reduce within batch, and between batch imprecision.
2b) To evaluate the performance of the developed antibody superoxide dismutase activity assay and determine the mechanism of action.	Assessment of albumin effects, heat-denaturation effects, and the effects of metal ions on activity would provide information about how the assay performs and elucidate mechanism of antibody superoxide dismutase activity.
3) To assess the pH dependency for superoxide dismutase activity of mouse IgG, human IgG, and SOD.	Superoxide dismutase activity would be optimal at slightly alkaline physiological pH (pH 7.0 – 7.5) and significantly reduced at inflammatory acidic pH, whereas antibody superoxide dismutase activity would be increased at inflammatory pH (pH 5.5 – 6.5) and significantly reduced at physiological pH.

4) To develop a method to isolate antibodies from human serum for the detection of superoxide dismutase activity.	Antibodies could be isolated from human serum using protein A/G agarose without removing antibody superoxide dismutase activity.
5) To study AbSOD activity of antibodies and antioxidant and oxidative stress markers in patient cohorts with immune dysfunction and oxidative stress-related diseases compared to 'healthy' patients.	Antibody superoxide dismutase activity and antioxidant and oxidative stress markers observed in disease states would be different from that of 'healthy' patients. Assay results would provide information to explain the oxidant / antioxidant status of patient cohorts and the role of antibodies in disease pathologies.
5a) To investigate the results with multivariate statistical analysis techniques	The use of principal components analysis and cluster analysis would provide information about previously unknown relationships between redox biology and the immune system in patient cohorts with complex disease states.

CHAPTER 2: Materials and methods

2.1 Reagents and Materials

Unless otherwise stated, all chemicals, reagents and materials were purchased from Sigma-Aldrich (Dorset, U.K.) and stored according to the manufacturer's instructions prior to use. Where reagents or chemicals were weighed, a Sartorius balance (CPA225D) was used unless otherwise stated. Where reagents were prepared to a specific pH, a Hanna HI 9321 pH meter was used (HANNA instruments); this was calibrated using pH reference solutions (Cat no: 961099, Orion Thermoscientific). The Jenway 6305 UV/Visible spectrophotometer (Jenway, Staffordshire, U.K.) was used for all spectroscopic measurements of solutions in cuvettes.

2.2 Characterisation of IgG from mouse ascites fluid

2.2.1 Protein A agarose purification of monoclonal IgG from mouse ascites fluid

Mouse monoclonal anti-human serum albumin IgG antibody (clone HSA-9 – Cat no: A2672) was purified using the Pierce™ protein A IgG purification kit (Cat no: 44667, Thermo Fisher Scientific). The mouse monoclonal antibody, produced from ascites, was supplied as a 0.2 millilitre (mL) solution with a protein concentration of 30.6 milligram per millilitre (mg/mL) containing 5.8 mg/mL of the isotype IgG_1, as determined by radial immunodiffusion. The protein A agarose had a binding capacity of 6 – 8 mg/mL of settled resin and was supplied in pre-packed 1.0 mL columns containing storage solution of 0.02 % sodium azide. Prior to use, all reagents were brought to room temperature (RT: 21 °C $\pm$ 2°C) and the column equilibrated. The top and bottom caps of the column were removed, and the storage solution discarded and replaced with 5.0 mL of protein A IgG binding buffer (Cat no: 21001, Thermo Fisher Scientific). This drained through the column before replacing the caps.

The antibody solution was slightly turbid and so was clarified by centrifugation at 10,000 g before use. The antibody (200 µg) was pipetted into the equilibrated column and the volume made up to 5.0 mL with binding buffer. The antibody-agarose resin slurry was incubated for 2 hours at room temperature on a roller mixer. After 2 hours the column caps were removed, and the antibody sample

was left to flow through the column with the residual flow-through being collected in 1.0 mL aliquots. The column was washed by allowing 15 mL of binding buffer to drain through the column, collecting the wash outs in 1.0 mL aliquots. To verify all unbound proteins were removed, the absorbance of the 1.0 mL aliquots was determined spectrophotometrically at 280 nm, in 10 mm path-length quartz cuvettes (cat no S-10SM), that had been blanked against equivalent volumes of binding buffer, until no further protein run-off could be detected.

The column-bound mouse IgG antibody was subsequently eluted from the protein A agarose by adding 5.0 mL of IgG elution buffer (Cat no:1851520, Thermo Fisher Scientific), with the eluate fractions collected in 1.0 mL aliquots. The pH of eluate aliquots was neutralised by adding 100 µL of protein A IgG binding buffer. To verify which eluate fractions contained the antibody the absorbance at 280 nm was spectrophotometrically determined. The concentration of the purified antibody solution was calculated using an extinction coefficient of 210,000 $M^{-1}cm^{-1}$, prior to storage in 100 µL aliquots at -80 °C for future use.

2.2.2 Spectrophotometric determination of IgG and superoxide dismutase protein concentration

The protein concentrations of mouse ascites fluid (Cat no: A2672), protein A-purified mouse monoclonal anti-human serum albumin IgG, superoxide dismutase (SOD) from bovine erythrocytes (Cat no: S7446-15KU) and SOD from human erythrocytes (Cat no: S9636-1KU) were determined based on their specific molar absorption coefficients.

The wavelength was adjusted to λ max for each protein (280 nm for determination of IgG concentration, 265 nm for human SOD and 258 nm for bovine SOD). Blank and protein absorbance measurements were determined using 1.0 mL, 10 mm path-length quartz cuvettes (Cat no: S-10SM).

For each protein, a buffer blank measurement of the buffer specific for the protein was completed at λ max wavelength. A blank of IgG elution buffer, neutralised with 100 µL of protein A binding buffer was spectrophotometrically determined at 280 nm for the protein A-purified mouse IgG antibody. The non-purified mouse IgG from ascites fluid was diluted in x 1 phosphate-buffered saline (x 1 PBS, pH 7.4: generated in-house from Sigma-Aldrich chemicals – refer to Appendix 2.1 for preparation) to a total volume of 1.0 mL; a blank of x 1 PBS was spectrophotometrically determined at 280 nm. Human and Bovine SOD were

reconstituted in x 1 PBS, pH 7.4; a blank of x 1 PBS was spectrophotometrically determined at 265 and 258 nm, respectively.

Following a blank measurement, the absorbance of 1.0 mL of protein solution was spectrophotometrically determined using quartz cuvettes at the respective λ max wavelength of each protein. The concentration of each protein sample was determined by substituting the molecular weight (g/mol), extinction coefficient (M^{-1} cm^{-1}) and λ max into the Beer-Lambert law equation (see fig 2.1).

This method was used for the determination of protein concentration for proteins used for protein agarose gel electrophoresis (PAGE), Western Blot and the cuvette antibody superoxide dismutase activity experiments (Chapter 3 and Chapter 4, sections 4.3.2 and 4.4.2).

Table 2.1: ***Proteins analysed***

Molecular Weights, Extinction Coefficients and λ max wavelength of proteins analysed.

Protein	Molecular Weight (Da)	Extinction Coefficient ($M^{-1}cm^{-1}$)	λ max wavelength
Immunoglobulin G	150,000	210,000	280 nm
Human SOD	32,000	18,400	265 nm
Bovine SOD	32,500	10,300	258 nm
Human serum albumin	66,450	35,219	280 nm
Bovine serum albumin	66,400	43,890	279 nm

The λ max wavelengths (nm), molar extinction coefficients ($M^{-1}cm^{-1}$) and molecular weight (Da) for Human SOD and Bovine SOD were obtained from the manufacturer data sheet (Sigma-Aldrich, Dorset, U.K.), for IgG from ThermoScientific technical notes 2013, and for Human and Bovine Serum Albumin from Pace *et al.* (1995).

$$Protein\ concentration\ (c), \mathrm{g/L} = \frac{Absorbance\ at\ \lambda\ max}{Extinction\ coefficient\ (\varepsilon) \times\ pathlength\ (l)} \times molecular\ weight\ (kDa)$$

Figure 2.1: **Beer-Lambert law**

Beer-Lambert law equation for calculation of protein concentration.

2.2.3 Colorimetric quantitation of IgG and SOD protein concentration

The protein concentrations of mouse ascites fluid (Cat no: A2672), protein A-purified mouse monoclonal anti-human serum albumin IgG, superoxide dismutase from bovine erythrocytes (Cat no: S7446-15KU) and superoxide dismutase from human erythrocytes (Cat no: S9636-1KU) were determined using a Colorimetric Pierce™ modified Lowry protein assay (Cat no: 23240, Thermo Fisher Scientific).

Under alkaline conditions (2 % $NaCO_3$ in 0.10 N NaOH), peptides in the protein sample were reacted with divalent cupric sulphate ($CuSO_4$) and tartrate ($C_4H_4O_6^{2-}$), which formed reduced monovalent tetradentate copper-peptide complexes. When the Folin-Ciocalteu reagent was added, copper-peptide complexes were further reduced, producing a water-soluble product molybdenum/tungsten blue, which absorbed at a wavelength of 750 nm.

The micro-titre plate assay procedure was used with the modified Lowry protein assay kit to conserve limited stocks of each protein solution. Bovine albumin (BSA) and gamma globulin (BGG) stock standard ampules (2.0 mg/mL, product no: 23209 and 23212, Thermo Fisher Scientific) were used to create separate standard curves. The stock ampules of BGG and BSA were serially diluted (1 in 2) in x 1 PBS, to produce standard curves of 1500, 750, 375, 125, 62.5, 31.3 and 15.6 µg/mL; x 1 PBS served as a blank internal standard (an example of a comparison between BGG and BSA calibration curves produced in Microsoft Excel can be viewed in Appendix 2.2). Prior to analysis, samples were diluted (1 in 5) in x 1 PBS for quantification within the assay calibration range.

The procedure was as follows. 40 µL of each standard and protein solutions were pipetted into a Perkin Elmer DELFIA® clear strip micro-titre plate (8 x 12 strips, Cat no: 1244-550) in duplicate. Thereafter, 200 µL of modified Lowry reagent were dispensed into each well with a multi-channel pipette and mixed for 30 seconds. The micro-titre plate was covered and incubated at room temperature (RT) for exactly 10 minutes. After incubation, 20 µL of x 1 Folin-Ciocalteu reagent were added to each well using a multi-channel pipette and mixed for 30 seconds. The plate was covered and incubated at RT for 30 minutes. The absorbance was determined spectrophotometrically at a wavelength of 750 nm using a Perkin Elmer 1420 Multilabel Counter Victor 3 plate reader. A blank correction was applied, subtracting the average blank absorbance from the test absorbance. A calibration

curve constructed with MultiCalc® software was used to calculate the concentration of the protein solutions.

This method was used for the determination of protein concentration for the 96-well antibody superoxide dismutase activity experiments (chapter 4, sections 4.3.3 to 4.3.9, and sections 4.4.3 to 4.4.9).

2.2.4 Protein agarose gel electrophoresis and Western blot of mouse ascites and purified IgG

Protein A-purified mouse monoclonal anti-human serum albumin IgG antibody (Cat no: A2672), non-purified ascites fluid, and the ascites fluid flow-through from protein A agarose purification were separated by reducing sodium dodecyl sulphate protein agarose gel electrophoresis (SDS-PAGE). Superoxide dismutase from human erythrocytes and albumin from mouse serum (Cat no: S9636-1KU and A3139-5MG, respectively) were used as controls. A 10-250 kDa Precision Plus protein dual colour standard was used as a protein molecular weight ladder (Cat no: 1610374, Bio-Rad Laboratories, Deeside, U.K.). Each protein was denatured using 2.5 µL of NuPAGE® LDS sample loading buffer (contains lithium dodecyl sulphate, pH 8.4 and tracking dye bromophenol blue) and 1.0 µL of 500 mM dithiothreitol (DTT x 10 concentrate – 50 mM end concentration), and made up to 10 µL with x 1 tris-buffered saline, before being heated for 10 minutes at 70 °C. The proteins and controls were loaded at 1 µg for pure proteins and 20 µg for complex protein mixtures in three sequential replicates and subjected to SDS-PAGE on the Novex NuPAGE midi system (Life technologies Corporation, Maryland, U.S.A.). A 4-12% gradient 26-well gel (13 cm × 8 cm, Cat no: WG1403BOX) was run in morpholinepropanesulfonic acid (MOPS, Cat no: NP0001) – SDS running buffer with NuPAGE™ antioxidant (Cat no: NP0005). The gel was electrophoresed in the XCell4 SureLock™ Midi-Cell at 200 Volts (V) for 55 minutes.

Electrophoretic transfer onto nitrocellulose membrane was performed using a regular size iBlot™ transfer stack and the iBlot transfer device on program 0 (20 V for 1 minute, 23 V for 4 minutes and 25 V for 2 minutes). Following transfer, the electrophoretic separation was visualised using reversible Ponceau S stain (Cat no: P7170, Sigma-Aldrich, Dorset, U.K.). The nitrocellulose membrane was placed in a container with Ponceau S solution on an orbital shaker for 5 minutes at RT and washed with deionised water to remove background staining. An image of the

stained membrane was then captured on the Bio-Rad ChemiDoc system. Once the banding was visualised, the nitrocellulose membrane was divided in to the three replicates. The membrane was de-stained with 0.1 N sodium hydroxide solution (NaOH) and washed with deionised water for 5 minutes.

The three nitrocellulose membrane replicates were blocked for 1 hour in 5 % fat-free milk (Marvel), washed three times with x 1 PBS for 5 minutes and incubated with a specific primary antibody on an orbital shaker overnight at +2 – 8 °C. One segment of the blot was incubated with HRP-linked anti-mouse IgG (Cat no: 7076, Cell signalling technologies), one with goat anti-mouse/human copper, zinc superoxide dismutase (Cat no: AF3418, BioTechne Ltd., Abingdon, U.K.), and the last with goat anti-mouse albumin (Cat no: A90-134A, Bethyl Laboratories, Texas, U.S.A.). The membranes were washed with x 1 PBS for 5 minutes, 3 times. The bound unconjugated goat antibodies were detected using HRP-linked donkey anti-goat IgG (Cat no: HAF109, BioTechne Ltd., Abingdon, U.K.) and incubated for 1 hour at RT. After a final wash step the blots were placed protein-side up on a clear plastic protector and incubated with Luminata Forte chemiluminescent HRP substrate (Cat no: WBLUF0500, Millipore U.K. Ltd, Watford, U.K.) for 5 minutes. Excess substrate was drained, and another sheet protector placed on top. The blots were exposed to initiate the chemiluminescent signal using the ChemiDoc MP System (Bio-Rad) for a total of 1 minute, and images were digitally captured at 0.1, 1.0, 2.0, 10, 30 and 60 second timepoints. The molecular weights of the bands were compared to the signal produced by standard protein ladder.

2.2.5 Immunoassay for quantitation of mouse immunoglobulin subclasses

The Meso Scale Discovery (MSD) mouse isotyping panel 1 kit is a non-competitive multiplex two-site sandwich eletrochemiluminescence (ECL) immunoassay (Meso Scale Diagnostics, Rockville, Maryland, U.S.A.). The assay was used to detect and quantify the different subclasses and subtypes of immunoglobulin present in the monoclonal anti-albumin antibody produced in mouse ascites fluid (Cat no: A2672). The concentration of each isotype in samples and quality controls were compared to a calibration curve of known concentrations of each isotype. Samples were analysed in duplicate.

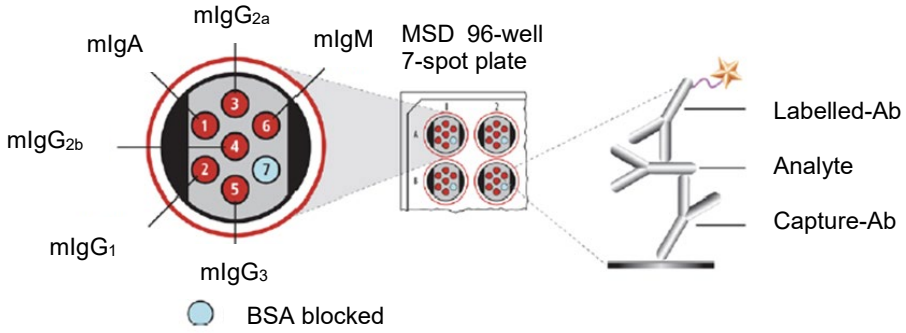

Figure 2.2: **MSD Isotyping assay**

MSD Multiplex Isotyping Panel 1 Immunoassay (Cat no: K15183B). On the left is a well diagram showing the spot placement in an MSD 96-well 7-spot plate. Each 'spot' is coated with a separate antibody (Ab) specific to a target mouse immunoglobulin (1- mIgA, 2- $mIgG_1$, 3- $mIgG_{2a}$, 4- $mIgG_{2b}$, 5- $mIgG_3$ and 6- mIgM) present in the sample, calibrators, or controls; the seventh spot is blocked with bovine serum albumin (BSA) to reduce non-specific binding of immunoglobulins being assayed. On the right is a schematic of the 'sandwich' complex of capture antibody (capture-Ab), analyte (isotype) and ruthenium-labelled detection antibody (labelled-Ab), that demonstrates how an immunoglobulin is detected. (Adapted from Mouse Isotyping Panel 1 Kit insert, Cat no: K15183B).

Primary capture antibody-specific epitopes present on each mouse isotype (IgA, IgG_1, IgG_{2a}, IgG_{2b}, IgG_3 and IgM) were pre-coated to specific spots of the base of the carbon-electrode 96-well plate by the manufacturer. When the samples were added, the capture antibodies formed complexes with the immunoglobulin isotypes present in the sample. A secondary labelled detection antibody, directed against a separate epitope specific to each isotype, was added to form a sandwich. The label is an electrochemiluminescent molecule called tris (2, 2'-bipyridine) ruthenium (II), ($Ru(bpy)_3^{2+}$). When MSD read buffer was added, which contains a co-reactant tripropylamine (TPA) and a voltage was applied to the plate electrodes, a reaction was initiated. Oxidation of TPA at the electrode surface formed a protonated TPA radical – the proton dissociated leaving a TPA radical. The simultaneous electrode oxidation of $Ru(bpy)_3^{2+}$ to $Ru(bpy)_3^{3+}$ enabled it to accept the TPA radical forming a $Ru(bpy)_3^{2+}$ radical and reduce TPA to its ground state. The excited state $Ru(bpy)_3^{2+}$ decayed, emitting a photon of light at 620 nm. The intensity of the emitted light was proportional to concentration (µg/mL) of the immunoglobulin isotype present. The plate was read using the Meso Scale Discovery sector imager S600.

2.3 Measurement of superoxide dismutase activity

The method used for detection of antibodies with superoxide dismutase activity (AbSOD) was modified and optimised from the method previously described for the detection of superoxide dismutase activity by Fried (1975) and for the detection of the apparent superoxide dismutase-like activity of immunoglobulin by Petyaev and Hunt (1996). This method utilises a non-enzymatic superoxide ($O_2^{-\cdot}$) generation step with nitroblue tetrazolium (NBT) detection system, whereby AbSOD or SOD compete with NBT for superoxide.

Firstly, superoxide ($O_2^{-\cdot}$) was generated when oxygen was reduced via the oxidation of reduced β-nicotinamide adenine dinucleotide (β-NADH) in the presence of the electron acceptor phenazine methosulphate (PMS). The resultant superoxide anion radical reduced the NBT detector to form a blue-coloured formazan with absorption maxima at a wavelength of 560 nm. In the presence of AbSOD or SOD, superoxide underwent dismutation inhibiting the reduction of NBT to formazan. The colour formation was inversely proportional to SOD activity; thus, the greater the activity of AbSOD / SOD, the less the colour formation (see Fig 2.3).

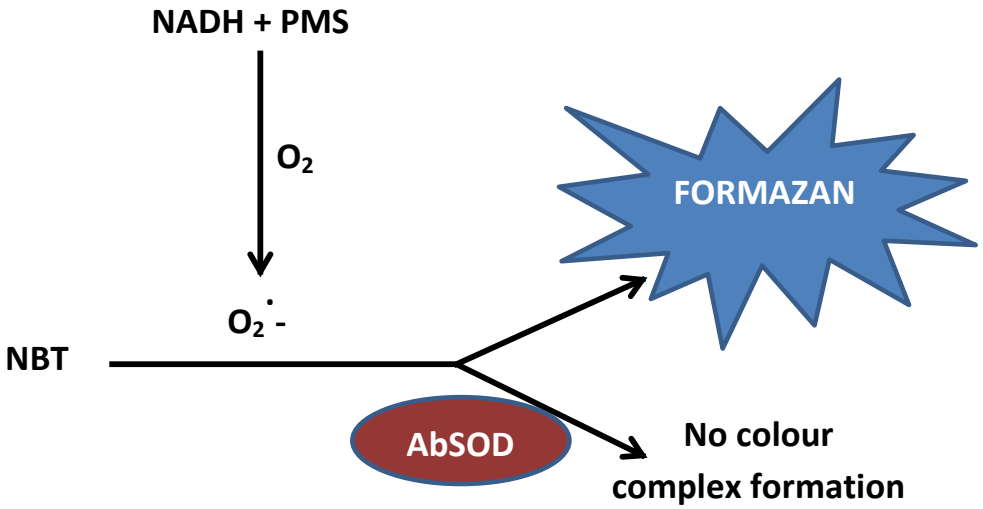

Figure 2.3: **AbSOD / SOD assay mechanism**

AbSOD / SOD assay mechanism. The system consisted of 100 mM K_2HPO_4 (potassium phosphate dibasic), 1.0 mM EDTA (Ethylenediaminetetraacetic acid), 0.66 µM PMS, 100 µM NBT and 5.0 mM NADH.

A 100 mM potassium phosphate dibasic (K_2HPO_4, 8.709 g, Cat no: P3786), 1.0 mM ethylenediaminetetraacetic acid (EDTA, $C_{10}H_{16}N2O_8$, 0.0146g, Cat no: ED) reaction buffer was prepared in a volumetric flask and made up to 500 mL with deionised water. Once dissolved and homogenised, the buffer was decanted into 40 mL vials and adjusted with 5 M hydrochloric acid (HCl) and 5 M potassium hydroxide (KOH) to pH 5.5, 6.5, 7.5 or 8.0 with a pH meter on the day of analysis. A 1.0 mM phenazine methosulphate (PMS, P9625) solution was prepared by adding 31 mg of PMS crystals and making up the solution to 10 mL with pH-adjusted 100 mM K_2HPO_4, 1.0 mM EDTA buffer. The solution was shielded from light and placed on a roller mixer for 15 minutes to dissolve and homogenise. Before use, the PMS 1.0 mM solution was diluted 1 in 30.3 to a concentration of 0.03 mM by adding 33 µL of 1.0 mM PMS to 967 µL of 100 mM K_2HPO_4, 1.0 mM EDTA buffer. A 100 mM reduced β-nicotinamide adenine dinucleotide (NADH, N6005) solution was prepared by combining 61 mg of NADH and 0.85 mL of 100 mM K_2HPO_4, 1.0 mM EDTA buffer (adjusted to correct pH). This was placed on a roller mixer for 15 minutes to dissolve and homogenise. A 0.5 mM nitroblue tetrazolium chloride (NBT, N6876) solution was prepared by adding 41 mg of NBT and making the solution up to 10 mL with 100 mM K_2HPO_4, 1.0 mM EDTA buffer (adjusted to correct pH). This was placed on a roller mixer for 15 minutes to dissolve and homogenise.

2.3.1 Cuvette-based SOD activity assay

A spectrophotometer was used to measure absorbance at a wavelength of 560 nm and prior to each measurement series was calibrated against 1.0 mL of 100 mM K_2HPO_4, 1.0 mM EDTA buffer. All assays were performed in polystyrene, 10 mm path-length spectrophotometer cuvettes (Cat no: C5416, Sigma-Aldrich).

To a 1.5 mL cuvette, 720 µL of 100 mM K_2HPO_4, 1.0 mM EDTA buffer were pipetted, followed by 10 µL of sample (3 µmol/L), 20 µL of 0.03 mM PMS and 200 µL of 0.5 mM NBT, before being stoppered and inverted to allow mixing. The cuvette was placed into the spectrophotometer and the first or ‘0 seconds’ absorbance measurement was recorded. The cuvette was removed from the spectrophotometer and the reaction was initiated by addition of 50 µL of 100 mM NADH to the cuvette, which was then stoppered and inverted. A timer was started, and an absorbance reading recorded every 10 seconds for 180 seconds. The reaction system consisted of 100 mM K_2HPO_4, 1.0 mM EDTA, 0.66 µM PMS, 100 µM NBT and 5.0 mM NADH. Experiments were completed in triplicate. The average change in absorbance was calculated for the ‘blank’ (x 1 PBS) and each sample.

The % inhibition was calculated for each sample, by dividing the average change in absorbance of the sample by the average change in absorbance of the blank, multiplied by 100. 100 was added to generate positive inhibition values.

$$Percentage\ inhibition\ (\%) = \left(\frac{Sample\ (average\ change\ in\ absorbance)}{Blank\ (average\ change\ in\ absorbance)}\ x\ 100\right) + 100$$

Figure 2.4: **AbSOD % inhibition equation**

Inhibition of superoxide formation equation for calculation of percentage inhibition (%).

2.3.2 96-well micro-titre plate SOD activity assay

A Perkin Elmer 1420 Multilabel Counter Victor 3 plate reader was used to measure absorbance at a wavelength of 560 nm. The reagents in section 2.3 were adjusted to pH 5.5, 6.0, 6.5, 7.0 or 7.4 and kept on wet ice until they were combined into two solutions, reagent 1 and 2. To produce reagent 1, 0.55 mL of 0.03 mM PMS and 5.5 mL of 0.5 mM NBT were added to 15.95 mL of 100 mM K_2HPO_4, 1.0 mM EDTA buffer; the reagent was shielded from light until use. To produce reagent 2, 1.5 mL of 100 mM NADH were added to 4.5 mL of 100 mM K_2HPO_4, 1.0 mM EDTA buffer.

Blank (x 1 PBS), controls (Human IgG and Bovine SOD) and samples were pipetted (10 µL) into the wells of a Perkin Elmer DELFIA® clear strip micro-titre plate (8 x 12 strips, Cat no: 1244-550) in duplicate followed by 200 µL of reagent 1 per well with a repeater pipette. Only one 12-well strip was used per run. The plate was mixed for 10 seconds on an orbital plate shaker and a blank reading measured at 560 nm. 50 µL of reagent 2 were added to each well using a repeater pipette and read immediately at 560 nm. The wells were read 25 times at 560 nm with a 1.0 second interval between wells and a 5.0 second delay between reads. The average change in absorbance was calculated for the ‘blank’ (x 1 PBS), controls and each sample. The % inhibition was calculated at 106, 185 and 661 seconds for each sample by dividing the sample change in absorbance by the change in absorbance of the blank, multiplied by 100. 100 was added to produce positive inhibition values.

2.4 Protein A/G agarose purification of polyclonal antibodies from human serum

Polyclonal antibodies were purified from human serum using protein A/G 6 % beaded agarose resin slurry (Cat no: 20423, Thermo Fisher Scientific). The binding buffer, resin slurry and elution buffer were brought to room temperature and mixed on a roller mixer for at least 30 minutes before use. The protein A/G agarose was mixed to homogenise the resin slurry and 140 µL pipetted immediately into a LoBind tube (Cat no: 022431081, Eppendorf Ltd, Stevenage, U.K.). To remove the storage solution and prepare for antibody binding, the agarose was washed 3 times with x 1 PBS, pH 8.0 in a LoBind tube. The PBS-agarose solution was thoroughly mixed for 5 seconds using a vortex mixer, the agarose pelleted by centrifugation at 10,000 g for 2.0 minutes (Eppendorf 5417 centrifuge) and the supernatant discarded using a Pasteur pipette.

Human serum samples (300 µL) were thawed, mixed and centrifuged (3000 g for 5.0 minutes) and 150 µL were pipetted into the tube containing the agarose pellet followed by 1.0 mL of x 1 PBS, pH 8.0. The tubes were vortex-mixed for 5.0 seconds to free the pellet and incubated on an end-over-end rotating mixer for 1 hour 40 minutes at room temperature. After incubation, the sample-agarose solution was centrifuged at 10,000 g for 2.0 minutes to pellet the antibody-bound agarose and the unbound fraction pipetted in to a 2.0 mL Sarstedt tube for storage at -80°C. The agarose pellet was then washed three times with 1.0 mL of x 1 PBS, pH 8.0, mixed by vortexing, centrifuged at 10,000 g for 2.0 minutes and supernatant was discarded. After washing the antibody, 300 µL of elution buffer (IgG Elution Buffer; Product No. 21004, Thermofisher scientific) were added to the agarose, incubated for 5.0 minutes on an end-over-end mixer and centrifuged at 10,000 g for 2.0 minutes. The supernatant was pipetted into a LoBind tube. This was completed a total of three times with the supernatant being pooled and neutralised with 90 µL of x 5 PBS, pH 10.0. The purified sample was stored at -80 °C and the total IgG concentration determined using Siemen's dimension EXL IgG method.

2.5 Turbidimetric quantitation of IgG, IgM and IgA concentration

The Siemens dimension EXL 200 immunoglobulin G, A and M assays (Siemens Healthcare Diagnostics, Camberley, Surrey, UK) are three separate quantitative, turbidimetric assays (Cat no: DF76, DF74, DF81). Each assay is based on the reaction of IgG, IgA or IgM from human serum with a specific rabbit anti-human polyclonal antibody to each subclass, forming complexes. The reaction is accelerated by the

addition of polyethylene glycol, furthering precipitation and formation of immune complexes between the IgG, IgA or IgM, and rabbit anti-serum. The resulting turbidity (scattering of light) is measured by bichromatic end-point measurements at 340 and 700 nm. The increase in turbidity is proportional to the concentration of IgG, IgA or IgM in the sample compared to calibrators of known immunoglobulin concentrations (reported in g/L). All three kits are CE-marked and use Bio-Rad liquicheck immunology level 1 and 3 quality controls.

2.6 Dye-binding protein concentration by pyrogallol red method

The Siemens Advia 2400 urine CSF protein assay (Siemens Healthcare Diagnostics, Camberley, Surrey, U.K.) is an adaptation of the pyrogallol red-molybdate method by Fujita, Mori and Kitano (1983). The method is based upon measuring the shift in absorption that occurs when the complex formed from pyrogallol red combining with sodium molybdate (pyrogallol red-molybdate complex) binds to basic amino acid groups of protein molecules. The pyrogallol red-molybdate complex has a maximum absorbance at 470 nm, but the protein in the sample reacting with this complex in acid solution forms a blue/purple coloured complex, which absorbs at 596/694 nm. The absorbance at 596/694 nm is directly proportional to the concentration of protein in the sample and is compared to an albumin calibration curve of known albumin concentrations. Samples were analysed on an automated system in singleton.

2.7 Detection of superoxide dismutase activity of human antibodies

Protein A/G agarose-purified polyclonal antibodies from human serum were assayed using the 96-well plate format AbSOD assay in section 2.3.2. The assay was run at pH 5.5, 6.0, 6.5, 7.0 and 7.4 for each sample. All antibody sample IgG concentrations were determined using the Siemens Dimension EXL IgG assay prior to analysis. Based on the IgG concentration, the antibody samples were diluted in Eppendorf LoBind tubes in x 1 PBS to an IgG concentration of 0.5 mg/mL (in-assay concentration 0.013 µmol/L). For each assay, x 1 PBS served as a blank, reagent-grade IgG from human serum as a control, and reagent-grade superoxide dismutase from bovine erythrocytes as a control. These were analysed alongside three antibody samples in duplicate, totalling six determinations per run.

Results were represented as calculated absorbance factor (patient absorbance / blank absorbance – see table 5.1) over 11 minutes.

2.7.1 Immunoglobulin G (IgG) control

An IgG control sample was prepared using reagent-grade IgG from human serum (Cat no: I4506, Sigma Aldrich, Dorset, U.K.). A vial of 10 mg IgG was reconstituted with 1.0 mL of x 1 PBS, pH 7.4, to produce a solution of approximately 10 mg/mL. This was then analysed on the siemens dimension EXL IgG assay to ascertain concentration. The solution was then diluted to a concentration of approximately 1.0 mg/mL using x 1 PBS in a LoBind tube and re-assayed in triplicate on the Siemens dimension EXL IgG assay. The IgG control was stored at -25 °C in 100 µL aliquots until analysis in the AbSOD assay, when it was diluted to 0.5 mg/mL in x 1 PBS in a LoBind tube (in-assay concentration 0.013 µmol/L).

2.7.2 Copper-zinc superoxide dismutase (SOD) control

A superoxide dismutase control sample was prepared using reagent-grade superoxide dismutase from bovine erythrocytes (Cat no: S7446-15KU, Sigma Aldrich, Dorset, U.K.). A vial was reconstituted with 1.0 mL of x 1 PBS to produce a solution of approximately 3.0 mg/mL. This was analysed on the Siemens Advia 2400 urine protein assay to ascertain concentration. The solution was then diluted to a concentration of approximately 1.0 mg/mL in x 1 PBS in a LoBind tube and stored at -25 °C in 100 µL aliquots. Prior to analysis in the AbSOD assay, the SOD control was diluted to 0.108 mg/mL in x 1 PBS in a LoBind tube for equimolar comparison of SOD and IgG (in-assay concentration 0.013 µmol/L).

2.8 Immunoassay for quantitation of serum catalase concentration

Serum catalase concentrations were analysed using an in-house two-step non-competitive two-site sandwich electrochemiluminescence immunoassay, using the Meso Scale Discovery (MSD) platform (Meso Scale Diagnostics, Rockville, Maryland, U.S.A.) and developed using antibodies from R & D Systems Ltd. (BioTechne Ltd., Abingdon, U.K.).

On day one, a vial of mouse monoclonal IgG_1 anti-human catalase (supplied as 100 µg of lyophilised antibody, Cat no: MAB3398) was reconstituted with 1.0 mL of x 1 PBS to produce a stock capture of 100 µg/mL stored in 80 µL vials at -80 °C. The stock capture was further diluted (1 in 50) in x 1 PBS to produce a working solution of 2.0 µg/mL. The capture antibody was pipetted, 30 µL/well, to a Sector ® imager standard

MULTI-ARRAY® 96-well plate (Cat no: L15XA-3) and incubated overnight at +2 – 8 °C.

On day two, the plate was washed three times with 300 µL MSD wash buffer (x 1 PBS, 0.05% Tween 20) per well using an automated plate washer (Wellwash™ Versa, Thermoscientific). The MSD blocker A was pipetted, 150 µL/well, and incubated on an orbital plate shaker at 600 rpm for 1 hour. A calibration curve was generated by dilution of recombinant human catalase protein (supplied as 20 µL of 0.2 µm filtered solution in PBS, pH 7.4, at a concentration of 0.57 mg/mL, Cat no: ab172164, AbCam, Cambridge, U.K.) from *E. coli*. The recombinant protein was diluted (1 in 114) in DELFIA diluent II (Cat no: B132-200, Perkin Elmer, Turku, Finland) to produce a stock solution of 5000 ng/mL which was stored at -80 °C in 100 µL aliquots. An 8-point standard curve was diluted in DELFIA diluent II from a stock solution of 5000 ng/mL to produce calibrators of 500, 250, 125, 62.5, 31.3, 15.6 and 7.8 ng/mL; DELFIA diluent II served as a zero standard. The samples and quality controls (in-house pooled human serum of low and high serum catalase concentrations) were thawed, thoroughly mixed, centrifuged at 3000 g for 5.0 minutes, and diluted (1 in 5) in DELFIA diluent II.

Once blocked, the plate was washed 3 times with 300 µL of MSD wash. 30 µL of DELFIA diluent II were dispensed into each well followed by 10 µL of calibrators, diluted serum samples and diluted quality controls analysed in duplicate. The plate was sealed and incubated on a plate shaker set to 600 rpm at room temperature for 2 hours. To detect the human catalase, goat polyclonal IgG anti-human catalase (supplied as 11.1 µL of solution at a concentration of 2.27 mg/mL, Cat no: AF3398) was used. The supplied stock was diluted (1 in 22.7) in x 1 PBS to produce a solution of 100 µg/mL stored at +2 – 8 °C in an Eppendorf LoBind tube. This was further diluted (1 in 250) in MSD diluent 100 (Cat no: R50AA-2, Meso Scale Diagnostics, Rockville, Maryland, U.S.A.) to produce a working solution of 400 ng/mL. The plate was washed three times with 300 µL of MSD wash, and 25 µL of the detection antibody pipetted per well. The plate was sealed and incubated on a plate shaker set to 600 rpm at room temperature for 1 hour. MSD sulpho-tag-labelled donkey anti-goat antibody (Cat no: R32AG-5, Meso Scale Diagnostics, Rockville, Maryland, U.S.A.) was used to detect the goat anti-human catalase antibody. The anti-goat sulpho-tag was diluted (1 in 1000) in MSD diluent 100, and 25 µL pipetted per well before being sealed and incubated on a plate shaker set to 600 rpm for 30 minutes. Finally, the plate was washed 3 times with 300 µL of MSD wash buffer per well and 150 µL of x 1 read buffer T were dispensed per well (Cat no: R92TC-2, Meso Scale Diagnostics, Rockville, Maryland, U.S.A.). The plate was read immediately on MSD sector S600. All results were multiplied by 5 to correct for the dilution factor.

2.9 Immunoassay for quantitation of serum CuZnSOD concentration

Serum concentrations of copper-zinc superoxide dismutase (CuZnSOD) were analysed using a one-step non-competitive two-site enzyme-linked immunosorbent assay (ELISA) using a matched antibody and calibrator protein kit (Cat no: BMS222MST, Bender MedSystems, Vienna, Austria).

On day one, a monoclonal anti-human CuZnSOD capture antibody was diluted to a concentration of 9.1 µg/mL in x 1 PBS, pH 7.4. A Perkin Elmer DELFIA® Clear StripPlate (Cat no: 1244-550, Turku, Finland) was coated with 100 µL/well of the diluted monoclonal anti-human CuZnSOD capture antibody (909 ng/well) and incubated overnight at 2 – 8 °C.

On day two, the plate was washed once with 300 µL/well of x 1 PBS, 0.05% Tween 20 (PBST) using an automatic plate washer and blotted on paper towels, before blocking with 250 µL/well of assay buffer (0.5% BSA, 0.05% Tween 20 in x 1 PBS) for 2 hours at RT. A 6-point calibration curve was produced from the kit stock – diluted in x 1 PBS, to produce calibrators of 5.0, 2.5, 1.25, 0.625, 0.313 and 0 ng/mL. Serum samples and quality controls (pool human serum control pre-diluted 1 in 5, 10 and 20) were thawed, mixed and centrifuged at 3000 g for 5 mins then diluted (1 in 10) in x 1 PBS prior to analysis. To remove the assay buffer, the plate wells were washed twice with 300 µL of PBST.

The calibrators were pipetted in duplicate, 100 µL/well, followed by 90 µL of x 1 PBS to the remaining wells and 10 µL of the diluted quality control and serum samples in duplicate. Before being sealed and incubated for 1 hour, 50 µL of CuZnSOD-HRP (horse radish peroxidase) conjugate (diluted 1 in 1000) was pipetted in to each well. The plate was then washed twice with 300 µL/well of PBST using an automatic plate washer and blotted on paper towels. The microplate wells were then incubated with 100 µL/well of 3,3',5,5'-tetramethylbenzidine (TMB, Cat no: T4444, Sigma-Aldrich, Dorset, U.K) for 30 minutes at 37 °C. After 30 minutes the reaction was stopped with 100 µL/well of 0.5 M sulphuric acid (H_2SO_4). The plate was then mixed for 10 seconds, and the colour development read at 450 nm with a 650 nm blank deduction on the Perkin Elmer 1420 Multilabel Counter Victor 3 plate reader. The results were multiplied by 100 to correct for the combined pre-dilution and in-plate dilution.

2.10 Colorimetric enzymatic activity assay of catalase activity

Serum catalase activity levels were analysed using a commercially available assay from Invitrogen™ (Cat no: EIACATC, Life technologies Corporation, Maryland, U.S.A.). Serum samples and quality controls (pooled human serum) were thawed, mixed and centrifuged at 3000 g for 5.0 minutes, then diluted (1 in 30) in x 1 assay buffer for analysis (quality controls were diluted 1 in 30, and 1 in 60).

Catalase in calibrators, quality controls or samples catalysed the decomposition of hydrogen peroxide (H_2O_2) to water and oxygen. The remaining unconverted hydrogen peroxide was then reacted with HRP in the presence of a chromogenic substrate to yield a pink/red coloured product detectable at 560 nm using the Perkin Elmer 1420 Multilabel Counter Victor 3 plate reader. The serum catalase activity was inversely proportional to the colour intensity and the results were expressed as enzyme units per mL (U/mL).

2.11 Colorimetric enzymatic activity assay of superoxide dismutase activity

Serum superoxide dismutase (SOD) activity levels were analysed using a commercially available assay from Invitrogen™ (Cat no: EIASOD, Life technologies Corporation, Maryland, U.S.A.). Serum samples and quality controls (pooled human serum) were thawed, mixed and centrifuged at 3000 g for 5.0 minutes, then diluted (1 in 5) in coloured assay buffer for analysis (quality controls were diluted 1 in 5 and 1 in 10).

Superoxide anions were produced by the reaction of xanthine oxidase in the presence of xanthine and oxygen. SOD in calibrators, quality controls or samples catalysed the dismutation of superoxide ($O_2^{-\cdot}$) to hydrogen peroxide and oxygen. The remaining excess unconverted superoxide anions then reduced the WST-1 (water-soluble tetrazolium-1) to produce a yellow-coloured product, WST-1 formazan, detectable at 450 nm using the Perkin Elmer 1420 Multilabel Counter Victor 3 plate reader. The serum SOD activity was inversely proportional to the colour intensity and the results were expressed as enzyme units per mL (U/mL).

2.12 Quantitation of serum hydroperoxides by ferrous oxidation – Xylenol orange assay

Serum hydroperoxides were measured by an adaptation of the peroxide measuring technique of Jiang, Woollard and Wolff (1990). The original method used 25 mM H_2SO_4, 100 µM xylenol orange, 100 mM sorbitol and 250 µM ammonium ferrous sulphate at pH 1.5. Increasing the concentration of the reagents to 50 mM H_2SO_4, 250 µM xylenol orange, 200 mM sorbitol and 500 µM ammonium ferrous sulphate at pH 1.5 and filtering the xylenol orange with 0.2 µM regenerated cellulose membrane syringe filter significantly improved the sensitivity and precision of the assay.

The ferrous oxidation xylenol orange assay detects serum hydroperoxides and various oxidant species (Erel, 2005); for this reason, it is sometimes used as a measure of total oxidant status in humans. The oxidant species in serum either oxidise the ferrous ions (Fe^{2+}) to ferric ions (Fe^{3+}) directly in the presence of sulphuric acid, or with the addition of sorbitol react to form a peroxyl radicals, which additionally oxidise Fe^{2+} ions to Fe^{3+} ions. The Fe^{3+} ions generated complex with xylenol orange (XO), to yield a purple adduct which absorbs at a wavelength of 560 nm.

Serum samples and quality controls (pooled human serum with low and high concentrations of hydroperoxides) were thawed, mixed and centrifuged at 3000 g for 5.0 minutes. Calibrators, controls and samples were pipetted (25 µL) into a 96-well micro-titre plate in duplicate. They were followed by 100 µL of 50 mM H_2SO_4, 25 µL of 2.5 mM xylenol orange and 50 µL of 1000 mM sorbitol. Finally, 50 µL of 2.5 mM ammonium ferrous sulphate were added to each well, and the plate incubated on a plate shaker for 30 minutes for colour development. The test absorbance was measured at 560 nm using the Perkin Elmer 1420 Multilabel Counter Victor 3 plate reader. The colour intensity was proportional to the concentration of oxidant species and hydroperoxides in the serum samples and quality controls. The assay was calibrated with hydrogen peroxide and the results expressed as micromoles of hydrogen peroxide equivalent per litre (µmol H_2O_2 equiv./L).

2.13 Experimental design and patient data analysis

2.13.1 Patients studied

Patients with diseases / conditions potentially associated with altered immune function and oxidative imbalance were identified through the pathology laboratory information system according to a list of biochemical inclusion criteria (see Appendix 2.3). Patients were excluded from the study at time of specimen retrieval where they – 1) were deceased, or – 2) were below the age of 18 years.

All patients had been referred for laboratory investigation to Clinical Biochemistry, Addenbrooke's Hospital, Cambridge University Hospitals NHS Foundation Trust, Cambridge. In total, analysis was undertaken on 115 subjects, made up of 94 patient samples and 21 'healthy' control samples. The patients studied included those with cancer (myeloma, breast, ovarian, colorectal and brain), cardiovascular disease (acute myocardial infarction (NSTEMI - non-ST segment elevation myocardial infarction) and ischemic heart disease), diabetes (type I and II), coeliac disease, rheumatoid arthritis, monoclonal gammopathy of unknown significance (MGUS) and Waldenström macroglobulinaemia. The 'healthy' control specimens were obtained by the Core Biochemical Assay Laboratory from Tissue Solution Ltd in Glasgow, a company that specializes in sourcing human tissue for research needs. The volunteers all gave informed consent for the use of their tissue in research.

Ninety-four patients and twenty-one 'healthy' controls were analysed in laboratory investigations; however, thirty-five patients and two 'healthy' controls were removed from the data analysis due to missing data points, analytical interference, and group sizes less than 6, details of which can be referred to in Appendix 2.4.

Data from fifty-nine patients – with rheumatoid arthritis, coeliac disease, myocardial infarction, breast cancer, monoclonal gammopathy of unknown significance and multiple myeloma – and nineteen 'healthy' controls were studied. The gender frequency and age range across disease and control groups can be seen in Appendix 2.5.

2.13.2 Ethical approval

Ethics approval was obtained from the Faculty Research Ethics Panel, Faculty of Science and Engineering (Ref: FST/FREP/17/705; see Appendix 2.6) and from the Research and Development Department, Addenbrooke's Hospital, Cambridge University Hospitals NHS Foundation Trust (Ref: A094438; see Appendix 2.7). All laboratory analysis was conducted at the Core Biochemical Assay Laboratory (CBAL), IMS annexe, Level 4, Laboratory Block, Addenbrooke's Hospital, CB2 0QQ. Laboratory studies and sample management were undertaken in accordance with the World Medical Association Declaration of Helsinki (2000). Patients gave blood samples voluntarily for clinical investigations via venepuncture, a well-tolerated blood sampling technique. The patient serum was surplus to clinical requirement and consent was not required as samples were anonymised and made nonidentifiable (given a unique study number) by a 'gatekeeper'.

2.13.3 Samples

Serum samples were used for human based analysis in this study. Serum was collected in serum gel separator tubes or plain collection tubes without additives, allowed to clot for at least 30 minutes then centrifuged within approximately 2 hours. The specimens then were either stored at 2-8 °C or ≤ -20 °C until they were analysed for clinical investigations. Once all clinical analysis was completed, the serum samples were re-stored at their previous pre-analysis storage temperature before being identified and collected by the project gatekeeper (a member of the clinical biochemistry team). They were then anonymised with a unique project code before being passed on and aliquoted. Up to four 300 µL aliquots were created and stored at -80 °C until research analysis was completed.

2.13.4 SPSS statistics

Data analysis of the patient-based experiments were completed using IBM SPSS Statistics 26. Patient groups and 'healthy' controls were compared across each continuous variable (AbSOD activity, serum catalase (activity and concentration), serum SOD (activity and concentration) and serum hydroperoxides). Where the assumption of homogeneity of variance was met ($p > 0.05$), one-way analysis of variance (ANOVA) was applied, and where assumption of homogeneity of variance was violated ($p < 0.05$), Welch's ANOVA was used to

investigate whether there were any statistically significant differences between patient group means ($p < 0.05$). Where statistically significant differences were discovered, either Tukey-Kramer (assumption of homogeneity of variance was met) or Games-Howell (assumption of homogeneity of variance was violated) post hoc tests were applied to determine whether there were any differences between patient groups and the 'healthy' control group. To determine the extent of the statistical difference, effect sizes were calculated using Hedge's *g* (where $g = 0.2$, small effect; 0.5, medium effect; 0.8, large effect; Cohen, 1988b).

Descriptive statistics (number of patients (N), mean, standard deviation (SD), skewness and kurtosis) are presented as tables (Tables 5.2, 5.4, 5.6, 5.7, 5.8, 5.9, 5.11, 5.12, 5.14, 5.16, 5.18, 5.20, 5.22, 5.24, 5.25, 6.1, 6.2, 6.4, 6.6, 6.8, 6.9 and 6.11). Post hoc tests (Tukey-Kramer or Games-Howell significance *p* values and Hedge's *g* effect size) are presented as tables (Tables 5.3, 5.5, 5.10, 5.13, 5.15, 5.17, 5.19, 5.21, 5.23, 5.26, 6.3, 6.5, 6.7, 6.10 and 6.12) and bar charts of group means and 95% confidence intervals (CI) in figures (Figures 5.1 to 5.15 and 6.1 to 6.6).

2.13.5 Adequate sample size

The nature of human research means sample size is dictated by timescales, funding, and availability of samples. Patient samples no longer required for clinical investigation were obtained and anonymised via a gatekeeper from the Department of Clinical Biochemistry and Immunology (Addenbrooke's Hospital). This was an elegant solution to obtain patient serum that would otherwise have been discarded, however samples took longer than expected to obtain and samples from patients with more rare conditions were, by nature, difficult to obtain. Consequently, the sample sizes for some groups were less than those that would generate a degree of statistical power (Power = 1-β, statistical standard is ≥ 0.8, i.e., 80% or greater probability a study will generate a statistically significant result) and could increase the probability of a type II error (β) (false negative – accept the null hypothesis when it is false) (Cohen, 1988a).

A study by Games and Howell (1976) investigated the effect of unequal variances and sample sizes. They recommended the use of the Games-Howell method if sample sizes are equal to or greater than 6 to maintain α close to 0.05, i.e., a 5% chance that a significant result is a result of a type I error (false positive) (Cohen, 1988a).

2.13.6 Removal of outliers and data points

Outliers and data points were only removed from data analysis based on sample integrity, measurement error (missing data points) and where the number of cases per patient group was less than 6 (Games and Howell, 1976). Genuine outliers (natural biological variation in population) were retained. Removal of outliers based on sample integrity removed any sample with visual haemolysis and lipaemia. Haemolysis is known to artificially increase the measured catalase and superoxide dismutase (concentration and activity), and lipaemia is known to artificially increase measured hydroperoxides. Where data points were removed or were missing, all data points from all analyses were omitted for that patient from the final analysis. All groups where cases were less than 6 were removed from final analysis, details of which can be seen in Appendix 2.4.

2.13.7 Assessing distribution and normality

Distribution of generated data and normality testing were assessed using a combination of histograms, boxplots, Shapiro-Wilk normality tests ($p > 0.05$), Q-Q plots and skewness and kurtosis analyses. Where distribution was associated with a skewness of $< \pm 2.0$ and was within two times the standard error of skewness, and where kurtosis was $< \pm 9.0$ and was within two times the standard error of kurtosis, the assumption of normality was determined to be satisfied (Schmider *et al.*, 2010). However, ANOVA and Welch ANOVA are particularly robust to deviations from normality with respect to type I errors (Wilcox, 2012). This means where the normality assumptions were violated, the probability of making a type 1 error (rejecting the null hypothesis when it is true) was still maintained at 5%.

2.13.8 Assessing homogeneity of variance

Levene's test for equality of variances tests the null hypothesis that population variances are equal. Therefore, Levene's test was used to determine whether the data from each measured variable had equal variances across all groups and had homoscedasticity. If the *p* value was greater than the alpha value ($p > 0.05$) the variances were equal and the assumption of homogeneity of variances was satisfied. If the *p* value was less than the alpha value ($p < 0.05$) the variances were unequal and the assumption of homogeneity of variances was violated.

2.13.9 One-way / Welch's ANOVA

One-way analysis of variance (ANOVA) and Welch's ANOVA were used to determine whether there were any statistically significant differences in the means of the measured variables (AbSOD activity, Catalase (activity and concentration), SOD (activity and concentration) and hydroperoxide concentration) between the investigated 'healthy' control and patient groups. One-way ANOVA assumes data generated from different groups has similar or equal variances (homogeneity of variance). Welch's ANOVA does not assume homogeneity of variance. Where the results from one-way ANOVA or Welch ANOVA were significantly different ($p < 0.05$), Tukey-Kramer (homogeneity of variance satisfied) or Games-Howell (homogeneity of variance violated) post hoc tests were used to determine which patient groups were different from the 'healthy' controls.

2.13.10 Tukey-Kramer post hoc analysis

If ANOVA determined a significant difference was present, the Tukey-Kramer test (1956) was used to determine where the statistical difference was – e.g., between 'healthy' controls and myeloma groups. The Tukey-Kramer test is a modification of the Tukey test, but for unequal sample sizes. To control type 1 error, this method was only used where the homogeneity of variance was equal. This method is robust against deviations from normality with regards to type 1 error (Dunnet, 1980; Stoline, 1981).

2.13.11 Games-Howell post hoc analysis

If Welch's ANOVA determined a significant difference was present, the Games-Howell test (1976) was used to determine where the statistical difference was – e.g., between 'healthy' controls and breast cancer groups. The Games-Howell test is Welch's extension of the Tukey-Kramer test, but for when the assumption of homogeneity of variance is violated. This method is robust against deviations from normality with regards to type I error (Toothaker, 1993; Day and Quinn, 1989).

2.13.12 Effect size

Effect sizes are used to represent the magnitude of significance in a standardised way, regardless of the scale used to measure a variable. This is useful for meta-analyses to investigate a group of independent studies, or when planning a study to determine the sample size required to achieve a set power level (1-β ≥0.8) whilst maintaining a set alpha level (α = 0.05). Cohen's *d* is the difference between observations of two groups, divided by the standard deviation of observations. Where sample group sizes are small (n = <20) Hedges' *g* is a preferred measure of effect size as it corrects for the biased estimate of population effect sizes calculated by Cohen's *d* (Hedges, 1985). Hedges' *g* uses pooled weighted standard deviations (instead of pooled standard deviations). Hedges' *g* was calculated alongside either the Tukey-Kramer or Games-Howell post hoc tests. Where the calculated Hedges' *g* was approximately 0.20, 0.50 and 0.80, a small, medium or large effect size was observed, respectively (Cohen, 1988b).

2.13.13 Multivariate analysis

2.13.13.1 Principal component analysis (PCA)

Principal component analysis was used to explore relationships between antibody superoxide dismutase activity (AbSOD activity), catalase (CAT; concentration and activity) and superoxide dismutase (SOD; concentration and activity) between 'healthy' controls and different disease groups. The patient data set generated from laboratory experiments consisted of 22 interrelated variables. Principal component analysis (PCA) was used to reduce the dimensionality of the data set while retaining as much of the variation as possible. This was achieved by transforming the data into a new set of uncorrelated variables, known as principal components (PCs).

Data were input into the MultiVariate Statistical Package (MVSP version 3.1, Kovach Computing Services, Pentraeth, Wales, U.K.). The data were centred, and natural log data transformation was applied to each variable. A cut-off value was not applied for retainment or omission of variables. Instead, a pragmatic approach was taken where variable loadings <0.1 and >0.9 (slightly and highly correlated with a PC, respectively) were further assessed to determine whether there was a sufficient relationship to include the variable, or an overwhelming relationship that decreased overall resolution. It was evident that some of the original variables that were highly correlated with each of the principal components caused a swamping

effect. This resulted in principal components that were only representative of the variance seen in just one of the original variables. Once those variables were removed from the PCA, a greater degree of variance was observed in each of the calculated principal components.

A PC was retained by applying Jolliffe's (1972) extension of Kaiser's rule, where PCs with eigenvalues below 0.7 times the average eigenvalue of all PCs were not retained for graphical visualisation. PC score plots and biplots (PC scores and variable loadings) were drawn for each comparison between PCs.

2.13.13.2 Network Cluster analysis

Network cluster analysis was used to identify and graphically represent groups of patients based on their antioxidant (CAT and SOD) and immune system (AbSOD activity) characteristics. By comparison of relationships between patients with oxidative stress-linked diseases, diseases of immune dysfunction and 'healthy' controls, similarities and differences between the different patient and control groups were discovered.

The MultiVariate Statistical Package (MVSP version 3.1, Kovach Computing Services, Pentraeth, Wales, U.K.) was used to perform cluster analysis and produce a distance matrix. Dimension reduction of 22 variables by principal component analysis resulted in retainment of 3 variables (catalase activity (U/ml), CuZnSOD (ng/ml) and AbSOD activity at pH 7.4, 661 seconds (Abs Factor)). The data were natural log (Log e)-transformed prior to UPGMA (unweighted pair group method with arithmetic mean) hierarchical clustering (Sokal and Michener, 1958) of euclidean distances.

Microsoft (MS) Excel was used to compute binary data matrices, ranking the nearest one, two, three, four or five 'neighbour patients' to every patient. Each data matrix and a list of commands were exported to MS Word for conversion to a network analysis command file (.txt / ascii / Unicode utf 8 file) suitable for the Pajek version 5.11 (De Nooy, Mrvar and Batagelj, 2018) network analysis software. The created network file was uploaded to Pajek where the Kamada-Kawai (1989) graph (network) algorithm (optimum display of patients ('nodes')) was applied. All networks were saved as '.jpeg' files for document import.

CHAPTER 3: Purification and characterisation of immunoglobulins from mouse ascites fluid

3.1 Background

In 1996, Petyaev and Hunt reported that commercially available mouse monoclonal anti-human albumin IgG antibodies (clone HSA-9) had superoxide dismutase activity which appeared comparable to that of CuZnSOD at pH 7.8. Furthermore, antibodies extracted from human atherosclerotic lesions were later reported to have SOD-like activity at pH 7.81 and 6.45 (Petyaev *et al.*, 1998). Although contamination of the antibody preparation by transition metals was eliminated (treatment with chelex resin), and the potential of enzymic metal ion catalytic centres proposed (treatment with Diethyldithiocarbamate – DDC), the involvement of associated CuZnSOD, presence of IgG and characterisation of immunoglobulin subclasses were neither excluded, verified, or determined, respectively. In these early investigations examining the SOD activity of intact immunoglobulin G (IgG), only limited attempts were made to confirm its identity and purity. To substantiate any claims IgG has true enzymatic SOD activity, purification and subsequent characterisation needed to be completed.

In this chapter, the antibody with superoxide dismutase activity (IgG_1 clone HSA-9, from ascites fluid; Cat no: A2672) used by Petyaev and Hunt (1996) was purified and analysed to determine the specific antibody isotypes present. Simultaneously, the possibility any of the other components of the ascites were responsible for the observed SOD activity was investigated. It was hypothesised the antibody ascites fluid would contain other host proteins, including additional antibody isotypes and CuZnSOD, which could account for the previously observed superoxide dismutase activity.

The overarching rationale of performing these experiments was to confirm whether antibodies were present in the ascites preparation and determine their isotype, investigate whether CuZnSOD was present and contributing to the observed SOD activity, and finally to confirm whether protein agarose sufficiently purified the antibody preparation to yield it suitable for further investigation in AbSOD activity and AbSOD activity pH dependency experiments (see sections 4.3.2, 4.4.9, 4.4.3 and 4.4.9).

3.2 Materials and methods

3.2.1 Protein A agarose – processing of mouse ascites fluid

Mouse monoclonal anti-human serum albumin IgG antibody (clone HSA-9) was purified from ascites fluid using the Pierce™ protein A IgG purification kit (see section 2.2.1). To determine which eluate fractions contained the antibody the absorbance of each eluate aliquot was measured at 280 nm. The concentration of protein present in the purified antibody solution was calculated using the molar extinction coefficient (ε) of 210,000 $M^{-1}cm^{-1}$ of an IgG with a molecular weight of 150 kDa. The first flow through after IgG capture by protein A agarose was collected and analysed by PAGE and Western blot.

3.2.2 Protein quantitation

The concentration of protein A agarose-purified IgG, non-purified IgG from ascites and Human CuZnSOD was determined spectrophotometrically (see section 2.2.2), before electrophoresis and Western blot analysis.

3.2.3 Electrophoresis and Western blot

3.2.3.1 SDS-PAGE

SDS-PAGE was performed under reducing conditions using an Invitrogen 4-12% gradient 26-well gel (13 cm × 8 cm, Cat no: WG1403BOX; see section 2.2.4). Each protein was prepared using 2.5 µL of NuPAGE® LDS sample loading buffer, 1 µL of 500 mM dithiothreitol (DTT x 10 concentrate – 50 mM end concentration) to ensure reduction of cysteine bonds for clearer visualisation of the protein bands. Standards, controls and samples were made up to 10 µL with x 1 Tris-buffered saline before being heated for 10 minutes at 70 °C. The proteins were loaded run at 1 µg/lane for pure proteins (mouse IgG and controls for human CuZnSOD and mouse albumin) and 20 µg/lane for complex protein mixtures (mouse ascites and purification flow through). An antioxidant (NuPAGE™ antioxidant – Cat no: NP0005) was added to NuPAGE™ MOPS SDS Running Buffer to maintain reduced proteins and prevent re-oxidation during electrophoresis. Sets of samples were run in triplicate in order to later be split in to

three blots for parallel Western blot analysis using anti-IgG, anti-CuZnSOD and anti-albumin antibodies, respectively.

3.2.3.2 Electroblotting and Ponceau S staining

An Invitrogen iBlot gel transfer device was used to transfer (blot) the separated proteins from the acrylamide gel to iBlot nitrocellulose membrane transfer stacks. The bands were then visualised using Ponceau S stain (see section 2.4.4).

3.2.3.3 Anti-IgG, anti-CuZnSOD and anti-mouse albumin Western blots

The triplicate samples applied to nitrocellulose membranes were separated into three blots, then blocked in 5% milk in Tris-buffered saline for an hour before being incubated overnight with HRP-conjugated anti-mouse IgG, goat anti-mouse/human CuZnSOD and goat anti-mouse albumin. After washing away the excess goat anti-mouse/human CuZnSOD antibodies and goat anti-mouse albumin the following day, the two blots with unconjugated antibodies were incubated for an hour with HRP-conjugated anti-goat IgG secondary antibody. All three blots were colour developed using Luminata Forte Western HRP substrate and read using chemiluminescence on the Bio-Rad ChemiDoc system. Using different exposure times, it was possible to elucidate where the antibodies bound to the protein bands (see section 2.4.4).

3.2.4 Mouse Isotyping panel 1 – Immunoglobulin ratio

The monoclonal IgG_1 antibody (clone HSA-9) investigated is produced in mouse ascites fluid from hybridoma cells. To produce monoclonal antibodies, hybridoma cells are injected into the abdomen of animals, causing the production of ascites in the peritoneal cavity (Köhler and Milstein, 1975). This is extracted but can contain many potentially interfering host proteins (host antibodies, superoxide dismutase, albumin etc.).

The Meso Scale Discovery (MSD) mouse isotyping panel 1 kit was used to determine the antibody subclasses present in ascites and so infer the likely subclass candidate for AbSOD activity. The assay was a multiplex (6-plex – six assays in one well) non-competitive sandwich immunoassay utilising the MSD ECL technology (see section 2.2.5).

3.3 Results

3.3.1 Electrophoresis and Western blot

Protein gel agarose electrophoresis (PAGE) and Western blot analysis were performed to determine whether the isolation of IgG by protein A/G agarose resulted in a purified antibody preparation.

In separate channels the staining patterns of proteins in mouse ascites (HSA-9), mouse IgG (purified from mouse ascites), first flow through (non-bound protein fraction of purification) and controls of Human CuZnSOD and mouse serum albumin were compared using a 10-250 kDa pre-stained protein molecular weight (MW) ladder to determine the molecular weight of the components of each sample.

3.3.1.1 Ponceau S staining of reducing PAGE

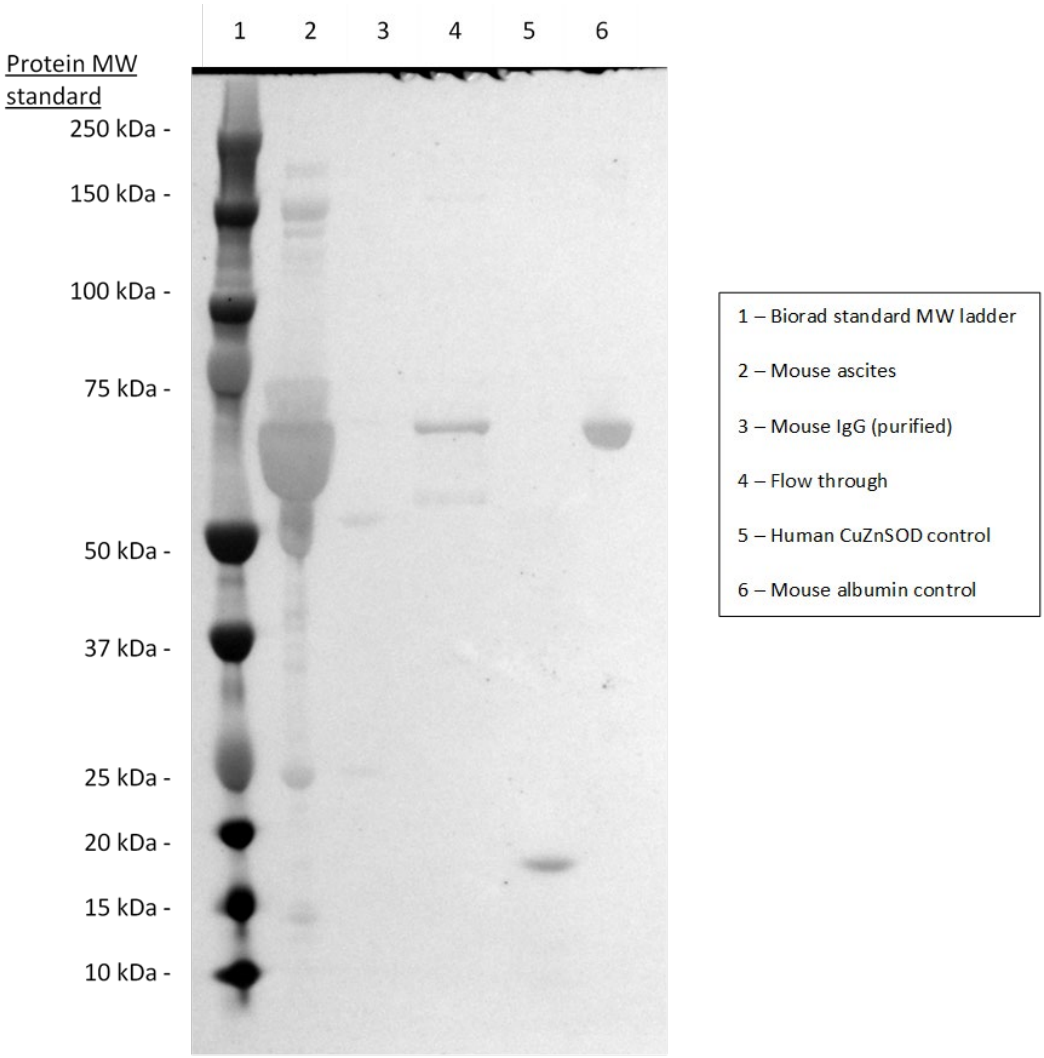

Figure 3.1: **Ponceau S protein staining of nitrocellulose blot.**
The blot visualises the protein band separation by SDS-PAGE under reducing conditions using Ponceau S stain. Colorimetric detection and image capture was achieved using the Bio-Rad ChemiDoc imaging system.

In lane 2 (ascites fluid) of Figure 3.1, heavy staining was observed between 50 and 75 kDa, with bands visible at 25, 50 and 150 kDa. Two faint bands were present in lane 3 (purified mouse IgG) at approximately 25 and 50 kDa. A distinct band was observed in lane 4 (purification flow through) at the same MW as the mouse albumin in lane 6. A clear band was visible between 15 and 20 kDa in lane 4 for human CuZnSOD control (mouse CuZnSOD could not be obtained). In lane 6 a band was visualised below 75 kDa for mouse albumin control.

3.3.1.2 Anti-IgG Western Blot

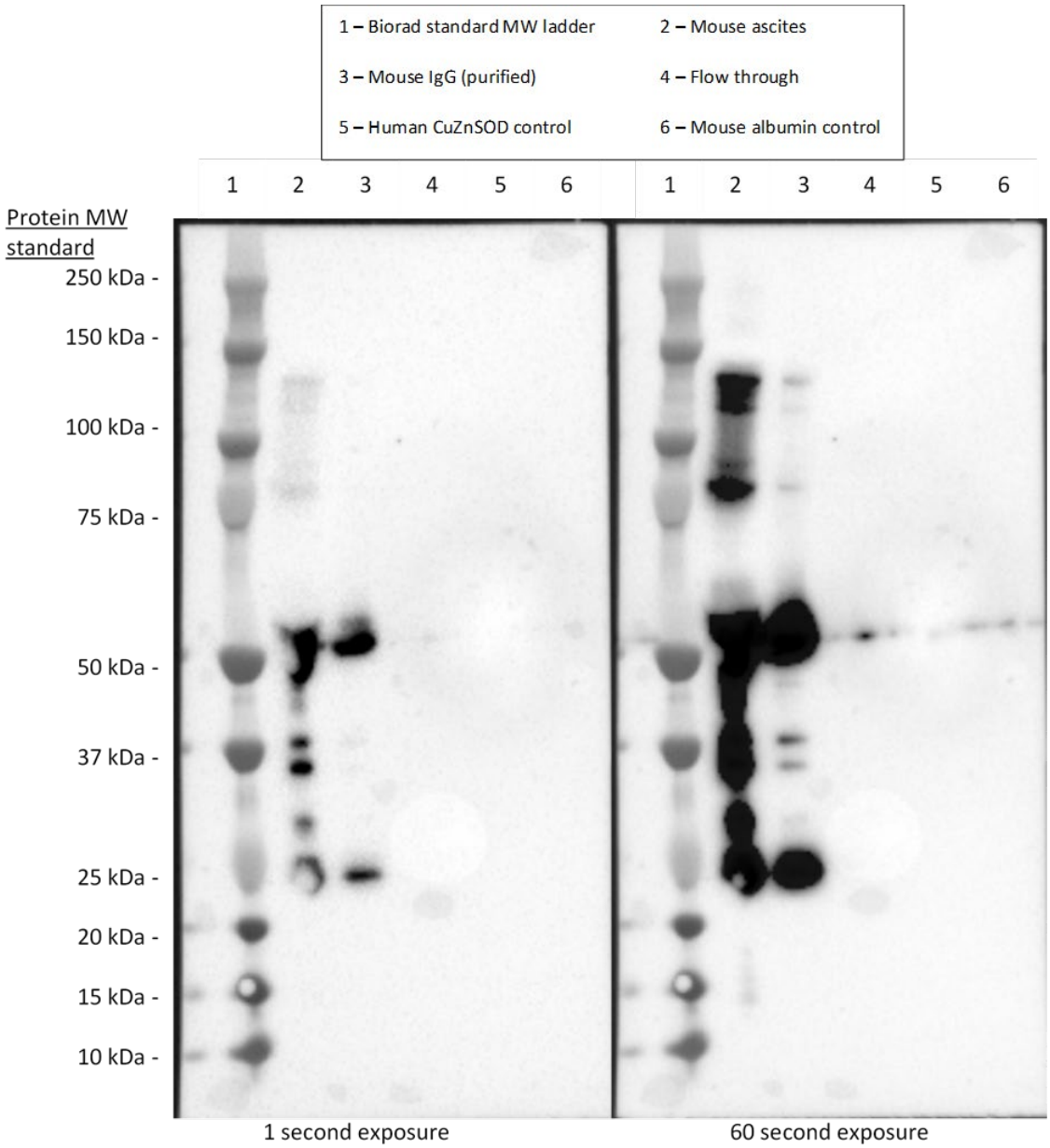

Figure 3.2: **IgG is present in ascites fluid and after protein A purification.** Anti-mouse IgG binding was visualised with chemiluminescence following 1- and 60-seconds' exposure. At both exposure times, binding was observed in the mouse ascites fluid and purified mouse IgG lanes. In the purification flow through, binding was observed following over exposure for 60-seconds. The blot was visualised with Luminata Forte Western HRP substrate and read by chemiluminescence on the Bio-Rad ChemiDoc following 1- and 60-seconds' exposure.

In lane 2 (ascites fluid) of Figure 3.2, at 1-second exposure, distinct, strongly stained bands at approximately 25, 28, 35, 40 and 50 kDa were observed. These

bands merged at 60-seconds exposure, with additional bands visible between 75 and 100 kDa and 100 and 150 kDa. In lane 3 (purified mouse IgG) following 1-second exposure, two bands were observed at approximately 25 and 50 kDa. At 60-seconds exposure, an additional two bands were observed in lane 3, exhibiting apparent molecular masses of approximately 35 and 40 kDa, with additional bands stained between 75 and 100 kDa and 100 and 150 kDa. A small band was observed in lane 4 (purification flow through) at approximately 50 kDa.

3.3.1.3 Anti-CuZnSOD Western Blot

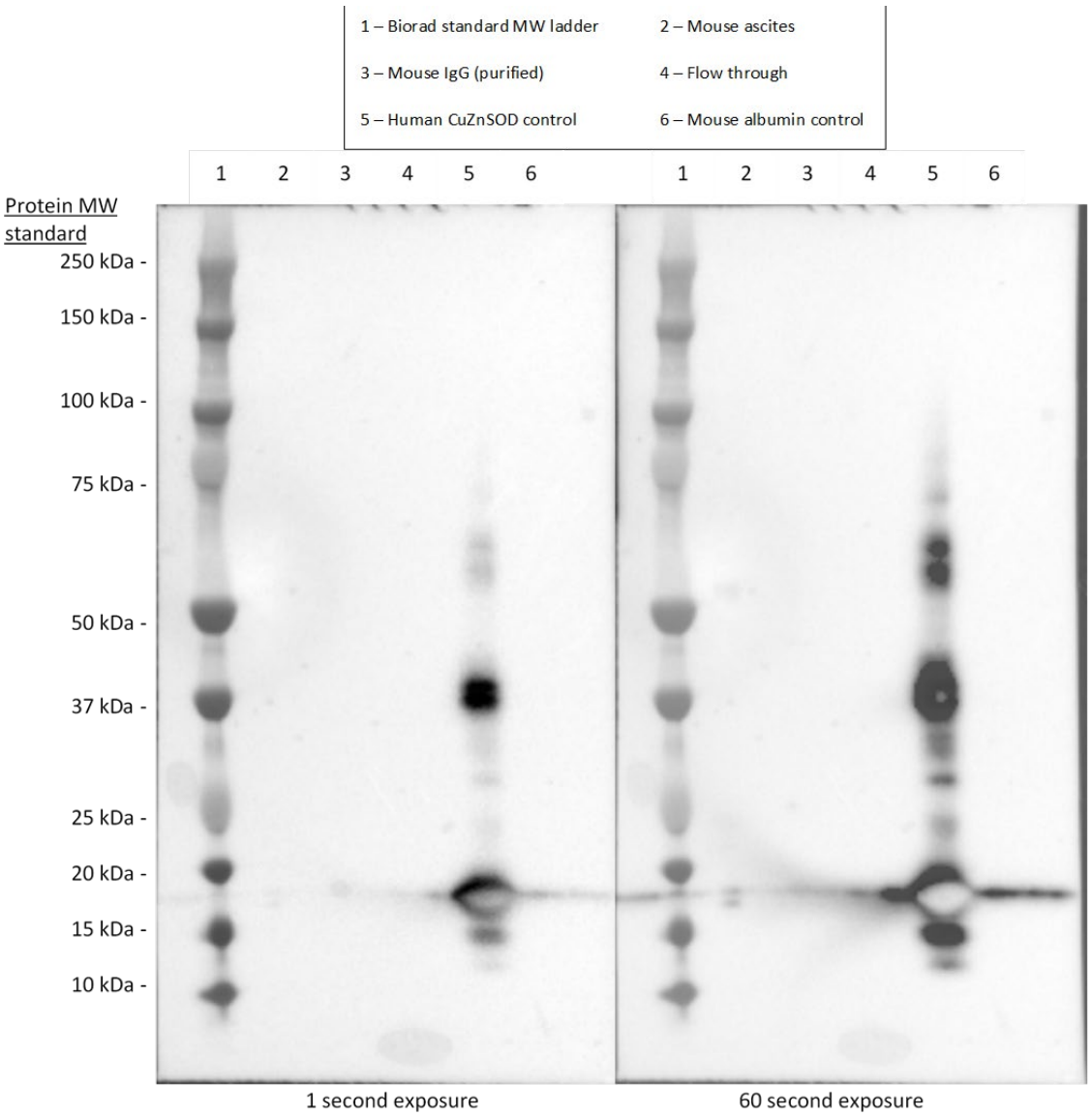

Figure 3.3: **CuZnSOD is present in ascites fluid and removed by protein A purification.**

Goat anti-mouse/human CuZnSOD binding was visualised with chemiluminescence following 1- and 60-seconds' exposure. In the ascites fluid lane, weak binding was observed following 1-second exposure and was slightly more distinct following 60-seconds over exposure. No binding was observed in the mouse IgG purified from ascites. The blot was visualised with Luminata Forte Western HRP substrate and read by chemiluminescence on the Bio-Rad ChemiDoc following 1- and 60-seconds' exposure.

In lane 2 (ascites fluid) of Figure 3.3, following 1-second exposure, only very faint bands were observed, but following 60-seconds' exposure two bands were observed between 15 and 20 kDa. In lane 3 (purified mouse IgG), following 1- and 60-seconds' exposure no visible banding was observed. In lane 4 (purification flow through), a small band was observed following 60-seconds exposure. In lane 5 (human CuZnSOD), following 1-second exposure bands were observed at 15 kDa, between 15 and 20 kDa, between 25 and 37 kDa, at 37 kDa and two bands between 50 and 75 kDa.

3.3.1.4 Anti-Albumin Western Blot

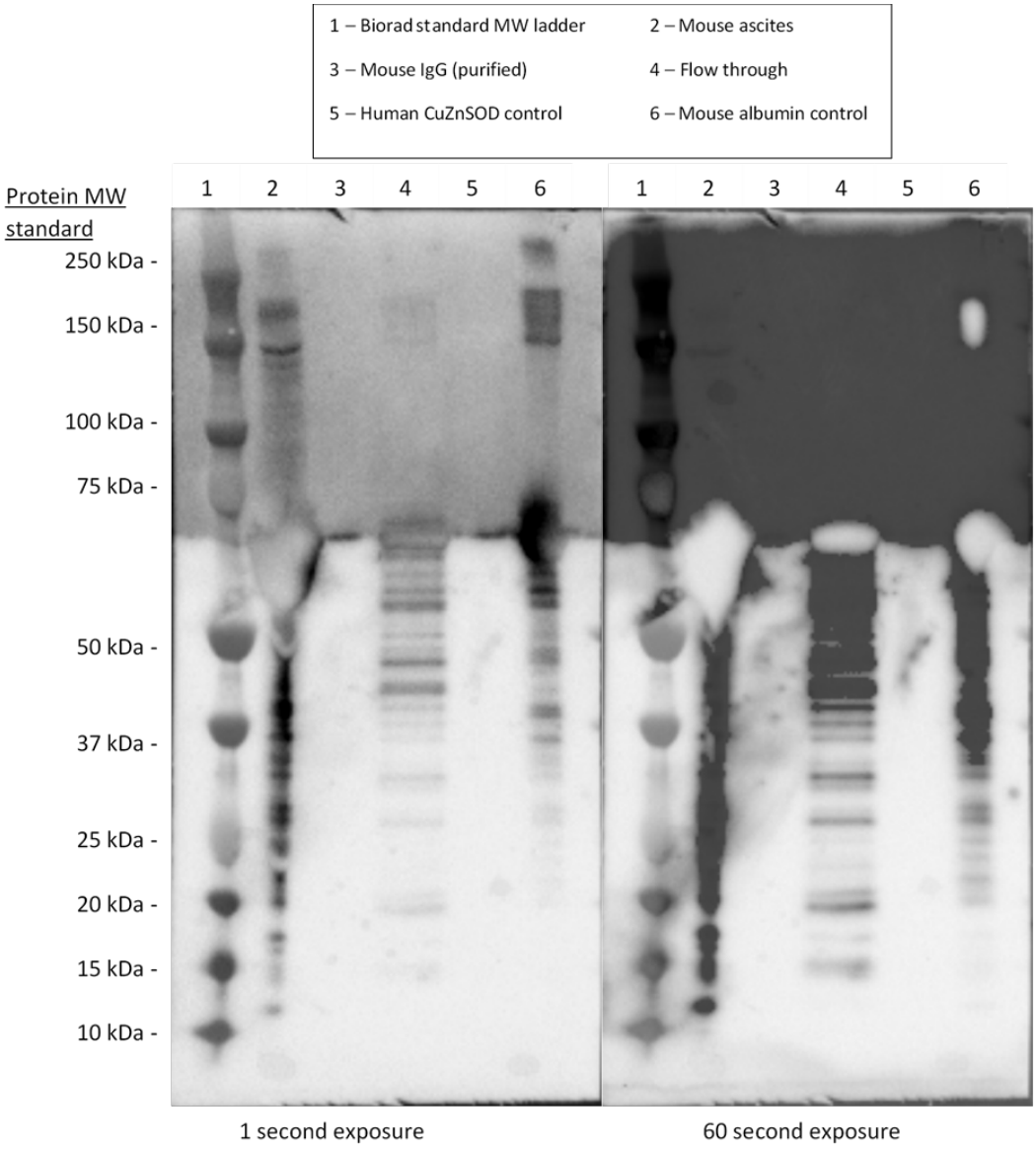

Figure 3.4: **Albumin is present in ascites fluid and removal cannot be confirmed by purification.**

Goat anti-mouse albumin binding was visualised with chemiluminescence following 1- and 60-seconds' exposure. In the ascites fluid, strong binding was observed at 1- and 60-seconds' exposure. Presence of albumin in the purified IgG could not be eradicated due to overstaining of the blot. The blot was visualised with Luminata Forte Western HRP substrate and read by chemiluminescence on the Bio-Rad ChemiDoc at 1- and 60-seconds' exposure.

The upper half of the blot in Figure 3.4 was overstained, less in the 1-second exposure and more in the 60-seconds exposure. In lane 2 (IgG ascites fluid), at 1-

second exposure, bands across the range of the molecular weight ladder were observed. At 60-seconds' exposure any bands in the upper half of the blot were obscured by overstaining, however at approximately 66 kDa a strong signal was observed (indicated by white spot). In lane 3 (purified mouse IgG), at 1-second and 60-seconds exposure, despite the overstaining there were no visible bands observed in the lower half or upper half of the blot, however a band was visible between 50 and 75 kDa. In lane 4 (purification flow through), at 1-second exposure, bands were observed across the molecular weight range. At 60-seconds exposure, bands were observed in the lower half of the blot and obscured in the upper of half of the blot by overstaining. In lane 5 (human CuZnSOD), at 1-second and 60-seconds' exposure, despite the overstaining there were no visible bands observed in the lower half or upper half of the blot, however a band was visible between 50 and 75 kDa. In lane 6 (mouse albumin control), at 1-second exposure bands across the range of the molecular weight ladder were observed. At 60-seconds exposure, any bands in the upper half of the blot were obscured by overstaining, however at approximately 66 kDa a strong signal was observed (indicated by white spot).

3.3.2 Mouse isotyping – immunoglobulin ratio

Table 3.1: ***Concentration of Ig subclasses in HSA-9***

Concentration (µg/mL) of immunoglobulin subclasses in murine monoclonal anti-human albumin antibody (HSA-9) from mouse ascites.

Antibody Subclasses	**Concentration (µg/mL)**
IgA	<0.25
IgG_1	189.5
IgG_{2a}	10.9
IgG_{2b}	4.1
IgG_3	0.9
IgM	3.9

The primary antibody subclass detected in mouse ascites fluid was IgG_1, consistent with manufacturer's certificate of analysis. However, significant concentrations of IgG_{2a}, IgG_{2b} and IgM were also detected.

3.4 Discussion

The mouse monoclonal HSA-9 antibody produced in mouse ascites (confirmed to have SOD activity – Petyaev and Hunt, 1996) was supplied and manufactured by Sigma Aldrich. The manufacturer's specification stated the mouse monoclonal was an IgG_1 isotype produced *in vivo* from mouse ascites.

The primary aim of the experiments described in this chapter were to determine whether an immunoglobulin with SOD activity was contaminated with host-derived proteins and / or associated with CuZnSOD. The second aim was to investigate the likely immunoglobulin subclass attributable to SOD activity. The final purpose of these experiments was to consider whether protein A agarose successfully purified the immunoglobulin. These data provided evidence that mouse monoclonal anti-human serum albumin IgG antibody (clone HSA-9), produced from ascites fluid was contaminated with mouse albumin and mouse CuZnSOD. Experiments confirmed the purification procedure yielded a solution of mouse IgG antibody, free from CuZnSOD, with negligible albumin contamination. Furthermore, it was confirmed that the antibody with reported SOD activity was primarily immunoglobulin subclass IgG_1, consistent with the manufacturer's certificate of analysis.

Ponceau S staining: purification removes albumin and CuZnSOD

Ponceau S staining after SDS-PAGE and electroblot (Figure 3.1) revealed mouse ascites (lane 2) was a complex sample matrix of many different proteins and not only IgG. A large band present between 50 and 75 kDa was indicative of albumin which can be compared to the mouse albumin control (approximately 66 kDa). The bands visible at 25 and 50 kDa were attributed to light and heavy immunoglobulin chains with a band at 150 kDa suggestive of a whole IgG molecule. The lack of a band between 15 and 20 kDa (mouse CuZnSOD subunit is approximately 15.9 kDa) suggests CuZnSOD was not present or at low concentrations not detectable using this method.

The staining in lane 3 (purified mouse IgG) at approximately 25 and 50 kDa was indicative of light and heavy immunoglobulin chains. The lack of presence of other bands suggested that purification with protein A agarose was successful and little or no CuZnSOD and albumin were present in the purified antibody.

Anti-IgG immunoblot: IgG is present post-purification

In the anti-IgG immunoblot shown in Figure 3.2, the visible bands in lane 2 (mouse ascites fluid) were attributed to antibody fragmentation due to heating with the reducing agent dithiothreitol (DTT). Bands were observed at the MW for light chains (25 kDa) and heavy chains (50 kDa) of immunoglobulins, but many other bands were also visible. Another or additional explanation for the number of separate bands visible was the lack of specificity of the anti-IgG antibody used. The anti-IgG used to detect IgG was not specific for the mouse IgG_1 only (the main isotype). Host-derived antibodies of various IgG isotypes (IgG_1, IgG_{2a}, IgG_{2b}, IgG_3 and IgG_4) would also be present in ascites. The anti-IgG antibody could likely bind to structures consistent across IgG isotypes.

The visible bands at 25 and 50 kDa in lane 3 (purified mouse IgG) at 1-second exposure were consistent with light and heavy chains of IgG. At 60-seconds' exposure, bands were visible at approximately 35 and 40 kDa, between 75 and 100 kDa and 100 and 150 kDa. The binding observed at 1-second exposure was consistent with the MW of Fv, Fc, F(ab) and $F(ab)_2$ fragments. The binding was comparable to the fragmentation of IgG observed in the mouse ascites. Although fragmentation and visualisation of 'artifact' bands can occur with incomplete denaturation or prolonged heating (Zhang, Wang and Li, 2019), this was not a concern as the detection of IgG presence was the sole purpose of this experiment. The different intensity of the bands was due to the higher and lower concentration analysed for each protein; 20 µg for ascites and 1 µg for purified mouse IgG. In lane 4 (purification flow-through), at 60-seconds' exposure, only a small band was visible at approximately 50 kDa, indicative of heavy chains. This suggested that although purification was not completely efficient, the method captured most of the antibody.

Anti-CuZnSOD immunoblot: CuZnSOD was not present post-purification

In the anti-human / mouse CuZnSOD immunoblot shown in Figure 3.3, the faint bands observed in lane 2 (mouse ascites fluid) between 15 and 20 kDa at 60-seconds' exposure were consistent with the mouse CuZnSOD subunit – evidence of presence in the ascites fluid. The lack of bands visible in the purified mouse IgG (lane 3) indicated purification removed any mouse CuZnSOD present in the ascites. The bands visible for the human CuZnSOD control (lane 5) show that the antibody detects human CuZnSOD.

Anti-albumin immunoblot: Albumin presence confirmed in ascites and not excluded post-purification

In the anti-mouse albumin immunoblot shown in Figure 3.4, the upper half of the blot was over-stained, which increased from the 1-second exposure to the 60-seconds' exposure. It was unknown why this interference occurred, however it was still possible to make necessary observations of albumin presence and absence in each of the protein solutions. In lane 2 (IgG ascites fluid), at 1-second exposure, bands across the range of the molecular weight ladder were indicative of the presence of albumin. At 60-seconds', a strong signal was observed at the MW of mouse albumin (66 kDa – indicated by a white spot). In lane 3 (purified mouse IgG), despite the overstaining, there were no visible bands observed in the lower half or upper half of the blot, however due to a visible band between 50 and 75 kDa, the presence of albumin could not be eradicated. In lane 4 (purification first flow-through), bands were observed across the molecular weight range attributable to the presence of albumin. In lane 5 (human CuZnSOD), despite the overstaining there were no visible bands observed in the lower half or upper half of the blot, however a band was visible between 50 and 75 kDa, therefore the presence of albumin could not be eliminated. In lane 6 (mouse albumin control) bands were visible across the range of the molecular weight ladder with a strong signal at the molecular weight for mouse albumin (66 kDa – indicated by white spot). It is possible the overstaining of the blot could have occurred due to cross-reactivity of the primary or secondary antibody – cross reactivity data was not available for the anti-mouse albumin antibody, however the manufacturer of the donkey anti-goat HRP-conjugated antibody (Cat no: HAF109, BioTechne Ltd., Abingdon, U.K.) did state, "this antibody shows approximately 5% cross-reactivity with human IgG, rabbit IgG, mouse IgG, rat IgG and less than 1% cross-reactivity with chicken IgY". Equally, inadequate blocking, which may have resulted in non-specific binding of the primary or secondary antibodies. Increasing the dilution of the primary or secondary antibody and changing the blocking solution may have reduced non-specific binding. Due to restrictions of time, cost and use of equipment this blot could not be repeated.

Mouse immunoglobulin isotyping: IgG1 is the primary isotype present

In Table 3.1, the concentration was highest for the IgG_1 isotype, approximately 17 times higher than IgG_{2a}. The results demonstrate that HSA-9, an antibody with SOD activity is a mix of subclasses and isotypes. In general, IgG_1 is the most abundant subclass; it is a primary immunoglobulin trigger of effector functions such as complement (Vidarsson, Dekkers and Rispens, 2014).

3.4.1 Conclusions

The results in this chapter provide evidence that mouse CuZnSOD and albumin were present in the mouse monoclonal antibody preparation (HSA-9) from ascites fluid (Figures 3.3 and 3.4). The activity of CuZnSOD and the postulation albumin has antioxidant activity (Kouoh *et al.*, 1999) means the SOD activity of whole immunoglobulin observed in earlier research (Petyaev and Hunt, 1996) could be in part attributed to CuZnSOD and albumin. Similarly, the SOD activity of whole IgG_1 in ascites preparations cannot be confirmed by these experiments due to the presence of a variety of immunoglobulin subclasses and isotypes in the antibody with proposed SOD activity. However, early experiments by Petyaev *et al.* (1998) demonstrated measured SOD activity of immunoglobulins in atherosclerotic lesions which are known to accumulate IgG. Immunoprecipitation (using protein A agarose – binds strongly to IgG) of atherosclerotic lesion extracts removed approximately 50% of SOD activity at pH 7.8 and more than 70% at pH 6.45, indicative of SOD activity resulting from antibodies (Petyaev *et al.*, 1998).

The purification of the antibody using protein A agarose was successful in that it yielded mouse IgG that was free from associated CuZnSOD. The presence of albumin in the purified mouse IgG could not be eradicated fully (fig 3.4), owing to the potential cross-reactivity or inadequate blocking in the anti-albumin blot. However, it was evident that the concentration of albumin in the purified mouse IgG was much less. The comparatively strong binding of anti-albumin in the ascites, flow through and albumin control lanes compared to the relatively extremely weak binding of bands in both the CuZnSOD control and purified mouse IgG, suggest the band could be an ‘artifact’ induced by bleeding across bands. As this could not be confirmed, the SOD activity of albumin was investigated in Chapter 4 (section 4.4.2.3).

The next chapter describes development and evaluation of a method to detect superoxide dismutase activity of mouse and human immunoglobulins, and bovine and human CuZnSOD. A study of the pH dependency of mouse and human immunoglobulin is presented in sections 4.4.2 and 4.4.4, to investigate whether antibodies contribute equivalent SOD activity to bovine and human CuZnSOD controls.

CHAPTER 4: Antibody superoxide dismutase activity and pH

4.1 Background

4.1.1 Causes of pH changes and its effect on proteins

Potential hydrogen (pH) is the logarithmic scale that represents the concentration of hydrogen ions in a solution. The pH *in vivo* is generally tightly regulated, however in pathological conditions (see section 1.2.2.1 for examples), local and systemic fluctuations can occur (Kellum, 2000). Changes in pH are significant because of the disruptive effects as even subtle changes can have on biochemical reactions and maintenance of homeostasis within cells (Rajamäki *et al.*, 2013). Local acidification can be caused by a combination of:

- Damage to capillaries, and infiltration and activation of leukocytes, resulting in tissue hypoxia, switching from aerobic to glycolytic metabolism causing an accumulation of lactic acid (Kopaniak, Issekutz and Movat, 1980; Menkin and Warner, 1937).
- An increased production by the NADPH oxidases of neutrophils and macrophages during the respiratory burst (Winterbourn, Kettle and Hampton, 2016).
- Bacterial production of short-chain fatty acids (Rotstein, Nasmith and Grinstein, 1987).

Protein (comprised of amino acids) structure is determined by non-covalent attractive forces such as hydrogen bonding or by salt bridges; interactions between positively and negatively charged side chains of amino acids. The charge of negative carboxyl (COO^-) and positive charged amino (NH_3^+) groups are neutralised by acidic and alkali environments. This alters the overall shape and structure of a protein (denaturation), which may affect its function (Talley and Alexov, 2010). All proteins have an optimal pH which is related to the environment in which it functions. The consequence of local acidification that accompanies acute and chronic inflammation, is that it can cause denaturation of proteins such as enzymes, inhibiting catalytic activity. Investigating the effects of pH on SOD and AbSOD activity may help to understand how and where they may function *in vivo*.

4.1.2 Improving the detection of AbSOD activity

To detect superoxide dismutase activity of SOD and antibodies, the assay employs a superoxide generation step via the reduction of oxygen by NADH in the presence of PMS. This is detected by the associated blue-colour change during the reduction of NBT to formazan. SOD activity of antibodies (AbSOD) or SOD suppresses the rate of NBT reduction. Although this assay has proved to be robust in detecting the SOD activity of SOD and antibodies alike, it has two significant limitations: firstly, the assay is extremely laborious and hence has low throughput, taking a whole day to complete analysis of a limited number of samples, and secondly, the assay is prone to batch-to-batch imprecision, due to the individual reagent additions inducing cumulative error.

The overall foundations of the experiments in this chapter were to develop an assay suitable for the detection of antibody SOD activity (AbSOD activity), to understand the relationship between pH and SOD / AbSOD activity and evaluate the assay for application in human studies.

4.2 Aims and hypotheses

The primary aim of this chapter was to develop and optimise an assay for the detection of SOD activity of antibodies, which was less laborious than the current cuvette-based method, had reduced imprecision and improved sensitivity across acidic and alkali pH ranges. A dual reagent addition, 96-well plate assay design was chosen for its simplicity and suitability for use with equipment commonly found in a 'wet' laboratory. It was hypothesised a 96-well plate assay would be less laborious, allowing higher throughput, more reliable and less prone to batch-batch variation, and have improved overall sensitivity, detecting changes between the AbSOD activity of patients with different diagnoses.

The secondary aim was to use the assay to investigate the effect of pH on superoxide dismutase activity of mouse monoclonal IgG_1 antibodies (HSA-9), alongside the activity of human and bovine superoxide dismutase. It was hypothesised HSA-9 antibodies would have optimal SOD activity at inflammatory pH (pH 6.5 – based on experiments by Petyaev and Hunt, 1996) and bovine and human CuZnSOD would have an optimum SOD activity at physiological pH (pH 7.0 – 7.5). Additionally, it was hypothesised protein A agarose-purified antibody and non-purified antibody, and bovine and human CuZnSOD would have similar pH dependency profiles.

The tertiary aim was to investigate the effects of proteins in the assay. Bovine and human albumin were assayed to investigate whether there was any observable SOD activity and thus protein matrix effects. It was hypothesised the observable SOD activity of albumin would be negligible.

The final aims were to investigate the effects of heat denaturation and metals ions on the SOD activity of antibodies and SOD1. It was hypothesised SOD activity of human IgG and SOD would diminish or reduce after heat-treatment, and SOD activity of human IgG incubated with metal ions would increase, and SOD remain unchanged.

4.3 Materials and methods

4.3.1 Optimisation of SOD activity assay

To define the optimum concentration of assay reagents for determination of superoxide dismutase activity, the generation of superoxide (detected by nitroblue tetrazolium chloride (NBT)) in the presence of x1 PBS (baseline) was assayed at varying concentrations of phenazine methosulfate (PMS) and nicotinamide adenine dinucleotide (NADH). Firstly, 0.11, 0.33 and 0.66 µM of PMS were analysed in the presence of 1.0 mM NADH and detected by 100 µM of NBT. The reaction profiles were compared, and the optimum concentration of PMS selected for the subsequent optimisation of NADH concentration. Secondly, 1.0, 2.0, 3.0, 4.0 and 5.0 mM of NADH were assayed in the presence of 0.66 µM of PMS and detected by 100 µM of NBT. A cuvette spectrophotometer was used to measure the reaction every 30 seconds for 3 minutes at 560 nm at room temperature; all assays were at pH 7.4. The aim was to develop an assay with an absorbance of approximately 1.0 at a wavelength of 560 nm, over 3 minutes.

4.3.2 pH dependency of AbSOD and SOD activity in cuvettes

The superoxide dismutase activity of SOD and antibodies was investigated at pH 5.5, 6.0, 6.5, 7.0, 7.5 and 8.0. The aim was to determine how pH affected SOD activity and whether the activity of purified-IgG was comparable to non-purified IgG from mouse ascites (HSA-9). Human SOD and bovine SOD were assayed as controls of superoxide dismutase activity and human serum albumin and bovine serum albumin as controls of protein matrix effects.

The assay was performed in cuvettes. SOD activity was recorded manually at 10 second intervals over 3 minutes at a wavelength of 560 nm; full details of the procedure are detailed in the methods section 2.3.1. Results of SOD activity of each protein are expressed percentage inhibition (Figure 2.4).

4.3.3 Development of micro-titre AbSOD activity assay

To increase assay throughput and reduce between-batch imprecision, a dual reagent assay was developed. Two different formats were investigated, one using a 1:16 ratio and the other a 1:26 ratio of sample to total reaction volume. For reagent 1, PMS and NBT were combined in a solution of pH adjusted K_2HPO_4 and EDTA; this was shielded from light until use. For reagent 2, NADH was combined with a solution of pH adjusted K_2HPO_4 and EDTA. Full details of the assay are in section 2.3.2. Human IgG, bovine SOD and human SOD were assayed at pH 6.5 for approximately 11 minutes and the resultant SOD activity compared. The aim was to determine whether a proportional increase in the concentration (1.4 to 2.3 µmol/L) of sample to reagents would improve assay sensitivity.

4.3.4 pH dependency of SOD and AbSOD activity micro-titre plates

The superoxide dismutase activity of SOD and antibodies was investigated at varying pH's (5.5, 6.0, 6.5, 7.0, 7.5 and 8.0). The aim was to determine how pH affected SOD activity and whether the activity of purified-mouse IgG was comparable to human IgG. Human SOD and bovine SOD were assayed as controls of superoxide dismutase activity.

The assay was performed in 96-well plates. SOD activity was recorded automatically at 26 second intervals for 11 minutes at a wavelength of 560 nm; full details of the procedure are detailed in the methods section 2.3.2. Results of SOD activity of each protein are expressed percentage inhibition (Figure 2.4).

4.3.5 Heat denaturation experiments

The pH dependency (pH 5.5 – 7.5) of human IgG, mouse IgG and bovine SOD subjected to intensive heat treatment (85°C for 1 hour) was investigated using method outlined in section 2.3.2. The SOD activity of these heat-treated proteins (at 0.2 µmol/L) was compared to fresh proteins alongside IgG and SOD controls.

4.3.6 Effects of metal ions (iron and copper)

To investigate the effects of metal ions on SOD activity, varying concentrations of iron (II) sulphate ($FeSO_4$) and copper (II) sulphate ($CuSO_4$) were incubated with human IgG (Cat no: I4506, Sigma Aldrich, Dorset, U.K.) and human SOD1 (Cat no: S9636-1KU, Sigma Aldrich, Dorset, U.K.). The reference range concentration of iron and copper in the body varies between approximately 10 – 30 µmol/L.

To simulate iron and copper in the body, x 10 concentrate iron and copper sulphate solutions were prepared: 0.0023g of $FeSO_4.7H_2O$ (Cat no: 31236, Sigma Aldrich, Dorset, U.K.) was added 50 mL of deionised water to create a 0.3 mM stock solution and 0.0024g of $CuSO_4.5H_2O$ (Cat no: 31293, Sigma Aldrich, Dorset, U.K.) and add 50 mL of deionised water to create a 0.3 mM stock solution. The copper sulphate and iron sulphate stock solutions were diluted (1:5 or 1:15) in deionised water to create 60 µmol/L or 20 µmol/L solutions. Human IgG and SOD1 (10 µmol/L) was diluted in Eppendorf LoBind tubes (1:2) separately in the copper sulphate and iron sulphate solutions to create the following: 30 µmol/L $CuSO_4$ or $FeSO_4$ and 5.0 µmol/L human IgG or human SOD1, and 10 µmol/L $CuSO_4$ or $FeSO_4$ and 5.0 µmol/L human IgG or human SOD1. The antibody-metal ion solutions were incubated for 48 hours at +4 °C on an end-over-end mixer.

After incubation, 1.0 mL of x 1 PBS (pH 7.4) was added to each tube, mixed and centrifuged. The entire volume of each vial was then pipetted in to a separate Amicon® Ultra-4 centrifugal filter unit with a 3 kDa (kilodalton) molecular weight cut-off. The cellulose filter tubes were then centrifuged at 3000 g for 30 minutes (25 °C). Centrifugation separated the solution where molecules less than 3 kDa flowed through the cellulose filter and all those greater than 3 kDa remained in the retention filter (the retentate). The concentrated protein solution was then obtained by pipetting from the filter using a sweeping motion and pipetted in to a LoBind tube.

The effect of metal ion treatment on the SOD activity of human IgG and SOD1 was then compared to untreated proteins at pH 5.5, 6.5 and 7.5 using the method outlined in section 2.3.2.

4.4 Results

4.4.1 Results for optimisation of SOD activity assay

4.4.1.1 Optimisation of PMS concentration

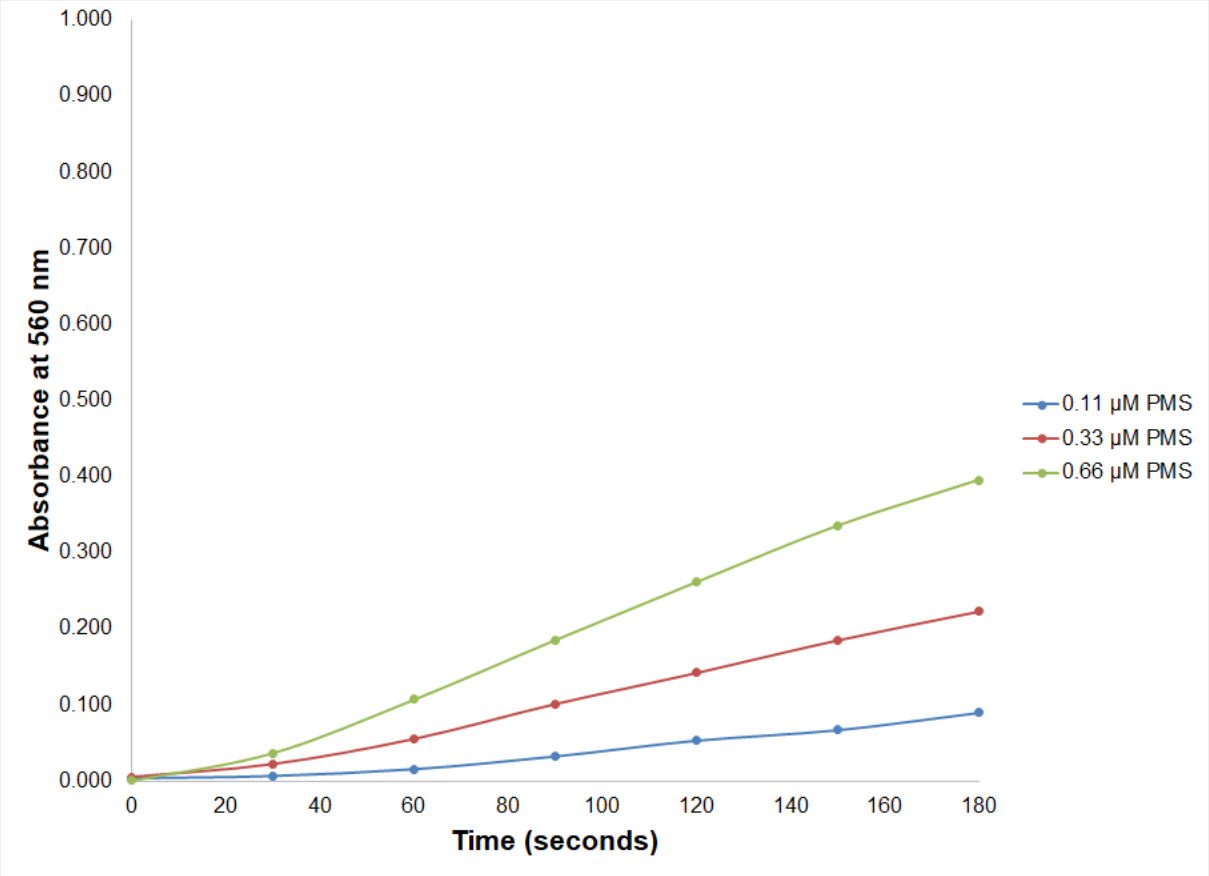

Figure 4.1: **Optimisation of PMS concentration**

The absorbance at 560 nm is plotted on the y-axis, versus the time (seconds) of the reaction on the x-axis. As the concentration of PMS was increased from 0.11 µM to 0.66 µM, there was a proportional increase in absorbance across the reaction profile of x1 PBS (baseline). The assay system consisted of 100 mM K_2HPO_4, 1.0 mM EDTA, 0.11, 0.33 or 0.66 µM of PMS, 1.0 mM NADH and 100 µM NBT (all reagents were adjusted to pH 7.4).

A PMS concentration of 0.66 µM resulted in significantly higher absorbance (0.395) at 180 seconds than the other concentrations of PMS analysed (0.11 µM, 0.090; 0.33 µM, 0.223). A 339% increase in absorbance was observed at a PMS concentration of 0.66 µM compared to 0.11 µM. A PMS concentration of 0.66 µM was selected for optimisation of NADH concentration.

4.4.1.2 Optimisation of NADH concentration

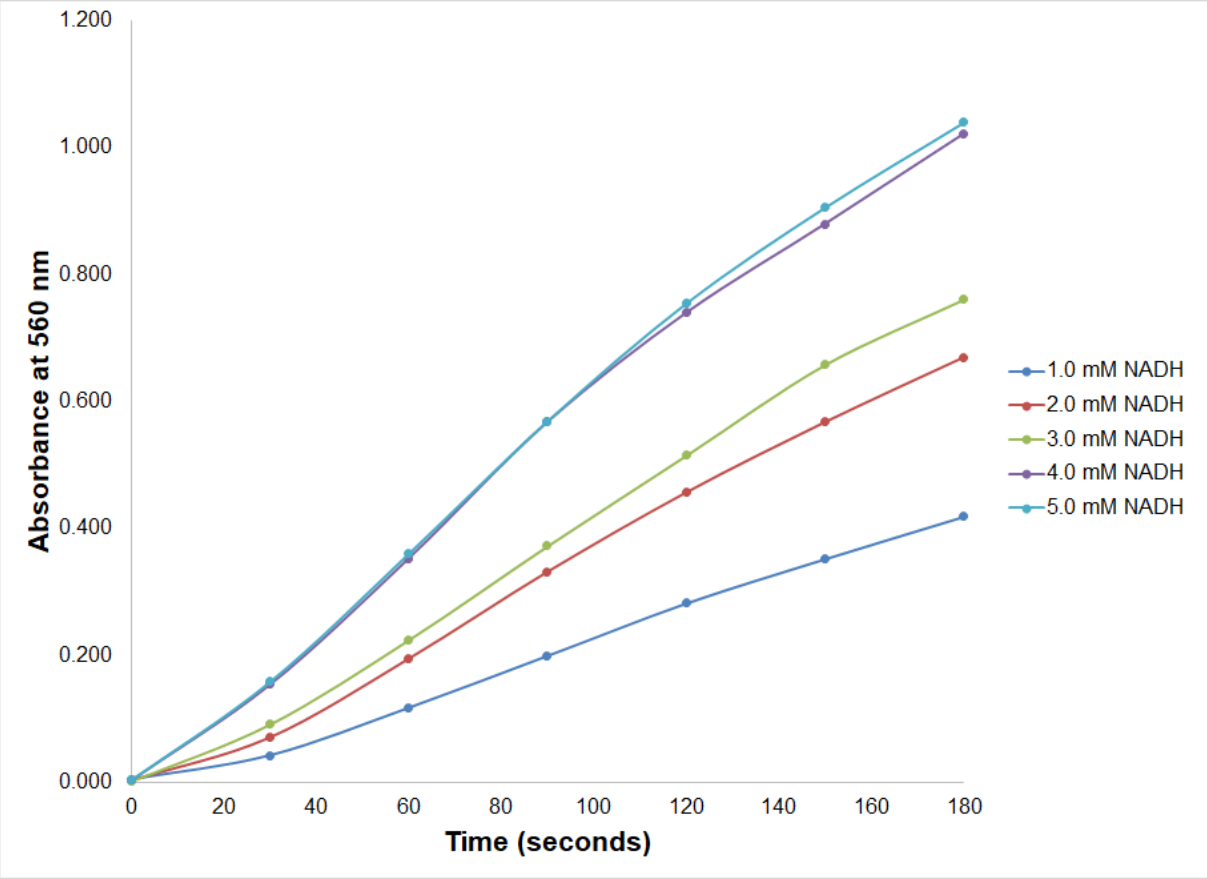

Figure 4.2: **Optimisation of NADH concentration**

The absorbance at 560 nm is plotted on the y-axis, versus the time (seconds) of the reaction on the x-axis. As the concentration of NADH was increased from 1.0 mM to 5.0 mM, there was a proportional increase in absorbance across the reaction profile of x1 PBS (baseline). The assay system consisted of 100 mM K_2HPO_4, 1.0 mM EDTA, 0.66 µM PMS, 1.0, 2.0, 3.0, 4.0 or 5.0 mM of NADH and 100 µM NBT (all reagents were adjusted to pH 7.4).

A NADH concentration of 5.0 mM resulted in significantly higher (1.040) absorbance at 180 seconds than the other concentrations of NADH analysed (1.0 mM, 0.419; 2.0 mM, 0.670; 3.0 mM, 0.761; 4.0 mM, 1.022). A 148% increase in absorbance was observed at a concentration of 5.0 mM NADH compared to 1.0 mM. A NADH concentration of 5.0 mM was selected for the SOD activity assay.

4.4.2 pH dependency of antibody SOD activity in cuvettes

The experiments described in this section (4.1.2) employed a SOD activity assay in cuvettes to investigate the effects of pH on the activity of purified mouse IgG, mouse ascites IgG, bovine CuZnSOD, human CuZnSOD, bovine albumin and human albumin. Proteins were all assayed at a molar concentration of 0.03 µmol/L in three independent experiments, recorded over 180 seconds, ranging from pH 5.5 – 8.0, increasing in 0.5 pH increments. Activity was represented as % inhibition – where positive values demonstrate SOD activity and negative values demonstrate pro-oxidant activity. The assay system consisted of 100 mM K_2HPO_4, 1.0 mM EDTA, 0.66 µM PMS, 5.0 mM of NADH and 100 µM NBT (see section 2.3.1).

4.4.2.1 pH dependency of human and bovine SOD

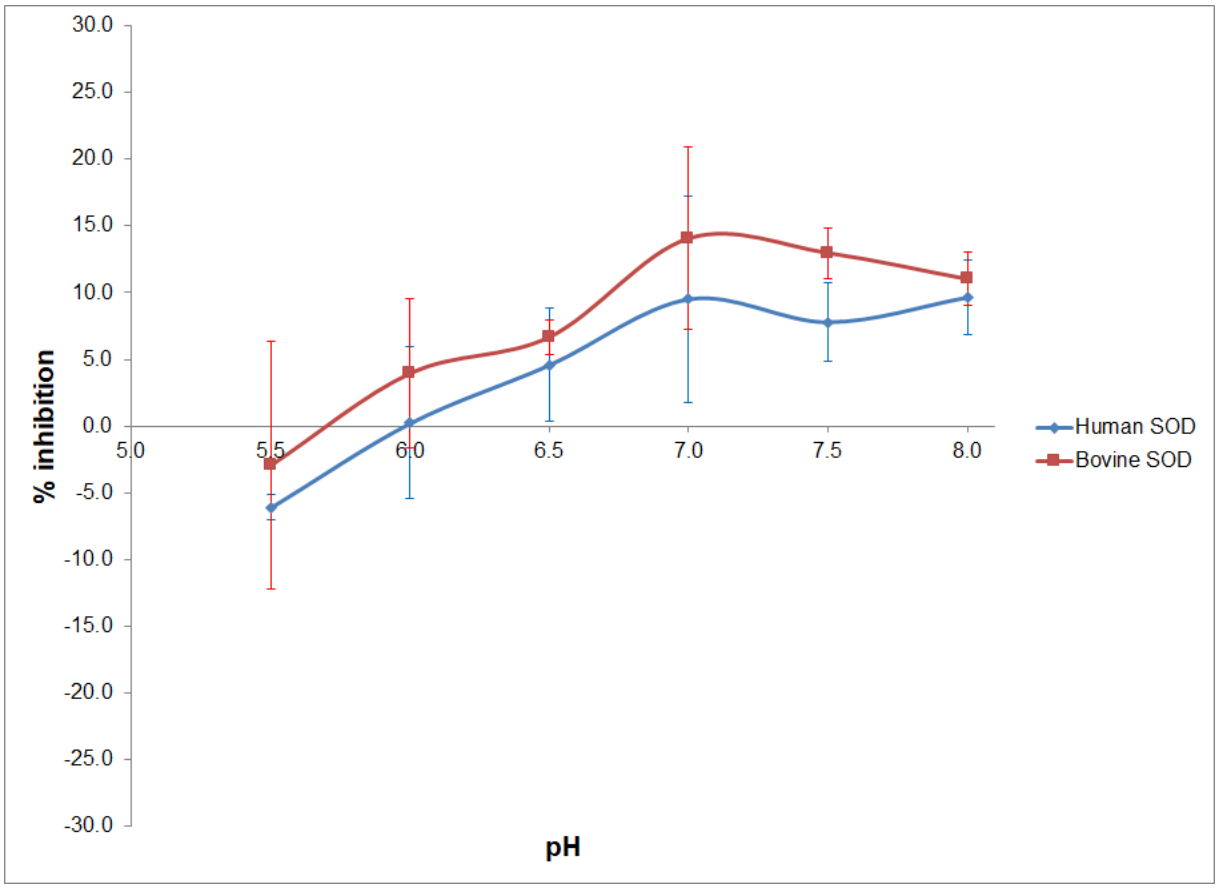

Figure 4.3: **CuZnSOD activity is increased between pH 7.0 and 7.5**

The percentage (%) inhibition is plotted on the y-axis, versus pH on the x-axis. The average % inhibition of bovine SOD and human SOD from pH 5.5 – 8.0 are visualised with error bars expressing ±1 standard deviation (SD).

The % inhibition of bovine and human SOD activity increased significantly from acidic pH to pH 7.0 (neutral), where the optimum inhibition was observed (Bovine SOD, 14.1 %; Human SOD, 9.5 %). Bovine SOD had increased inhibition compared to human SOD across the pH range.

4.4.2.2 pH dependency of purified mouse IgG and ascites IgG

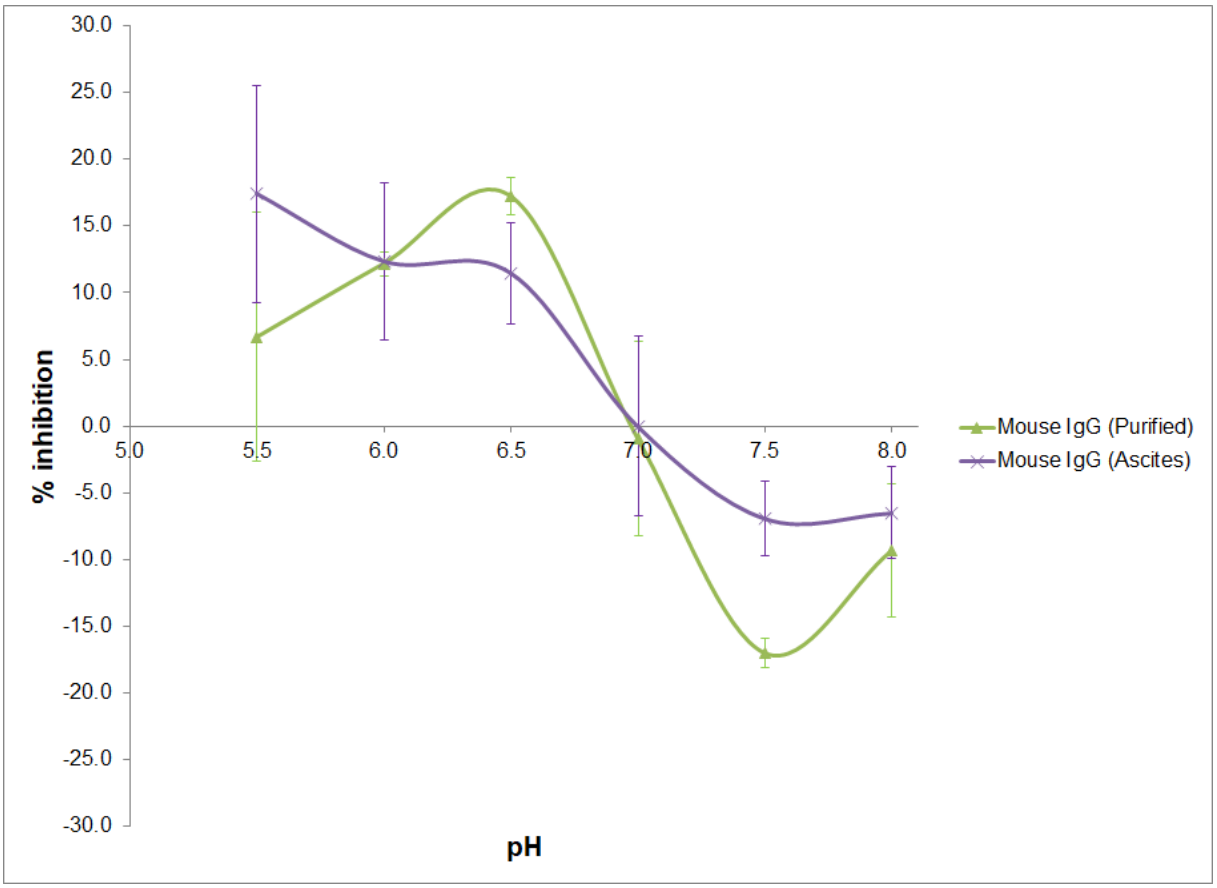

Figure 4.4: **Mouse IgG has increased SOD activity at acidic pH**
The percentage (%) inhibition is plotted on the y-axis, versus pH on the x-axis. The average % inhibition of purified mouse IgG and mouse ascites IgG from pH 5.5 – 8.0 are visualised with error bars, expressing ±1 SD.

Optimum % inhibition was observed at pH 5.5 for mouse ascites IgG (17.4 %), and pH 6.5 for purified mouse IgG (17.2 %). Negative % inhibition of purified mouse IgG was observed at pH 7.5 (-17.0 %). Mouse ascites IgG and purified mouse IgG had similar activity profiles across the pH range investigated.

4.4.2.3 pH dependency of human and bovine albumin

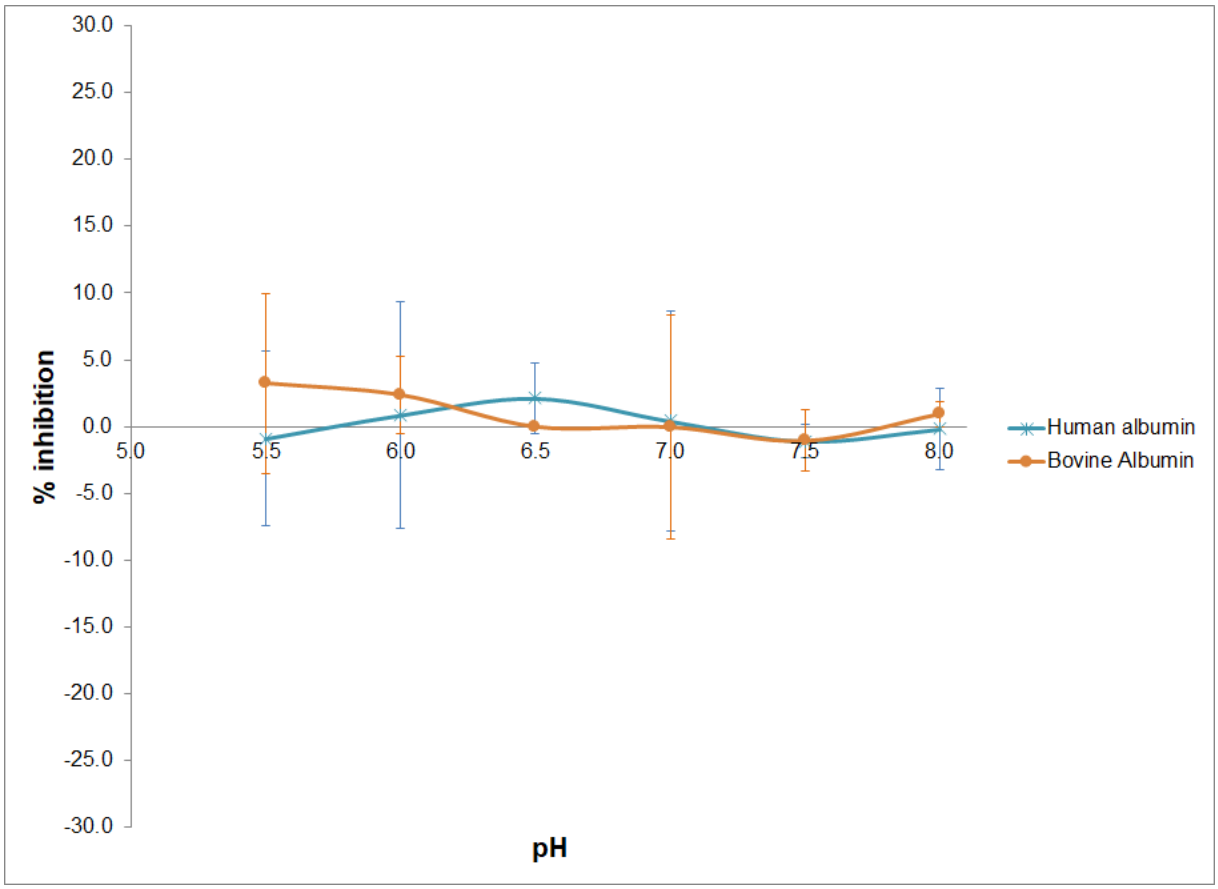

Figure 4.5: **Human and bovine albumin have negligible activity**
The percentage (%) inhibition is plotted on the y-axis, versus pH on the x-axis. The average % inhibition of human albumin and bovine albumin from pH 5.5 – 8.0 are visualised with error bars, expressing ±1 SD.

The inhibition of bovine and human SOD was negligible, ranging between an average of 2.1 and -1.1 % for human albumin and 3.2 to -1.1 % for bovine albumin.

4.4.2.4 Comparing the activity of SOD and IgG across pH

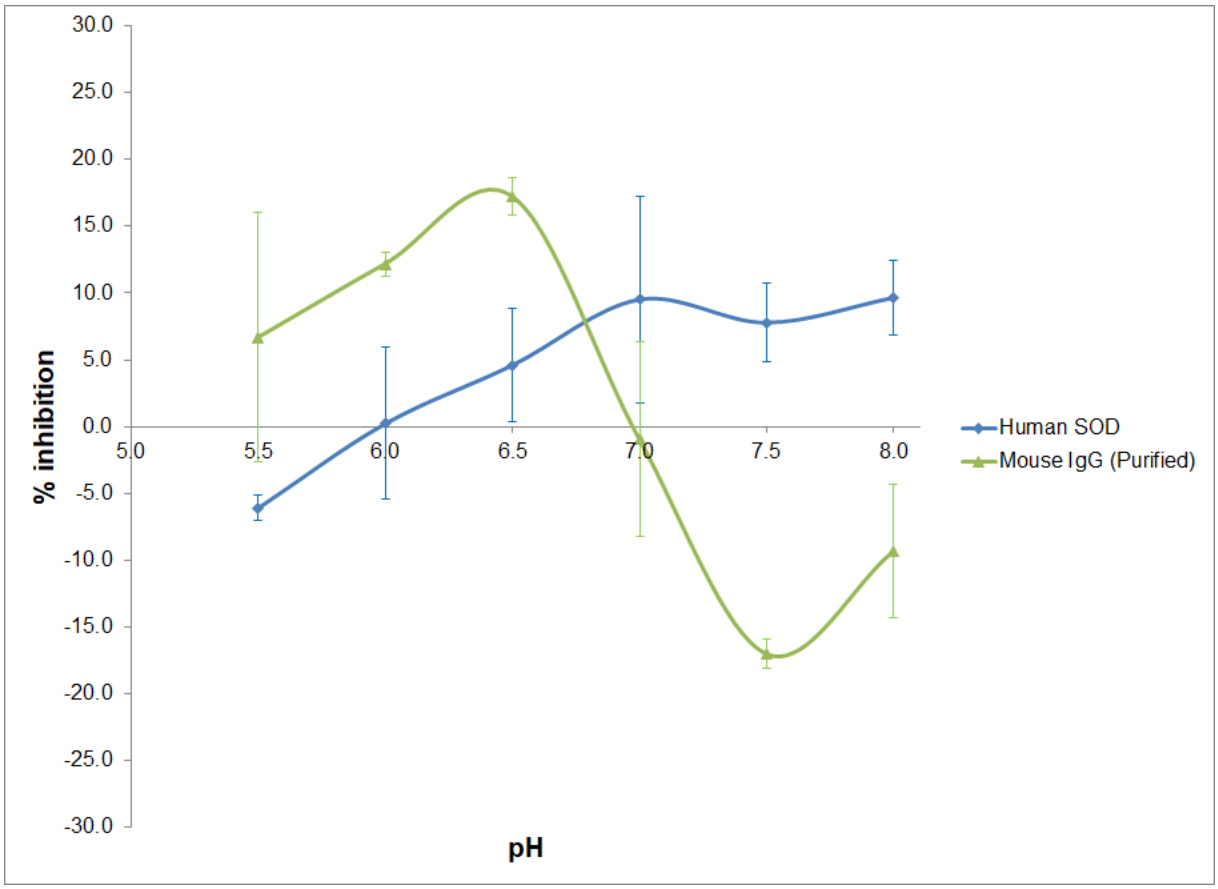

Figure 4.6: **Human SOD and mouse IgG have opposing activity**
The percentage (%) inhibition is plotted on the y-axis, versus pH on the x-axis. The average % inhibition of human SOD and purified mouse IgG from pH 5.5-8.0 are visualised with error bars, expressing ±1 SD.

Between pH 5.5 and 6.5, human SOD was decreased (-6.1 to 4.6 % inhibition) in comparison to purified mouse IgG (6.7 to 17.2 % inhibition). At pH 7.0 and 7.5 optimum inhibition was observed for human SOD (9.5 and 7.8 %), and at pH 7.5 mouse IgG (-17.0 %) catalysed the formation of superoxide.

4.4.3 Development of a high throughput SOD activity assay

4.4.3.1 Dual reagent assay (1:16 ratio – sample to reagent)

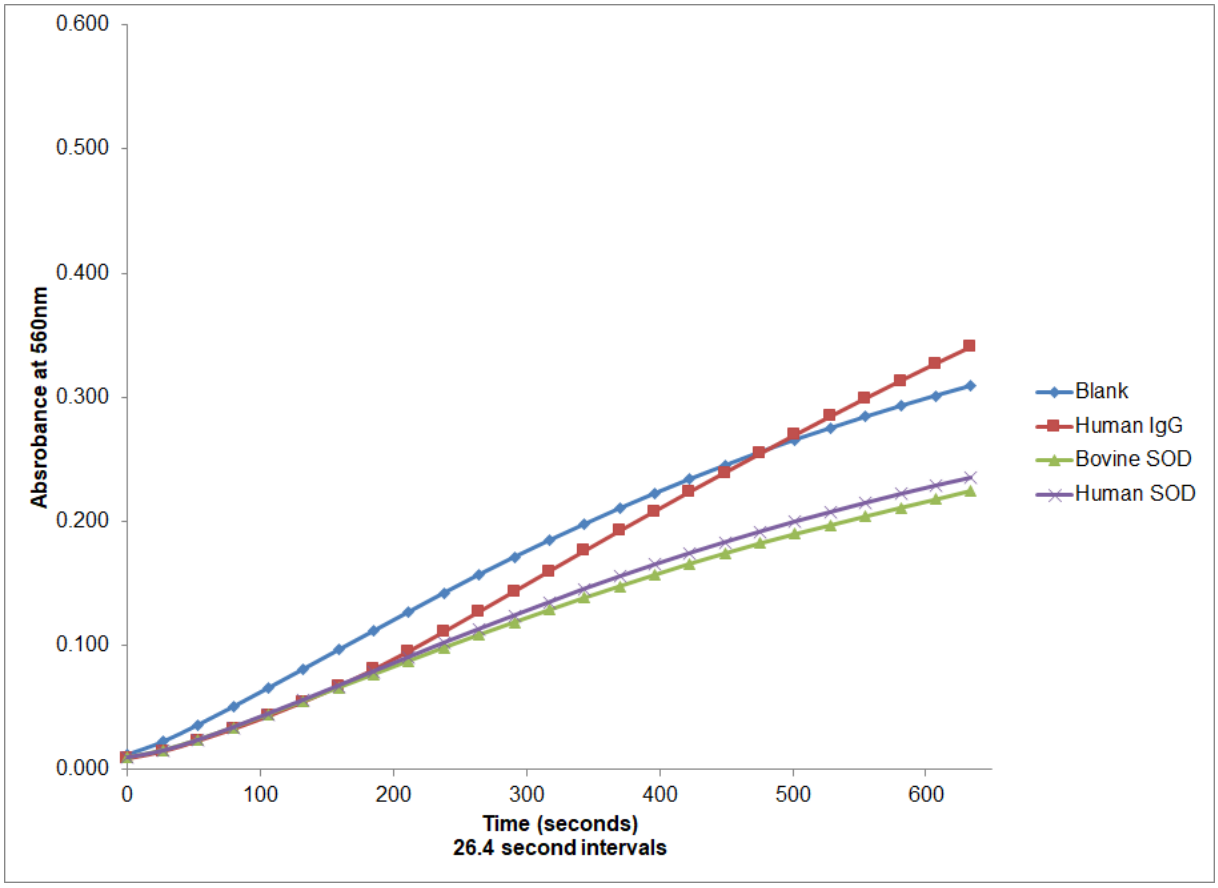

Figure 4.7: **Dual reagent AbSOD activity assay – 1:16 ratio**

The absorbance at 560 nm is plotted on the y-axis, versus the time (seconds) of the reaction on the x-axis. The absorbance of human IgG, bovine SOD and human SOD are visualised on the graph over 11 minutes. The assay used a ratio of 1:16 of sample to reagents and was performed in 96-well micro-tire plates.

At 3 minutes, the human IgG, bovine SOD and human SOD had a % inhibition of 17.4, 22.7 and 19.8 %, respectively, and at 11 minutes a % inhibition of -11.7, 27.5 and 23.9 %, respectively. Although the inhibitory action of bovine and human SOD slightly increased from 3 to 11 minutes, the SOD activity of human IgG diminished by 11 minutes, indicating a switch from antioxidant to pro-oxidant activity.

4.4.3.2 Dual reagent assay (1:26 ratio – sample to reagent)

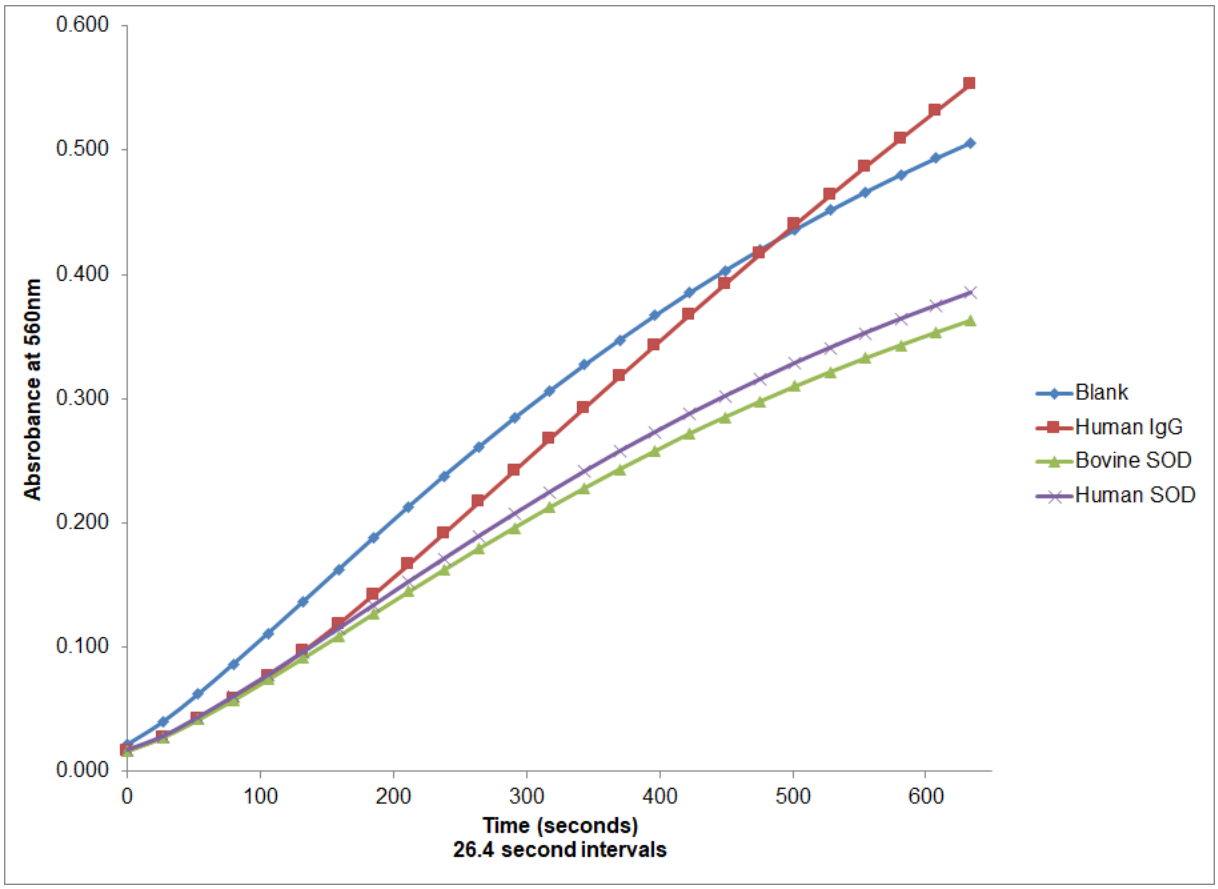

Figure 4.8: **Dual reagent AbSOD activity assay – 1:26 ratio**

The absorbance at 560 nm is plotted on the y-axis, versus the time (seconds) of the reaction on the x-axis. The absorbance of human IgG, bovine SOD and human SOD are visualised on the graph over 11 minutes. The assay used a ratio of 1:26 of sample to reagents and was performed in 96-well micro-tire plates.

At 3 minutes, the human IgG, bovine SOD and human SOD had a % inhibition of 11.0, 22.1 and 17.5 % and at 11 minutes, -10.9, 28.5 and 24.0 %, respectively. Similar to the 1:16 ratio of reagents, with 1:26 ratio the inhibitory action of bovine and human SOD increased from 3 to 11 minutes, the SOD activity of human IgG diminished by 11 minutes, indicating a switch from antioxidant to pro-oxidant activity.

It was determined the increased absorbance with the 1:26 format would improve the differentiation between patients and reduce imprecision between batches due to a reduction in the emphasis of a small change in absorbance, generating a larger change in absorbance. The 1:26 format was selected for all future experiments.

4.4.4 pH dependency of IgG in 96-well plates

The experiments described in this section (4.1.3) employed a SOD activity assay (1:26 format) in 96-well micro-titre plates, to investigate the effects of pH on the activity of purified mouse IgG, human IgG, bovine CuZnSOD and human CuZnSOD. All proteins were assayed at a molar concentration of 0.19 µmol/L, in three independent experiments ranging from pH 5.5 – 8.0, increasing in 0.5 pH increments. The reaction was recorded for 11 minutes. SOD activity was represented as % inhibition, where positive values were interpreted at observed SOD activity and negative values as pro-oxidant activity. The assay system consisted of 100 mM K_2HPO_4, 1.0 mM EDTA, 0.66 µM PMS, 5.0 mM of NADH and 100 µM NBT (see section 2.3.2).

4.4.4.1 pH dependency of bovine and human SOD

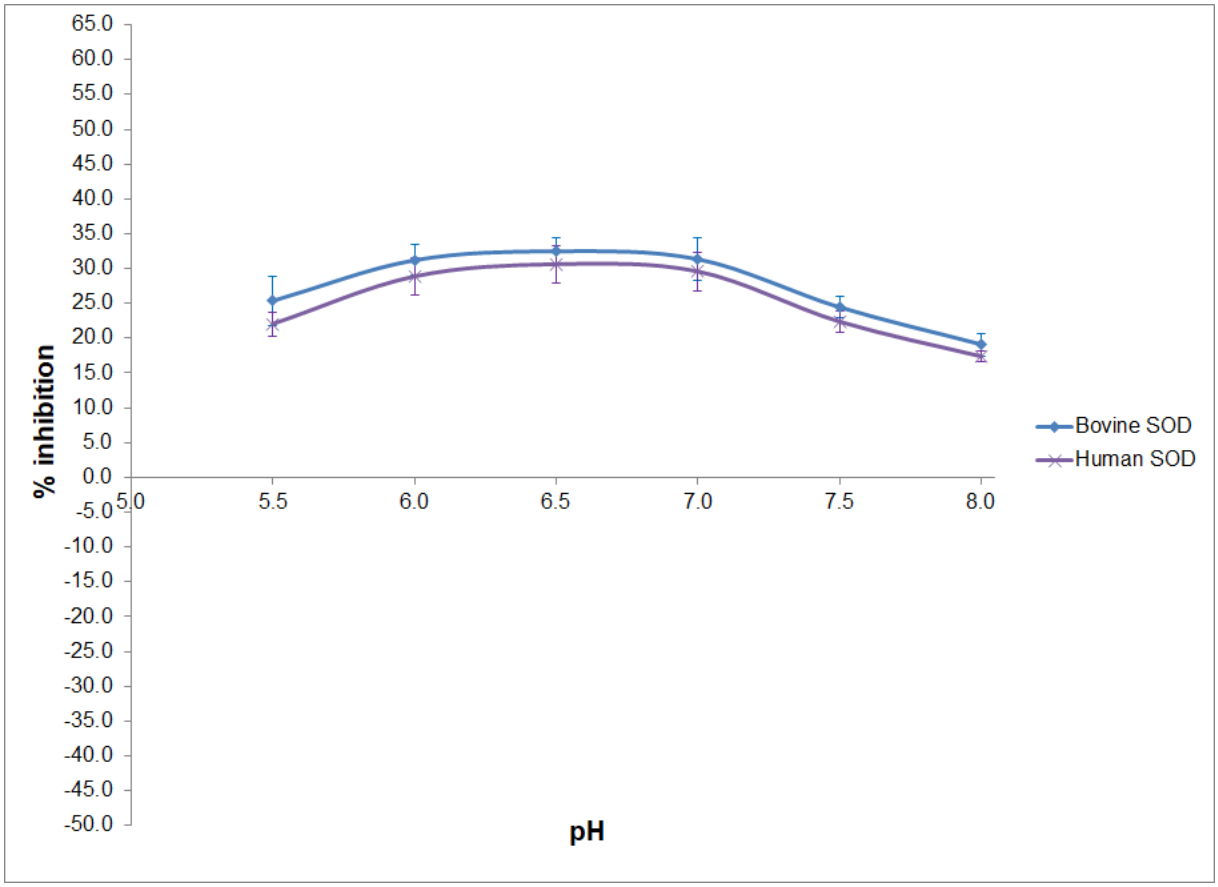

Figure 4.9: **CuZnSOD activity is independent of pH**

The percentage (%) inhibition is plotted on the y-axis, versus pH on the x-axis. The average % inhibition over 3 minutes of bovine SOD and human SOD from pH 5.5-8.0 are visualised, with error bars expressing ±1 SD.

Over 3 minutes, the % inhibition of human and bovine SOD from pH 5.5 to 7.5 was relatively constant (bovine SOD, 24.4 – 32.5 %; human SOD, 22.0 – 30.6%). Only at pH 8.0 was there a significant decrease in % inhibition for both enzymes (bovine SOD, 19.1 %; human SOD, 17.4%). Bovine SOD had slightly increased % inhibition compared to human SOD across the pH range.

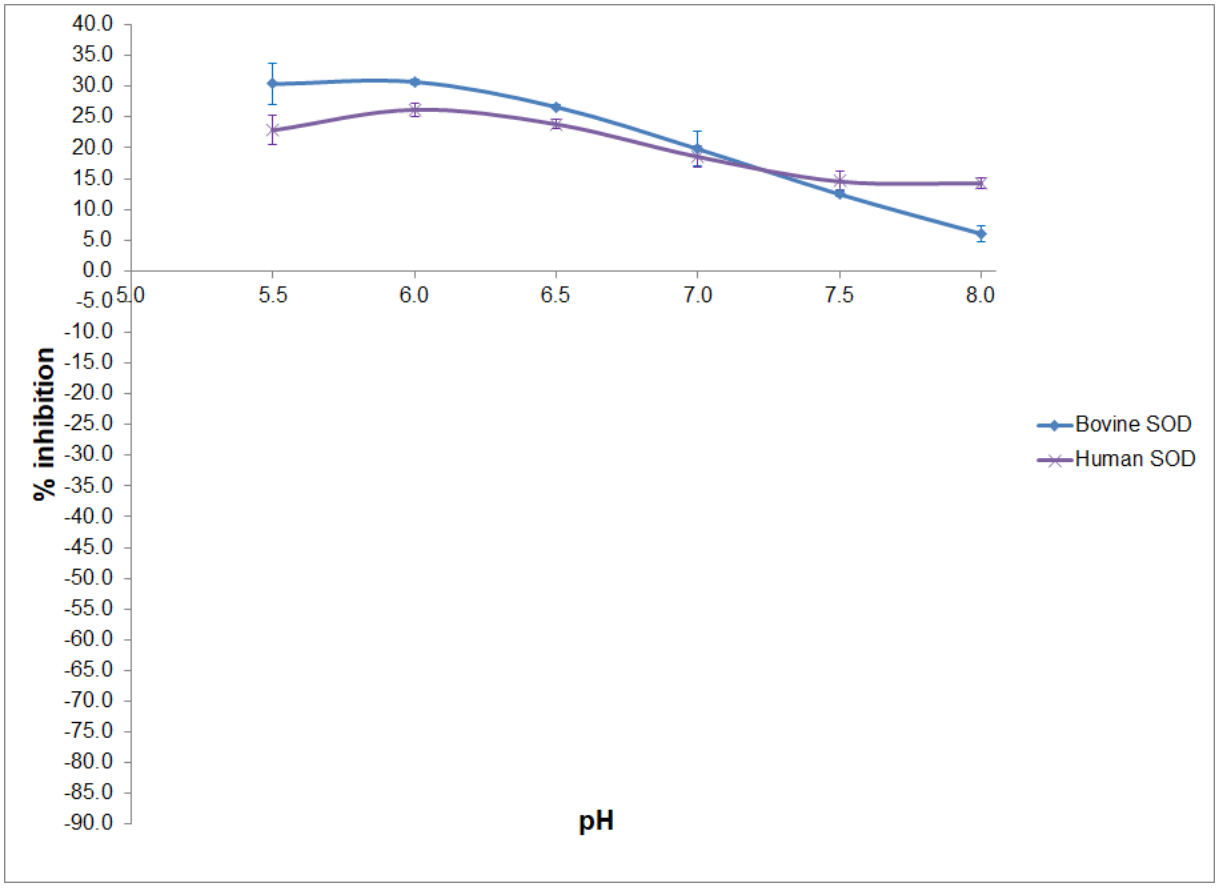

Figure 4.10: **CuZnSOD activity decreases from acid to alkali pH**
The percentage (%) inhibition is plotted on the y-axis, versus pH on the x-axis. The average % inhibition over 11 minutes of bovine SOD and human SOD from pH 5.5 – 8.0 are visualised, with error bars expressing ±1 standard deviation (SD).

The % inhibition of bovine and human SOD decreased as pH changed from acidic to alkaline (bovine SOD, 30.4 – 6.0 %; human SOD, 22.9 – 14.3 %) upon prolonged reaction time (11 minutes) with superoxide.

4.4.4.2 pH dependency of human and mouse IgG

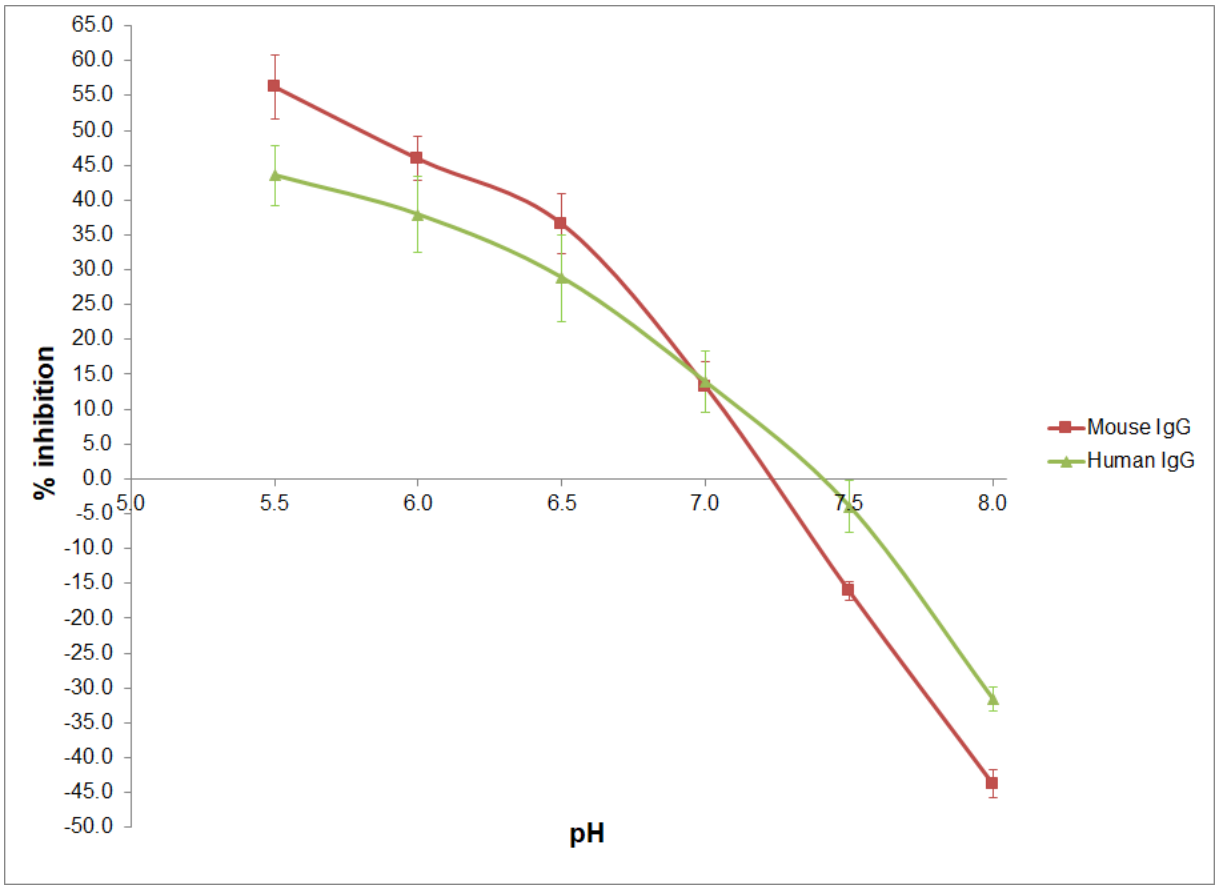

Figure 4.11: **AbSOD activity is inhibited from acid to alkali pH**
The percentage (%) inhibition is plotted on the y-axis, versus pH on the x-axis. The average % inhibition over 3 minutes of purified mouse IgG and human IgG from pH 5.5 – 8.0 are visualised with error bars, expressing ±1 standard deviation (SD).

Over 3 minutes, the % inhibition of mouse IgG and human IgG decreased as pH changed from acidic to alkaline (mouse IgG, 56.3 to -43.8 %; human IgG, 43.6 to -31.6 %). The change in % inhibition was greater for the mouse IgG (-100.1 %) than the human IgG (-75.2 %).

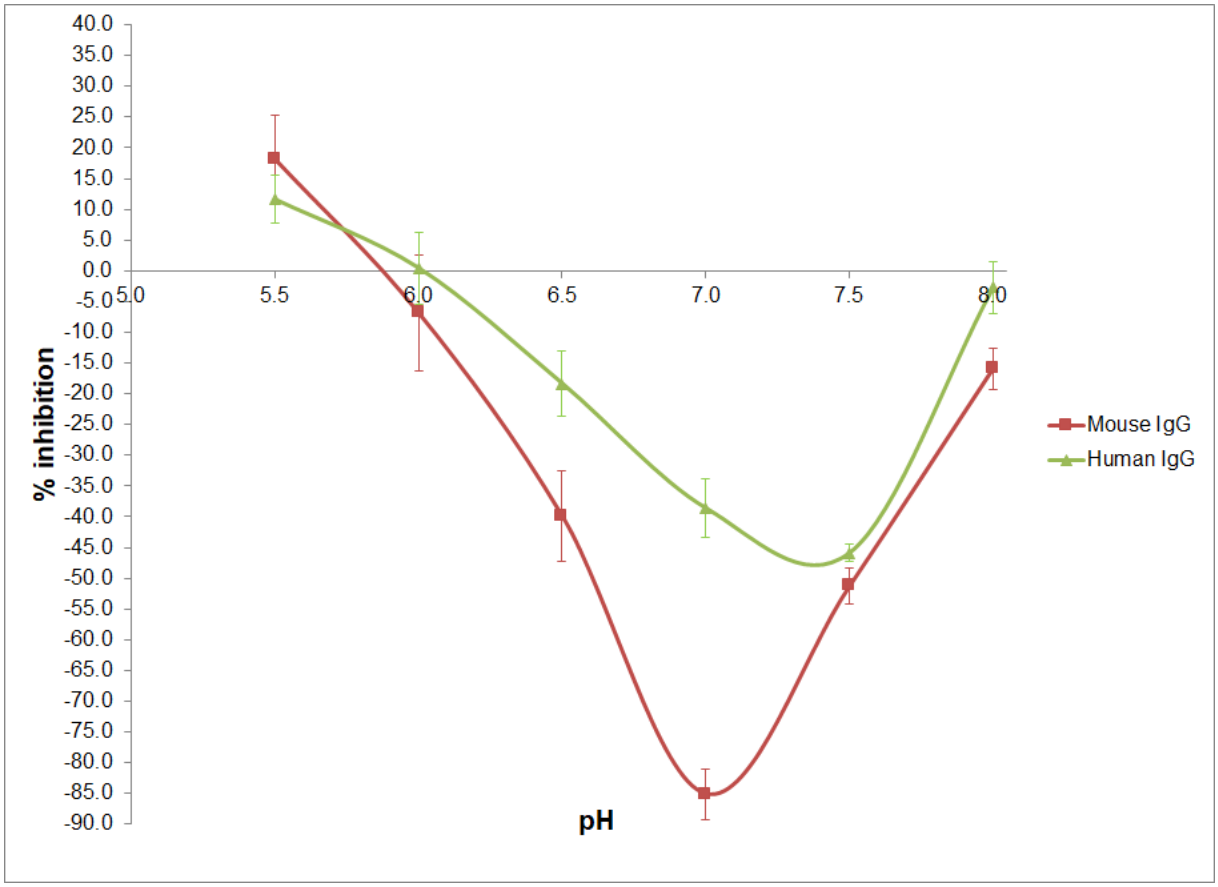

Figure 4.12: **Antibodies have pro-oxidant activity between pH 7.0 and 7.5**
The percentage (%) inhibition is plotted on the y-axis, versus pH on the x-axis. The average % inhibition over 11 minutes of mouse IgG and human IgG from pH 5.5 – 8.0 are visualised with error bars, expressing ±1 standard deviation (SD).

Over 11 minutes, as pH decreased from pH 5.5 to 7.0, the % inhibition of mouse IgG decreased (18.2 to -85.1 %), and from pH 5.5 to 7.5, the % inhibition of human IgG decreased (11.6 to -45.9 %). The change in decrease was greater for the mouse IgG (103.3 %) than human IgG (57.5 %). At pH 7.0 to 8.0, for mouse IgG (-85.1 to -15.9 %), and pH 7.5 to 8.0 for human IgG (-45.9 to -2.7 %) the % inhibition increased.

4.4.4.3 Comparing the activity of human SOD and IgG across pH

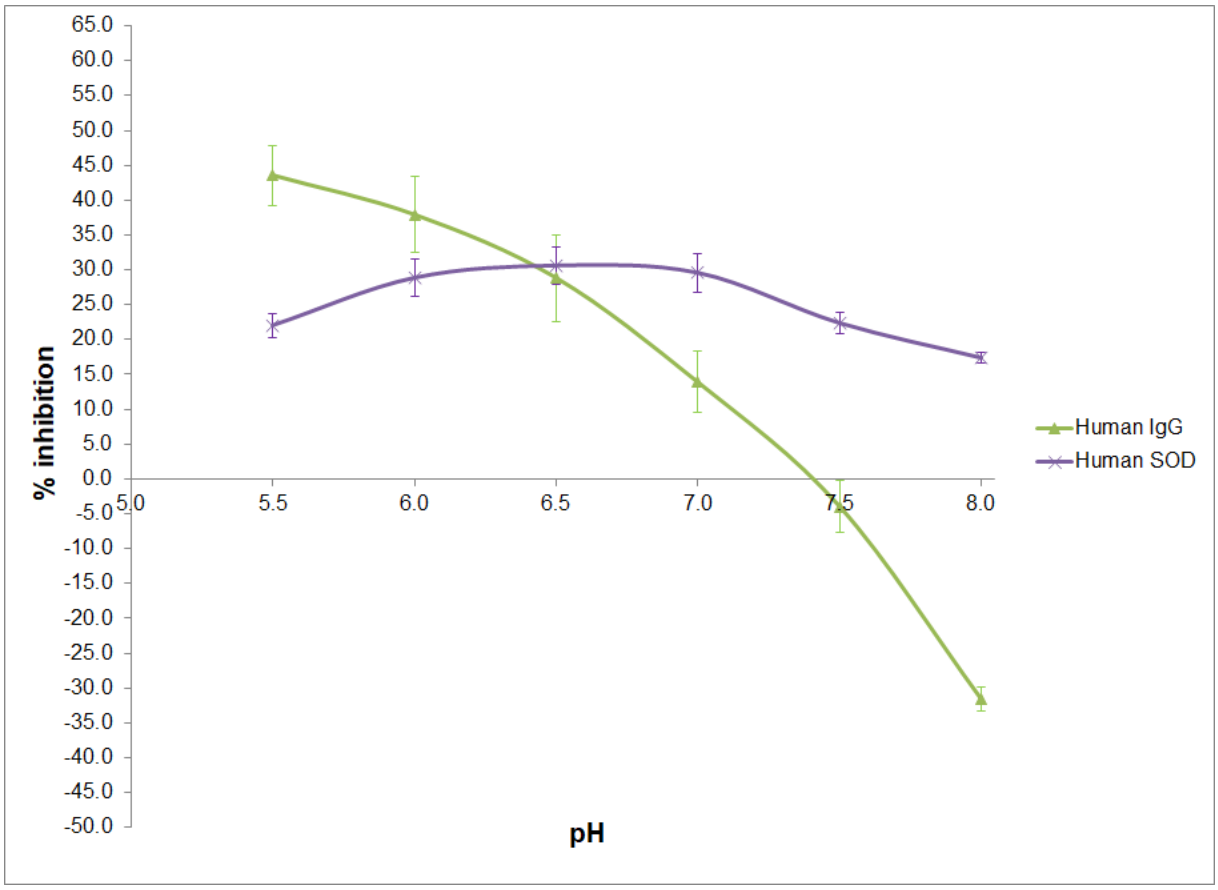

Figure 4.13: **Human SOD and IgG have opposing activity**

The percentage (%) inhibition is plotted on the y-axis, versus pH on the x-axis. The average % inhibition over 3 minutes of human SOD and purified mouse IgG from pH 5.5 – 8.0 are visualised with error bars, expressing ±1 standard deviation (SD).

Over 3 minutes, the % inhibition of human IgG significantly decreased as pH changed from acidic to alkaline (human IgG, 43.6 to -31.6 %). The % inhibition of human SOD from pH 5.5 to 7.5 was relatively static (human SOD, 22.0 – 30.6%). Only at pH 8.0 was there a significant decrease in % inhibition for human SOD (17.4%).

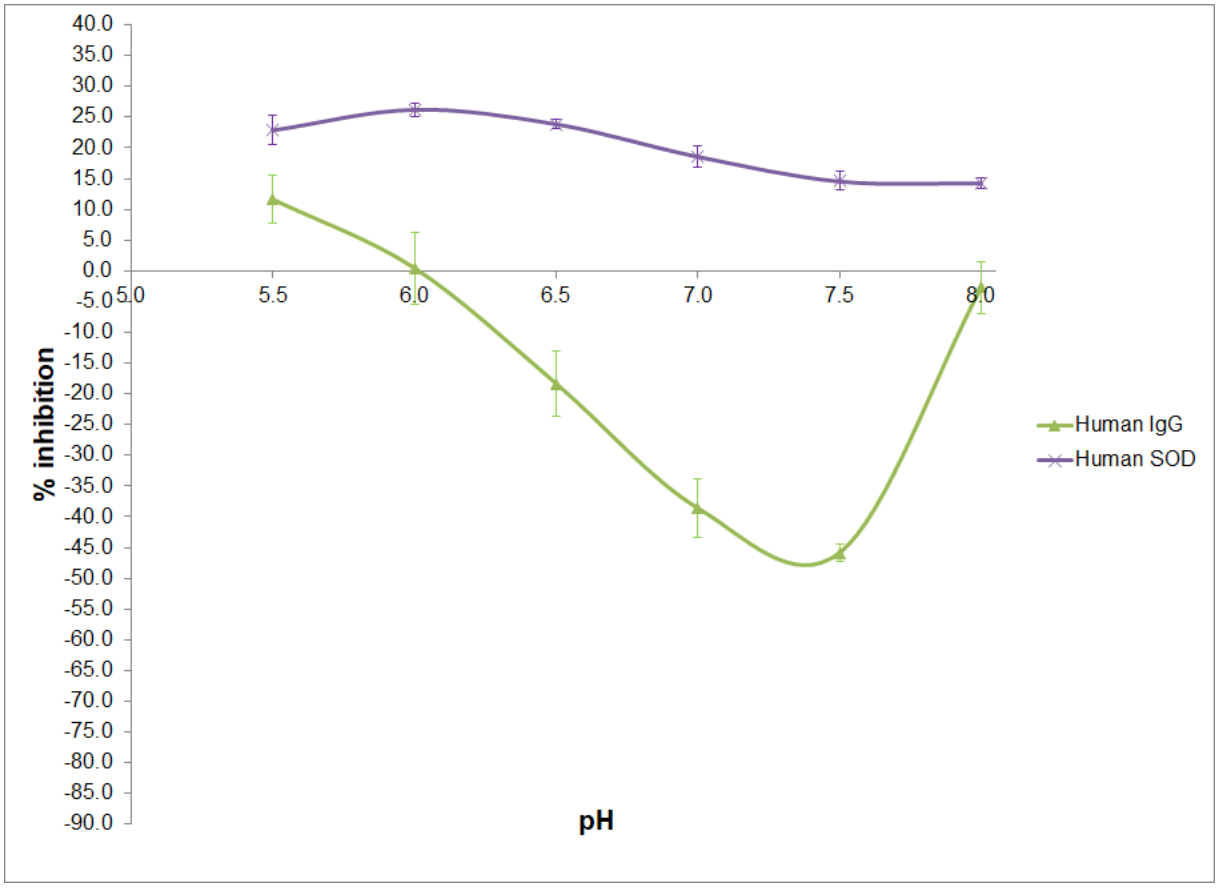

Figure 4.14: **Human SOD and mouse IgG have opposing activity**

The percentage (%) inhibition is plotted on the y-axis, versus pH on the x-axis. The average % inhibition over 11 minutes of human SOD and purified mouse IgG from pH 5.5 – 8.0 are visualised with error bars, expressing ±1 standard deviation (SD).

Over 11 minutes, as pH decreased from pH 5.5 to 7.5, the % inhibition of human IgG decreased (11.6 to -45.9 %). From pH 7.5 to 8.0, the % inhibition for human IgG (-45.9 to -2.7 %) increased. The % inhibition of human SOD decreased as pH changed from acidic to alkaline (human SOD, 22.9 – 14.3 %) upon prolonged reaction time with superoxide.

4.4.5 SOD activity after heat denaturation

The results reported in this section (4.4.5) were generated using a SOD activity assay (1:26 format) in 96-well micro-titre plates, to investigate the effects of heat treatment (85°C for 1 hour) on the activity of human IgG, purified mouse IgG and bovine CuZnSOD. All proteins were assayed at a molar concentration of 0.20 µmol/L, ranging from pH 5.5 – 7.5, increasing in 0.5 pH increments. The reaction was recorded for 3 minutes. SOD activity was represented as % inhibition, where positive values were interpreted at observed SOD activity and negative values as pro-oxidant activity. The assay system consisted of 100 mM K_2HPO_4, 1.0 mM EDTA, 0.66 µM PMS, 5.0 mM of NADH and 100 µM NBT (see section 2.3.2).

Table 4.1: ***Heat treatment of human IgG, mouse IgG and bovine SOD***

	% Inhibition									
pH	**5.5**		**6.0**		**6.5**		**7.0**		**7.5**	
Protein	**Fresh**	**Heat treated**	**Fresh**	**Heat treated**	**Fresh**	**Heat treated**	**Fresh**	**Heat treated**	**Fresh**	**Heat treated**
Human IgG	46.2	10.5	39.6	20.6	31.0	7.6	26.8	4.9	-0.6	0.1
Mouse IgG	56.5	56.4	45.3	59.6	39.4	48.1	26.0	36.5	-15.5	-34.0
Bovine SOD	28.0	50.4	30.4	49.4	33.3	43.5	34.9	43.3	26.2	5.3

After heat treatment the AbSOD activity of human IgG was decreased (pH 5.5 – 7.0) compared to human IgG that was not heat treated. However, at pH 7.5 the effect of heat treatment on AbSOD activity was negligible.

After heat treatment the AbSOD activity of mouse IgG was increased (pH 5.5 – 7.0). At pH 7.5 the mouse IgG had significantly higher pro-oxidant activity after heat treatment.

After heat treatment the activity of bovine SOD was increased (pH 5.5 – 7.0). At pH 7.5, the effect of heat treatment caused a reduction in SOD activity.

4.4.6 SOD activity after metal ion incubation

The results reported in this section (4.4.6) employed a SOD activity assay (1:26 format) in 96-well micro-titre plates, to investigate the effects of incubation of various concentrations of iron (II) sulphate (FeSO4) and copper (II) sulphate (CuSO4) on the SOD activity of human IgG and bovine SOD. All proteins were assayed at a molar concentration of 5.0 µmol/L, ranging from pH 5.5 – 7.5, increasing in 1.0 pH increments. The reaction was recorded for a total of 11 minutes with recordings of % inhibition taken at 3 and 11 minutes. The assay system consisted of 100 mM K_2HPO_4, 1.0 mM EDTA, 0.66 µM PMS, 5.0 mM of NADH and 100 µM NBT (see section 2.3.2).

Table 4.2: ***Copper and iron sulphate treatment of human SOD***

	% Inhibition					
pH	**5.5**		**6.5**		**7.5**	
Protein	**3 minutes**	**11 minutes**	**3 minutes**	**11 minutes**	**3 minutes**	**11 minutes**
Human SOD	17.3	15.8	29.6	22.0	22.7	10.5
Human SOD + 30 µM $CuSO_4$	10.8	11.6	25.5	20.6	20.7	10.9
Human SOD + 10 µM $CuSO_4$	12.0	12.2	25.9	20.5	21.5	13.8
Human SOD + 30 µM $FeSO_4$	14.4	12.3	23.2	19.1	20.4	14.4
Human SOD + 10 µM $FeSO_4$	11.4	11.6	22.5	19.3	18.9	13.7

The effect on SOD activity of human SOD, subjected to 48-hour incubation with physiological concentrations of copper and iron (in form sulphate salts), was investigated at pH 5.5, 6.5 and 7.5. A decrease in SOD activity was observed when SOD was incubated with $CuSO_4$ and $FeSO_4$ for 48 hours. At pH 5.5 and 6.0 the effect was negligible – however the decrease was more pronounced at pH 7.5 over 3 minutes reaction time. At pH 7.5, over 11 minutes reaction time there was a slight increase in inhibition observed with SOD incubated with metal ions.

Table 4.3: ***Copper and iron sulphate treatment of human IgG***

	% Inhibition					
pH	**5.5**		**6.5**		**7.5**	
Protein	**3 minutes**	**11 minutes**	**3 minutes**	**11 minutes**	**3 minutes**	**11 minutes**
Human IgG	34.9	11.9	27.6	-20.2	-16.8	-42.4
Human IgG + 30 µM $CuSO_4$	28.6	11.6	26.9	-18.4	-18.0	-27.5
Human IgG + 10 µM $CuSO_4$	32.7	13.8	30.3	-12.1	-12.3	-36.0
Human IgG + 30 µM $FeSO_4$	40.0	19.8	34.0	-5.4	-8.7	-42.7
Human IgG + 10 µM $FeSO_4$	36.4	12.4	30.6	-11.1	-12.6	-41.3

The effect of SOD activity of human IgG, subjected to 48-hour incubation with physiological concentrations of copper and iron (in form sulphate salts), was investigated at pH 5.5, 6.5 and 7.5. At pH 5.5, an increase in AbSOD activity was observed for antibodies incubated with $FeSO_4$, and a decrease in AbPro activity was observed at pH 6.5. At pH 6.5 and 7.5, there was a decrease in AbPro activity observed in antibodies incubated with $CuSO_4$ over a reaction time of 11 minutes.

4.5 Discussion

The experiments in chapter 4 set out to optimise a SOD activity assay for the determination of AbSOD activity. By assaying various concentrations of the reagents required for superoxide generation it was possible to generate an assay that had a blank (uninhibited production and detection of superoxide) absorbance of 1.0 over approximately 3 minutes at pH 7.4. The subsequent investigation of the effects of pH on AbSOD and SOD activity, first using a cuvette format of the assay, then a micro-titre plate format, enabled an increase in the concentration of SOD and IgG which increased the differences in response observed between the two proteins. Finally, heat-treatment and metal ion treatment, aimed to postulate the origin of the potential mechanism of enzyme activity by IgG's. The data generated was analysed and graphically represented in scatter plots using Microsoft Excel. The results in this chapter support the hypothesis that antibodies have superoxide dismutase activity, but for the first time highlight the potential pro-oxidant activity antibodies may have.

4.5.1 Superoxide detection from acid to alkali pH

There may be concerns about the reaction of superoxide across varying pH; acidic pH compared to alkali pH. The pH (potential of hydrogen) scale is logarithmic meaning for every change in 1 pH unit of a solution the concentration of hydrogen ions (H^+) changes by a factor of 10. In turn, as the number of H^+ ions increase so does the likelihood of superoxide existing in its protonated form. For this reason, it is important to have an appreciation of the pKa of the reaction $HO_2^{\bullet} \leftrightarrow H^+ + O_2^{\bullet -}$, which is approximately 4.8 (Bielski *et al.*, 1985). When the pH of a solution or environment is less numerically than the pKa of reaction, the compound will exist predominately in its protonated form. In contrast when the pH of a solution or environment is greater than the pKa of the reaction, the compound will exist predominantly in its deprotonated form.

Although the ratio of superoxide to hydroperoxyl will change across the pH range due to the change in hydrogen ions, with the pH range used in the experiments (pH 5.5 – 8.0) superoxide would be present predominantly in its deprotonated anionic form ($O_2^{\bullet -}$).

4.5.2 Increased concentration of NADH and PMS improves assay response

The reaction between NADH and PMS in presence of oxygen results in the formation of superoxide. The superoxide then reduces NBT to a formazan which has absorbance maxima at 560 nm. Increasing the concentration of NADH (from 1.0 – 5.0 mM) and PMS (0.11 to 0.66 µM) resulted in an increased absorbance obtained over 3 minutes of reaction at pH 7.4.

4.5.3 The SOD activity of albumin was negligible

The pH dependency of human and bovine albumin showed negligible effects on SOD activity in the assay. Although the antioxidant properties of albumin are well known (Taverna *et al.*, 2013), it did not affect the determination of superoxide dismutase activity. Thus, it can be concluded, it is unlikely the superoxide dismutase activity of antibodies is caused merely by interfering protein matrix effects.

4.5.4 Effects of heat-denaturation on SOD activity

The AbSOD activity of heat-treated human IgG was decreased between pH 5.5 – 7.0. It was likely the human IgG was denatured by heat, which could have caused unravelling of structure. Experiments by Petyaev and Hunt (1996), showed the AbSOD activity was localised to the binding site. Structural changes induced by heating may have obscured the binding site. In mouse IgG it was evident the heating may have been favourable for AbSOD activity. It is possible the increase in AbSOD activity observed was due to aggregation. Aggregation may have formed an immune complex that increased the effectiveness of superoxide dismutation.

Surprisingly, after heat treatment the activity of bovine SOD was increased (pH 5.5 – 7.0) and at pH 7.5, the effect of heat treatment caused a reduction in SOD activity. This may be because not all the SOD was denatured. CuZnSOD is an extremely stable enzyme resistant to heating and freezing, evident from its isolation during the manufacture of commercial SOD products. A study of CuZnSOD from *E. coli* observed dimeric structure was not required for efficient catalytic activity of SOD (Battistoni and Rotilio, 1995). It is possible even if denaturation of SOD occurred, it may have caused release of free copper (Cu^{2+}), which in may compete with NBT for superoxide ions.

4.5.5 Effects of metal ion treatment on SOD activity

The SOD activity of human CuZnSOD was generally decreased by incubation with metal ions for 48-hours. It is possible excess metal ions did not remain in the retentate after filter centrifugation. Alternatively, metal ions may have bound to the SOD, but upon exposure to acidic pH may have dissociated. In either circumstance, in the case of copper it may have caused an increase in free copper (Cu^{2+}), resulting in reduction of copper instead of reduction of NBT. Or in the case of iron, free iron (Fe^{2+}) may have participated in Fenton chemistry. In each case, copper and iron did not result in significantly different SOD activity of human CuZnSOD compared to native SOD.

The SOD activity of human IgG incubated with metal ions was more variable. With $FeSO_4$, there was an increase in AbSOD activity at pH 5.5 and a decrease in AbPro activity at pH 6.5. With $CuSO_4$, there was a decrease in AbPro activity at pH 6.5 – 7.5 over 11 minutes. Overall, these responses are the similar, i.e., a decreased formazan formation observed. This indicates iron ions may enhance AbSOD activity at acidic pH and copper ions may inhibit prooxidant activity from acidic to physiological pH. It is also possible, as observed with CuZnSOD, the copper ions may simply be competing with NBT for superoxide radicals.

4.5.6 pH dependency of CuZnSOD

The experiments in cuvettes and micro-titre plates yielded slightly different results for CuZnSOD. In the cuvette assay, the activity of bovine and human SOD increased from pH 5.5 – 8.0, whereas in the micro-titre plate assay the activity was almost independent of pH. It was likely the imprecision observed in the cuvette assay and the reduced concentration of SOD used were the primary causes of the differences between results. Although the results in cuvettes concur with those by Petyaev and Hunt (1996), the consensus in the literature aligns with our findings in the micro-titre assay, that the activity of CuZnSOD is independent of pH (Rotilio, Bray and Fielden, 1972; Ellerby *et al.*, 1996; Halliwell and Gutteridge, 2015d).

In the micro-titre plate experiments, the reaction recorded over 3 minutes and 11 minutes. This resulted in some inhibition of activity for bovine and human SOD, however bovine SOD was most adversely affected between pH 7.0 – 8.0. The prolonged reaction likely enabled an increased conversion of superoxide, causing accumulation of H_2O_2. It is known that H_2O_2 can have inhibitory effects on the activity of SOD and potentially cause the dissociation of copper from the active

site of SOD, which may participate in Fenton chemistry (Hodgson and Fridovich, 1975; Gottfredsen *et al.*, 2013).

4.5.7 pH dependency of IgG

The experiments between cuvettes and micro-titre plates were similar for IgG. In the cuvette experiments protein A agarose-purified mouse IgG and mouse IgG-ascites were compared, whereas in the micro-titre plate experiments purified mouse IgG and human IgG were compared. The general pattern observed gradual inhibition of AbSOD activity as pH changed from acid to alkali (pH 5.5 – 8.0). Although comparable to the work by Petyaev and Hunt (1996) between pH 5.5 – 6.5, beyond pH 6.5 superoxide dismutation by whole IgG was inhibited. In the pH dependency experiments by Petyaev and Hunt, NQ11.7.22-Fv fragments were compared to activity of CuZnSOD. In these experiments whole IgG was used, which is the likely cause of the differences in activity between pH 7.0 and 8.0.

Interestingly, the AbSOD activity at 11 minutes was observed to be very different to that at 3 minutes. At pH 7.0 for mouse IgG and at pH 7.5 for human IgG maximal pro-oxidant activity of antibodies (AbPro activity) was observed.

4.5.8 Function of AbPro activity?

The reason for the change from antioxidant (dismutation) to pro-oxidant activity is difficult to interpret as there are numerous possibilities. From a basic view, antibodies are causing the increased reduction of NBT to formazan. This indicates antibodies are producing excess superoxide. Antibodies may enhance the production of superoxide to aid in bacteria killing, similar in the way to phagocytes. There may also be other mechanisms causing the increase in reduction of NBT to formazan, more work would be required to determine how this occurs.

4.5.9 Conclusion

In summary, AbSOD activity (antioxidant activity) occurs over a short period of exposure to superoxide at acidic pH. Upon prolonged exposure to superoxide AbPro activity (pro-oxidant activity) follows, which occurs over a shorter time-course as the pH increases from acid to alkali (see section 5.3.1).

4.5.9.1 Clinical relevance of findings

It is likely the clinical implications of AbPro activity *in vivo* may be limited. The prolonged reaction time required for AbPro activity to occur is unlikely to be physiologically relevant. This is because the short half-life of free radicals, ROS and pro-oxidants such as superoxide (Marklund, 1976; Sies,1993), and the antioxidant capacity of tissues such as the blood which contain free dietary antioxidants and serum antioxidants such as albumin (Roche *et al.*, 2008), combined with the knowledge that the pH environments at which oxidative stress takes place in disease (sites of inflammation) are generally acidic (Lardner, 2001) and not alkali, when AbPro activity is more likely to occur, drastically reduces the potential impact of this type of AbPro activity.

However, the finding that AbSOD activity occurs over a shorter period of exposure at acidic pH may shed new light on the role and application of AbSOD in inflammation (inflammatory environments are associated with acidic pH (Lardner, 2001). The increase in immune cells that can produce superoxide such as neutrophils in acute inflammation and macrophages in chronic inflammation (Winterbourn, Kettle and Hampton, 2016), would increase the demand for molecules that can detoxify free radicals. The experiments in this chapter demonstrated that CuZnSOD activity is independent of pH, which may suggest there is not a requirement for antibodies with SOD activity. However, antibodies are far more ubiquitous and likely to be present at sites of infection and inflammation, so it's likely AbSOD activity would have a role here. There is potential that antibodies that yield this activity could be used therapeutically to provide antioxidant protection, injected directly to sites with inflammation and oxidative stress, e.g., rheumatic joints.

Chapter 5 explores the relationship between AbSOD and AbPro activity of antibodies isolated from patients with diseases associated with oxidative stress and immune dysfunction. This enhances the understanding of the potential role of redox antibodies in disease.

CHAPTER 5: AbSOD and pro-oxidant activity of antibodies in patients

5.1 Background

The role of antibodies with superoxide dismutase activity (AbSOD activity) is not yet fully understood. Petyaev *et al.* (1998), demonstrated the SOD activity detected in diseased atherosclerotic lesions was attributable to antibodies, which was increased at acidic pH (5.5-6.5) compared to physiological pH (7.0-7.4). It was suggested antibodies could serve to deliver SOD activity to sites of tissue damage (Petyaev *et al.*, 1998).

5.1.1 Physiological relevance of pH

From the work by Petyaev *et al.* (1996 and 1998) and the results presented in Chapter 4, it is apparent the local pH environment is key in the mechanism of AbSOD activity. This is significant as pH fluctuations occur frequently under pathological conditions at the cell surface, in local tissue, and even systemically. In cancer, the pH at the surfaces of highly metastatic cells within tumours was found to be pH 6.1 – 6.4 and in nonmetastatic tumours pH 6.7 – 6.9 (Anderson *et al.*, 2016). This is thought to be a common hallmark of cancers cells, due to the production of lactic acid in anaerobic glucose metabolism (Fais *et al.*, 2014) Additionally, acidic pH environments have been demonstrated in a variety of other tissues (Rajamäki *et al.*, 2013):

- In atherosclerotic plaques where values drop to pH 6.8.
- In synovial fluid of rheumatic joints where values may reach pH 6.8 – 7.1.
- Ischemic tissues during myocardial infarction and stroke where pH can fall to 6.0 – 6.5.
- In asthma, where the pH of exhaled breath condensate was measured to be pH 5.2 compared with pH 7.7 in ‘healthy’ controls.

Whether the SOD activity of antibodies at acidic and physiological pH are different in patients with cancer, autoimmune disease, and cardiovascular disease compared to ‘healthy’ controls has yet to be examined experimentally and this is the primary focus of this chapter.

5.1.2 Physiological relevance of time exposure

In general, ROS are highly reactive, short-lived molecules, having half-lives of nanoseconds (OH•), microseconds (HOO•) and seconds ($O_2^{\bullet-}$) (Sies, 1993), consequently, *in vivo* ROS will primarily react at their site of formation. However, the protonated form of superoxide, the hydroperoxyl radical ($HO_2^{\bullet}$), due to its lack of charge, can traverse membranes (de Grey, 2002). It has also been shown hydrogen peroxide (H_2O_2) can diffuse through specific members of the aquaporin family (Bienert *et al.*, 2007). Despite this, tissues such as the blood contain free dietary antioxidants and serum antioxidants such as albumin (Roche *et al.*, 2008). It is therefore unlikely the investigation of AbSOD activity over 185 seconds are reflective of AbSOD activity *in vivo.* However, the production of ROS is a dynamic process and in chronic conditions the continuous generation of ROS such as superoxide could mean prolonged exposure is representative of these circumstances. It has been shown where proteins are isolated from their cellular compartment (pH change) and antioxidant environment (lack of antioxidant defenses), they can be oxidatively modified and have enhanced pro-oxidant activity (Reeder *et al.*, 2002).

5.1.3 The redox activity of antibodies is multifaceted

The experiments carried out in Chapter 4, demonstrated the SOD activity of antibodies (AbSOD) was following short exposure to superoxide (oxidative stress environment), elevated at acidic pH, but significantly decreased at physiological pH. It was also revealed that AbSOD activity is a transient antioxidant process that switches to pro-oxidant activity upon prolonged exposure to superoxide (AbPro activity). The increase in alkalinity from pH 5.5 to 7.5 resulted in this transition occurring more rapidly.

Part of the experiments in this chapter investigated the initiation of pro-oxidant activity by human antibodies after prolonged exposure to an oxidative stress environment. Data presented in these chapters showed significant increases in the AbSOD activity and decreased AbPro activity for patients with multiple myeloma, between pH 6.0 – 7.4, and for breast cancer at pH 7.4, compared to ‘healthy’ controls. Additionally, on shorter exposure, significant increases in AbSOD activity were observed in antibodies isolated from serum samples at pH 5.5 for myocardial infarction and rheumatoid arthritis groups. Increased antioxidant activity

and decreased pro-oxidant activity of antibodies may therefore play a role in the pathology of cancer, autoimmune diseases, and cardiovascular diseases.

5.1.4 Patient group-specific hypotheses

5.1.4.1 'Healthy' controls

In previous studies, it was reported AbSOD activity was increased in atherosclerotic lesions (Petyaev *et al.*, 1998) and in multiple sclerosis (Smirnova *et al.*, 2020) compared to 'healthy' controls. It was therefore hypothesised the AbSOD activity of 'healthy' controls would be decreased in comparison to diseases associated with immune dysfunction and oxidative stress.

5.1.4.2 Rheumatoid Arthritis and Coeliac disease

Autoantibodies are detected in autoimmune diseases (such as coeliac disease and rheumatoid arthritis). Autoantibodies, which bind and react with self-antigens, arise from the diminishment of self-tolerance, which develops to induce pathology (Delves *et al.*, 2017b).

Rheumatoid arthritis (RA) is characterised by the presence of autoantibodies called rheumatoid factors, directed to the Fc region of IgG (Delves *et al.*, 2017c). Although not limited to a single immunoglobulin isotype, rheumatoid factors are commonly IgM or IgG. With this and the knowledge that the pH of synovial tissue is acidic in RA, it was hypothesised that AbSOD activity would be significantly increased at acidic pH in RA patients, compared to 'healthy' controls.

In coeliac disease (CD), an autoimmune reaction occurs that causes damage to the small intestine, the wheat protein gliadin undergoes deamidation by the enzyme tissue transglutaminase (TTG) increasing its immunogenicity. An immune response is mounted against gliadin, resulting in the development of antibodies to TTG, gliadin, and actin, however the mechanisms of how this occurs is unclear (Lebwohl, Sanders and Green, 2018). A study of the pH of the intestinal tract using the IntelliCap® system (an ingestible capsule that measures real-time pH), reported the small intestine had pH values of around pH 6.0 in proximal regions and slightly higher pH values of pH 7.0–8.0 in distal areas (Koziolek *et al.*, 2015). It was hypothesised the AbSOD activity in CD would be significantly increased at acidic pH in comparison to 'healthy' controls.

5.1.4.3 Myocardial infarction

Myocardial infarction (MI) is characterised by partial or complete blockage of blood flow (ischemia) to the myocardium (heart muscle) and an associated fall in pH (Rajamäki *et al.*, 2013). This results in damage to the myocardium due to lack of oxygen delivery to the tissue and release of troponin. Troponin is a protein that mediates muscle contraction. Anti-troponin I antibodies (ATAs) have been detected in Myocardial infarction and their presence has been associated with reduced improvement in left ventricular function (Leuschner *et al.*, 2008). Conversely, the presence of ATAs has also been associated with improved survival in chronic dilated cardiomyopathy, suggesting they may have protective effects (Doesch *et al.*, 2011). It was hypothesised the AbSOD activity observed in MI would be significantly increased in comparison to 'healthy' controls, at acidic pH.

5.1.4.4 Breast cancer

Breast cancer is characterised by the uncontrollable growth of malignant cells. Tumour-reactive antibodies can bind to cancer cells, which can result in disruption of their activity and several autoantibodies to tumour associated antigens (TAAs) have been detected in breast cancer (Garaud *et al.*, 2018). The pH at the surface and extracellular space near tumour cells is often acidic (Kato *et al.*, 2013).

It was hypothesised at acidic pH, the AbSOD activity observed in breast cancer would be significantly increased in comparison to 'healthy' controls.

5.1.4.5 Multiple myeloma and MGUS

Proliferations of monoclonal antibodies are produced in myeloma and MGUS which are malignant and pre-malignant disorders of the plasma B-cells characterised by the over-production of abnormal monoclonal immunoglobulins, respectively (Matsuura *et al.*, 2006). It was hypothesised the AbSOD activity observed in myeloma would be significantly increased in comparison to 'healthy' controls, at acidic pH. Similarly, it was hypothesised the AbSOD activity observed in MGUS would be significantly increased in comparison to 'healthy' controls, at acidic pH, however reduced in comparison to myeloma.

5.2 Aim

The aim of the work in this chapter was to determine whether the superoxide dismutase activity (AbSOD) and pro-oxidant activity (AbPro) of antibodies isolated from the serum of patients with clinically verified autoimmune diseases (coeliac disease and rheumatoid arthritis), various classes of cancer / pre-cancer (breast cancer, myeloma and MGUS) and cardiovascular disease (myocardial infarction), were increased or decreased compared to 'healthy' controls.

5.3 Materials and methods

The serum of patients (described in section 2.13.1) was purified using protein A/G agarose (described in detail in section 2.4). The results of assaying a random subset of 15 of the purified serum samples for IgG, IgM and IgA (appendix 5.1), revealed IgG was the primary immunoglobulin isotype captured during purification, with non-detectable concentrations of IgA or IgM.

All purified antibody samples were assayed with the Siemens IgG assay (described in section 2.5) and diluted to a concentration of 0.5 mg/mL, prior to antibody superoxide dismutase activity (AbSOD factor) determination, detailed in section 2.7. In total, the data from 19- 'healthy' controls and 59- patients (were analysed using IBM SPSS Statistics 26. Details for the selection of the statistical tests are described in section 2.13. The gender frequency and age range across disease and control groups can be seen in appendix 2.5.

5.3.1 AbSOD activity (AbSOD factor)

Antibody superoxide dismutase (AbSOD) activity was measured using the AbSOD activity assay (NADH/PMS – NBT) described in section 2.3.2. For the comparison of AbSOD activity between patients across varying pH ranges (5.5 - 7.4), over extended time periods (approximately 3, 5 and 11 minutes), AbSOD activity is represented as calculated AbSOD factor (Figure 5.1).

$$AbSOD\ factor = \frac{Patient\ AbSOD\ activity\ absorbance}{'Blank'\ absorbance}$$

Figure 5.1: AbSOD factor equation.

A patients AbSOD activity absorbance divided by the 'Blank' reaction absorbance is the AbSOD factor.

Table 5.1: ***AbSOD activity (AbSOD factor) explained.***

The purpose of AbSOD absorbance factor (AbSOD factor) is to enable the comparison of the SOD and pro-oxidant activity of antibodies between the pH ranges assayed, over different periods of exposure.

Patient absorbance related to 'blank' absorbance	AbSOD factor
When patient absorbance at time 'x' is greater than the 'blank' absorbance at time 'x', the antibody superoxide dismutase activity is decreased, and antibodies have pro-oxidant activity.	If AbSOD factor is >1.0 then antibodies have AbPro / pro-oxidant activity.
When patient absorbance at time 'x' is less than the 'blank' at time 'x', the antibody superoxide dismutase activity is increased, and antibodies have antioxidant activity.	If AbSOD factor is <1.0 then antibodies have AbSOD / antioxidant activity.
When patient absorbance at time 'x' is the same as the 'blank' at time 'x', the antibody superoxide dismutase activity is neither increased or decreased, and antibodies have neither pro-oxidant nor antioxidant activity.	If AbSOD factor is 1.0 then antibodies have neither antioxidant nor pro-oxidant activity.

5.4 Results

5.4.1 Antibody superoxide dismutase activity pH 5.5-7.4 – 185 seconds

5.4.1.1 pH 5.5 – 185 seconds

The descriptive statistics associated with AbSOD activity (antibody superoxide dismutase activity – AbSOD factor) at pH 5.5, over approximately 3 minutes, across the seven patient groups are reported in Table 5.2. The rheumatoid arthritis group was associated with the numerically smallest mean AbSOD factor (*M* = 0.749), and the 'healthy' control group was associated with the highest mean AbSOD factor (*M* = 0.803). To test the hypothesis that the seven patient groups had different AbSOD activity (AbSOD factor), a one-way (between-groups) ANOVA was performed. Prior to conducting the ANOVA, the assumption of normality was evaluated and determined to be satisfied as the seven groups' distributions were associated with a skew and kurtosis less than |<2.0| and |<9.0|, respectively (Schmider, Zielger, Danay, Beyer and Bühner, 2010; see Table 5.2). Furthermore, the assumption of homogeneity of variances was tested and satisfied via Levene's F test, $F(6, 71) = 1.772$, $p = .117$.

The independent between-groups ANOVA generated a statistically significant result, $F(6, 71) = 2.881$, $p = .014$. Thus, the null hypothesis of no differences between the AbSOD factor means in different disease groups was rejected. To evaluate the differences between the seven means further, simultaneous single step Tukey Kramer multiple comparisons were performed. As can be seen in Table 5.3, one of the six comparisons were statistically significant ($p < 0.05$). Furthermore, the statistically significant differences between the means were associated with a small to moderate effect size based on Cohen's (1992) guidelines. A visual depiction of the means and 95% confidence intervals is presented in Figure 5.2.

It can be observed that the mean AbSOD factor (pH 5.5 at 185 seconds) of all groups was less than 1.0. This showed all antibodies at pH 5.5, demonstrated antioxidant activity. The AbSOD factor of disease groups tended to be lower than the 'healthy' control group, indicating increased AbSOD activity in these disease groups. The rheumatoid arthritis group had significantly increased AbSOD activity compared to the 'healthy' control group.

Table 5.2: ***Descriptive statistics – AbSOD factor at pH 5.5 (185 seconds)***

Descriptive statistics for antibody superoxide dismutase activity (AbSOD factor) at pH 5.5 (185 seconds) observed in control and patient disease groups

Disease group	N	M (Absorbance factor)	SD	Skew	Kurtosis
'Healthy' Control	19	0.803	0.041	-0.438	-0.316
Rheumatoid Arthritis	7	0.749	0.010	-0.627	0.232
Coeliac Disease	11	0.793	0.030	1.123	2.093
Myocardial Infarction	6	0.759	0.035	0.205	-2.392
Breast Cancer	7	0.785	0.042	-1.052	0.286
Monoclonal Gammopathy of Unknown Significance	7	0.763	0.037	0.140	0.072
Myeloma	21	0.795	0.044	-0.048	-0.325

Table 5.3: ***Tukey Kramer – AbSOD factor at pH 5.5 (185 seconds)***

Results associated with Tukey Kramer multiple comparisons analysis

Comparison			*p*	*g*
'Healthy' Control	-	Rheumatoid Arthritis	0.035	0.30
'Healthy' Control	-	Coeliac Disease	0.991	0.06
'Healthy' Control	-	Myocardial Infarction	0.180	0.24
'Healthy' Control	-	Breast Cancer	0.930	0.10
'Healthy' Control	-	Monoclonal Gammopathy of Unknown Significance	0.228	0.22
'Healthy' Control	-	Myeloma	0.994	0.04

Note. N = 19 for 'Healthy' Control, 7 for Rheumatoid Arthritis, 11 for Coeliac Disease, 6 for Myocardial Infarction, 7 for Breast Cancer, 7 for Monoclonal Gammopathy of Unknown Significance and 21 for Myeloma; p = significance; g = Hedge's g

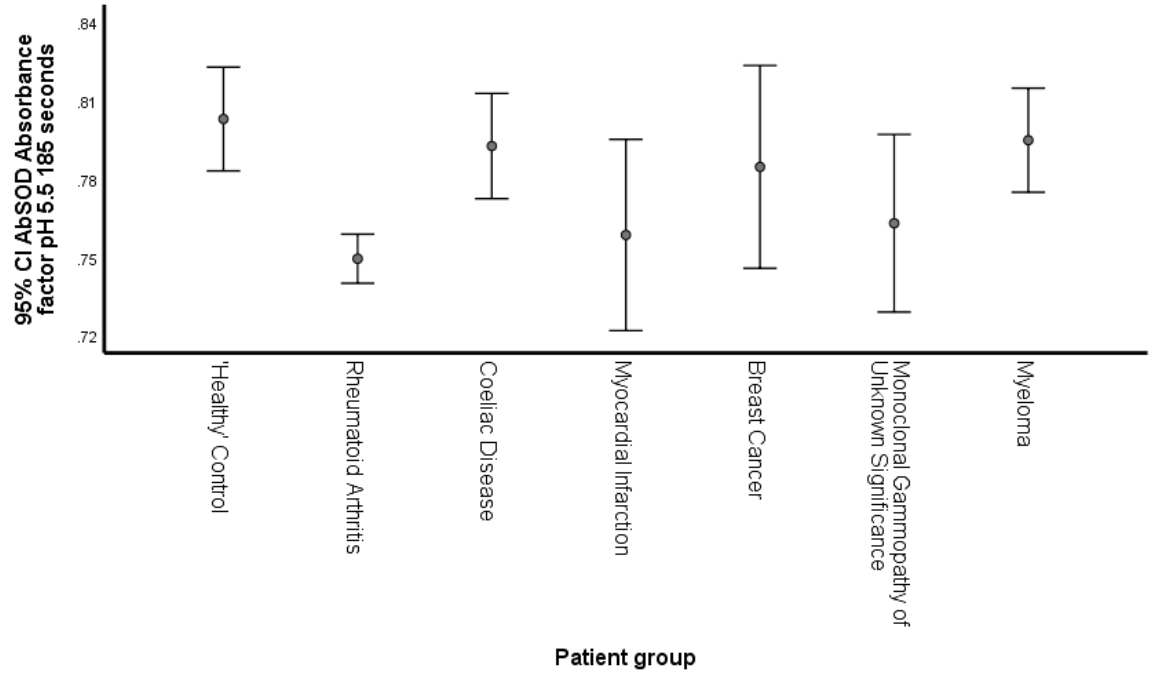

Figure 5.2: **Bar chart of AbSOD factor pH 5.5 at 185 seconds**

Bar chart with antibody superoxide dismutase activity (AbSOD factor pH 5.5 at 185 seconds) means and 95% confidence intervals observed in 'healthy' control and disease groups.

5.4.1.2 pH 6.0 – 185 seconds

The descriptive statistics associated with AbSOD activity (antibody superoxide dismutase activity – AbSOD factor) at pH 6.0, over approximately 3 minutes, across the seven patient groups are reported in Table 5.4. The rheumatoid arthritis group was associated with the numerically smallest mean AbSOD factor (M = 0.748) and myeloma group was associated with the highest mean AbSOD factor (M = 0.787). To test the hypothesis that the seven patient groups had different AbSOD activity (AbSOD factor), a one-way (between-groups) ANOVA was performed. Prior to conducting the ANOVA, the assumption of normality was evaluated and determined to be satisfied for six of the seven groups, where distributions were associated with a skew and kurtosis less than |<2.0| and |<9.0|, respectively but violated for myocardial Infarction, where skewness was greater than 2.0; (Schmider, Zielger, Danay, Beyer and Bühner, 2010; see Table 5.4). Furthermore, the assumption of homogeneity of variances was tested and satisfied via Levene's F test, $F(6, 71) = 1.794$, $p = .113$.

The independent between-groups ANOVA generated a statistically non-significant result, $F(6, 71) = 1.743$, $p = .124$. Thus, the null hypothesis of no differences between the AbSOD factor means could not be rejected. A visual depiction of the means and 95% confidence intervals are presented in Figure 5.3.

It can be observed that the mean AbSOD factor (pH 6.0 at 185 seconds) of all groups was less than 1.0, showing AbSOD activity. The error bars of AbSOD factor of the disease and 'healthy' control groups overlap indicating no statistically significant differences were present.

Table 5.4: ***Descriptive statistics – AbSOD factor at pH 6.0 (185 seconds)***

Descriptive statistics for antibody superoxide dismutase activity (AbSOD factor) at pH 6.0 (185 seconds) observed in control and patient disease groups

Disease group	N	M (Absorbance factor)	SD	Skew	Kurtosis
'Healthy' Control	19	0.775	0.021	-1.607	2.813
Rheumatoid Arthritis	7	0.748	0.021	1.680	3.305
Coeliac Disease	11	0.784	0.029	-1.553	2.584
Myocardial Infarction	6	0.757	0.031	2.303	5.496
Breast Cancer	7	0.779	0.037	-0.434	-1.320
Monoclonal Gammopathy of Unknown Significance	7	0.777	0.034	0.327	-0.873
Myeloma	21	0.787	0.042	0.196	-0.730

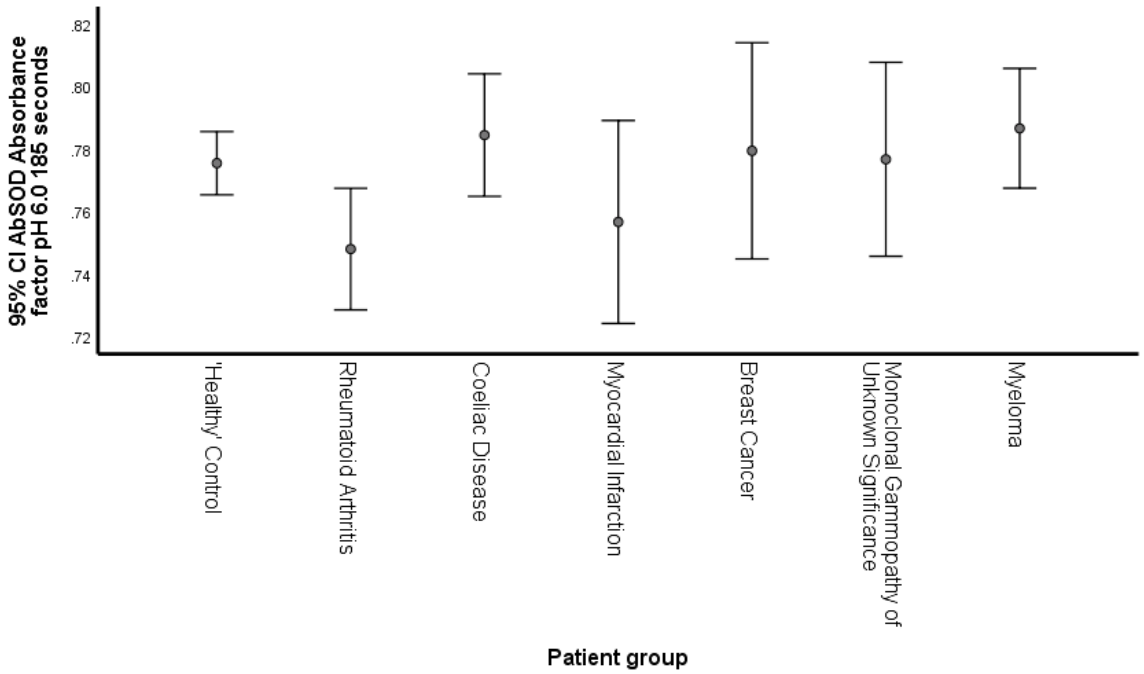

Figure 5.3: **Bar chart of AbSOD factor pH 6.0 at 185 seconds**

Bar chart with antibody superoxide dismutase activity (AbSOD factor pH 6.0 at 185 seconds) means and 95% confidence intervals observed in 'healthy' control and disease groups.

5.4.1.3 pH 6.5 – 185 seconds

The descriptive statistics associated with AbSOD activity (antibody superoxide dismutase activity – AbSOD factor) at pH 6.5, over approximately 3 minutes, across the seven patient groups are reported in Table 5.5. The myocardial infarction group was associated with the numerically smallest mean AbSOD factor (*M* = 0.724) and 'healthy' control group was associated with the highest mean AbSOD factor (*M* = 0.795). To test the hypothesis that the seven patient groups had different AbSOD activity (AbSOD factor), a one-way (between-groups) ANOVA was performed. Prior to conducting the ANOVA, the assumption of normality was evaluated and determined to be satisfied as the seven groups' distributions were associated with a skew and kurtosis less than |<2.0| and |<9.0|, respectively (Schmider, Zielger, Danay, Beyer and Bühner, 2010; see Table 5.5). The assumption of homogeneity of variances was tested and violated, as assessed by Levene's F test, $F(6, 71) = 3.069$, $p = .010$.

The independent between-groups Welch ANOVA generated a statistically non-significant result, $F(6, 21.424) = 1.293$, $p = .302$. Thus, the null hypothesis of no differences between the AbSOD factor means could not be rejected. A visual depiction of the means and 95% confidence intervals are presented in Figure 5.4.

It can be observed that the mean AbSOD factor (pH 6.5 at 185 seconds) of all groups was less than 1.0, showing AbSOD activity. The error bars of AbSOD factor across the disease and 'healthy' control groups overlap indicating no statistically significant differences were present. Although the average AbSOD activity is much lower for the myocardial infarction group, the standard deviation in comparison to the other groups is much larger.

Table 5.5: ***Descriptive statistics – AbSOD factor at pH 6.5 (185 seconds)***

Descriptive statistics for antibody superoxide dismutase activity (AbSOD factor) at pH 6.5 (185 seconds) observed in control and patient disease groups

Disease group	N	M (Absorbance factor)	SD	Skew	Kurtosis
'Healthy' Control	19	0.795	0.019	0.280	-1.109
Rheumatoid Arthritis	7	0.786	0.024	-0.113	-1.170
Coeliac Disease	11	0.783	0.048	-1.263	1.244
Myocardial Infarction	6	0.724	0.061	-0.454	-1.221
Breast Cancer	7	0.794	0.024	-0.305	-0.384
Monoclonal Gammopathy of Unknown Significance	7	0.794	0.048	1.520	3.487
Myeloma	21	0.791	0.040	0.968	1.484

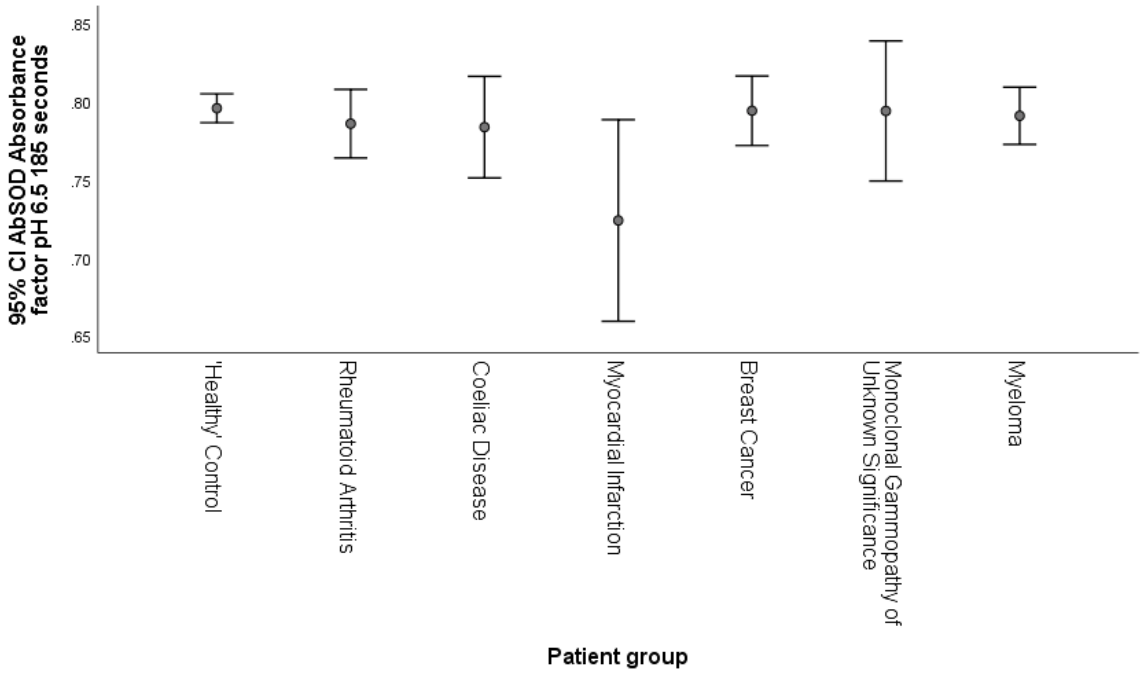

Figure 5.4: **Bar chart of AbSOD factor pH 6.5 at 185 seconds**

Bar chart with antibody superoxide dismutase activity (AbSOD factor pH 6.5 at 185 seconds) means and 95% confidence intervals observed in 'healthy' control and disease groups.

5.4.1.4 pH 7.0 – 185 seconds

The descriptive statistics associated with AbSOD activity (antibody superoxide dismutase activity – AbSOD factor) at pH 7.0, over approximately 3 minutes, across the seven patient groups are reported in Table 5.6. The myeloma group was associated with the numerically smallest mean AbSOD factor (*M* = 0.829) and 'healthy' control group was associated with the highest mean AbSOD factor (*M* = 0.876). To test the hypothesis that the seven patient groups had different AbSOD activity (AbSOD factor), a one-way (between-groups) ANOVA was performed. Prior to conducting the ANOVA, the assumption of normality was evaluated and determined to be satisfied as the seven groups' distributions were associated with a skew and kurtosis less than |<2.0| and |<9.0|, respectively (Schmider, Zielger, Danay, Beyer and Bühner, 2010; see Table 5.6). The assumption of homogeneity of variances was tested and violated, as assessed by Levene's F test, $F(6, 71) = 2.902$, $p = .014$.

The independent between-groups Welch ANOVA generated a statistically significant result, $F(6, 21.353) = 2.597$, $p = 0.048$. Thus, the null hypothesis of no differences between the AbSOD factor means in different disease groups was rejected. To evaluate the differences between the seven means further, Games-Howell comparisons were performed. As can be seen in Table 5.7, one of the six comparisons were statistically significant ($p < 0.05$). Furthermore, the statistically significant differences between the means were associated with a moderate to large effect size based on Cohen's (1992) guidelines. A visual depiction of the means and 95% confidence intervals is presented in Figure 5.5.

It can be observed that the mean AbSOD factor (pH 7.0 at 185 seconds) of all the groups was less than 1.0 (AbSOD activity) and the disease groups tended to be lower than the 'healthy' control group. The myeloma group had significantly increased AbSOD activity compared to the 'healthy' control group.

Table 5.6: ***Descriptive statistics – AbSOD factor at pH 7.0 (185 seconds)***

Descriptive statistics for antibody superoxide dismutase activity (AbSOD factor) at pH 7.0 (185 seconds) observed in control and patient disease groups

Disease group	N	M (Absorbance factor)	SD	Skew	Kurtosis
'Healthy' Control	19	0.876	0.015	1.175	1.546
Rheumatoid Arthritis	7	0.874	0.024	-1.177	2.403
Coeliac Disease	11	0.862	0.045	-1.176	2.972
Myocardial Infarction	6	0.846	0.039	-0.654	-0.449
Breast Cancer	7	0.874	0.018	0.022	-2.319
Monoclonal Gammopathy of Unknown Significance	7	0.870	0.056	1.459	2.280
Myeloma	21	0.829	0.054	1.261	2.646

Table 5.7: ***Games-Howell – AbSOD factor at pH 7.0 (185 seconds)***

Results associated with Games-Howell multiple comparisons analysis

Comparison			*p*	*g*
'Healthy' Control	-	Rheumatoid Arthritis	1.000	0.03
'Healthy' Control	-	Coeliac Disease	0.961	0.20
'Healthy' Control	-	Myocardial Infarction	0.696	0.43
'Healthy' Control	-	Breast Cancer	1.000	0.03
'Healthy' Control	-	Monoclonal Gammopathy of Unknown Significance	1.000	0.09
'Healthy' Control	-	Myeloma	0.007	0.61

Note. N = 19 for 'Healthy' Control, 7 for Rheumatoid Arthritis, 11 for Coeliac Disease, 6 for Myocardial Infarction, 7 for Breast Cancer, 7 for Monoclonal Gammopathy of Unknown Significance and 21 for Myeloma; *p* = significance; *g* = Hedge's g

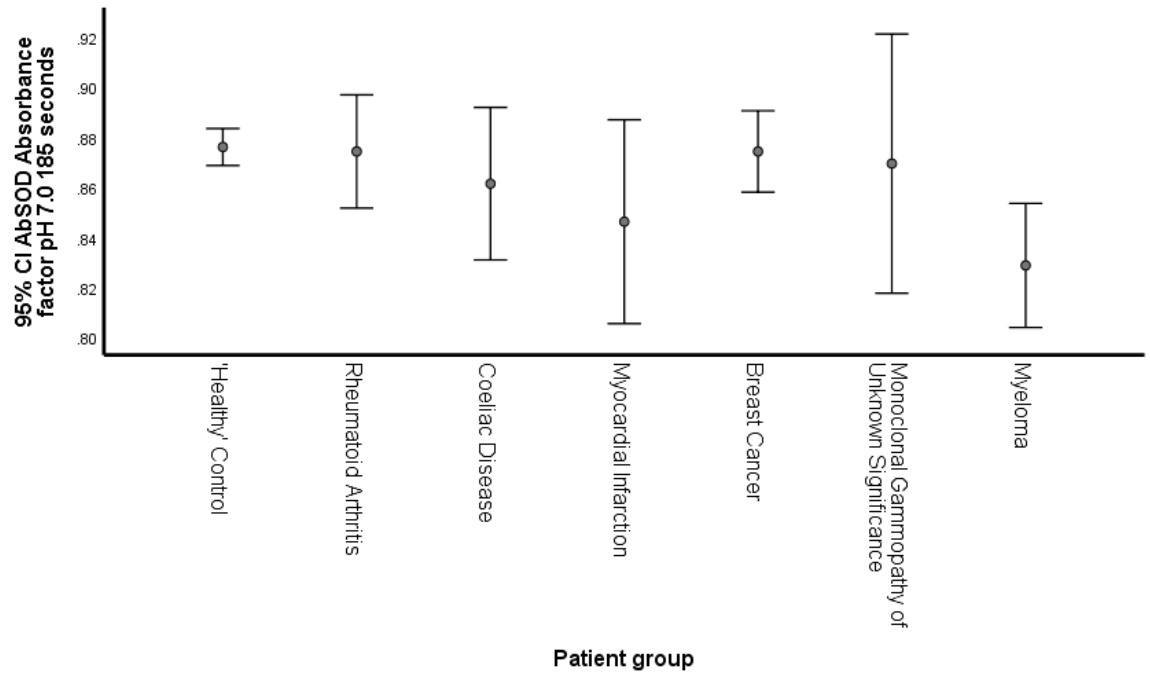

Figure 5.5: **Bar chart of AbSOD factor pH 7.0 at 185 seconds**

Bar chart with antibody superoxide dismutase activity (AbSOD factor pH 7.0 at 185 seconds) means and 95% confidence intervals observed in 'healthy' control and disease groups.

5.4.1.5 pH 7.4 – 185 seconds

The descriptive statistics associated with AbSOD activity (antibody superoxide dismutase activity – AbSOD factor) at pH 7.0, over approximately 3 minutes, across the seven patient groups are reported in Table 5.8. The myeloma group was associated with the numerically smallest mean AbSOD factor (*M* = 0.904) and rheumatoid arthritis group was associated with the highest mean AbSOD factor (*M* = 0.973). To test the hypothesis that the seven patient groups had different AbSOD activity (AbSOD factor), a one-way (between-groups) ANOVA was performed. Prior to conducting the ANOVA, the assumption of normality was evaluated and determined to be satisfied as the seven groups' distributions were associated with a skew and kurtosis less than |<2.0| and |<9.0|, respectively (Schmider, Zielger, Danay, Beyer and Bühner, 2010; see Table 5.8). The assumption of homogeneity of variances was tested and violated, as assessed by Levene's F test, $F(6, 71) = 2.904$, $p = .014$.

The independent between-groups Welch ANOVA generated a statistically significant result, $F(6, 20.902) = 3.259$, $p = .020$. Thus, the null hypothesis of no differences between the AbSOD factor means in different disease groups was rejected. To evaluate the differences between the seven means further, Games-Howell comparisons were performed. As can be seen in Table 5.9, one of the six comparisons were statistically significant ($p < 0.05$). Furthermore, the statistically significant differences between the means were associated with a moderate to large effect size based on Cohen's (1992) guidelines. A visual depiction of the means and 95% confidence intervals is presented in Figure 5.6. It can be observed that the AbSOD factor (pH 7.4 at 185 seconds) of all the groups was less than 1.0 (AbSOD activity). The myeloma group had significantly increased AbSOD activity compared to the 'healthy' control group.

Table 5.8: ***Descriptive statistics – AbSOD factor at pH 7.4 (185 seconds)***

Descriptive statistics for antibody superoxide dismutase activity (AbSOD factor) at pH 7.4 (185 seconds) observed in control and patient disease groups

Disease group	N	M (Absorbance factor)	SD	Skew	Kurtosis
'Healthy' Control	19	0.958	0.023	0.387	-0.466
Rheumatoid Arthritis	7	0.973	0.046	-0.213	-0.718
Coeliac Disease	11	0.954	0.036	-0.944	1.178
Myocardial Infarction	6	0.920	0.072	-0.181	-2.694
Breast Cancer	7	0.960	0.037	-0.134	-2.265
Monoclonal Gammopathy of Unknown Significance	7	0.939	0.057	0.514	1.419
Myeloma	21	0.904	0.051	0.735	0.436

Table 5.9: ***Games-Howell – AbSOD factor at pH 7.4 (185 seconds)***

Results associated with Games-Howell multiple comparisons analysis

Comparison			*p*	*g*
'Healthy' Control	-	Rheumatoid Arthritis	0.972	-0.15
'Healthy' Control	-	Coeliac Disease	1.000	0.04
'Healthy' Control	-	Myocardial Infarction	0.852	0.35
'Healthy' Control	-	Breast Cancer	1.000	-0.02
'Healthy' Control	-	Monoclonal Gammopathy of Unknown Significance	0.973	0.18
'Healthy' Control	-	Myeloma	0.003	0.51

Note. N = 19 for 'Healthy' Control, 7 for Rheumatoid Arthritis, 11 for Coeliac Disease, 6 for Myocardial Infarction, 7 for Breast Cancer, 7 for Monoclonal Gammopathy of Unknown Significance and 21 for Myeloma; *p* = significance; *g* = Hedge's g

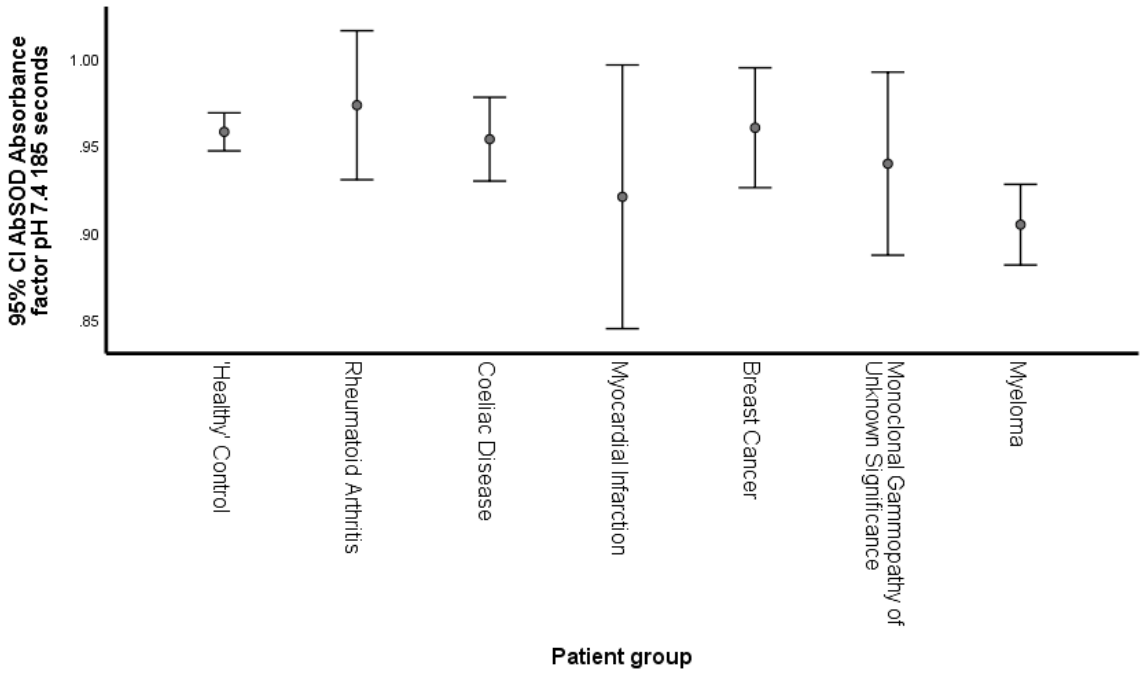

Figure 5.6: **Bar chart of AbSOD factor pH 7.4 at 185 seconds**

Bar chart with antibody superoxide dismutase activity (AbSOD factor pH 7.4 at 185 seconds) means and 95% confidence intervals observed in 'healthy' control and disease groups.

5.4.2 Antibody superoxide dismutase activity pH 5.5-7.4 – 317 seconds

5.4.2.1 pH 5.5 – 317 seconds

The descriptive statistics associated with AbSOD activity (antibody superoxide dismutase activity – AbSOD factor) at pH 5.5, over approximately 5 minutes, across the seven patient groups are reported in Table 5.10. The rheumatoid arthritis group was associated with the numerically smallest mean AbSOD factor (M = 0.778) and 'healthy' control group was associated with the highest mean AbSOD factor (M = 0.803). To test the hypothesis that the seven patient groups had different AbSOD activity (AbSOD factor), a one-way (between-groups) ANOVA was performed. Prior to conducting the ANOVA, the assumption of normality was evaluated and determined to be satisfied as the seven groups' distributions were associated with a skew and kurtosis less than |<2.0| and |<9.0|, respectively (Schmider, Zielger, Danay, Beyer and Bühner, 2010; see Table 5.10). Furthermore, the assumption of homogeneity of variances was tested and satisfied via Levene's F test, $F(6, 71) = 1.644$, $p = .148$

The independent between-groups ANOVA generated a statistically significant result, $F(6, 71) = 2.950$, $p = .013$. Thus, the null hypothesis of no differences between the AbSOD factor means in different disease groups was rejected. To evaluate the differences between the seven means further, simultaneous single step Tukey Kramer multiple comparisons were performed. As can be seen in Table 5.11, one of the six comparisons were statistically significant ($p < 0.05$). Furthermore, the statistically significant differences between the means were associated with a small to moderate effect size based on Cohen's (1992) guidelines. A visual depiction of the means and 95% confidence intervals is presented in Figure 5.7.

It can be observed that the mean AbSOD factor (pH 5.5 at 317 seconds) of all groups was less than 1.0 and the disease groups tended to be lower than the 'healthy' control group. The myocardial infarction group had significantly increased AbSOD activity compared to the 'healthy' control group.

Table 5.10: ***Descriptive statistics – AbSOD factor at pH 5.5 (317 seconds)***

Descriptive statistics for antibody superoxide dismutase activity (AbSOD factor) at pH 5.5 (317 seconds) observed in control and patient disease groups

Disease group	N	M (Absorbance factor)	SD	Skew	Kurtosis
'Healthy' Control	19	0.778	0.030	-0.268	1.340
Rheumatoid Arthritis	7	0.732	0.021	0.687	0.134
Coeliac Disease	11	0.761	0.033	0.290	1.920
Myocardial Infarction	6	0.724	0.029	-0.859	0.659
Breast Cancer	7	0.769	0.056	-0.444	-0.854
Monoclonal Gammopathy of Unknown Significance	7	0.749	0.030	-0.778	1.117
Myeloma	21	0.769	0.040	-0.363	-0.277

Table 5.11: ***Tukey Kramer – AbSOD factor at pH 5.5 (317 seconds)***

Results associated with Tukey Kramer multiple comparisons analysis

Comparison			*p*	*g*
'Healthy' Control	-	Rheumatoid Arthritis	0.061	0.35
'Healthy' Control	-	Coeliac Disease	0.870	0.13
'Healthy' Control	-	Myocardial Infarction	0.030	0.40
'Healthy' Control	-	Breast Cancer	0.997	0.07
'Healthy' Control	-	Monoclonal Gammopathy of Unknown Significance	0.536	0.22
'Healthy' Control	-	Myeloma	0.985	0.07

Note. N = 19 for 'Healthy' Control, 7 for Rheumatoid Arthritis, 11 for Coeliac Disease, 6 for Myocardial Infarction, 7 for Breast Cancer, 7 for Monoclonal Gammopathy of Unknown Significance and 21 for Myeloma; *p* = significance; *g* = Hedge's g

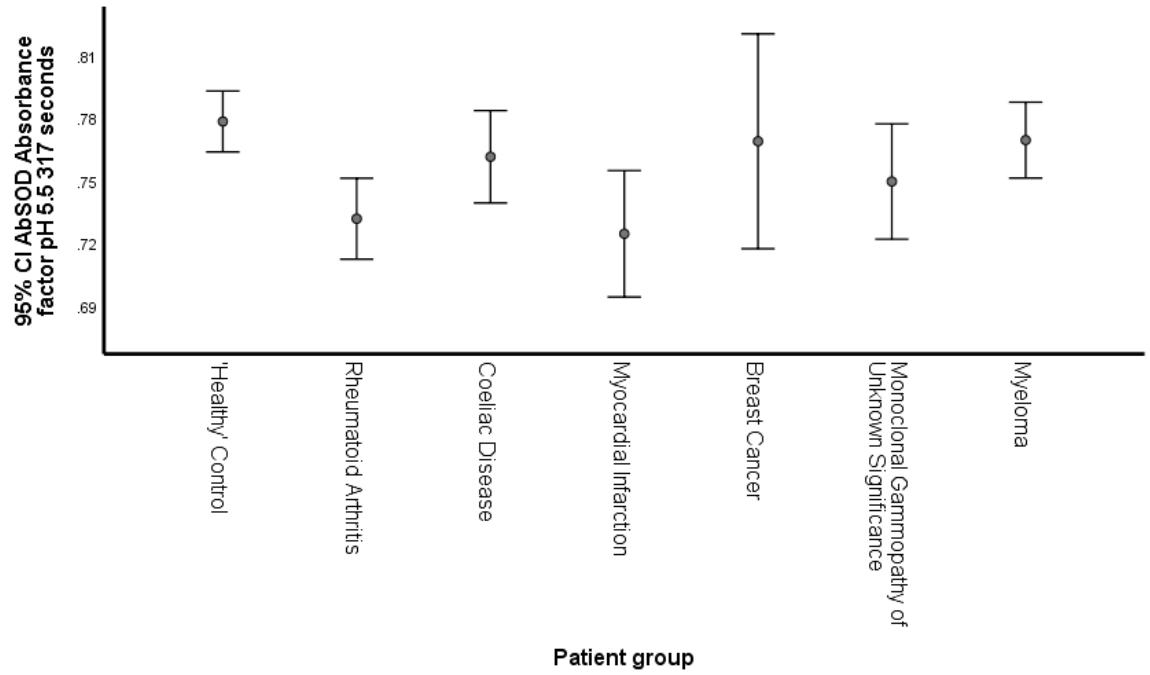

Figure 5.7: **Bar chart of AbSOD factor pH 5.5 at 317 seconds**

Bar chart with antibody superoxide dismutase activity (AbSOD factor pH 5.5 at 317 seconds) means and 95% confidence intervals observed in 'healthy' control and disease groups.

5.4.2.2 pH 6.0 – 317 seconds

The descriptive statistics associated with AbSOD activity (antibody superoxide dismutase activity – AbSOD factor) at pH 6.0, over approximately 5 minutes, across the seven patient groups are reported in Table 5.12. The myocardial infarction group was associated with the numerically smallest mean AbSOD factor (*M* = 0.768) and MGUS (Monoclonal Gammopathy of Unknown Significance) group was associated with the highest mean AbSOD factor (*M* = 0.803). To test the hypothesis that the seven patient groups had different AbSOD activity (AbSOD factor), a one-way (between-groups) ANOVA was performed. Prior to conducting the ANOVA, the assumption of normality was evaluated and determined to be satisfied for six of the seven groups, where distributions were associated with a skew and kurtosis less than |<2.0| and |<9.0|, respectively but violated for MGUS, where skewness was greater than 2.0; (Schmider, Zielger, Danay, Beyer and Bühner, 2010; see Table 5.12). Furthermore, the assumption of homogeneity of variances was tested and satisfied via Levene's F test, $F(6, 71) = 2.065$, $p = .068$.

The independent between-groups ANOVA generated a statistically non-significant result, $F(6, 71) = 0.678$, $p = .667$. Thus, the null hypothesis of no differences between the AbSOD factor means could not be rejected. A visual depiction of the means and 95% confidence intervals are presented in Figure 5.8.

It can be observed that the mean AbSOD factor (pH 6.0 at 317 seconds) of all groups was less than 1.0, showing AbSOD activity. The error bars of AbSOD factor across the disease and 'healthy' control groups overlap indicating no statistically significant differences were present.

Table 5.12: ***Descriptive statistics – AbSOD factor at pH 6.0 (317 seconds)***

Descriptive statistics for antibody superoxide dismutase activity (AbSOD factor) at pH 6.0 (317 seconds) observed in control and patient disease groups

Disease group	N	M (Absorbance factor)	SD	Skew	Kurtosis
'Healthy' Control	19	0.799	0.018	-1.552	2.309
Rheumatoid Arthritis	7	0.792	0.029	-0.015	-1.024
Coeliac Disease	11	0.783	0.042	-1.715	3.569
Myocardial Infarction	6	0.768	0.051	0.248	-1.969
Breast Cancer	7	0.786	0.034	0.457	-1.630
Monoclonal Gammopathy of Unknown Significance	7	0.803	0.048	2.075	4.790
Myeloma	21	0.789	0.049	0.791	1.560

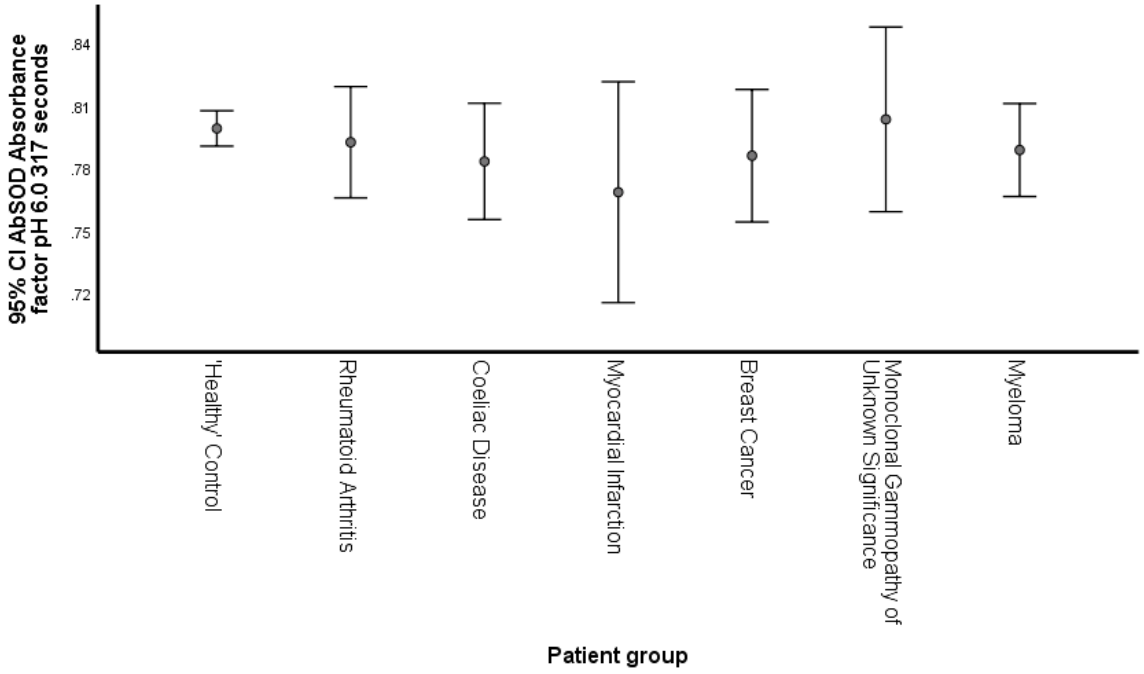

Figure 5.8: **Bar chart of AbSOD factor pH 6.0 at 317 seconds**

Bar chart with antibody superoxide dismutase activity (AbSOD factor pH 6.0 at 317 seconds) means and 95% confidence intervals observed in 'healthy' control and disease groups.

5.4.2.3 pH 6.5 – 317 seconds

The descriptive statistics associated with AbSOD activity (antibody superoxide dismutase activity – AbSOD factor) at pH 6.5, over approximately 5 minutes, across the seven patient groups are reported in Table 5.13. The myocardial infarction group was associated with the numerically smallest mean AbSOD factor (*M* = 0.798) and 'healthy' control group was associated with the highest mean AbSOD factor (*M* = 0.869). To test the hypothesis that the seven patient groups had different AbSOD activity (AbSOD factor), a one-way (between-groups) ANOVA was performed. Prior to conducting the ANOVA, the assumption of normality was evaluated and determined to be satisfied as the seven groups' distributions were associated with a skew and kurtosis less than |<2.0| and |<9.0|, respectively (Schmider, Zielger, Danay, Beyer and Bühner, 2010; see Table 5.13). The assumption of homogeneity of variances was tested and violated, as assessed by Levene's F test, $F(6, 71) = 4.823$, $p = .000$.

The independent between-groups Welch ANOVA generated a statistically significant result, $F(6, 19.978) = 2.662$, $p = .046$. Thus, the null hypothesis of no differences between the AbSOD factor means in different disease groups was rejected. To evaluate the differences between the seven means further, Games-Howell comparisons were performed. Although the Welch ANOVA was significant, the post-hoc comparisons were not statistically significant ($p > 0.05$) as can be seen in Table 5.14. Only the Post-hoc comparisons to healthy controls are presented here, therefore the statistically significant difference must be between two of the disease groups. A visual depiction of the means and 95% confidence intervals is presented in Figure 5.9.

It can be observed that the AbSOD factor (pH 6.5 at 317 seconds) of all groups was less than 1.0 (AbSOD activity). Although the myeloma group was lower than the 'healthy' control group, the error bars of AbSOD factor across the disease and 'healthy' control groups overlap indicating no statistically significant differences were present.

Table 5.13: ***Descriptive statistics – AbSOD factor at pH 6.5 (317 seconds)***

Descriptive statistics for antibody superoxide dismutase activity (AbSOD factor) at pH 6.5 (317 seconds) observed in control and patient disease groups

Disease group	N	M (Absorbance factor)	SD	Skew	Kurtosis
'Healthy' Control	19	0.869	0.015	-0.566	0.164
Rheumatoid Arthritis	7	0.864	0.045	-1.440	3.179
Coeliac Disease	11	0.841	0.076	-0.968	-0.241
Myocardial Infarction	6	0.798	0.068	0.324	-1.397
Breast Cancer	7	0.851	0.029	-0.958	-0.394
Monoclonal Gammopathy of Unknown Significance	7	0.858	0.076	1.267	0.942
Myeloma	21	0.825	0.062	1.682	4.274

Table 5.14: ***Games-Howell – AbSOD factor at pH 6.5 (317 seconds)***

Results associated with Games-Howell multiple comparisons analysis

Comparison			*p*	*g*
'Healthy' Control	-	Rheumatoid Arthritis	1.000	0.08
'Healthy' Control	-	Coeliac Disease	0.877	0.35
'Healthy' Control	-	Myocardial Infarction	0.295	0.99
'Healthy' Control	-	Breast Cancer	0.695	0.28
'Healthy' Control	-	Monoclonal Gammopathy of Unknown Significance	1.000	0.14
'Healthy' Control	-	Myeloma	0.062	0.56

Note. N = 19 for 'Healthy' Control, 7 for Rheumatoid Arthritis, 11 for Coeliac Disease, 6 for Myocardial Infarction, 7 for Breast Cancer, 7 for Monoclonal Gammopathy of Unknown Significance and 21 for Myeloma; *p* = significance; *g* = Hedge's g

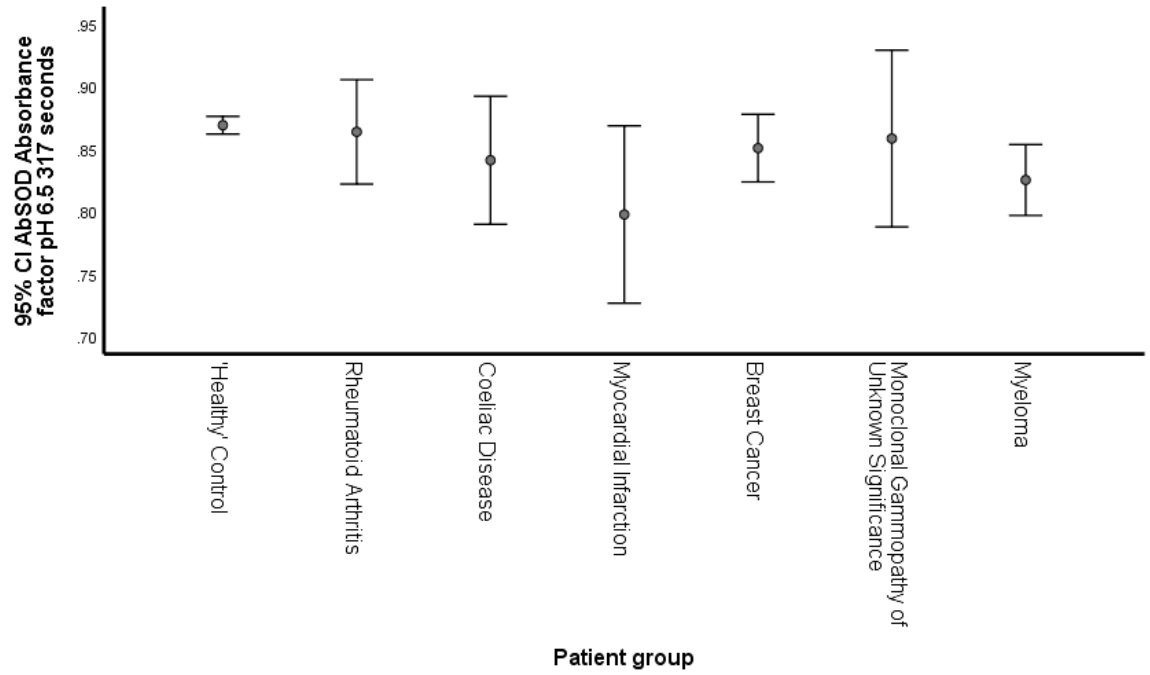

Figure 5.9: **Bar chart of AbSOD factor pH 6.5 at 317 seconds**

Bar chart with antibody superoxide dismutase activity (AbSOD factor pH 6.5 at 317 seconds) means and 95% confidence intervals observed in 'healthy' control and disease groups.

5.4.2.4 pH 7.0 – 317 seconds

The descriptive statistics associated with AbSOD activity (antibody superoxide dismutase activity – AbSOD factor) at pH 7.0, over approximately 5 minutes, across the seven patient groups are reported in Table 5.15. The myeloma group was associated with the numerically smallest mean AbSOD factor (*M* = 0.921) and rheumatoid arthritis group was associated with the highest mean AbSOD factor (*M* = 1.013). To test the hypothesis that the seven patient groups had different AbSOD activity (AbSOD factor), a one-way (between-groups) ANOVA was performed. Prior to conducting the ANOVA, the assumption of normality was evaluated and determined to be satisfied as the seven groups' distributions were associated with a skew and kurtosis less than |<2.0| and |<9.0|, respectively (Schmider, Zielger, Danay, Beyer and Bühner, 2010; see Table 5.15). The assumption of homogeneity of variances was tested and violated, as assessed by Levene's F test, $F(6, 71) = 2.510$, $p = .029$.

The independent between-groups Welch ANOVA generated a statistically significant result, $F(6, 21.990) = 3.498$, $p = .014$. Thus, the null hypothesis of no differences between the AbSOD factor means in different disease groups was rejected. To evaluate the differences between the seven means further, Games-Howell comparisons were performed. As can be seen in Table 5.16, one of the six comparisons were statistically significant ($p < 0.05$). Furthermore, the statistically significant differences between the means were associated with a moderate to large effect size based on Cohen's (1992) guidelines. A visual depiction of the means and 95% confidence intervals is presented in Figure 5.10. It can be observed that the AbSOD factor (pH 7.0 at 317 seconds) of the 'healthy' control, rheumatoid arthritis and breast cancer groups were greater than 1.0 (AbPro activity) and the coeliac disease, myocardial infarction, MGUS and myeloma groups were less than 1.0 (AbSOD activity). The Myeloma group had significantly increased AbSOD activity compared to the 'healthy' control group.

Table 5.15: ***Descriptive statistics – AbSOD factor at pH 7.0 (317 seconds)***

Descriptive statistics for antibody superoxide dismutase activity (AbSOD factor) at pH 7.0 (317 seconds) observed in control and patient disease groups

Disease group	N	M (Absorbance factor)	SD	Skew	Kurtosis
'Healthy' Control	19	1.002	0.027	0.355	-0.142
Rheumatoid Arthritis	7	1.013	0.051	0.133	-0.513
Coeliac Disease	11	0.986	0.048	0.927	0.955
Myocardial Infarction	6	0.982	0.030	0.006	-3.157
Breast Cancer	7	1.006	0.034	-0.111	-0.805
Monoclonal Gammopathy of Unknown Significance	7	0.985	0.089	0.555	-0.252
Myeloma	21	0.921	0.076	1.393	1.051

Table 5.16: ***Games-Howell – AbSOD factor at pH 7.0 (317 seconds)***

Results associated with Games-Howell multiple comparisons analysis

Comparison			*p*	*g*
'Healthy' Control	-	Rheumatoid Arthritis	0.996	-0.09
'Healthy' Control	-	Coeliac Disease	0.941	0.13
'Healthy' Control	-	Myocardial Infarction	0.766	0.16
'Healthy' Control	-	Breast Cancer	1.000	-0.03
'Healthy' Control	-	Monoclonal Gammopathy of Unknown Significance	0.998	0.13
'Healthy' Control	-	Myeloma	0.002	0.62

Note. N = 19 for 'Healthy' Control, 7 for Rheumatoid Arthritis, 11 for Coeliac Disease, 6 for Myocardial Infarction, 7 for Breast Cancer, 7 for Monoclonal Gammopathy of Unknown Significance and 21 for Myeloma; *p* = significance; *g* = Hedge's g

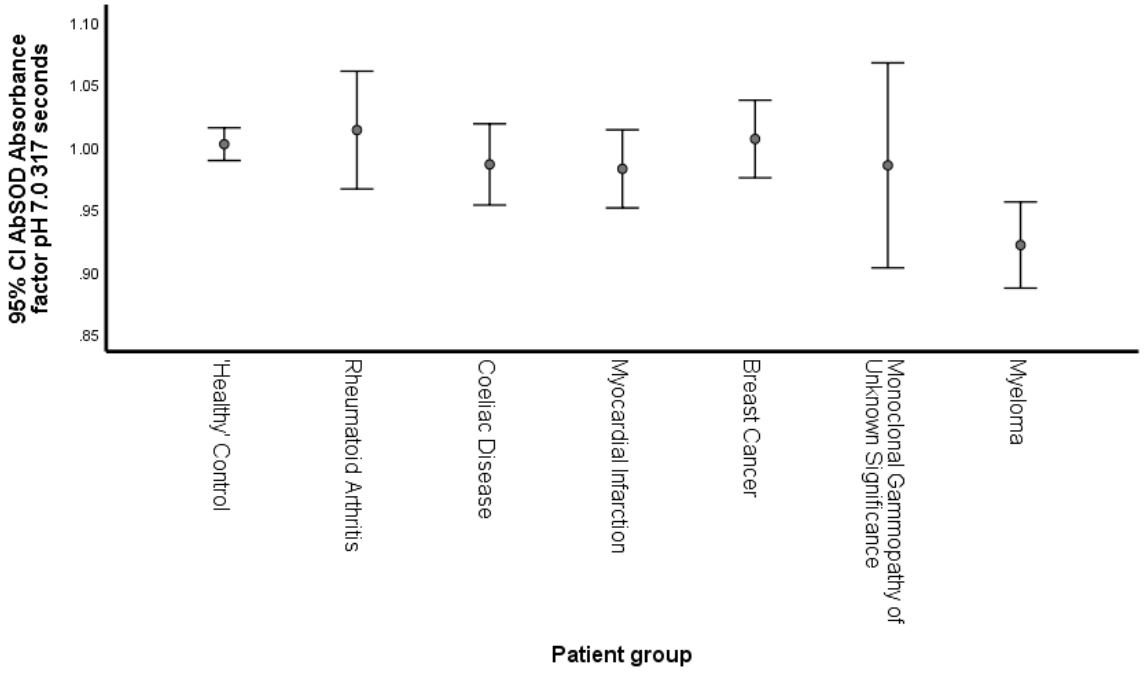

Figure 5.10: Bar chart of AbSOD factor pH 7.0 at 317 seconds

Bar chart with antibody superoxide dismutase activity (AbSOD factor pH 7.0 at 317 seconds) means and 95% confidence intervals observed in 'healthy' control and disease groups.

5.4.2.5 pH 7.4 – 317 seconds

The descriptive statistics associated with AbSOD activity (antibody superoxide dismutase activity – AbSOD factor) at pH 7.4, over approximately 5 minutes, across the seven patient groups are reported in Table 5.17. The myeloma group was associated with the numerically smallest mean AbSOD factor (*M* = 1.078) and rheumatoid arthritis group was associated with the highest mean AbSOD factor (*M* = 1.182). To test the hypothesis that the seven patient groups had different AbSOD activity (AbSOD factor), a one-way (between-groups) ANOVA was performed. Prior to conducting the ANOVA, the assumption of normality was evaluated and determined to be satisfied as the seven groups' distributions were associated with a skew and kurtosis less than |<2.0| and |<9.0|, respectively (Schmider, Zielger, Danay, Beyer and Bühner, 2010; see Table 5.17). The assumption of homogeneity of variances was tested and violated, as assessed by Levene's F test, $F(6, 71) = 3.619$, $p = .003$.

The independent between-groups Welch ANOVA generated a statistically non-significant result, $F(6, 20.354) = 1.963$, $p = .119$. Thus, the null hypothesis of no differences between the AbSOD factor means could not be rejected. A visual depiction of the means and 95% confidence intervals are presented in Figure 5.11. It can be observed that the AbSOD factor (pH 7.4 at 317 seconds) of all groups was greater than 1.0 (AbPro activity). The error bars of AbSOD factor across the disease and 'healthy' control groups overlap indicating no statistically significant differences were present.

Table 5.17: ***Descriptive statistics – AbSOD factor at pH 7.4 (317 seconds)***

Descriptive statistics for antibody superoxide dismutase activity (AbSOD factor) at pH 7.4 (317 seconds) observed in control and patient disease groups

Disease group	N	M (Absorbance factor)	SD	Skew	Kurtosis
'Healthy' Control	19	1.113	0.033	0.045	0.845
Rheumatoid Arthritis	7	1.182	0.104	0.353	1.098
Coeliac Disease	11	1.150	0.068	-0.051	-1.179
Myocardial Infarction	6	1.101	0.104	0.360	-1.826
Breast Cancer	7	1.173	0.078	-1.346	1.064
Monoclonal Gammopathy of Unknown Significance	7	1.098	0.100	-0.969	0.407
Myeloma	21	1.078	0.090	0.077	-1.357

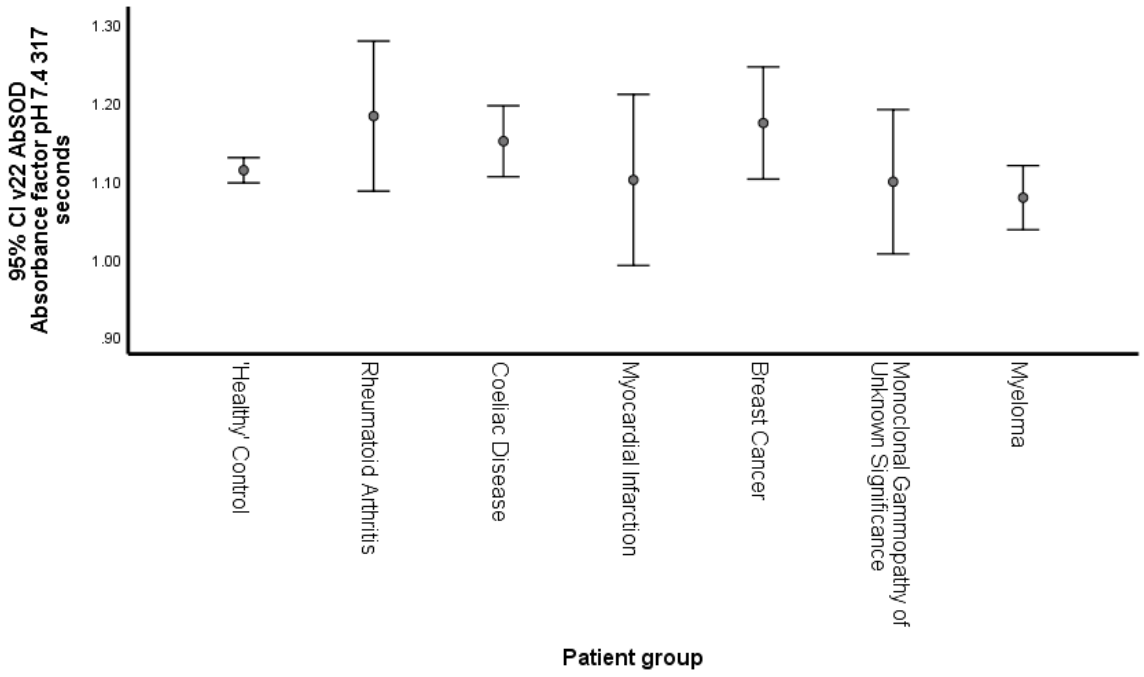

Figure 5.11: **Bar chart of AbSOD factor pH 7.4 at 317 seconds**

Bar chart with antibody superoxide dismutase activity (AbSOD factor pH 7.4 at 317 seconds) means and 95% confidence intervals observed in 'healthy' control and disease groups.

5.4.3 Antibody superoxide dismutase activity pH 5.5-7.4 – 661 seconds

5.4.3.1 pH 5.5 – 661 seconds

The descriptive statistics associated with AbSOD activity (antibody superoxide dismutase activity – AbSOD factor) at pH 5.5, over approximately 11 minutes, across the seven patient groups are reported in Table 5.18. The myocardial infarction group was associated with the numerically smallest mean AbSOD factor (*M* = 0.801) and breast cancer group was associated with the highest mean AbSOD factor (*M* = 0.855). To test the hypothesis that the seven patient groups had different AbSOD activity (AbSOD factor), a one-way (between-groups) ANOVA was performed. Prior to conducting the ANOVA, the assumption of normality was evaluated and determined to be satisfied as the seven groups' distributions were associated with a skew and kurtosis less than |<2.0| and |<9.0|, respectively (Schmider, Zielger, Danay, Beyer and Bühner, 2010; see Table 5.18). Furthermore, the assumption of homogeneity of variances was tested and satisfied via Levene's F test, $F(6, 71) = 1.788$, $p = .114$.

The independent between-groups ANOVA generated a statistically non-significant result, $F(6, 71) = 0.780$, $p = .588$. Thus, the null hypothesis of no differences between the AbSOD factor means could not be rejected. A visual depiction of the means and 95% confidence intervals are presented in Figure 5.12.

It can be observed that the mean AbSOD factor (pH 5.5 661 at seconds) of all groups was less than 1.0, showing AbSOD activity. The error bars of AbSOD factor of the disease and 'healthy' control groups overlap indicating no statistically significant differences were present.

Table 5.18: ***Descriptive statistics – AbSOD factor at pH 5.5 (661 seconds)***

Descriptive statistics for antibody superoxide dismutase activity (AbSOD factor) at pH 5.5 (661 seconds) observed in control and patient disease groups

Disease group	N	M (Absorbance factor)	SD	Skew	Kurtosis
'Healthy' Control	19	0.830	0.025	0.352	-1.137
Rheumatoid Arthritis	7	0.846	0.046	0.334	0.883
Coeliac Disease	11	0.833	0.058	-1.219	1.885
Myocardial Infarction	6	0.801	0.068	-0.353	-1.816
Breast Cancer	7	0.855	0.059	-0.778	-0.138
Monoclonal Gammopathy of Unknown Significance	7	0.845	0.077	1.561	2.512
Myeloma	21	0.822	0.061	1.371	3.853

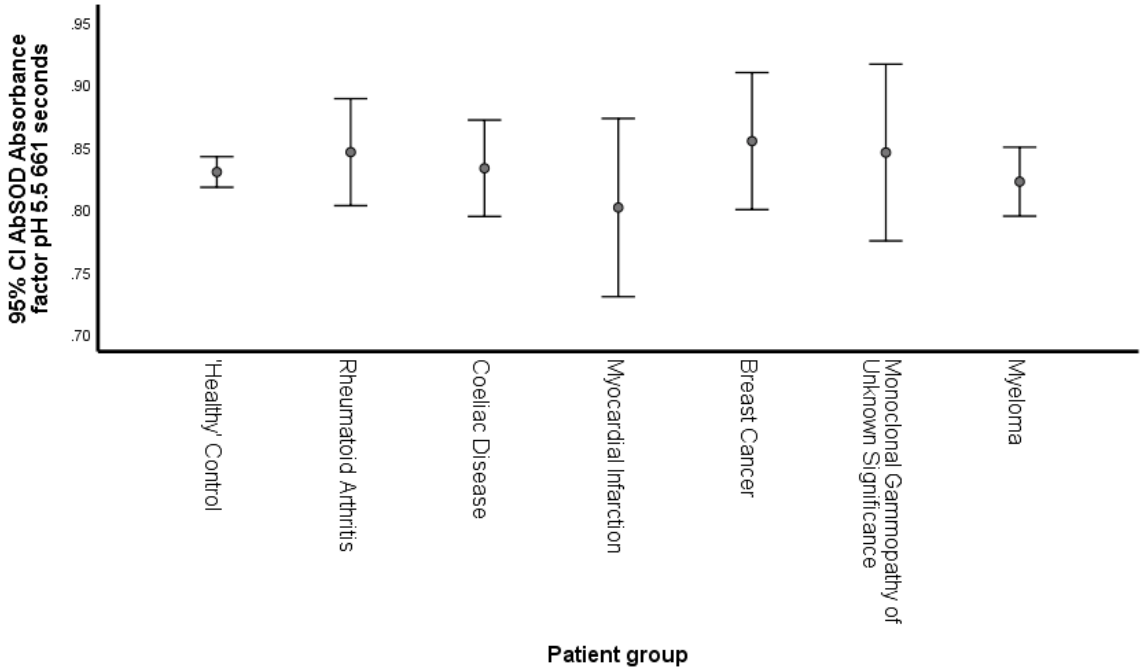

Figure 5.12: **Bar chart of AbSOD factor pH 5.5 at 661 seconds**

Bar chart with antibody superoxide dismutase activity (AbSOD factor pH 5.5 at 661 seconds) means and 95% confidence intervals observed in 'healthy' control and disease groups.

5.4.3.2 pH 6.0 – 661 seconds

The descriptive statistics associated with AbSOD activity (antibody superoxide dismutase activity – AbSOD factor) at pH 6.0, over approximately 11 minutes, across the seven patient groups are reported in Table 5.19. The myeloma group was associated with the numerically smallest mean AbSOD factor (*M* = 0.923) and rheumatoid arthritis group was associated with the highest mean AbSOD factor (*M* = 1.021). To test the hypothesis that the seven patient groups had different AbSOD activity (AbSOD factor), a one-way (between-groups) ANOVA was performed. Prior to conducting the ANOVA, the assumption of normality was evaluated and determined to be satisfied as the seven groups' distributions were associated with a skew and kurtosis less than |<2.0| and |<9.0|, respectively (Schmider, Zielger, Danay, Beyer and Bühner, 2010; see Table 5.19). The assumption of homogeneity of variances was tested and violated, as assessed by Levene's F test, $F(6, 71) = 3.297$, $p = .006$.

The independent between-groups Welch ANOVA generated a statistically significant result, $F(6, 19.880) = 2.789$, $p = 0.039$. Thus, the null hypothesis of no differences between the AbSOD factor means in different disease groups was rejected. To evaluate the differences between the seven means further, Games-Howell comparisons were performed. As can be seen in Table 5.20, one of the six comparisons were statistically significant ($p < 0.05$). Furthermore, the statistically significant differences between the means were associated with a medium to large effect size based on Cohen's (1992) guidelines. A visual depiction of the means and 95% confidence intervals is presented in Figure 5.13.

It can be observed that the mean AbSOD factor (pH 6.0 at 661 seconds) of all groups was less than 1.0 (AbSOD activity), except the rheumatoid arthritis group which was greater than 1.0 (AbPro activity). The myeloma group had significantly increased AbSOD activity compared to the 'healthy' control group.

Table 5.19: ***Descriptive statistics – AbSOD factor at pH 6.0 (661 seconds)***

Descriptive statistics for antibody superoxide dismutase activity (AbSOD factor) at pH 6.0 (661 seconds) observed in control and patient disease groups

Disease group	N	M (Absorbance factor)	SD	Skew	Kurtosis
'Healthy' Control	19	0.988	0.020	0.057	-1.197
Rheumatoid Arthritis	7	1.021	0.086	-1.266	-0.149
Coeliac Disease	11	0.949	0.064	-0.565	0.256
Myocardial Infarction	6	0.962	0.098	0.875	-1.674
Breast Cancer	7	0.964	0.047	-0.682	-1.244
Monoclonal Gammopathy of Unknown Significance	7	0.990	0.099	0.562	-0.002
Myeloma	21	0.923	0.077	1.807	4.808

Table 5.20: ***Games-Howell – AbSOD factor at pH 6.0 (661 seconds)***

Results associated with Games-Howell multiple comparisons analysis

Comparison			*p*	*g*
'Healthy' Control	-	Rheumatoid Arthritis	0.933	-0.33
'Healthy' Control	-	Coeliac Disease	0.484	0.40
'Healthy' Control	-	Myocardial Infarction	0.991	0.25
'Healthy' Control	-	Breast Cancer	0.837	0.25
'Healthy' Control	-	Monoclonal Gammopathy of Unknown Significance	1.000	-0.03
'Healthy' Control	-	Myeloma	0.017	0.62

Note. N = 19 for 'Healthy' Control, 7 for Rheumatoid Arthritis, 11 for Coeliac Disease, 6 for Myocardial Infarction, 7 for Breast Cancer, 7 for Monoclonal Gammopathy of Unknown Significance and 21 for Myeloma; *p* = significance; *g* = Hedge's g

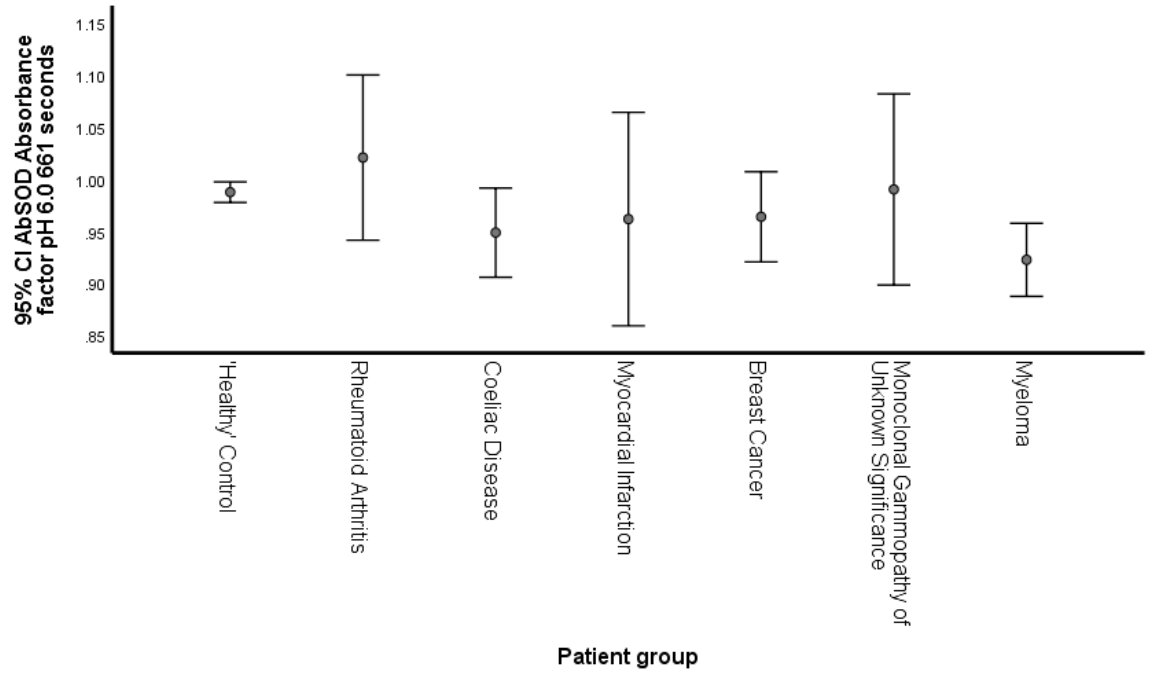

Figure 5.13: **Bar chart of AbSOD factor pH 6.0 at 661 seconds**

Bar chart with antibody superoxide dismutase activity (AbSOD factor pH 6.0 at 661 seconds) means and 95% confidence intervals observed in 'healthy' control and disease groups.

5.4.3.3 pH 6.5 – 661 seconds

The descriptive statistics associated with AbSOD activity (antibody superoxide dismutase activity – AbSOD factor) at pH 6.5, over approximately 11 minutes, across the seven patient groups are reported in Table 5.21. The myeloma group was associated with the numerically smallest mean AbSOD factor (*M* = 1.004) and rheumatoid arthritis group was associated with the highest mean AbSOD factor (*M* = 1.123). To test the hypothesis that the seven patient groups had different AbSOD activity (AbSOD factor), a one-way (between-groups) ANOVA was performed. Prior to conducting the ANOVA, the assumption of normality was evaluated and determined to be satisfied as the seven groups' distributions were associated with a skew and kurtosis less than |<2.0| and |<9.0|, respectively (Schmider, Zielger, Danay, Beyer and Bühner, 2010; see Table 5.21). Furthermore, the assumption of homogeneity of variances was tested and satisfied via Levene's F test, $F(6, 71) = 1.987$, $p = .079$.

The independent between-groups ANOVA generated a statistically significant result, $F(6, 71) = 4.502$, $p = .001$. Thus, the null hypothesis of no differences between the AbSOD factor means in different disease groups was rejected. To evaluate the differences between the seven means further, simultaneous single step Tukey Kramer multiple comparisons were performed. As can be seen in Table 5.22, one of the six comparisons was statistically significant ($p < 0.05$). Furthermore, the statistically significant differences between the means were associated with a moderate effect size based on Cohen's (1992) guidelines. A visual depiction of the means and 95% confidence intervals is presented in Figure 5.14.

It can be observed that the mean AbSOD factor (pH 6.5 at 661 seconds) of all groups was greater than 1.0 (AbPro activity) and the disease groups (except for rheumatoid arthritis) tended to be lower than the 'healthy' control group. The myeloma group had significantly decreased AbPro activity compared to the 'healthy' control group and other patient groups which all demonstrated increased antibody pro-oxidant activity (AbPro activity).

Table 5.21: ***Descriptive statistics – AbSOD factor at pH 6.5 (661 seconds)***

Descriptive statistics for antibody superoxide dismutase activity (AbSOD factor) at pH 6.5 (661 seconds) observed in control and patient disease groups

Disease group	N	M (Absorbance factor)	SD	Skew	Kurtosis
'Healthy' Control	19	1.113	0.045	-0.025	-0.424
Rheumatoid Arthritis	7	1.123	0.074	-0.449	0.052
Coeliac Disease	11	1.096	0.063	0.075	0.034
Myocardial Infarction	6	1.084	0.047	0.919	-0.824
Breast Cancer	7	1.086	0.058	0.349	-1.278
Monoclonal Gammopathy of Unknown Significance	7	1.070	0.128	0.496	-0.694
Myeloma	21	1.004	0.092	1.693	2.438

Table 5.22: ***Tukey Kramer – AbSOD factor at pH 6.5 (661 seconds)***

Results associated with Tukey Kramer multiple comparisons analysis

Comparison			*p*	*g*
'Healthy' Control	-	Rheumatoid Arthritis	1.000	-0.05
'Healthy' Control	-	Coeliac Disease	0.997	0.09
'Healthy' Control	-	Myocardial Infarction	0.981	0.15
'Healthy' Control	-	Breast Cancer	0.984	0.14
'Healthy' Control	-	Monoclonal Gammopathy of Unknown Significance	0.862	0.21
'Healthy' Control	-	Myeloma	0.000	0.53

Note. N = 19 for 'Healthy' Control, 7 for Rheumatoid Arthritis, 11 for Coeliac Disease, 6 for Myocardial Infarction, 7 for Breast Cancer, 7 for Monoclonal Gammopathy of Unknown Significance and 21 for Myeloma; *p* = significance; *g* = Hedge's g

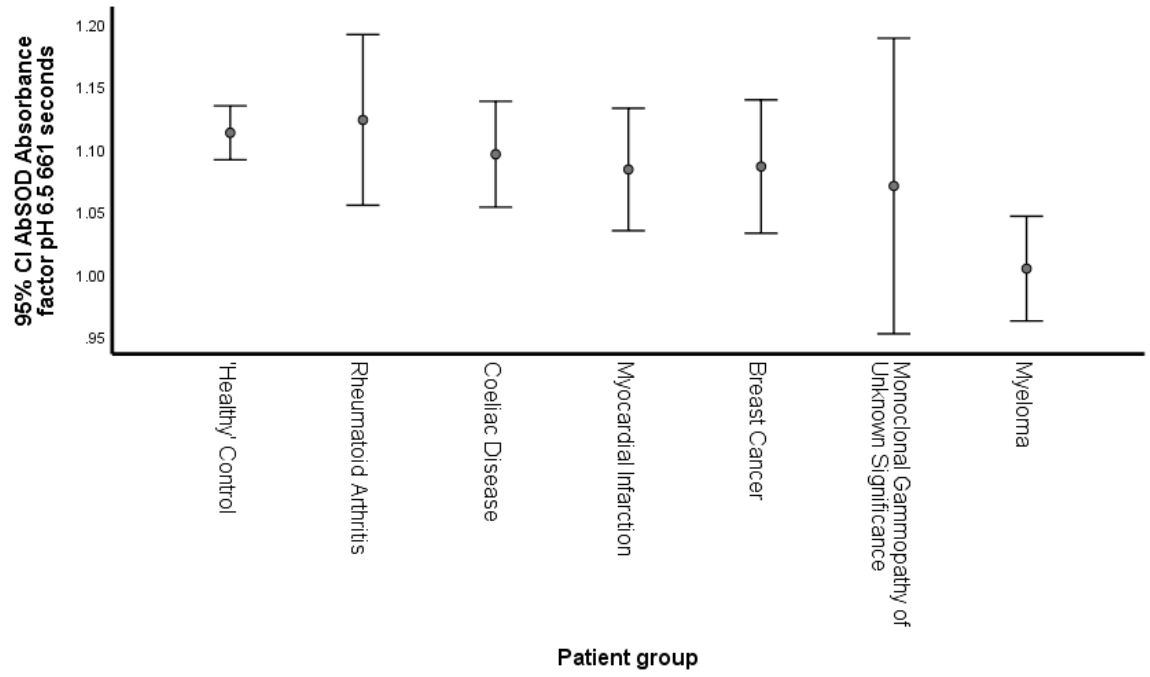

Figure 5.14: **Bar chart of AbSOD factor pH 6.5 at 661 seconds**

Bar chart with antibody superoxide dismutase activity (AbSOD factor pH 6.5 at 661 seconds) means and 95% confidence intervals observed in 'healthy' control and disease groups.

5.4.3.4 pH 7.0 – 661 seconds

The descriptive statistics associated with AbSOD activity (antibody superoxide dismutase activity) (AbSOD factor) at pH 7.0, over approximately 11 minutes, across the seven patient groups are reported in Table 5.23. The myeloma group was associated with the numerically smallest mean AbSOD factor (*M* = 1.213) and rheumatoid arthritis group was associated with the highest mean AbSOD factor (*M* = 1.383). To test the hypothesis that the seven patient groups had different AbSOD activity (AbSOD factor), a one-way (between-groups) ANOVA was performed. Prior to conducting the ANOVA, the assumption of normality was evaluated and determined to be satisfied as the seven groups' distributions were associated with a skew and kurtosis less than |<2.0| and |<9.0|, respectively (Schmider, Zielger, Danay, Beyer and Bühner, 2010; see Table 5.23). The assumption of homogeneity of variances was tested and violated, as assessed by Levene's F test, $F(6, 71) = 4.128$, $p = .001$.

The independent between-groups Welch ANOVA generated a statistically significant result, $F(6, 23.371) = 3.483$, $p = .013$. Thus, the null hypothesis of no differences between the AbSOD factor means in different disease groups was rejected. To evaluate the differences between the seven means further, Games-Howell comparisons were performed. Although the Welch ANOVA was significant, the post-hoc comparisons were not statistically significant ($p > 0.05$) as can be seen in Table 5.24. Only the post-hoc comparisons to healthy controls are presented here, therefore the statistically significant difference must be between two of the disease groups. A visual depiction of the means and 95% confidence intervals is presented in Figure 5.15. It can be observed that the AbSOD factor (pH 7.0 at 661 seconds) of all groups was greater than 1.0 (AbPro activity). Although the myeloma group was lower than the 'healthy' control group, the error bars of AbSOD factor across the disease and 'healthy' control groups overlap indicating no statistically significant differences were present.

Table 5.23: ***Descriptive statistics – AbSOD factor at pH 7.0 (661 seconds)***

Descriptive statistics for antibody superoxide dismutase activity (AbSOD factor) at pH 7.0 (661 seconds) observed in control and patient disease groups

Disease group	N	M (Absorbance factor)	SD	Skew	Kurtosis
'Healthy' Control	19	1.291	0.062	0.942	2.404
Rheumatoid Arthritis	7	1.383	0.137	1.423	1.628
Coeliac Disease	11	1.328	0.089	0.592	-0.411
Myocardial Infarction	6	1.339	0.034	0.636	-1.697
Breast Cancer	7	1.356	0.062	-0.492	-1.259
Monoclonal Gammopathy of Unknown Significance	7	1.281	0.146	-0.581	-0.763
Myeloma	21	1.213	0.132	0.627	-0.196

Table 5.24: ***Games-Howell – AbSOD factor at pH 7.0 (661 seconds)***

Results associated with Games-Howell multiple comparisons analysis

Comparison			*p*	*g*
'Healthy' Control	-	Rheumatoid Arthritis	0.635	-0.33
'Healthy' Control	-	Coeliac Disease	0.884	-0.13
'Healthy' Control	-	Myocardial Infarction	0.248	-0.18
'Healthy' Control	-	Breast Cancer	0.297	-0.24
'Healthy' Control	-	Monoclonal Gammopathy of Unknown Significance	1.000	0.04
'Healthy' Control	-	Myeloma	0.217	0.28

Note. N = 19 for 'Healthy' Control, 7 for Rheumatoid Arthritis, 11 for Coeliac Disease, 6 for Myocardial Infarction, 7 for Breast Cancer, 7 for Monoclonal Gammopathy of Unknown Significance and 21 for Myeloma; *p* = significance; *g* = Hedge's g

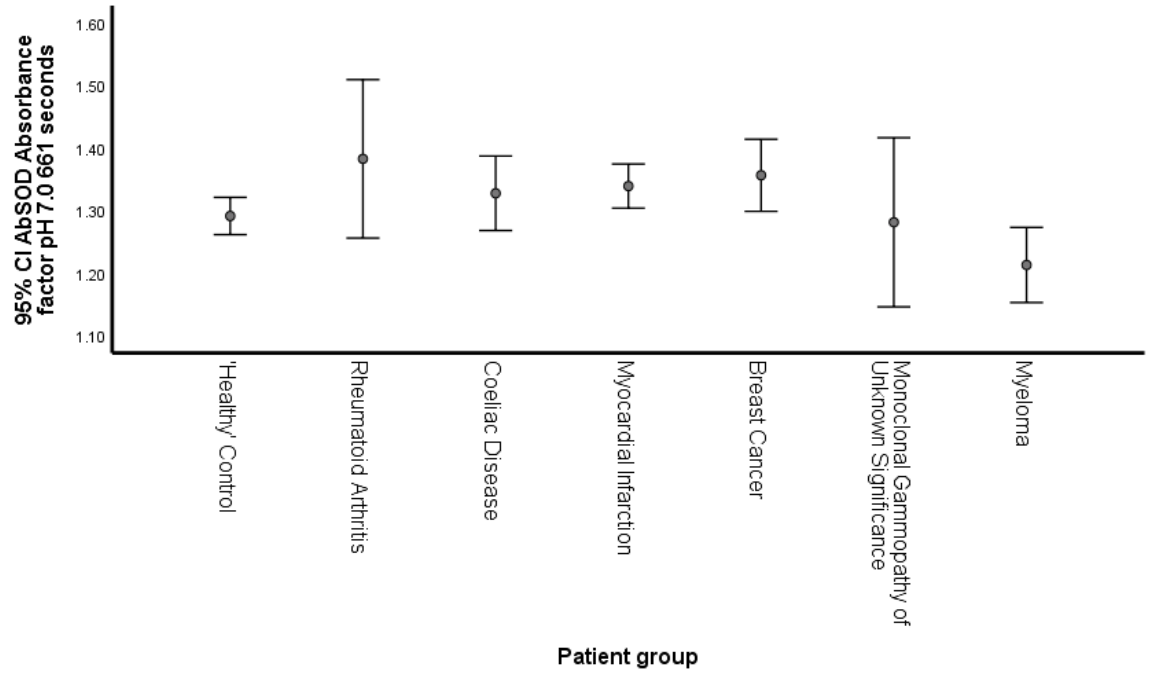

Figure 5.15: **Bar chart of AbSOD factor pH 7.0 at 661 seconds**

Bar chart with antibody superoxide dismutase activity (AbSOD factor pH 7.0 at 661 seconds) means and 95% confidence intervals observed in 'healthy' control and disease groups.

5.4.3.5 pH 7.4 – 661 seconds

The descriptive statistics associated with AbSOD activity (antibody superoxide dismutase activity – AbSOD factor) at pH 7.4, over approximately 11 minutes, across the seven patient groups are reported in Table 5.25. The monoclonal gammopathy of unknown significance (MGUS) group was associated with the numerically smallest mean AbSOD factor (*M* = 1.359) and 'healthy' control group was associated with the highest mean AbSOD factor (*M* = 1.441). To test the hypothesis that the seven patient groups had different AbSOD activity (AbSOD factor), a one-way (between-groups) ANOVA was performed. Prior to conducting the ANOVA, the assumption of normality was evaluated and determined to be satisfied as the seven groups' distributions were associated with a skew and kurtosis less than |<2.0| and |<9.0|, respectively (Schmider, Zielger, Danay, Beyer and Bühner, 2010; see Table 5.25). The assumption of homogeneity of variances was tested and violated, as assessed by Levene's F test, $F(6, 71) = 2.586$, $p = .025$.

The independent between-groups Welch ANOVA generated a statistically significant result, $F(6, 21.989) = 4.569$, $p = .004$. Thus, the null hypothesis of no differences between the AbSOD factor means in different disease groups was rejected. To evaluate the differences between the seven means further, Games-Howell comparisons were performed. As can be seen in Table 5.26, two of the six comparisons were statistically significant ($p < 0.05$). Furthermore, the statistically significant differences between the means were associated with a small to moderate effect size based on Cohen's (1992) guidelines. A visual depiction of the means and 95% confidence intervals is presented in Figure 5.16. It can be observed that the AbSOD factor (pH 7.4 at 661 seconds) of all the groups was greater than 1.0. This indicated all the antibodies over this time of exposure at pH 7.4 demonstrated pro-oxidant activity. Antibody pro-oxidant activity (AbPro) was highest in the 'healthy' control group which suggested a potential redox regulatory or immunological role of pro-oxidant antibodies. The AbSOD factor of disease groups was lower than the 'healthy' control group, indicating decreased pro-oxidant activity in these disease groups, suggesting a role for AbPro activity in 'health' homeostasis e.g., bacterial killing by antibodies. The breast cancer and myeloma groups demonstrated statistically decreased pro-oxidant activity compared to the 'healthy' control group and other patient groups. The AbPro activity of the MGUS group was also lower, however standard deviation was larger, possibly due to differences in disease stage.

Table 5.25: ***Descriptive statistics – AbSOD factor at pH 7.4 (661 seconds)***

Descriptive statistics for antibody superoxide dismutase activity (AbSOD factor) at pH 7.4 (661 seconds) observed in control and patient disease groups

Disease group	N	M (Absorbance factor)	SD	Skew	Kurtosis
'Healthy' Control	19	1.441	0.038	0.120	2.192
Rheumatoid Arthritis	7	1.419	0.077	1.149	0.803
Coeliac Disease	11	1.405	0.058	1.219	2.477
Myocardial Infarction	6	1.416	0.053	0.762	-0.775
Breast Cancer	7	1.364	0.037	-1.509	3.396
Monoclonal Gammopathy of Unknown Significance	7	1.359	0.089	-0.863	-0.220
Myeloma	21	1.362	0.092	1.171	1.771

Table 5.26: ***Games-Howell – AbSOD factor at pH 7.4 (661 seconds)***

Results associated with Games-Howell multiple comparisons analysis

Comparison			*p*	*g*
'Healthy' Control	-	Rheumatoid Arthritis	0.987	0.13
'Healthy' Control	-	Coeliac Disease	0.549	0.21
'Healthy' Control	-	Myocardial Infarction	0.923	0.15
'Healthy' Control	-	Breast Cancer	0.009	0.46
'Healthy' Control	-	Monoclonal Gammopathy of Unknown Significance	0.334	0.47
'Healthy' Control	-	Myeloma	0.018	0.44

Note. N = 19 for 'Healthy' Control, 7 for Rheumatoid Arthritis, 11 for Coeliac Disease, 6 for Myocardial Infarction, 7 for Breast Cancer, 7 for Monoclonal Gammopathy of Unknown Significance and 21 for Myeloma; *p* = significance; *g* = Hedge's g

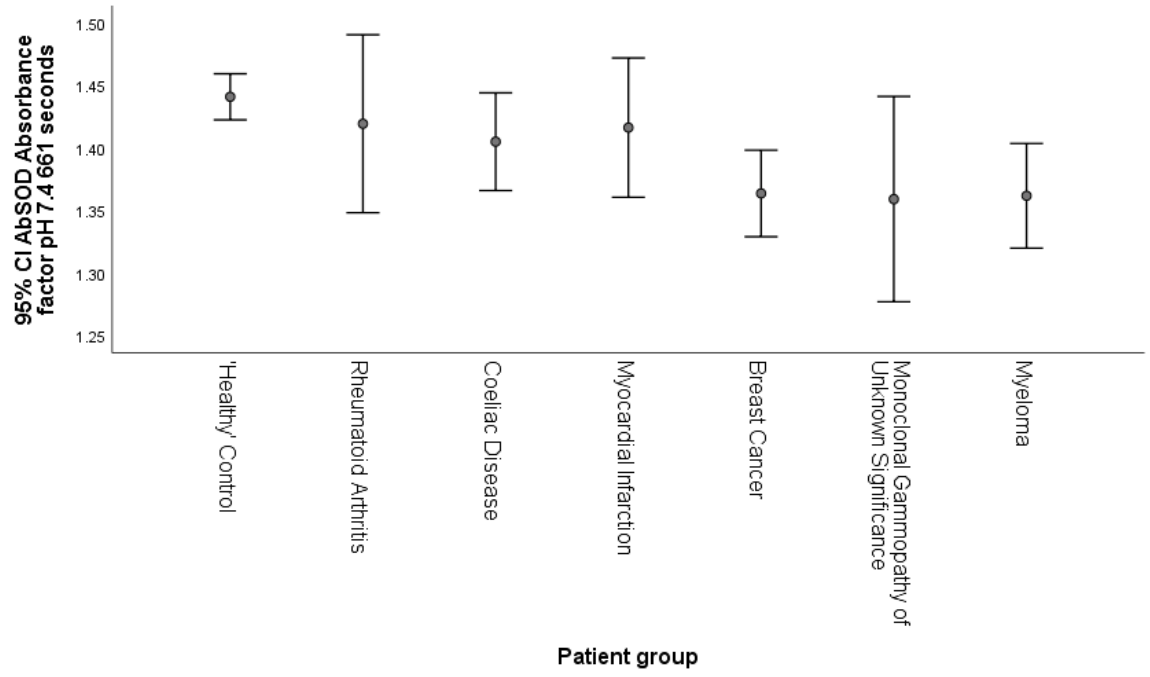

Figure 5.16: **Bar chart of AbSOD factor pH 7.4 at 661 seconds**

Bar chart with antibody superoxide dismutase activity (AbSOD factor pH 7.4 at 661 seconds) means and 95% confidence intervals observed in 'healthy' control and disease groups.

5.4.4 General summary of AbSOD absorbance factor results

5.4.4.1 pH 5.5 – 7.4 (185 seconds)

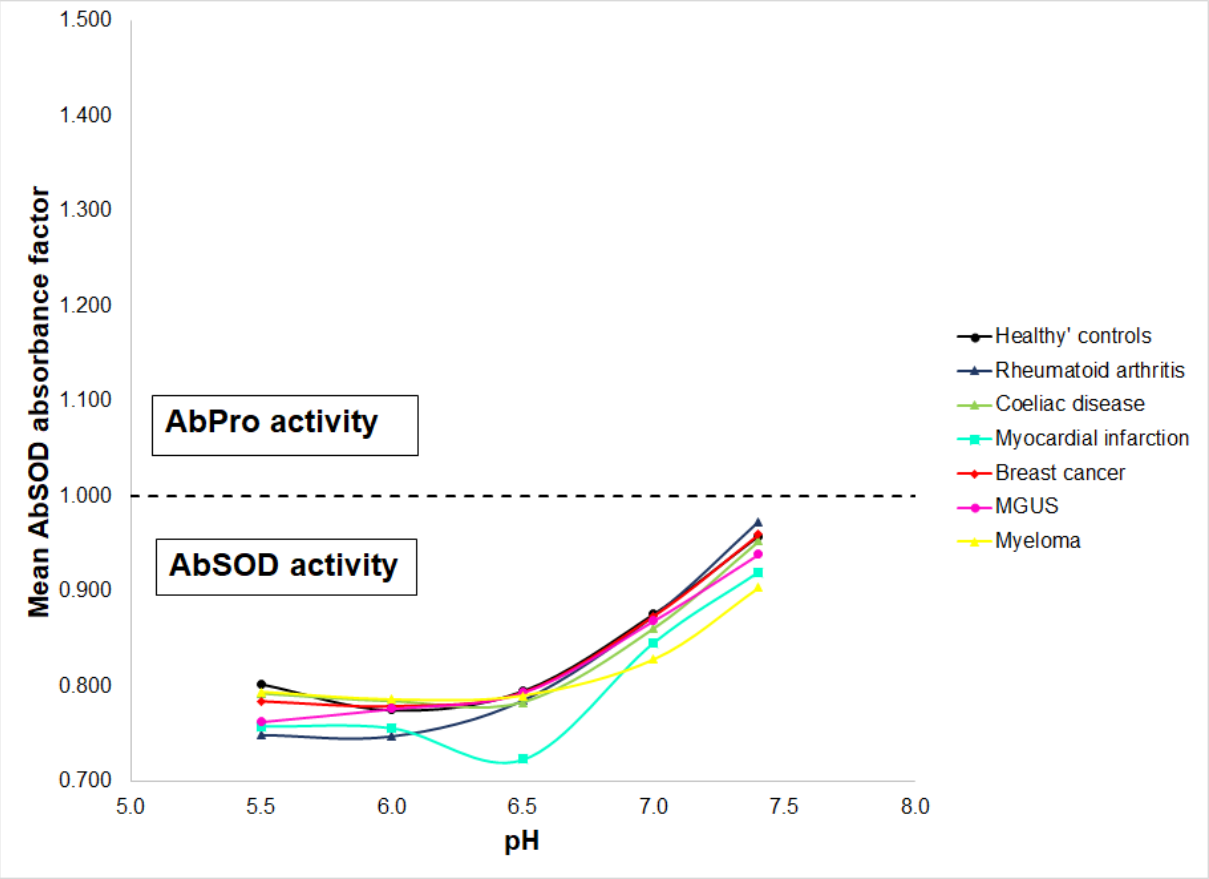

Figure 5.17: **AbSOD factor at 185 seconds, between patient groups**

The average AbSOD factor for all groups across the pH range studied was <1.0. This indicated AbSOD activity over short exposure. The AbSOD activity gradually decreased as pH rose from 5.5 (acidic) to 7.4 (physiological pH).

5.4.4.2 pH 5.5 – 7.4 (317 seconds)

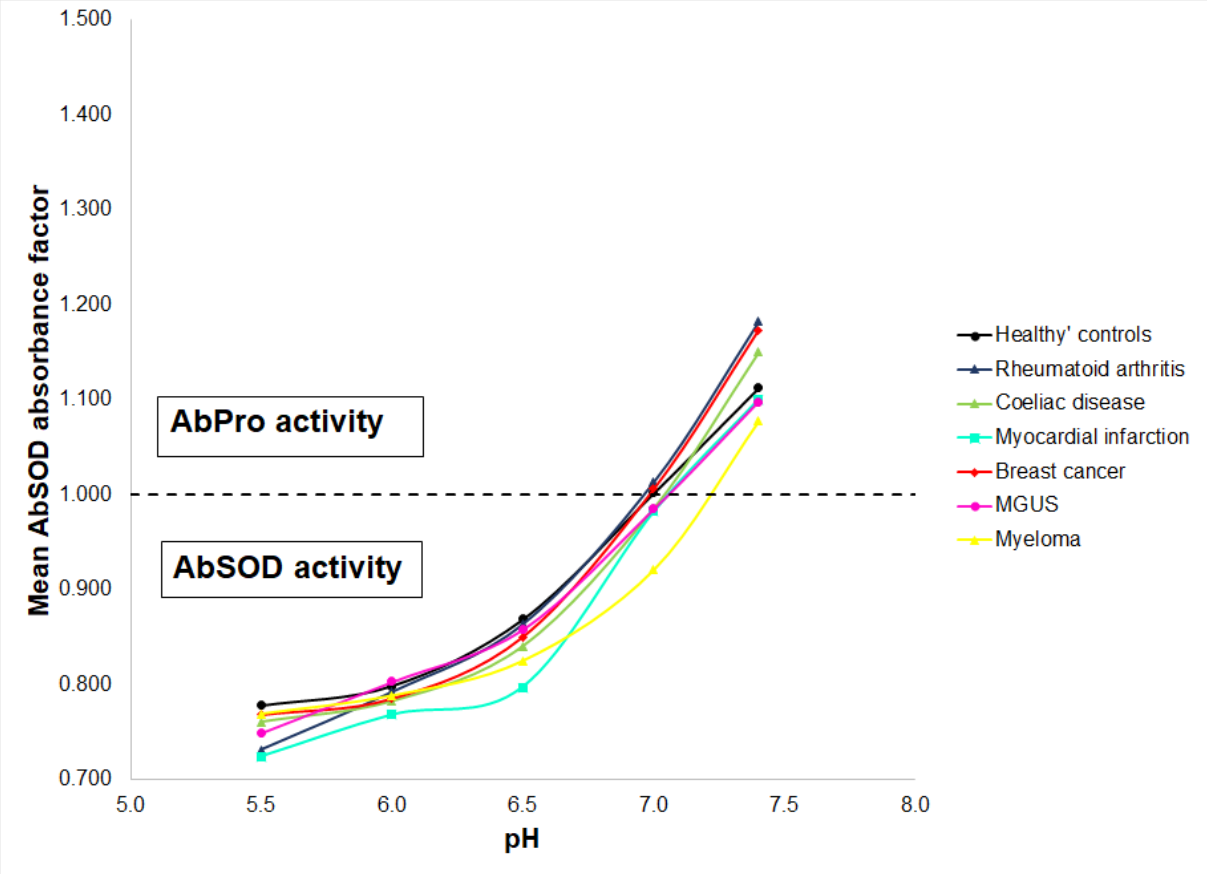

Figure 5.18: AbSOD factor at 317 seconds, between patient groups

The average AbSOD factor for all groups across the pH range studied was variable. From pH 5.5 to 6.5 the AbSOD activity was <1.0, indicating AbSOD activity. At pH 7.0, the average AbSOD factor was approximately 1, indicating neither AbPro, nor AbSOD activity was grossly detectable. By pH 7.4, the AbSOD factor was >1.0, signifying AbPro activity. The AbSOD activity gradually decreased from pH 5.5 to 6.5, before it diminished and transitioned to AbPro activity at pH 7.4.

5.4.4.3 pH 5.5 – 7.4 (661 seconds)

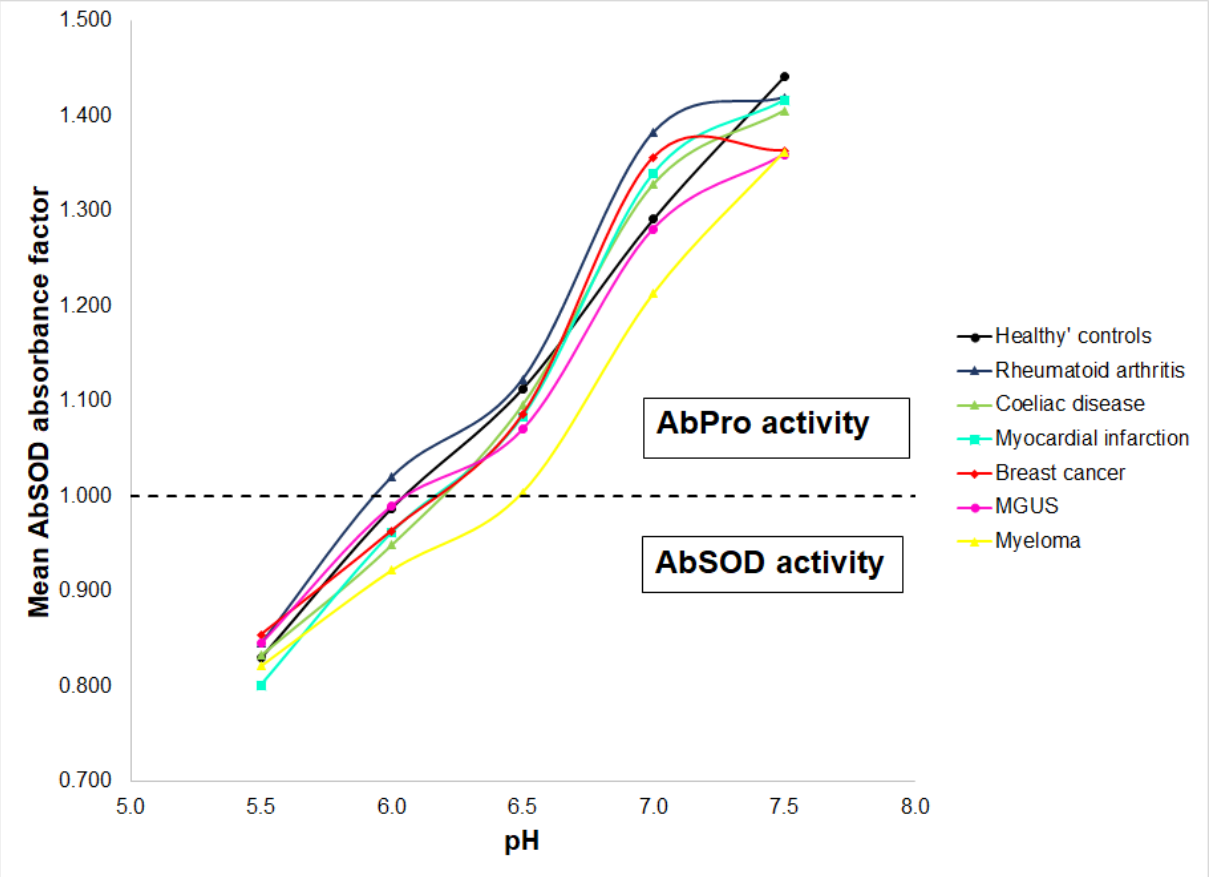

Figure 5.19: AbSOD factor at 661 seconds, between patient groups

The average AbSOD factor for all groups across the pH range studied was variable. At pH 5.5, AbSOD factor was <1.0, indicating AbSOD activity. At pH 6.0, the average AbSOD factor for all groups except the rheumatoid arthritis group were <1.0. At pH 6.5, AbSOD factor was >1.0 for all groups except the myeloma group, which was approximately 1.0. At pH 7.0 and 7.4, the AbSOD factor for all groups was >1.0, indicating strong AbPro activity. The AbSOD activity rapidly decreased from pH 5.5 to 6.0, before it diminished and transitioned to strong AbPro activity between pH 6.5 to 7.4.

5.5 Discussion

The experiments in Chapter 5 were designed to investigate the superoxide dismutase activity of antibodies isolated from serum over pH ranges associated with the inflammatory and pathophysiological environments of diseases associated with oxidative stress, such as cancer and autoimmune aetiology, compared to 'healthy' controls. The experiments were the first to investigate the superoxide dismutase activity of antibodies isolated from serum at pH 5.5 – 7.4. In total, data from 19- 'healthy' controls and 59- patients were analysed using one-way ANOVA, followed by subsequent Tukey-Kramer, or Games-Howell post-hoc analysis. Data described in this chapter supports the hypothesis antibodies of the immune system play a role in pathological and physiological redox processes.

5.5.1 The effect of pH and time exposure was variable between groups

The results of this study indicated that pH and time course of exposure are important factors in the redox activity of antibodies in disease and physiology. The AbSOD / antioxidant activity observed over the initial period of reaction (185 seconds – pH 5.5 – 7.4) transitioned to pro-oxidant activity thereafter (by 661 seconds – pH 6.5 – 7.4). The progressive increase in superoxide generation was not observed in blank readings, where there was a steady generation of superoxide and increase in formazan formation.

5.5.1.1 AbSOD activity at acidic pH

At 185 seconds over the pH range investigated, at 317 seconds between pH 5.5 and 6.5, and at 661 seconds between pH 5.5 and 6.0, AbSOD activity (antioxidant activity) was inherent to all patient groups studied. AbSOD activity was increased at acidic pH; a possible explanation for this might be due to the association of acidic pH environments with inflammation. The increase in immune cells that can produce superoxide such as neutrophils in acute inflammation and macrophages in chronic inflammation (Winterbourn, Kettle and Hampton, 2016), would increase the demand for molecules that can detoxify free radicals. In Chapter 4, it was demonstrated CuZnSOD activity is independent of pH, which may suggest there is not a requirement for antibodies with SOD activity, however antibodies are far more ubiquitous and likely to be present at sites of infection and inflammation. Secondly, antibodies may act as signalling molecules, generating H_2O_2 to signal

recruitment of leukocytes in wound healing (Niethammer, Grabher, Look and Mitchison, 2009), or in response to bacterial infection, in a similar fashion to the respiratory burst by NADPH oxidases.

Prior studies evaluating the AbSOD activity of murine antibodies at pH 5.4 to 6.4, observed IgG had superoxide dismutase activity comparable to that of CuZnSOD (Petyaev and Hunt, 1996). In addition, a study of antibodies isolated from human arteries and atherosclerotic lesions demonstrated superoxide dismutase activity increased with severity of lesion progression at pH 6.45 and pH 7.81 leading to the speculation antibodies contribute to the mechanisms which control the progression of atherosclerosis through supply of SOD activity (Petyaev *et al.*, 1998). More recently, a study at pH 10.2, observed IgG-dependent dismutation in patients with multiple sclerosis (MS) (Smirnova *et al.*, 2020). Only the initial rate of reaction was investigated, with reaction times between 5 and 7 minutes, using the superoxide generation system of xanthine-xanthine oxidase, and detection with NBT. The group reported, IgG-dependent dismutation (AbSOD activity) in MS was significantly increased compared to 'healthy' donors, but decreased with increasing disease severity, which the group considered to be a protective anti-inflammatory mechanism in the extracellular environment.

5.5.1.2 AbSOD activity and AbPro activity and time exposure

Prolonged incubation of antibodies with the superoxide generating system resulted in a reduction in AbSOD activity and an increase in the production of superoxide or AbPro (pro-oxidant) activity; this is the first time this has been reported. The transition from AbSOD to AbPro activity occurred more rapidly as the pH rose from acidic to physiological pH. Reports of antioxidant to pro-oxidant switches are scarce but have been described with dehydroascorbate during LDL oxidation by copper(II) ions (Horsley *et al.*, 2007), and with damage to DNA by phenolic compounds in the presence of copper (II) ions (Jomová *et al.*, 2019). Additionally, CuZnSOD has been reported to act as a pro-oxidant under certain conditions (Yim *et al.*, 1998). A note of caution is due here since the exact mechanism of AbPro activity is unknown; a reserved description of the results is there was increased conversion of NBT to formazan, caused by the presence of antibodies.

5.5.2 AbSOD activity was reduced in ‘healthy’ controls at pH 5.5

It was hypothesised the AbSOD activity of ‘healthy’ controls would be decreased in comparison to diseases associated with immune dysfunction and oxidative stress. Over 3 and 5 minutes of assay reaction time, AbSOD activity was decreased the most in the ‘healthy’ control group compared to disease groups, which may support the hypothesis that increased AbSOD activity is activated by antibody exposure to acidic pH (pH 5.5). The acidic pH associated with local inflammatory environments, could result in a decreased activity of peroxidase enzymes such as catalase (pH optimum 6.8 – 7.5; Aebi, 1984) and glutathione peroxidase (pH optimum 8.5; Guo *et al.*, 2014), which may have the repercussions of localised increase in H_2O_2 concentration.

5.5.3 AbSOD activity was increased in rheumatoid arthritis at pH 5.5

It was hypothesised that AbSOD activity would be significantly increased at acidic pH in RA patients, compared to ‘healthy’ controls. At pH 5.5 (185 seconds), patients with rheumatoid arthritis had significantly increased AbSOD activity (lower AbSOD factor than ‘healthy’ controls). Although the effect size was small (Hedge’s g = 0.30), these results provide further support to the hypothesis that increased AbSOD activity at pH 5.5 may serve as a protective mechanism to reduce free radical damage. On the other hand, it could be suggested that the production of H_2O_2 by antibodies, such as rheumatoid factor or antibodies bound by rheumatoid factor, would not be sequestered due to the acidic environment where peroxidase enzymes do not function optimally, and could in turn exacerbate the symptoms observed in this disease.

5.5.4 AbSOD activity was increased in myocardial infarction at pH 5.5

It was hypothesised the AbSOD activity observed in MI would be significantly increased in comparison to ‘healthy’ controls, at acidic pH. At pH 5.5 (317 seconds), patients that had experienced myocardial infarction had significantly increased AbSOD activity (lower AbSOD factor) than ‘healthy’ controls. The small-medium effect size (Hedge’s g = 0.40) suggested the results between the two groups were practically significant. This result was interesting as it pointed further towards the hypothesis that AbSOD activity at pH 5.5 may confer antioxidant protection at myocardial tissue post-infarction. A possible mechanism for this could

be the AbSOD activity of anti-cardiac troponin antibodies (ATAs), which develop when troponin is released from myocardial tissue into the circulation. A study of 390 patients with chronic heart failure, found 72 patients developed detectable ATAs, which were associated with improved survival and increased left ventricular ejection fraction (LVEF), suggesting they may have protective effects (Doesch *et al.*, 2011). However, a study of 108 patients with myocardial infarction reported the recovery of left ventricular ejection fraction was hindered in patients with anti-cardiac troponin antibodies (Leuschner *et al.*, 2008). The increased damage to myocardium in myocardial infarction, suggests AbSOD activity of anti-cardiac troponin antibodies at cardiac tissue in this circumstance could equally offer a potential mechanism by which reactive species are formed in ischemic tissue.

5.5.5 AbSOD activity was increased in the myeloma between pH 6.0-7.4

It was hypothesised the AbSOD activity observed in myeloma would be significantly increased in comparison to 'healthy' controls, at acidic pH. Myeloma cells produce lactic acid which results in dissociation of protons because of anaerobic glucose metabolism, leading to extracellular acidification, reducing pH to between 6.2 and 6.8 (Amachi *et al.*, 2016). Therefore, it is likely that all immunoglobulins produced by myeloma cells are transiently exposed to an acidic environment, which may be the reason why AbSOD / AbPro activity was aberrant at pH 6.0-7.4 when other diseases were not significantly different from 'healthy' controls.

At pH 6.0 (661 seconds), myeloma patients had significantly increased AbSOD activity compared to 'healthy' controls. The medium-large effect size (Hedge's g = 0.62) suggested results between the two groups were practically significant. This finding was consistent with the underlying results of Petyaev *et al.* (1998), who found AbSOD activity was increased in atherosclerotic lesions, and that of Smirnova *et al.* (2020), who demonstrated IgG-dependent dismutation was increased in multiple sclerosis, compared to 'healthy' controls. Both research groups hypothesised, in the diseases they studied, antibodies gave antioxidant protection against free radicals.

5.5.6 AbPro activity was decreased in myeloma between pH 6.5-7.4

AbPro activity was significantly decreased in myeloma patients at:

- pH 6.5 (661 seconds) – medium effect size (Hedge's g = 0.53)
- pH 7.0 (185 seconds) – medium-large effect size (Hedge's g = 0.61)
- pH 7.0 (317 seconds) – medium-large effect size (Hedge's g = 0.62)
- pH 7.4 (185 seconds) – medium effect size (Hedge's g = 0.51)
- pH 7.4 (661 seconds) – medium effect size (Hedge's g = 0.44)

The medium and medium-large effect sizes of all the results suggested the results between myeloma and 'healthy' controls are practically significant. The finding that antibodies in myeloma demonstrated reduced pro-oxidant activity was expected. It was apparent AbSOD activity lasted longer in myeloma patients before transitioning to AbPro activity. There are several possible explanations for these results.

The monoclonal antibodies formed in myeloma could be structurally unstable (Stevens and Argon, 1999) and may be more susceptible to protein modifications, which might cause folding of immunoglobulin into a confirmation more favourable for SOD activity.

Another hypothesis could be during protein A/G agarose purification, serum free light chains (immunoglobulin light chains) may have been co-purified with intact IgG. There was no information available in the manufacturers kit insert (Siemens, Ref: DF76) that indicated serum free light chains were detected by the IgG method used for IgG quantitation (see section 2.7). Petyaev and Hunt (1996), discovered SOD activity of immunoglobulins could be localised to the antigen binding site, i.e., variable region of light chains. This may have resulted in the reduced AbPro activity observed.

It is possible the high titer of monoclonal antibodies observed in myeloma, may result in reduced diversity of normal polyclonal antibodies (Chicca *et al.*, 2020). Based on the results from 'healthy' controls, where polyclonal antibodies of diverse repertoire are produced and AbSOD activity is decreased / AbPro activity increased, a reduction in different types of antibodies observed in myeloma could well account for the increased AbSOD activity / decreased AbPro activity. It is likely *in vivo* the AbSOD activity response could also be further increased than observed in these experiments due to the high concentrations of monoclonal antibodies in myeloma. In these experiments, each patient was standardised using the IgG assay, which may have negated this observation.

Finally, there may also be potential of the damaging effects of increased AbSOD activity and reduced AbPro activity. The catalytic activity of Bence Jones proteins (light chains) have been reported to have cytotoxic effects which lead to renal damage (Matsuura *et al.*, 2006). The production of H_2O_2 by intact IgG and light chains may induce cytotoxic effects that contributes to renal cellular injury (Paul *et al.*, 1995).

5.5.7 AbPro activity was decreased in breast cancer at pH 7.4

It was hypothesised the AbSOD activity observed in breast cancer would be significantly increased in comparison to 'healthy' controls, at acidic pH. At pH 7.4 (661 seconds), breast cancer patients had significantly decreased AbPro activity compared to 'Healthy' Controls. The medium effect size (Hedge's g = 0.46) indicated the difference was practically significant. The result may be explained by the presence of tumour-reactive antibodies in breast cancer (Garaud *et al.*, 2018). It was also possible patients included in the study were being treated with monoclonal antibodies such as trastuzumab (Herceptin). The specific monoclonal antibody could have increased AbSOD activity at pH 7.4, nullifying the polyclonal AbSOD response.

5.5.8 Why were coeliac disease and MGUS not significantly different?

The antibodies against TTG, gliadin, and actin that characterise coeliac disease are primarily of the IgA subclass, however there are occurrences where IgA deficiency occurs in patients with coeliac disease and there is a class-switch to antibodies of the IgG subclass. The protein agarose treatment of serum samples would not have isolated the IgA subclass as it only binds weakly to this subclass (see binding characteristics of Cat no: 20423, Thermo Fisher Scientific). Hence, the contribution of AbSOD activity by the pathological antibody would have likely been unobservable. Future work may use protein L agarose after protein A/G agarose treatment, or alternatively anti-IgA affinity chromatography or a similar technique could be used to isolate and investigate IgA antibodies. Secondly, but less likely the cause is the pH of 'healthy' mucosal surface of the jejunum is approximately pH 6.0. Whereas in coeliac disease, the pH increases to approximately 6.7 (Rawlings, Lucas and Russell, 1987; McEwan *et al.*, 1990). Unlike the other disease states investigated, there is a reduction in acidity of tissues observed in the disease.

In MGUS, the abnormal proliferation of monoclonal antibodies would suggest the AbSOD activity may be significantly different to 'healthy' controls, however this was not the case. MGUS is a non-cancerous condition but may lead to the formation of diseases such as myeloma. The mean AbPro activity of the MGUS group was lower than myeloma at pH 7.4 (661 seconds), however the standard deviation was larger, possibly due to differences in disease severity.

5.5.9 Is AbSOD activity protective?

The similarity in tertiary structure between the immunoglobulin domain and the copper-zinc superoxide dismutase subunit led to the postulation of an evolutionary and functional relationship between antibodies and CuZnSOD (Richardson *et al.*, 1976). The structural similarity and potential evolutionary relationship suggest antibodies may well have antioxidant protective abilities. Although it has been proven that antibodies can inhibit the formation of formazan in the NADH/PMS-NBT assay (Petyaev and Hunt, 1996 and Smirnova *et al.*, 2020, Chapter 4 and Chapter 5) and increase hydrogen peroxide formation (Petyaev *et al.*, 1998), thus offering antioxidant protection, the mechanisms and enzymatic pathways are complex.

Antibodies dismutate superoxide radicals to hydrogen peroxide, offering antioxidant protection at pH values conducive to the optimal functioning of enzymes that decompose hydrogen peroxide. The pH optimum for human catalase is 6.8 – 7.5 (Aebi, 1984) and human glutathione peroxidase is 8.5 (Guo *et al.*, 2014). An accumulation of hydrogen peroxide may occur at pH values outside the range of optimal functioning for enzymes that decompose this molecule.

During myocardial infarction, the pH of ischemic tissues can decrease between pH 6.0 – 6.5, and in rheumatoid arthritis the pH of synovial fluid can reduce to pH 6.8 – 7.1 (Rajamäki *et al.*, 2013). However, it is possible that areas of localised pH below this level could develop. At acidic pH 5.5 (associated with inflammation), AbSOD activity was statistically significantly increased in patients with rheumatoid arthritis and myocardial infarction. In terms of myeloma, the clinical significance of acidic pH in kidneys should be considered. In 1985, a study showed that infusion of a human Bence Jones proteins in to aciduric rats (pH 6.0) can produce acute renal failure (Holland *et al.*, 1985). In this study, at pH 6.0 myeloma patients had statistically significantly increased AbSOD activity compared to 'healthy' controls. Without the simultaneous increase of hydrogen peroxide catalysing enzymes such

as catalase or glutathione peroxidases, AbSOD activity could increase hydrogen peroxide accumulation in these pathologies.

5.5.10 Conclusion

In conclusion, it is hypothesised that antibodies in general offer antioxidant protection in the form of AbSOD activity. However, in some pathologies or with increasing severity of disease, due to the suboptimal peroxidase and catalase pH conditions, AbSOD activity may result in an accumulation of hydrogen peroxide, which could exacerbate oxidative stress and inflammation in diseased tissues.

5.5.10.1 Clinical relevance of findings

The results in this chapter may have clinical applications in identification and treatment of patients at risk of cast nephropathy and provide deeper insight into the mechanism of renal toxicity induced by this disease complication. In research by Petyaev and Hunt (1996), the SOD activity of antibodies was localised to the variable region of antibodies, which constitutes the light and heavy chains of the antigen binding site. In myeloma, there is an increased production of monoclonal free light chains (FLCs), which can result in kidney injury via formation of casts, caused by precipitation light chains which bind to Tamm-Horsfall protein in the kidney. One of the factors that promotes formation of casts is acidic urine (Cancarini *et al.*, 2021). The acidic pH promotes aggregation of FLCs (Basnayake *et al.*, 2011).

The findings that AbSOD activity is increased at acidic pH (myeloma) and results in the formation of hydrogen peroxide, according to the hypothesis above would mean the accumulation of hydrogen peroxide in the kidney, which could exacerbate oxidative stress and inflammation in this tissue. If AbSOD activity in the absence of sufficient hydrogen peroxide decomposition was a mechanism of nephrotoxicity in myeloma, urinary pH monitoring (approximate pH 7.0; Cancarini *et al.*, 2021) and subsequent corrective urine alkalinisation treatment to neutralise the pH, e.g., sodium bicarbonate treatment, would be recommended. The mechanism of action for alkalinisation treatment is thought to occur through the reduction of protein aggregation (cast formation) induced by acidic pH (Ray *et al.*, 2018).

The investigation of AbSOD activity at pH 5.5 has shown that it was increased in myocardial infarction and rheumatoid arthritis. The acidic pH at

synovial joints associated with inflammation and the localised acidic pH in myocardium post infarction, suggest that although AbSOD activity is an antioxidant mechanism, the conversion of superoxide to hydrogen peroxide without sufficient catalase or peroxidase activity could increase the levels of ROS at these sites. There is potential that hydrogen peroxide in the presence of metal ions, such as iron, could participate in Fenton chemistry.

In rheumatoid arthritis and myocardial infarction, it is hypothesised that administration of chelation therapy could improve outcomes for patients. While chelation therapy in rheumatoid arthritis has shown good clinical outcomes, it has only been trialled in limited studies (Leipzig *et al.*, 1970; Bamonti *et al.*, 2011). Tan and Smolen (2016), suggested administration of chelation therapy targeted directly to inflamed joints could be conceivable. Trials assessing the efficacy of chelation therapy in myocardial infarction are more comprehensive. The 'Trial To Assess Chelation Therapy (TACT1)' concluded intravenous administration of disodium EDTA, post myocardial infarction, 'modestly' reduced the risk of adverse cardiovascular outcomes, however a 'striking' reduction was observed in diabetic patients (Escolar *et al.*, 2014). A study investigating metal ions in diabetic patients found iron levels were raised (Kaple *et al.*, 2020). The TACT2 trial is currently underway, with the aim to reproduce the findings of TACT1. From this study's perspective it is hypothesised chelation therapy would reduce oxidative stress by removal of metal ions, that along with the products of AbSOD activity may participate in Fenton chemistry.

Chapter 6 investigates the levels of antioxidant and oxidative stress markers in diseases associated with oxidative stress and immune dysfunction compared to healthy controls. These findings highlight the potential of antioxidant measurements as prognostic tools for cancer.

CHAPTER 6: Investigation of antioxidant and pro-oxidant biomarkers in patients

6.1 Background

Antioxidants play a crucial role in the protection of lipids, proteins, and DNA from oxidative stress-induced damage *in vivo*. Endogenous antioxidants, superoxide dismutase, catalase and glutathione peroxidase are the first line of defence against ROS. Superoxide radicals, which are the precursor to most RS *in vivo* are generated as a by-product of mitochondria respiration, by NADPH oxidases and xanthine oxidase (Handy and Loscalzo, 2012).

Superoxide radicals are catalytically dismutated by superoxide dismutase (SOD) to form hydrogen peroxide and oxygen (McCord and Fridovich, 1969). When hydrogen peroxide accumulates, it is toxic to cells, and in the presence of ferrous irons (Fe^{2+}) can be converted to the potent hydroxyl radical ($^{\bullet}OH$) via the Fenton reaction (Liochev and Fridovich, 1999). Peroxidases and catalase prevent the damaging effects of hydrogen peroxide by catalytically decomposing it to water and oxygen (Halliwell and Gutteridge, 2015d).

Cell membranes function as a biological barrier that are composed of lipids. Due to their structure consisting of carbon-carbon double bonds near methylene groups (Bast, 1993), and the proximity of membranes to metabolic activity and reactions that generate reactive species, they are susceptible to oxidative damage. Reactions of the lipid bilayer with RS can result in lipid peroxidation (Halliwell and Gutteridge, 2015a), which causes an increase in measurable by-products such as hydroperoxides (Jiang, Woollard and Wolff, 1991).

6.2 Patient specific hypotheses

Rheumatoid arthritis

In rheumatoid arthritis (RA), it was reported that plasma catalase activity (CAT) was significantly decreased, and lipid peroxidation was increased compared to 'healthy' controls (Kamanli *et al.*, 2004). In another study, erythrocyte SOD activity was decreased in RA patients (Kiziltunc, Coğalgil, and Cerrahoğlu, 1998).

It was hypothesised in RA that serum catalase (activity and concentration) and SOD (activity and concentration) would be decreased and serum hydroperoxides would be increased in comparison to 'healthy' controls.

Coeliac disease

A study of 39 paediatric patients found hydroperoxides and SOD activity were significantly increased in active coeliac disease (CD). CAT activity was increased in CD patients that were following a gluten free diet (Stojiljković *et al.*, 2007).

It was hypothesised in CD that serum catalase (activity and concentration), serum SOD (activity and concentration) and serum hydroperoxide concentration would be increased in comparison to 'healthy' controls.

Myocardial infarction

Several studies of lipid peroxidation after myocardial infarction (MI) agreed lipid peroxidation was increased (Bagatini *et al.*, 2011; Noichri *et al.*, 2013). On the other hand, reports of measured SOD and CAT activity was more inconsistent. Bagatini *et al.* (2011), observed increases in both SOD and CAT activity amongst MI subjects, whereas Patil, Chavan and Karnik (2007) observed a decrease and Noichri *et al.* (2013) observed a decrease in CAT activity. Additionally, a study observed increased plasma SOD activity was a marker of successful myocardial reperfusion and myocardial salvage (reversibly injured myocardium) in MI (Tomoda, Morimoto and Aoki, 1996).

It was hypothesised in MI that serum hydroperoxides would be increased compared to 'healthy' controls, and that serum catalase (activity and concentration) and SOD (activity and concentration) would be variable, resulting in large differences within this group.

Breast cancer

In breast cancer (BC) tissues, it was reported lipid peroxidation and SOD activity were increased in malignant tissue compared to non-malignant tissue, whereas catalase was significantly decreased (Tas *et al.*, 2005). A later study found plasma lipid peroxidation was significantly increased in BC and reported total erythrocyte CAT and SOD activity were decreased (Kasapović *et al.*, 2008). The differences between the SOD activity results are likely due to the differences in sample type, where cancer cells may utilise SOD for cell survival.

It was hypothesised in BC that serum catalase (activity and concentration) and SOD (activity and concentration) would be decreased and serum hydroperoxides would be increased in comparison to 'healthy' controls.

Myeloma and MGUS

A study of myeloma (MM), where MGUS was used as a control reported SOD1 expression was increased in MGUS (n = 44) compared to 'healthy' controls (Salem *et al.*, 2015). In 2009, Sharma *et al.* observed the activity of SOD, GPx and CAT were significantly decreased, and lipid peroxidation was increased in myeloma compared to controls.

It was hypothesised in myeloma it was hypothesised that serum catalase (activity and concentration) and SOD (activity and concentration) would be decreased and serum hydroperoxides would be increased. In MGUS it was hypothesised that SOD (activity and concentration), catalase (activity and concentration) and serum hydroperoxide concentration would be increased in comparison to 'healthy' controls.

6.3 Aims

The aim of the work in this chapter was to quantify levels of antioxidant (serum catalase and serum SOD activity and concentration) and pro-oxidant biomarkers (lipid hydroperoxide concentration) in serum to determine the antioxidant status of patients with clinically verified autoimmune diseases (coeliac disease and rheumatoid arthritis), various classes of cancer / pre-cancer (breast cancer, myeloma and MGUS) and cardiovascular disease (myocardial infarction), were increased or decreased compared to 'healthy' controls.

6.4 Materials and methods

6.4.1 Patients, samples and data analysis

Patients

Fifty-nine patients – with rheumatoid arthritis, coeliac disease, myocardial infarction, breast cancer, monoclonal gammopathy of unknown significance and multiple myeloma – and nineteen 'healthy' controls were studied (see section 2.13.1). All patients had been referred for laboratory investigation to Clinical Biochemistry, Addenbrooke's Hospital, Cambridge University Hospitals NHS Foundation Trust, Cambridge. Laboratory studies and sample management were undertaken in accordance with the World Medical Association Declaration of Helsinki (2000). The gender frequency and age range across disease and control groups can be seen in appendix 2.5.

Ninety-four patients and twenty-one 'healthy' controls were analysed in laboratory investigations; however, thirty-five patients and two 'healthy' controls were removed from the data analysis due to analytical interference and group sizes less than 6, details of which can be referred to in appendix 2.4.

Samples

Serum samples were used for catalase (activity and concentration), superoxide dismutase (activity and concentration) and lipid hydroperoxide concentration determinations. Details of sample collection are described in detail in section 2.13.3.

Data analysis

The data was analysed using IBM SPSS statistics 26. The approach taken is described in section 2.13 was used to perform one way ANOVA's / Welch's ANOVA's, and Tukey-Kramer / Games Howell post hoc tests. Additionally, Hedge's g (a measured of effect size) was calculated to determine the relative significance of any statistically significant results generated.

6.4.2 Immunoassays

All samples, calibrators and quality controls were analysed in duplicate, and the average concentration reported for all immunoassays.

Quantitative measurement of catalase concentration was performed using a catalase immunoassay (section 2.8) on the Meso Scale Discovery (MSD) platform. The assay was developed using matched antibodies from R&D systems (Cat no: MAB3398 and AF3398) and a calibrator from AbCam (Cat no: ab172164). Low and high pooled serum controls were run at the beginning and end of every batch. Dilutions of serum and controls were prepared in DELFIA diluent II (1 in 5; Cat no: B132-200) prior to analysis.

Quantitative measurement of CuZnSOD was performed using a CuZnSOD enzyme-linked immunosorbent assay (ELISA) – see section 2.9. The assay used a matched antibody and calibrator protein kit (Cat no: BMS222MST, Bender MedSystems, Vienna, Austria) and was run according to the manufacturer guidelines. Dilutions of serum and controls were prepared in x1 PBS (1 in 100) prior to analysis.

6.4.3 Colorimetric assays

All samples, calibrators and quality controls were analysed in duplicate and the average concentration reported for all colorimetric assays.

Serum catalase activity levels were analysed using a commercially available assay from Invitrogen™ (Cat no: EIACATC, Life technologies Corporation, Maryland, U.S.A.) – see section 2.10. Serum samples and quality controls (pooled human serum) were thawed, mixed and centrifuged at 3000 g for 5.0 minutes, then diluted (1 in 30) in x 1 assay buffer for analysis (quality controls were diluted 1 in 30, and 1 in 60).

Serum superoxide dismutase (SOD) activity levels were analysed using a commercially available assay from Invitrogen™ (Cat no: EIASOD, Life technologies Corporation, Maryland, U.S.A.) – see section 2.11. Serum samples and quality controls (pooled human serum) were thawed, mixed and centrifuged at 3000 g for

5.0 minutes, then diluted (1 in 5) in coloured assay buffer for analysis (quality controls were diluted 1 in 5 and 1 in 10).

Serum hydroperoxides were measured by an adaptation of the peroxide measuring technique of Jiang, Woollard and Wolff (1990) – see section 2.12. A reaction system of 50 mM H_2SO_4, 250 µM xylenol orange, 200 mM sorbitol and 500 µM ammonium ferrous sulphate at pH 1.5 was used. The xylenol orange with filtered with a 0.2 µM regenerated cellulose membrane syringe filter, as it significantly improved the sensitivity and precision of the assay.

6.4.4 Serum adjusted catalase and SOD

Serum adjusted catalase and SOD were calculated by dividing the activity of the enzyme (U/mL) by the concentration (ng/mL) to give a calculation of overall enzymic efficiency. It was hypothesised that by assaying the concentration and the activity of the enzymes, it would improve the specificity, to give an overall evaluation of SOD and catalase.

6.5 Results

6.5.1 Serum catalase concentration

The descriptive statistics associated with serum catalase concentration (ng/ml) across the seven patient groups are reported in Table 6.1. The breast cancer group was associated with the numerically smallest mean serum catalase concentration (*M* = 124), and the myocardial infarction group was associated with the highest mean serum catalase concentration (*M* = 170). To test the hypothesis that the seven patient groups had different serum catalase concentrations (ng/ml), a one-way (between-groups) ANOVA was performed. Prior to conducting the ANOVA, the assumption of normality was evaluated and determined to be satisfied as the seven groups' distributions were associated with a skew and kurtosis less than |<2.0| and |<9.0|, respectively (Schmider, Zielger, Danay, Beyer and Bühner, 2010; see Table 6.1). Furthermore, the assumption of homogeneity of variances was tested and satisfied via Levene's F test, $F(6, 71) = .755$, $p = .608$.

The independent between-groups ANOVA generated a statistically non-significant result, $F(6, 71) = 1.715$, $p = .130$. Thus, the null hypothesis of no differences between the serum catalase concentration means could not be rejected. A visual depiction of the means and 95% confidence intervals are presented in Figure 6.1. It can be observed that the error bars of serum catalase concentration across the disease and 'healthy' control groups overlap.

Table 6.1: ***Descriptive statistics – serum catalase concentration***

Descriptive statistics for serum catalase concentration (ng/ml) observed in control and patient disease groups

Disease group	N	M (ng/ml)	SD	Skew	Kurtosis
'Healthy' Control	19	126	39	0.167	-1.353
Rheumatoid Arthritis	7	143	29	0.488	-0.705
Coeliac Disease	11	166	49	0.654	0.193
Myocardial Infarction	6	170	56	1.419	1.746
Breast Cancer	7	124	29	-0.191	-1.639
Monoclonal Gammopathy of Unknown Significance	7	151	41	-0.040	0.464
Myeloma	21	131	51	0.955	-0.159

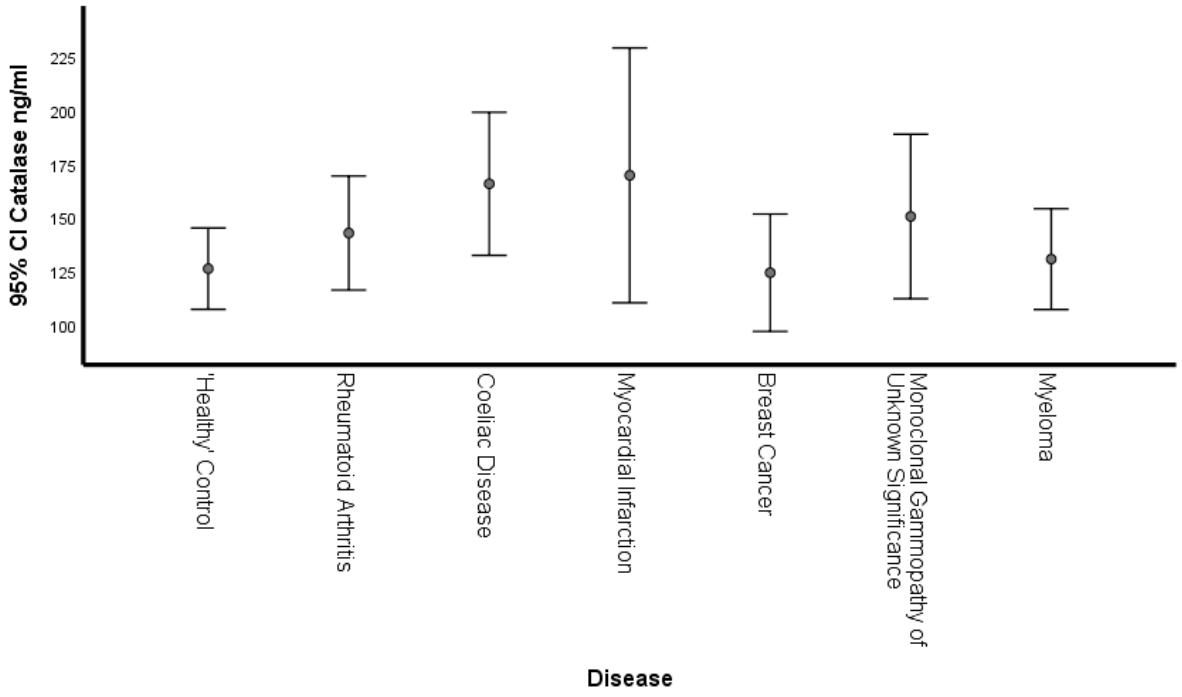

Figure 6.1: **Bar chart of serum catalase concentration**

Bar chart with serum catalase concentration (ng/ml) means and 95% confidence intervals observed in 'healthy' control and disease groups

6.5.2 Serum catalase activity

The descriptive statistics associated with serum catalase activity (U/ml) across the seven patient groups are reported in Table 6.2. The myeloma group was associated with the numerically smallest mean serum catalase activity (M = 48), and the myocardial infarction group was associated with the highest mean serum catalase activity (M = 114). To test the hypothesis that the seven patient groups had different serum catalase activity (U/ml), a one-way (between-groups) ANOVA was performed. Prior to conducting the ANOVA, the assumption of normality was evaluated and determined to be satisfied as the seven groups' distributions were associated with a skew and kurtosis less than |<2.0| and |<9.0|, respectively (Schmider, Zielger, Danay, Beyer and Bühner, 2010; see Table 6.2). The assumption of homogeneity of variances was tested and violated, as assessed by Levene's F test, $F(6, 71) = 5.137$, $p = .000$.

The independent between-groups Welch ANOVA generated a statistically significant result, $F(6, 22.617) = 5.780$, $p = .001$. Thus, the null hypothesis of no differences between the serum catalase activity means in different disease groups was rejected. To evaluate the differences between the seven means further, Games-Howell multiple comparisons were performed. As can be seen in Table 6.3, two of the six comparisons were statistically significant ($p < 0.05$). However, the statistically significant differences between the means were associated with low effect sizes based on Cohen's (1992) guidelines. A visual depiction of the means and 95% confidence intervals is presented in Figure 6.2. It can be observed that the serum catalase activity of disease groups associated with cancer tended to be lower than the other groups, including the 'healthy' control group.

Table 6.2: ***Descriptive statistics – serum catalase activity***

Descriptive statistics for serum catalase activity (U/ml) observed in control and patient disease groups

Disease group	N	M (U/ml)	SD	Skew	Kurtosis
'Healthy' Control	19	84	24	0.662	-0.200
Rheumatoid Arthritis	7	63	31	0.584	-1.161
Coeliac Disease	11	89	32	-0.159	-1.041
Myocardial Infarction	6	114	67	0.707	-0.798
Breast Cancer	7	49	13	-1.016	-0.806
Monoclonal Gammopathy of Unknown Significance	7	55	23	0.839	-1.126
Myeloma	21	48	28	1.839	2.805

Table 6.3: ***Games-Howell – serum catalase activity***

Results associated with Games-Howell multiple comparisons analysis

Comparison			*p*	*g*
'Healthy' Control	-	Rheumatoid Arthritis	0.676	0.20
'Healthy' Control	-	Coeliac Disease	0.998	-0.05
'Healthy' Control	-	Myocardial Infarction	0.906	-0.28
'Healthy' Control	-	Breast Cancer	0.003	0.33
'Healthy' Control	-	Monoclonal Gammopathy of Unknown Significance	0.157	0.27
'Healthy' Control	-	Myeloma	0.002	0.34

Note. N = 19 for 'Healthy' Control, 7 for Rheumatoid Arthritis, 11 for Coeliac Disease, 6 for Myocardial Infarction, 7 for Breast Cancer, 7 for Monoclonal Gammopathy of Unknown Significance and 21 for Myeloma; *p* = significance; *g* = Hedge's g

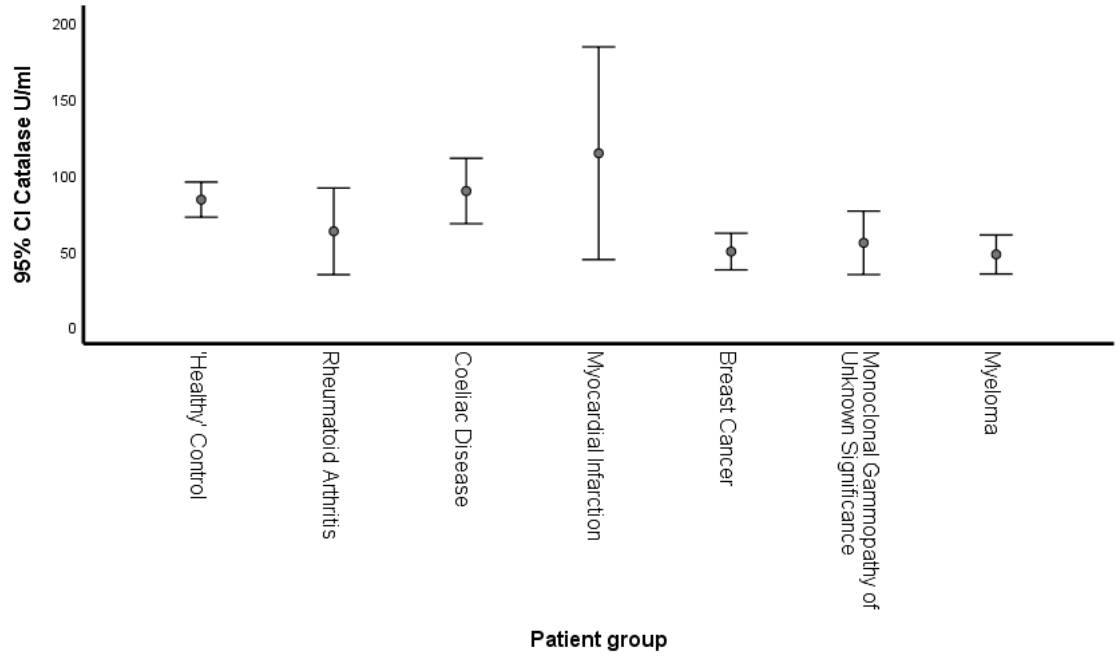

Figure 6.2: **Bar chart of serum catalase activity**

Bar chart with serum catalase activity (U/ml) means and 95% confidence intervals observed in 'healthy' control and disease groups

6.5.3 Adjusted Catalase activity

The descriptive statistics associated with serum adjusted catalase activity (U/ng) across the seven patient groups are reported in Table 6.4. The MGUS group was associated with the numerically smallest mean serum adjusted catalase concentration (*M* = 0.37), and the 'healthy' control group was associated with the highest mean serum adjusted catalase concentration (*M* = 0.68). To test the hypothesis that the seven patient groups had different serum adjusted catalase concentration (U/ng), a one-way (between-groups) ANOVA was performed. Prior to conducting the ANOVA, the assumption of normality was evaluated and determined to be satisfied as the seven groups' distributions were associated with a skew and kurtosis less than |<2.0| and |<9.0|, respectively (Schmider, Zielger, Danay, Beyer and Bühner, 2010; see Table 6.4). Furthermore, the assumption of homogeneity of variances was tested and satisfied via Levene's F test, $F(6, 71) = 1.819$, $p = .108$.

The independent between-groups ANOVA generated a statistically significant result, $F(6, 71) = 8.201$, $p = .000$. Thus, the null hypothesis of no differences between the serum adjusted catalase activity means in different disease groups was rejected. To evaluate the differences between the seven means further, simultaneous single step Tukey-Kramer multiple comparisons were performed. As can be seen in Table 6.5, four of the six comparisons were statistically significant ($p < 0.05$). Furthermore, the statistically significant differences between the means were associated with moderate effect sizes based on Cohen's (1992) guidelines. A visual depiction of the means and 95% confidence intervals is presented in Figure 6.3. It can be observed that the serum adjusted catalase activity of disease groups tended to be lower than the 'healthy' control group.

Table 6.4: ***Descriptive statistics – serum adjusted catalase activity***

Descriptive statistics for serum adjusted catalase activity (U/ng) observed in control and patient disease groups

Disease group	N	M (U/ng)	SD	Skew	Kurtosis
'Healthy' Control	19	0.68	0.12	1.014	2.679
Rheumatoid Arthritis	7	0.45	0.24	1.083	0.244
Coeliac Disease	11	0.55	0.19	1.161	3.210
Myocardial Infarction	6	0.64	0.22	0.322	-2.216
Breast Cancer	7	0.41	0.12	-0.211	0.507
Monoclonal Gammopathy of Unknown Significance	7	0.37	0.09	0.135	-0.726
Myeloma	21	0.37	0.16	1.139	0.718

Table 6.5: ***Tukey-Kramer – serum adjusted catalase activity***

Results associated with Tukey-Kramer multiple comparisons analysis

Comparison			*p*	*g*
'Healthy' Control	-	Rheumatoid Arthritis	0.031	0.44
'Healthy' Control	-	Coeliac Disease	0.394	0.24
'Healthy' Control	-	Myocardial Infarction	0.998	0.08
'Healthy' Control	-	Breast Cancer	0.007	0.52
'Healthy' Control	-	Monoclonal Gammopathy of Unknown Significance	0.001	0.61
'Healthy' Control	-	Myeloma	0.000	0.59

Note. N = 19 for 'Healthy' Control, 7 for Rheumatoid Arthritis, 11 for Coeliac Disease, 6 for Myocardial Infarction, 7 for Breast Cancer, 7 for Monoclonal Gammopathy of Unknown Significance and 21 for Myeloma; *p* = significance; *g* = Hedge's g

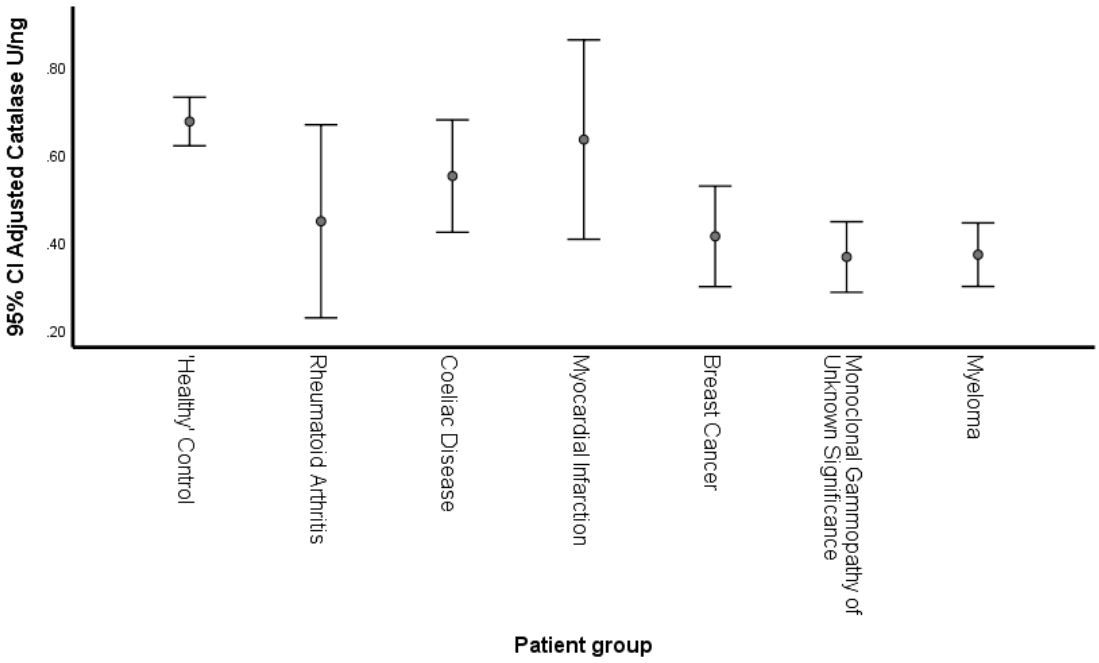

Figure 6.3: **Bar chart of serum adjusted catalase activity**

Bar chart with serum adjusted catalase activity (U/ng) means and 95% confidence intervals observed in 'healthy' control and disease groups

6.5.4 Copper-zinc superoxide dismutase concentration

The descriptive statistics associated with serum CuZnSOD concentration (ng/ml) across the seven patient groups are reported in Table 6.6. The breast cancer group was associated with the numerically smallest mean serum CuZnSOD concentration (M = 53), and the myocardial infarction group was associated with the highest mean serum CuZnSOD concentration (M = 230). To test the hypothesis that the seven patient groups had different serum CuZnSOD concentrations (ng/ml), a one-way (between-groups) ANOVA was performed. Prior to conducting the ANOVA, the assumption of normality was evaluated and determined to be satisfied for five of the groups, where distributions were associated with a skew and kurtosis less than |<2.0| and |<9.0|, respectively, but violated for the breast cancer and myocardial infarction groups, where skewness was greater than 2.0; (Schmider, Zielger, Danay, Beyer and Bühner, 2010; see Table 6.6). The assumption of homogeneity of variances was tested and violated, as assessed by Levene's F test, $F(6, 71) = 4.413$, $p = .001$.

The independent between-groups Welch ANOVA generated a statistically significant result, $F(6, 22.122) = 5.046$, $p = .002$. Thus, the null hypothesis of no differences between the serum CuZnSOD concentration means in different disease groups was rejected. To evaluate the differences between the seven means further, Games-Howell multiple comparisons were performed. As can be seen in Table 6.7, one of the six comparisons were statistically significant ($p < 0.05$). However, the statistically significant differences between the means were associated with low effect size based on Cohen's (1992) guidelines. A visual depiction of the means and 95% confidence intervals is presented in Figure 6.4. It can be observed that the serum CuZnSOD concentration of the breast cancer group was lower than the 'healthy' control group; both groups had similar standard deviation, however the standard deviation for the other groups were much larger.

Table 6.6: ***Descriptive statistics – serum CuZnSOD concentration***

Descriptive statistics for serum CuZnSOD (ng/ml) observed in control and patient disease groups

Disease group	N	M (ng/ml)	SD	Skew	Kurtosis
'Healthy' Control	19	135	72	0.562	0.082
Rheumatoid Arthritis	7	216	206	1.735	2.444
Coeliac Disease	11	180	75	0.884	3.470
Myocardial Infarction	6	230	274	2.276	5.263
Breast Cancer	7	53	37	2.564	6.666
Monoclonal Gammopathy of Unknown Significance	7	230	181	1.617	2.707
Myeloma	21	121	94	1.196	0.372

Table 6.7: ***Games-Howell – serum CuZnSOD concentration***

Results associated with Games-Howell multiple comparisons analysis

Comparison			*p*	*g*
'Healthy' Control	-	Rheumatoid Arthritis	0.933	-0.24
'Healthy' Control	-	Coeliac Disease	0.686	-0.14
'Healthy' Control	-	Myocardial Infarction	0.969	-0.28
'Healthy' Control	-	Breast Cancer	0.016	0.26
'Healthy' Control	-	Monoclonal Gammopathy of Unknown Significance	0.814	-0.29
'Healthy' Control	-	Myeloma	0.998	0.04

Note. N = 19 for 'Healthy' Control, 7 for Rheumatoid Arthritis, 11 for Coeliac Disease, 6 for Myocardial Infarction, 7 for Breast Cancer, 7 for Monoclonal Gammopathy of Unknown Significance and 21 for Myeloma; *p* = significance; *g* = Hedge's g

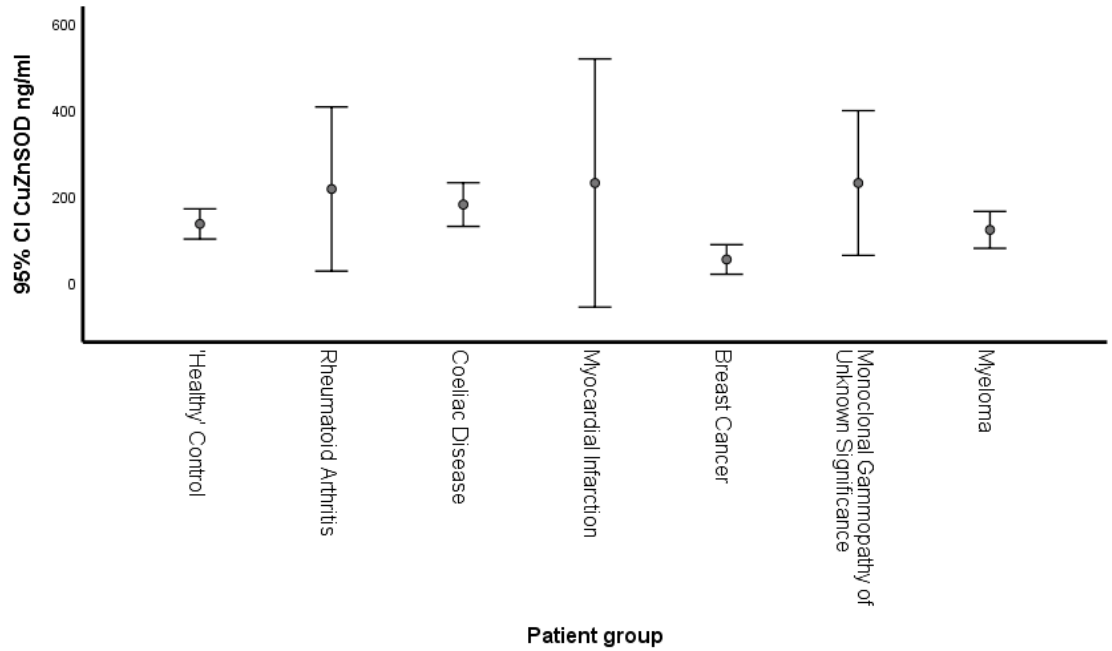

Figure 6.4: **Bar chart of serum CuZnSOD concentration**

Bar chart with serum CuZnSOD concentration (ng/ml) means and 95% confidence intervals observed in 'healthy' control and disease groups

6.5.5 Superoxide dismutase activity

The descriptive statistics associated with serum SOD activity (U/ml) across the seven patient groups are reported in Table 6.8. The myeloma group was associated with the numerically smallest mean serum SOD activity (M = 0.62), and the myocardial infarction group was associated with the highest mean serum SOD activity (M = 1.01). To test the hypothesis that the seven patient groups had different serum SOD activity (U/ml), a one-way (between-groups) ANOVA was performed. Prior to conducting the ANOVA, the assumption of normality was evaluated and determined to be satisfied for five of the groups, where distributions were associated with a skew and kurtosis less than |<2.0| and |<9.0|, respectively but violated for the 'healthy' control and coeliac disease groups, where skewness was greater than 2.0; (Schmider, Zielger, Danay, Beyer and Bühner, 2010; see Table 6.8). Furthermore, the assumption of homogeneity of variances was tested and satisfied via Levene's F test, $F(6, 71) = 1.925$, $p = .089$.

The independent between-groups ANOVA generated a statistically non-significant result, $F(6, 71) = 2.028$, $p = .073$. Thus, the null hypothesis of no differences between the serum SOD activity means could not be rejected. A visual depiction of the means and 95% confidence intervals are presented in Figure 6.5. It can be observed that the error bars of serum SOD activity across the disease and 'healthy' control groups overlap.

Table 6.8: ***Descriptive statistics – serum SOD activity***

Descriptive statistics for serum SOD activity (U/ml) observed in control and patient disease groups

Disease group	N	M (U/ml)	SD	Skew	Kurtosis
'Healthy' Control	19	0.84	0.46	2.547	5.624
Rheumatoid Arthritis	7	0.67	0.26	1.797	4.266
Coeliac Disease	11	0.86	0.38	2.573	7.391
Myocardial Infarction	6	1.01	0.45	1.737	2.820
Breast Cancer	7	0.71	0.09	0.561	-0.478
Monoclonal Gammopathy of Unknown Significance	7	0.63	0.11	0.471	0.824
Myeloma	21	0.62	0.12	0.798	0.298

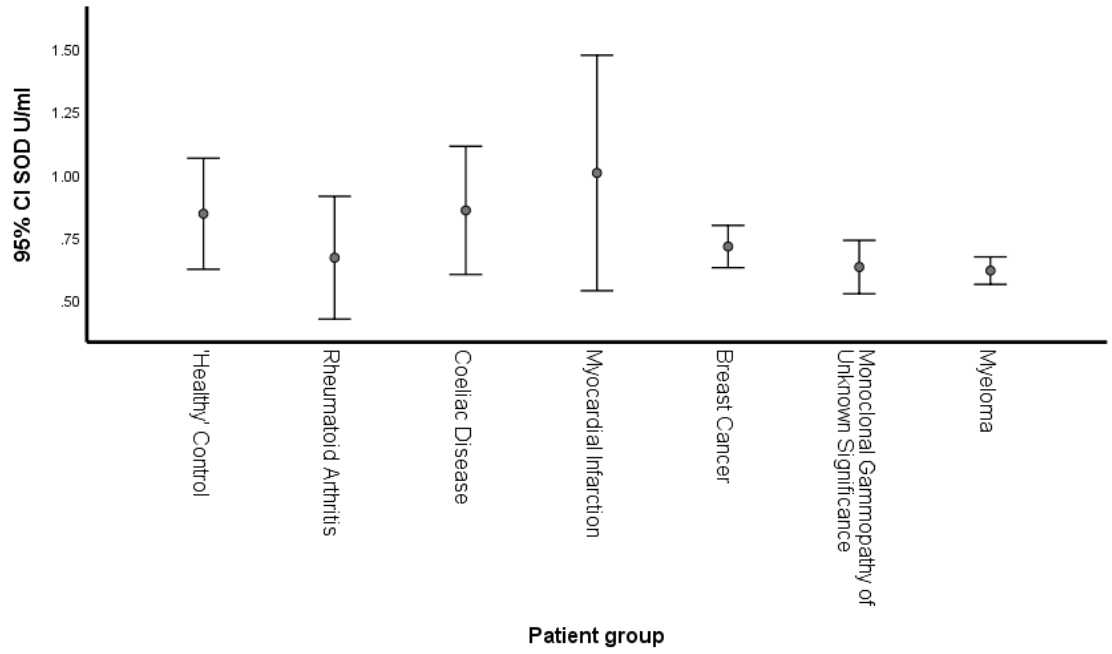

Figure 6.5: **Bar chart of serum SOD activity**

Bar chart with serum SOD activity (U/ml) means and 95% confidence intervals observed in 'healthy' control and disease groups

6.5.6 Adjusted superoxide dismutase activity

The descriptive statistics associated with serum adjusted SOD activity (U/ng) across the seven patient groups are reported in Table 6.9. The MGUS group was associated with the numerically smallest mean serum adjusted SOD activity (M = 0.004), and the breast cancer group was associated with the highest mean serum adjusted SOD activity (M = 0.017). To test the hypothesis that the seven patient groups had different serum adjusted SOD activity (U/ng), a one-way (between-groups) ANOVA was performed. Prior to conducting the ANOVA, the assumption of normality was evaluated and determined to be satisfied as the seven groups' distributions were associated with a skew and kurtosis less than |<2.0| and |<9.0|, respectively (Schmider, Zielger, Danay, Beyer and Bühner, 2010; see Table 6.9). Furthermore, the assumption of homogeneity of variances was tested and satisfied via Levene's F test, $F(6, 71) = 2.201$, $p = .053$.

The independent between-groups ANOVA generated a statistically significant result, $F(6, 71) = 5.553$, $p = .000$. Thus, the null hypothesis of no differences between the serum adjusted SOD activity means in different disease groups was rejected. To evaluate the differences between the seven means further, simultaneous single step Tukey-Kramer multiple comparisons were performed. As can be seen in Table 6.10, one of the six comparisons was statistically significant ($p < 0.05$). However, the statistically significant differences between the means were associated with a low effect size based on Cohen's (1992) guidelines. A visual depiction of the means and 95% confidence intervals is presented in Figure 6.6. It can be observed that the serum adjusted SOD activity of the breast cancer group was higher than the 'healthy' control group.

Table 6.9: ***Descriptive statistics – serum adjusted SOD activity***

Descriptive statistics for serum adjusted SOD activity (U/ng) observed in control and patient disease groups

Disease group	N	M (U/ng)	SD	Skew	Kurtosis
'Healthy' Control	19	0.008	0.006	1.172	0.351
Rheumatoid Arthritis	7	0.005	0.002	-1.374	1.062
Coeliac Disease	11	0.006	0.004	1.695	1.636
Myocardial Infarction	6	0.008	0.005	0.862	1.962
Breast Cancer	7	0.017	0.006	-1.093	2.027
Monoclonal Gammopathy of Unknown Significance	7	0.004	0.003	0.789	-0.211
Myeloma	21	0.008	0.005	0.543	-0.707

Table 6.10: ***Tukey-Kramer – serum adjusted SOD activity***

Results associated with Tukey-Kramer multiple comparisons analysis

Comparison			*p*	*g*
'Healthy' Control	-	Rheumatoid Arthritis	0.572	0.15
'Healthy' Control	-	Coeliac Disease	0.775	0.10
'Healthy' Control	-	Myocardial Infarction	1.000	0.02
'Healthy' Control	-	Breast Cancer	0.003	-0.32
'Healthy' Control	-	Monoclonal Gammopathy of Unknown Significance	0.486	0.16
'Healthy' Control	-	Myeloma	1.000	0.01

Note. N = 19 for 'Healthy' Control, 7 for Rheumatoid Arthritis, 11 for Coeliac Disease, 6 for Myocardial Infarction, 7 for Breast Cancer, 7 for Monoclonal Gammopathy of Unknown Significance and 21 for Myeloma; *p* = significance; *g* = Hedge's g

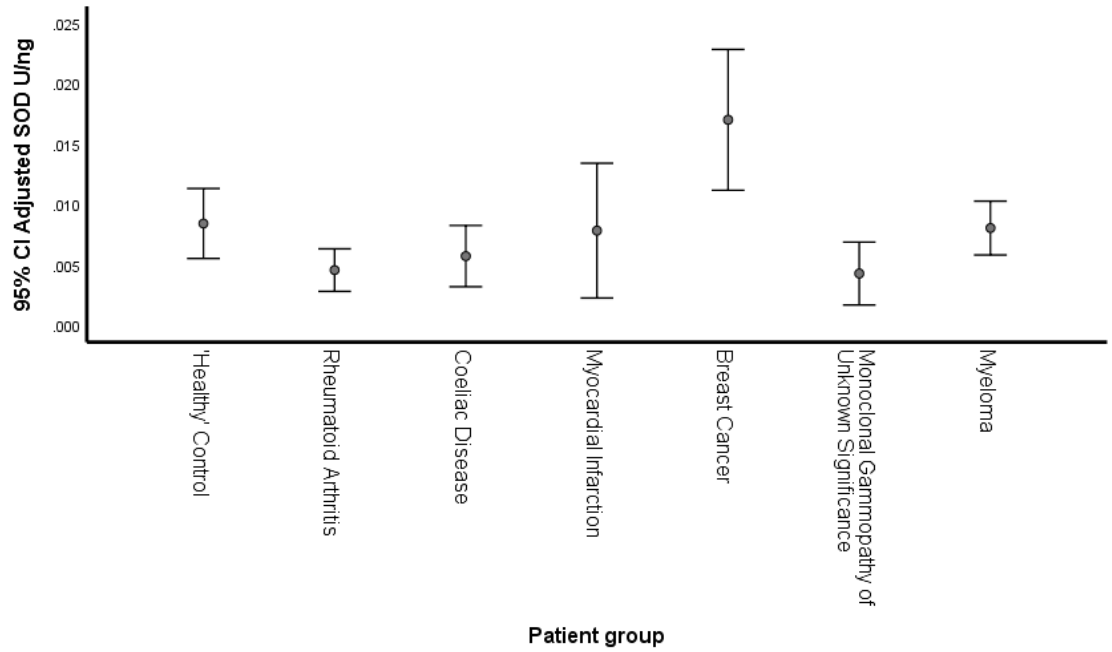

Figure 6.6: **Bar chart of serum adjusted SOD activity**

Bar chart with serum adjusted SOD activity (U/ng) means and 95% confidence intervals observed in 'healthy' control and disease groups.

6.5.7 Hydroperoxides concentration

The descriptive statistics associated with serum hydroperoxide concentration (μmol H_2O_2 equivalents/L) across the seven patient groups are reported in Table 6.11. The breast cancer group was associated with the numerically smallest mean serum hydroperoxide concentration (*M* = 4.7), and rheumatoid arthritis group was associated with the highest serum hydroperoxide concentration (*M* = 11.0). To test the hypothesis that the seven patient groups had different serum hydroperoxide concentration (μmol H_2O_2 equivalents/L), a one-way (between-groups) ANOVA was performed. Prior to conducting the ANOVA, the assumption of normality was evaluated and determined to be satisfied for five of the groups, where distributions were associated with a skew and kurtosis less than |<2.0| and |<9.0|, respectively, but violated for rheumatoid arthritis and coeliac disease, where skewness was greater than 2.0; (Schmider, Zielger, Danay, Beyer and Bühner, 2010; see Table 6.11). The assumption of homogeneity of variances was tested and violated, as assessed by Levene's F test, $F(6, 71) = 4.130$, $p = .001$.

The independent between-groups Welch ANOVA generated a statistically significant result, $F(6, 22.588) = 5.661$, $p = 0.001$. Thus, the null hypothesis of no differences between the serum hydroperoxide concentration means in different disease groups was rejected. To evaluate the differences between the seven means further, Games-Howell multiple comparisons were performed. As can be seen in Table 6.12, one of the six comparisons were statistically significant ($p < 0.05$). However, the statistically significant differences between the means were associated with low effect size based on Cohen's (1992) guidelines. A visual depiction of the means and 95% confidence intervals is presented in Figure 6.7. It can be observed that the serum hydroperoxide concentration of the MGUS disease group was higher than the 'healthy' control group; both groups had similar standard deviation, however the standard deviation for the other groups tended to be larger.

Table 6.11: ***Descriptive statistics – serum hydroperoxide concentration***

Descriptive statistics for serum hydroperoxide concentration (µmol H_2O_2 equivalents/L) observed in control and patient disease groups

Disease group	N	M (µmol H_2O_2 equiv. /L)	SD	Skew	Kurtosis
'Healthy' Control	19	6.4	1.9	1.124	0.815
Rheumatoid Arthritis	7	11.0	10.9	2.460	6.270
Coeliac Disease	11	10.6	8.4	2.028	4.392
Myocardial Infarction	6	5.8	3.7	0.035	-0.668
Breast Cancer	7	4.7	1.9	0.165	-1.415
Monoclonal Gammopathy of Unknown Significance	7	9.1	1.3	-0.288	-0.174
Myeloma	21	9.5	4.8	0.501	-0.793

Table 6.12: ***Games-Howell – serum hydroperoxide concentration***

Results associated with Games-Howell multiple comparisons analysis

Comparison			*p*	*g*
'Healthy' Control	-	Rheumatoid Arthritis	0.909	-0.45
'Healthy' Control	-	Coeliac Disease	0.659	-0.43
'Healthy' Control	-	Myocardial Infarction	0.999	0.07
'Healthy' Control	-	Breast Cancer	0.451	0.20
'Healthy' Control	-	Monoclonal Gammopathy of Unknown Significance	0.012	-0.32
'Healthy' Control	-	Myeloma	0.131	-0.34

Note. N = 19 for 'Healthy' Control, 7 for Rheumatoid Arthritis, 11 for Coeliac Disease, 6 for Myocardial Infarction, 7 for Breast Cancer, 7 for Monoclonal Gammopathy of Unknown Significance and 21 for Myeloma; *p* = significance; *g* = Hedge's g

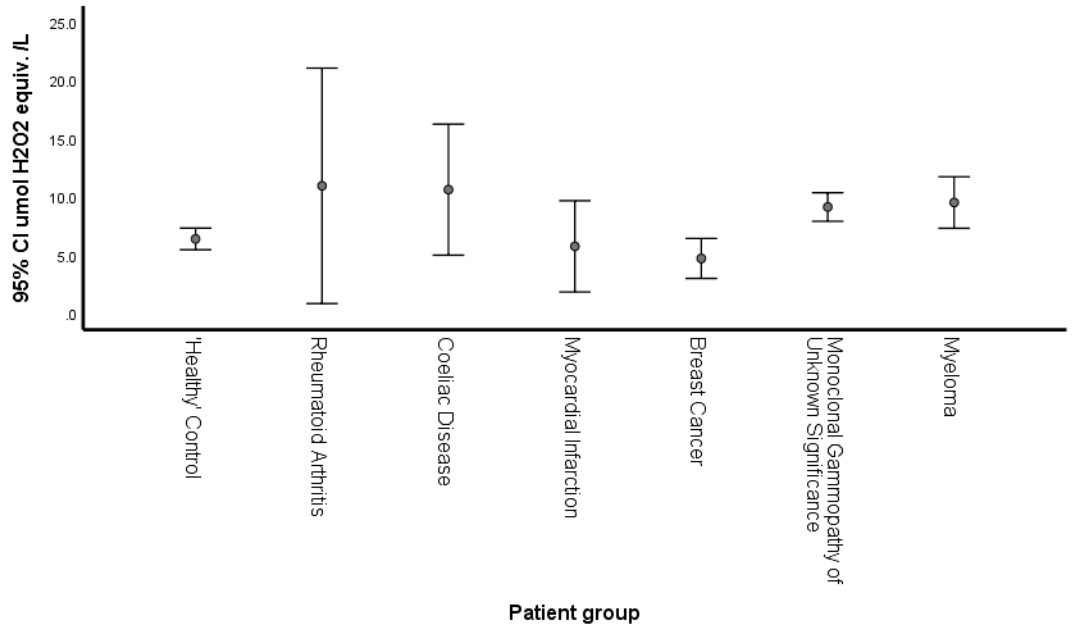

Figure 6.7: **Bar chart of serum hydroperoxide concentration**

Bar chart with serum hydroperoxide concentration (µmol H_2O_2 equivalents/L) means and 95% confidence intervals observed in 'healthy' control and disease groups

6.6 Discussion

The experiments in Chapter 6 were designed to investigate the concentrations and activity of antioxidant enzymes catalase and superoxide dismutase, and the oxidative stress marker hydroperoxides, in the serum of patients with oxidative stress associated conditions and in 'healthy' controls.

6.6.1 Serum catalase activity and concentration

It was hypothesised in BC and MM that serum catalase (activity and concentration) would be decreased in comparison to 'healthy' controls. Significant differences were observed in the breast cancer and myeloma groups compared to 'healthy' control group – the activity was lower than the 'healthy' control group. Despite the low effect sizes, this is result is consistent with findings in breast cancer (Tas *et al.*, 2005; Kasapović *et al.*, 2008) and in myeloma (Sharma *et al.*, 2009). It can therefore be assumed that serum catalase activity could be lower in other cancer conditions, which may suggest it is directly involved in disease pathogenesis / pathophysiology.

Surprisingly, there were no significant differences in the measurement of serum catalase concentration across all patient groups. Although this result is unexpected, it suggests catalase activity is more sensitive antioxidant marker. Potentially, it may have been more worthwhile investigating alternate peroxidases, e.g., glutathione peroxidase and peroxiredoxins.

Significant differences were observed for serum adjusted catalase in rheumatoid arthritis, breast cancer, MGUS and myeloma groups compared to 'healthy' control group. Adjusted catalase activity was lower than the 'healthy' control group with moderate effect sizes. This suggests the catalase enzyme in these groups were not as efficient as the 'healthy' controls. This is the first-time specific activity of catalase in patients has been described. Factoring in both concentration and activity together results in better differentiation of patients from 'healthy' controls. Specific catalase activity is a better indicator of catalase activity efficiency than either concentration or activity alone.

6.6.2 Serum CuZnSOD activity and concentration

It was hypothesised in BC that serum SOD (activity and concentration) would be decreased compared to 'healthy' controls. Surprisingly, no significant differences were observed SOD activity between patient groups and 'healthy' controls. Although this result is unexpected, it suggests SOD concentration is more sensitive antioxidant marker.

Significant differences were observed in the breast cancer group compared to 'healthy' control group – the concentration was lower than the 'healthy' control group. Despite the low effect size, this result is consistent with a study by Kasapović *et al.* (2008), supporting the oxidative stress hypothesis of cancer. The reduction observed in CuZnSOD concentration may be a result of treatment. A reports noted x-rays decreased concentration and activity of CuZnSOD (Symonyan and Nalbandyan, 1979).

The breast cancer group was significantly different for serum adjusted activity to the 'healthy' control group. Adjusted activity was higher than the 'healthy' control group, with a low effect size. This suggests the SOD enzymes in breast cancer despite having lower concentration were more efficient. There was no improvement in differentiation between 'healthy' controls and disease groups by calculation serum adjusted SOD activity.

6.6.3 Serum hydroperoxide concentration

In MGUS it was hypothesised that serum hydroperoxide concentration would be increased in comparison to 'healthy' controls. A significant difference was observed in the MGUS group compared to 'healthy' control group. Concentration was higher than the 'healthy' control group, however low effect size. A study of bisphosphonates (part of treatment to maintain bone density) can induce lipid peroxidation (Nagano *et al.*, 2012).

6.6.4 Difficulties of interpretation of AO and OS data

Interpretation of antioxidant measurement is complex. Increased antioxidants can indicate the potential to protect against free radicals but can also indicate an increased challenge against free radicals. However, an increase or decrease in antioxidants can also indicate the type of free radicals produced in a disease, which aid in determining the underlying redox mechanisms.

Very few studies have investigated the concentration and activity of these enzymes in serum, and generally erythrocyte lysate measurements are favoured. There are also difficulties with measurement of CAT and SOD concentration and activity, such as time on cells (serum).

6.6.5 Conclusions

In summary, serum catalase activity (U/mL) is decreased in patients with multiple myeloma and breast cancer compared to ‘healthy’ controls, suggesting lower catalase activity may contribute to the pathophysiology of these diseases. Although significant differences were not observed in catalase concentration (ng/mL) between ‘healthy’ controls and disease groups, calculation of adjusted catalase improved the differentiation between disease states, resulting in observed significant differences between rheumatoid arthritis, breast cancer, MGUS and myeloma groups compared to ‘healthy’ controls. Despite the significantly decreased serum catalase activity and adjusted activity for some of the patient groups compared to healthy controls, surprisingly the concentration of serum hydroperoxides were only significantly increased in MGUS patients compared to ‘healthy’ controls. It can be assumed that alternative peroxidases (e.g., glutathione peroxidases and peroxiredoxins) may have caused a decreased in measured serum hydroperoxides.

The concentration of serum CuZnSOD was significantly lower in the breast cancer group than ‘healthy’ controls, supporting the oxidative stress hypothesis of cancer. Calculation of adjusted SOD activity showed an increased activity in breast cancer compared to ‘healthy’ controls, suggesting although the concentration was lower in breast cancer, the efficiency of the enzyme counteracted the lower concentration. Combined with the lack of observed significant differences in serum SOD activity between the other disease groups and ‘healthy’ controls, it can be concluded serum SOD is tightly regulated in disease pathology.

6.6.5.1 Clinical relevance of findings

The current data in this chapter highlight the clinical potential of catalase activity as a prognostic tool in breast cancer and myeloma, where lower activity could be indicative of poorer outcomes. Comparably, the calculation of adjusted catalase activity (specific enzyme activity) may improve the detection of aberrant catalase functionality. The concept of assessing enzymatic efficiency through specific enzyme activity measurements (concentration and activity) could be applied to other categories of enzymes, e.g., liver enzymes, to better understand raised or low activity in asymptomatic patients.

Chapter 7 uses exploratory multivariate data analysis techniques to investigate the relationships between antioxidant and oxidative stress markers and the redox activity of antibodies isolated from patients with diseases associated with oxidative stress and immune dysfunction. Potential relationships, which may shed light on the similar and different underlying mechanisms of autoimmune diseases and cancer are explored.

CHAPTER 7: Investigating relationships between antibodies and antioxidant enzymes: A multivariate analysis

7.1 Background

In previous chapters (chapter 5 and 6), the redox action of antibodies (AbSOD and AbPro activity), the concentration and activity of antioxidant enzymes (catalase and SOD) and overall oxidant status (hydroperoxide concentration) in 'healthy' patients, cancer and monoclonal gammopathies (myeloma and MGUS), autoimmune diseases (rheumatoid arthritis, coeliac disease) and myocardial infarction were studied.

The primary focus of many previously reported studies has been to investigate a biomarker in isolation (e.g., SOD activity only). A criticism of such research is the reported conclusions and associations disguise the bigger picture; a combination of multiple biological systems working synergistically and antagonistically resulting in redox imbalance or homeostasis. The data collected in this study consisted of many interrelated variables, in multiple disease states. Despite the approach to comprehensively investigate catalase, SOD and redox action of antibodies, it was impossible to draw precise conclusions from the results generated. However, it was evident that relationships between antioxidants, free radicals and the immune system are extremely complex due to the pleiotropic action of these molecules, e.g., defence, signalling and regulation.

Analysis of the combined data using traditional parametric analysis methods would make it challenging to explore any novel relationships; non-parametric methods offered a solution to this problem. The aim of this chapter was to use principal component analysis (PCA), cluster analysis (CA) and network analysis (NA) to explore any correlations between antioxidant enzymes (CuZnSOD and catalase) and AbSOD activity. The analogous patterns and relationships identified may inform future research into the redox mechanisms and physiological processes underlying 'health' and diseases associated with oxidative stress and immune dysfunction.

7.1.1 Introduction to principal component analysis

PCA is known as a dimension reduction technique and is a way of consolidating a large dataset with many interrelated observed variables. In PCA, a high-dimensional dataset with many variables (dimensions) that may be correlated, is reduced to a low-dimensional space, by generating 'artificial' uncorrelated variables, called principal components (PCs). These summarise the data whilst retaining the maximal variation, without a loss of important information (Jolliffe and Cadima, 2016). The first PC (axis) always accounts for the largest proportion of the variance, the second the second largest, and so on. When the scales of variables are different, standardisation may be required, e.g., natural log transformation. Observed variables are 'loaded' on to PCs, depending on how highly correlated (weighted) with the PC they are (Jolliffe, 2002a). Observed variables with larger weightings tend to have larger component loadings (eigenvalues), meaning the variable has an increased contribution to the overall variance observed in a PC. Where the component loading of a variable is particularly low, it can be omitted from analysis as its contribution is negligible. Based on these points, it may be possible to infer what each principal component represents, and hence the overall characteristics of the data.

Once the component loadings of variables are complete for each PC, the correlation of each individual case (patient), to each PC is represented by a component score, which is plotted on a scatterplot (score plots). A score represents how strongly correlated a case is to a PC and is calculated by multiplying the component loadings by the original data (raw or transformed data). Where cases are plotted in a similar dimensional space on each PC, they share similar characteristics with each PC. Components scores which are positioned further apart on the first PCA axis (PC1 – axis that spans the most variation in the data) are more different than those that are different on second or third axis (PC2 / PC3 – the axes that span the next most variation in the data). Therefore, the data varies a lot left to right and a smaller amount up and down. The PCA scores at the extreme points of the axis have the greatest influence on that axis (Jolliffe, 2002b). Additionally, plotting of vectors (representative of the direction of variables) enables visualisation of the strength of correlation of individual cases with each variable. Where cases are furthest towards the vector arrowhead, the value and correlation of the case with that vector is the greatest.

For this study, variables / biomarkers with the largest variation between patient groups will have the most influence on the principal components, and where

groups of case scores form, would suggest the cases / patients are highly correlated. It was hypothesised patients with the same diagnosis should group and diagnoses that share underlying relationships would be revealed.

7.1.2 Introduction to cluster analysis

Clustering is a group of data analysis techniques used to classify 'objects' (including patients) into groups that share common characteristics (Kaufman and Rousseeuw, 1990a). In this context, a group or cluster of objects share a discrete set of characters that are 'different' to those of outliers and other clusters. Clusters are based on 'numbers' representing either binary (1/0 = presence/absence) or scalar values of particular parameters (or variables) describing the samples (or cases). Variables may describe very different volumes (for example assays in ranges of 10^{-6} to 10^{-3} and 100 to 1000 magnitude), which must be reconciled to a common relationship between cases. This is achieved using a clustering coefficient which expresses the relationships between all cases, and patients in terms of all variables in the form of a triangular matrix. This 'cluster matrix' represents the relationships between cases / patients in terms of maximal similarity or minimal distance. Finally, a cluster algorithm derives clusters from the triangular matrix using simple rules such as maximal similarity or minimal distance (Kaufman and Rousseeuw, 1990b). It was hypothesised patients with the same diagnosis and diseases that share underlying relationships would group into clusters.

7.1.3 Introduction to network analysis

Data from CA can be represented using a variety of graphical techniques, most commonly a clustergram or dendrograms, which visually reflects the relationships in the triangular similarity / distance matrix. While dendrograms are a 'standard' tool in ecology, where most variables are minor and become incorporated within cluster driven by the dominant variable (usually temperature, rainfall or other broad-brush descriptors of climate), this is not the case with biochemical data where there may be neither a hierarchy or dominant variables. To counter this, proximity ranking was applied to the data matrix, to identify the 1st, 2nd, 3rd, and 4th nearest neighbour to each patient as described in the triangular matrix.

7.2 Materials and methods

7.2.1 Principle component analysis of patient data: methods

The cases (patients) and variable numerical values (variable results, e.g., 100 ng/mL of catalase) were the same that were used in the ANOVA and post hoc analysis in SPSS. Cases were previously removed from analysis based on interfering factors, e.g., haemolysis and lipaemia, and cases were also removed where groups were <6 – although this is not required for PCA, for consistency and complete data analysis across all groups, it was decided analysis of only the 78 cases with patient groups >6 would be agreeable (see section 2.13.13.1). To enhance the signal (variance) obtained in PCA, the data from each measured variable was natural log transformed prior to analysis. A Euclidean biplot of PCA scores and variable vectors of antioxidant enzymes (Catalase activity (U/mL) and CuZnSOD concentration (ng/mL)) and AbSOD factor (pH 7.4 (661 seconds)) is presented Figure 7.1.

7.2.2 Cluster analysis of patient data: methods

The MVSP (version 3.1) software platform was used to perform cluster analysis and produce a distance matrix. For consistency between the CA and PCA, only the same 3 variables used for PCA were used for the CA. The data were natural log (Log e) transformed prior to UPGMA (unweighted pair group method with arithmetic mean) hierarchical clustering (Sokal and Michener, 1958) of Euclidean distances. Traditional cluster analysis would reduce (n x n-1) distances to n/2 nodes; so, a sample of 20 patients would be described by 20 x 19 (=380) ‘distances’, but with only 19 key nodes and connections. This approach allowed the initial 19 connections to be expanded to include up to 38, 57, 76 or 95 (see section 2.13.13.2).

7.2.3 Network analysis of patient data: methods

All computations based on the triangular Euclidean distance matrix were performed in Microsoft Excel.

The initial triangular Euclidean matrix was converted to a square, individual data columns ranked shortest to longest, scored 1 to 5 (first, second, third, fourth and fifth) shortest, or '0' (residuals), and then returned to their matrix positions. Five copies of this 'rationalised' square matrix were further reduced to describe the nearest one, two, three, four or five 'neighbour patients' to every sampled patient. All (one to five) distances were thus described purely as '1' (versus '0'), i.e., present, or absent.

7.2.4 Drawing a network with Pajek software

A bespoke network analysis command file suitable for the Pajek version 5.11 (Mrvar and Batagelj, 2020) network analysis software was compiled in MS Excel. The list of commands and one of the five rationalised binary data matrices exported to MS Word, formatted, and saved as text (.txt / ascii / Unicode utf 8 file). This network file was uploaded to the Pajek and output using both Kamada-Kawai (1989) (optimum display of patients ('nodes') and Fruchterman-Reingold (optimum display of connections ('edges') between patients. The Kamada-Kawai (optimised nodes) proved most suitable and is the only method presented here ('best' three connections only – Figure 7.2). The Kamada-Kawai (1989) algorithm positions the nodes in a two-dimensional space connected by edges of equal length and with as few crossed edges as possible. For final presentation, some nodes were manually moved to minimize the overlaps of either symbols or labels. All networks were saved as '.jpeg' files for document import (see section 2.13.13.2).

7.3 Results

7.3.1 Scatter plot of principal component analysis

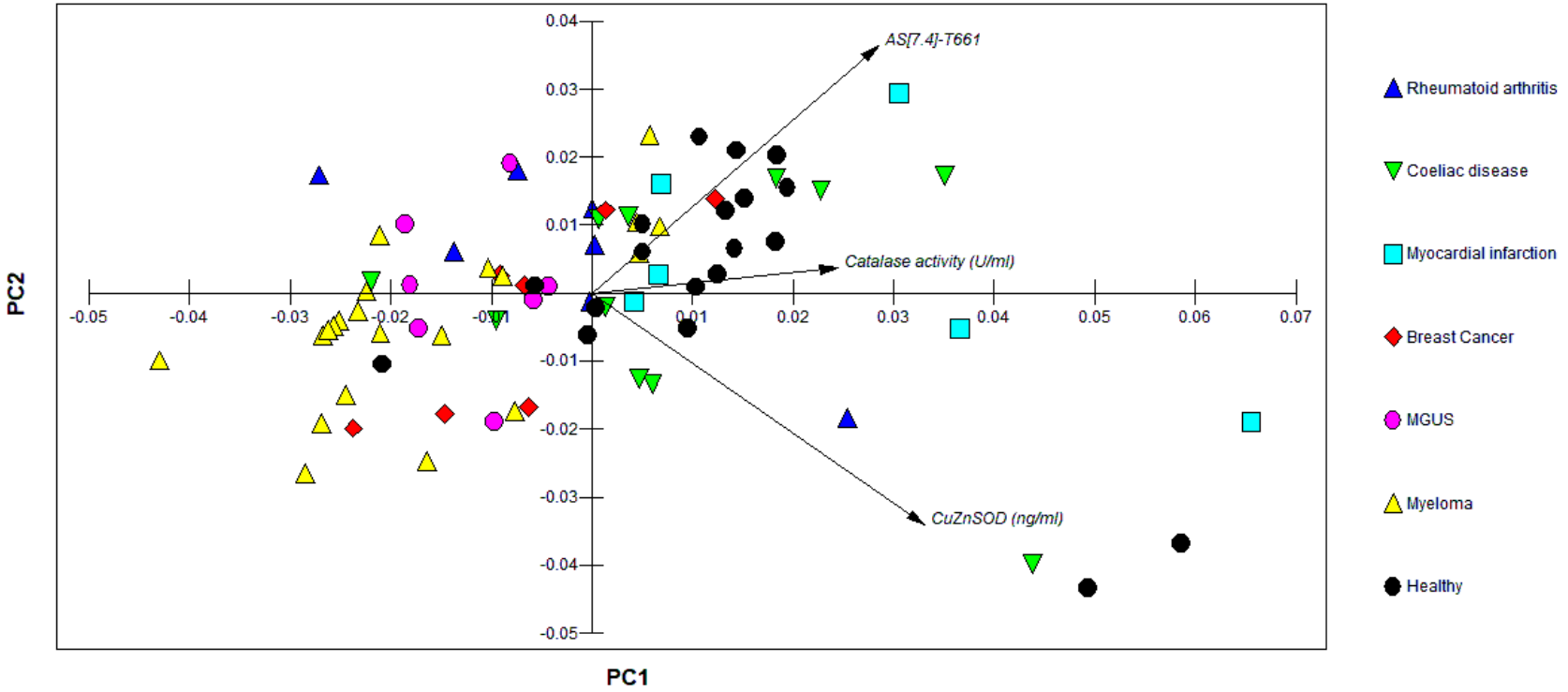

Figure 7.1: **A PCA biplot of PCA scores (PC1 vs. PC2).** PCA component scores of 3 variables are plotted from 'healthy' controls and different diagnosis groups with vectors of antioxidant enzymes (Catalase activity (U/mL) and CuZnSOD concentration (ng/mL)) and AbSOD factor (pH 7.4 (661 seconds)). PC1 (plotted on the x-axis) contributed 53% and PC2 (plotted on the y-axis) contributed 27% of the variation observed in the data. The first two components accounted for a total 80% of the variation observed in the data.

7.3.2 General comments on PCA and biplot

From dimension reduction only 3 variables were retained, resulting in improved signal for PC1 and PC2 (45% to 53% and 24% to 27% increase). The PCA plot for PC1 vs PC2 with reduced dimensions was very similar in structure and position of patient plot points compared to the PC1 vs PC2 for 19 variables. The number of principal components retained were reduced and a higher signal-noise ratio achieved.

In general, myeloma, MGUS and breast cancer patients tended to group further to the left away from the direction of the vectors, whereas ‘healthy’, coeliac disease and myocardial infarction tended to group to the right of the graph, in the direction of the vectors.

7.3.3 Cluster analysis and network analysis results

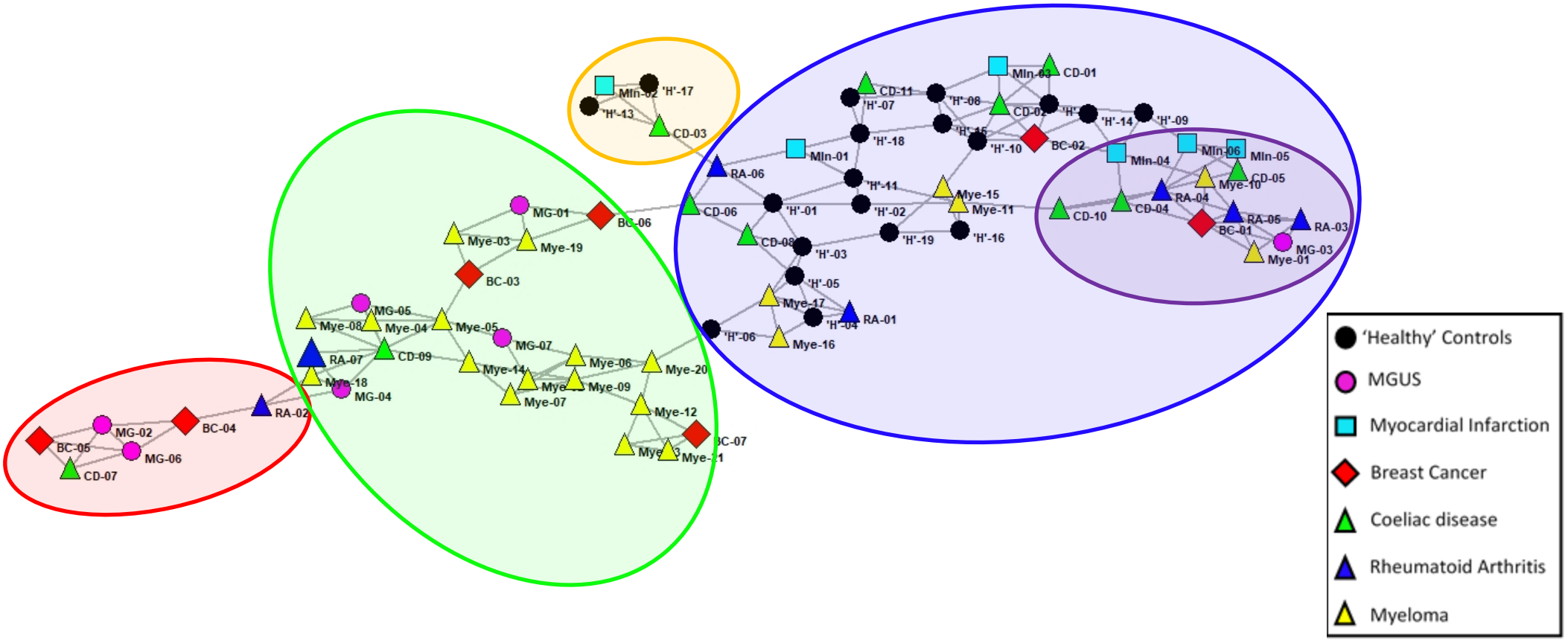

Figure 7.2: **A network analysis of antioxidant enzymes and AbSOD activity between patient groups.**

The network graph was drawn using the Kamada-Kawai (1989) algorithm, where analysis represents the three 'best' connections between patients and healthy controls.

7.3.4 General comments on cluster and network analysis

There are four main groups evident in this network. The first group (bottom left red oval) is separate, consisting of two patients with breast cancer (red diamond), two with monoclonal gammopathy of unknown significance (MGUS – pink circle), one with coeliac disease (green triangle) and one with rheumatoid arthritis (blue triangle). The second group (middle left green oval) predominantly harbours patients with myeloma (15 – yellow triangle), MGUS (four), breast cancer (three), rheumatoid arthritis (one) and coeliac disease (one). The third and smallest group (upper middle yellow oval) is formed of two 'healthy' controls (black circle), one myocardial infarction (cyan square) and one coeliac disease. The fourth and largest group (right blue oval) is formed predominantly of 'healthy' controls (17 of 19), but all other patient groups are present; eight patients with coeliac disease, six with myeloma, four with rheumatoid arthritis, six with myocardial infarction (cyan square), rheumatoid arthritis, two with breast cancer and one with MGUS.

7.4 Discussion

7.4.1 Principal component analysis

7.4.1.1 Vector correlations with principal components

Catalase activity (U/mL) had a positive correlation with PC1 and a weak positive correlation with PC2. Very few patients plotted along this vector, towards the arrowhead, mostly from the 'healthy' control group. However, several groups (myeloma, breast cancer and MGUS) had a negative correlation with this vector. A negative correlation with the catalase activity variable-vector is suggestive of lower catalase activity.

CuZnSOD concentration (ng/ml) had a strong positive correlation with PC1 and strong negative correlation with PC2. Very few patient groups plotted along this vector, towards the arrowhead. However, several groups (breast cancer, MGUS, rheumatoid arthritis and myeloma) had a negative correlation with this vector. A negative correlation with the CuZnSOD concentration variable-vector is suggestive of lower CuZnSOD concentration.

AbSOD factor (at pH 7.4, 661 seconds) had a strong positive correlation with both PC1 and PC2. Patient groups plotted along this vector, towards the arrowhead, tended to have a larger AbSOD factor. In general, 'healthy' patients had a larger AbSOD factor than the other patient groups, whereas the myeloma patients had a smaller AbSOD factor. In all patients, prolonged exposure of antibodies to superoxide at pH 7.4 resulted in increased production of the reaction product formazan. This was most marked in the 'healthy' patient group and least in myeloma patient group. A negative correlation with the AbSOD factor variable-vector is indicative of decreased AbPro activity.

7.4.1.2 Myeloma, breast cancer and MGUS are negatively correlated with catalase activity

The negative correlation of multiple myeloma and breast cancer with the catalase activity vector are expected and consistent with observations from ANOVA and Games-Howell multiple comparisons analysis (section 6.4.2). Equally, because of the similarities between myeloma and MGUS (pre-cancerous condition), the negative correlation of MGUS is expected. However, this is not consistent with

findings from parametric analysis, where no significant differences were observed compared to 'healthy' controls.

The findings from PCA analysis are supported by several studies – a study by Sharma *et al.* (2009), observed patients with Multiple Myeloma at stage II of international staging system, had significantly lower levels of catalase in haemolysate compared to healthy controls. Similarly, a study in 2005 of 40 women newly diagnosed with breast cancer, found catalase activity was significantly decreased in breast cancer tissue (Tas *et al.*, 2005). The discrepancies observed between breast cancer cases in Figure 7.1, is likely due to differences in disease severity. Catalase activity was found to decrease with increasing BI-RADS (breast imaging-reporting and data system) staging (Radenkovic *et al.*, 2013).

7.4.1.3 None of the groups studied were strongly correlated with CuZnSOD

Serum CuZnSOD concentration is not commonly assayed, with researchers generally measuring SOD activity of haemolysate. The increased specificity of an immunoassay (section 2.9) compared to an activity assay would have been preferred. The variability within patient groups could be explained by serum concentration of CuZnSOD being tightly regulated, i.e., does not differ significantly in the pathologies investigated.

In parametric data analysis, CuZnSOD concentration was only significantly different from 'healthy' controls in breast cancer, where it was lower (section 6.4.4). There is an apparent lack of definitive correlation between any of the disease groups and the vector. Due to the results from parametric data analysis, a negative correlation to breast cancer was expected. However, the lack of correlation is likely representative of the smaller effect size (Hedge's g = 0.26 – Cohen, 1988b) associated with the significant Games-Howell p value (p = 0.016) for CuZnSOD concentration of breast cancer compared to 'healthy' controls.

7.4.1.4 'Healthy' controls are positively correlated with AbSOD factor

The positive correlation of 'healthy' controls with AbSOD factor is consistent with the results from parametric analysis. The increased conversion of NBT to formazan by antibodies at pH 7.4, in 'healthy' controls, suggests this activity

(apparent pro-oxidant activity) is part of normal physiology. Consequently, the reduced conversion of NBT to formazan appears to be a characteristic of patients with myeloma, breast cancer and to a lesser extent MGUS.

The mechanism of increased formazan production at pH 7.4 is not known, however, pro-oxidant activity of antibodies at pH 7.4 is likely related to their physiological function in immune responses or cellular signalling. RS are produced in immune responses to infection by NADPH oxidases (nicotinamide adenine dinucleotide phosphate oxidases), NOS (nitric oxide synthases), mitochondrial electron transport chain and MPO (myeloperoxidase) (Steck and Grassl, 2014).

The decreased formation of formazan in the myeloma, breast cancer and to a lesser extent MGUS groups is potentially due to the abnormal ratio of antibodies present in these conditions. It is possible monoclonal antibodies that occur naturally as part of the disease process, or from pharmaceutical treatments, may account for the hinderance / down-regulation in homeostatic AbPro activity. In Myeloma, cancerous plasma B-cells results in increased proliferations of monoclonal antibodies. The production of these monoclonal antibodies overtakes the production of normal antibody production, which consequently may result in a reduction in antibodies with AbPro activity. Comparably, the treatments used in breast cancer such as radiotherapy and chemotherapy, which have suppressive effects on the immune system and immunoglobulin levels (van Tilburg *et al.*, 2012), combined with monoclonal antibody treatments such as Trastuzumab (Herceptin), ultimately result in the similar reduction in AbPro proficient antibodies.

7.4.1.5 Catalase and CuZnSOD are positively correlated

The angle between catalase activity and CuZnSOD was <90 degrees. The variables had some correlation (a relationship), perhaps unsurprisingly as catalase and SOD have a synergistic relationship – SOD dismutates superoxide to oxygen and hydrogen peroxide, catalase decomposes hydrogen peroxide to water and oxygen. In general, as the activity of SOD increases, the demands of catalase increase to cope with the excess production of hydrogen peroxide. Correspondingly, where SOD activity decreases, the demands of catalase decrease.

7.4.1.6 Catalase and AbSOD factor are positively correlated

Similarly, the angle between catalase activity and AbSOD activity is <90 degrees. This is interesting as a correlation between these two variables could suggest they are mechanistically linked, i.e., catalase is required to decompose hydrogen peroxide produced by antibodies; alternatively, it could also just be the product of the SOD-catalase relationship. This could also be reflective of the lower catalase activity levels and decreased AbPro activity seen in myeloma.

7.4.1.7 AbSOD factor and CuZnSOD are limitedly correlated

Finally, in terms of vector orientations to each other, there was limited correlation between AbSOD activity and CuZnSOD, indicated by an angle ≥ 90°. This may suggest the two are independent of each other, and thus may have different functions at pH 7.4. Where immunoglobulins function to catalyse the formation of superoxide as part of homeostatic mechanisms, SOD and catalase function to regulate the levels of free radicals produced in this process.

7.4.2 Cluster and network analysis

Both exogenous antioxidants such as vitamins, polyphenols and carotenoids, and endogenous antioxidants such as SOD, catalase, and glutathione peroxidase function as part of human antioxidant defence mechanisms in response to free radicals and oxidants produced in physiological, metabolic and disease processes. The redox action of antibodies was seldom appreciated and their roles in 'health' and diseases associated with oxidative stress and immune dysfunction unknown. The apparent decrease in catalase activity, antibody pro-oxidant activity, and to a lesser extent CuZnSOD concentration in myeloma, MGUS and breast cancer, compared to 'healthy' controls, suggests a potential role in the pathophysiology of cancer and a physiological role in 'health'.

7.4.2.1 Clustering of cancer and pre-cancer conditions

The results of network analysis revealed there was a relationship between the primary antioxidants SOD and catalase, and antibodies of the immune system. This was evident due to the clustering (green oval) of patients with pre-cancerous (MGUS) and cancerous conditions (myeloma and breast cancer). It is clear there are cases where patients from these groups do not follow the 'rule', though it is possible disease severity, stage and even misdiagnosis (e.g., smouldering myeloma, myeloma and Waldenström macroglobulinemia – misdiagnosed as MGUS) could reasonably account for these differences. Another consideration is the differing mechanisms of the underlying aetiology for these diseases. Myeloma and MGUS for example are not simply diseases of the IgG subclass (although the most common), it can result in the proliferation of immunoglobulin paraproteins of IgA, IgM, IgD and IgE subclasses, light and heavy chains and even a combination of several subclasses (Sheikh *et al.*, 2020). Likewise, breast cancer has several types including ductal carcinoma in situ, invasive ductal carcinoma (most common), inflammatory breast cancer and metastatic breast cancer, all of which vary in severity, and histological / biochemical criteria (Li *et al.*, 2005).

7.4.2.2 Clustering of ‘healthy’ controls

Equally important to note is the separation between the predominantly pre-cancerous / cancerous groups (red and green ovals) and the group with principally ‘healthy’ controls (blue oval). The separation and distance between these groups suggests the relationships between redox action of SOD and catalase, and antibodies of the immune system are distinct from one another. It is apparent the increased activity of catalase, increased concentration of CuZnSOD and increased pro-oxidant activity of antibodies are required for ‘health’ and redox homeostasis. Subtle deviations from ‘healthy’ ranges of CuZnSOD concentration, catalase activity and antibody pro-oxidant activity do not result in formation of separate groups in the network.

7.4.2.3 Are outliers to ‘healthy’ control group predisposed to cancer?

There are as in the pre-cancerous / cancerous type groups, outliers to the ‘healthy’ group. In these cases, deviations from ‘rule’ could suggest increased susceptibility to cancer type conditions. There have been several studies (Baecklund *et al.*, 2005, and Zintzaras *et al.*, 2005) suggesting patients with rheumatoid arthritis have approximately double the risk for developing lymphoma, a condition characterised by cancer of the T and B-cells. This is likely caused by chronic inflammatory stimulation of the immune system where increased activity of lymphocytes increases their likelihood of becoming malignant (Yadlapati and Efthimiou, 2016). This has been evidenced when patients with poorly controlled inflammation have the highest risk for developing lymphoma (Franklin *et al.*, 2006). Similarly, in coeliac disease studies reported a 2- to 5-fold increased risk of Hodgkin lymphoma (HL) in CD patients compared to the general population (Marafini *et al.*, 2020).

The myocardial infarction group (except for 1 case) are the only ‘disease’ group which remained contained to the cluster with predominantly ‘healthy’ cases. As a condition characterised by acute tissue damage and localised oxidative stress, myocardial infarction is mechanistically the most dissimilar to the other conditions investigated in this study. However, the chronic repercussions of such an event should be considered, as although the increased risk of cardiovascular events in cancer are well reported, the risks of cancer pathogenesis associated with a cardiovascular event are

seldom reported. A large register-based study of Danish residents from 1996 to 2012 found patients after a myocardial infarction have increased incidence of cancer (Malmborg *et al.*, 2018). A later study of a syngeneic mouse model of breast cancer reported surgically induced myocardial infarction accelerated tumour growth, suggesting it was associated with an immunosuppressive tumour environment (Koelwyn *et al.*, 2020).

7.4.2.4 Is the purple cluster associated with chronic inflammation?

To the extremity of the 'healthy' group (blue oval) there is emergence of a smaller group (purple oval), consisting of patients with rheumatoid arthritis, coeliac disease, breast cancer, myeloma, MGUS and myocardial infarction. It could be argued that the common relationship between this subset of cases is chronic inflammation. Rheumatoid arthritis and coeliac disease are conditions characterised by chronic inflammation with periods of acute inflammation or 'flare ups' (Firestein, 2003; Green and Jabri, 2003). Parallels can be drawn with myocardial infarction, which is often secondary to a chronic condition such as type 2 diabetes or atherosclerosis (Palasubramaniam *et al.*, 2019; Liang *et al.*, 2014). The near proximity of this group to the 'healthy' control group, suggests the antioxidant and antibody redox response is only slightly aberrant.

7.4.3 Conclusions

The purpose of this chapter was to reveal relationships between 'healthy controls and patient groups associated with oxidative stress and immune dysfunction, based on their antioxidant enzyme and antibody redox activity status. Using multivariate statistical methods of PCA and CA, it was possible to elucidate similarities and differences between groups. The results of this investigation show that pre-cancerous (MGUS) and cancerous (breast cancer and myeloma), share similar responses in antioxidant enzyme and redox antibody response, evidenced by grouping of these groups in both PCA and CA. A second major finding was that CuZnSOD, and antibody redox activity are independent of one another, suggesting they have different functions at physiological pH (pH 7.4). This chapter highlights the potential synergism between the immune system and antioxidant defences, and the pleiotropic function of antibodies.

Despite its exploratory nature Chapter 7 offers some insight into the parallels between myeloma, breast cancer and MGUS in their antioxidant and redox antibody response, suggesting they play an important role in pathophysiology of these diseases. The precise mechanism of the apparent pro-oxidant activity of antibodies upon prolonged exposure to superoxide at pH 7.4, remains to be elucidated, and this would be a fruitful area for further work. Further research might explore the production of free radicals by antibodies. Similarly, although the current study is based on a small sample of patients, the findings suggest the relationships between CuZnSOD concentration, catalase activity and redox antibody activity, may indicate susceptibility to cancer in coeliac disease, rheumatoid arthritis, and myocardial infarction. Further work, with larger cohorts need to be completed to fully understand the implications of these findings.

7.4.3.1 Clinical relevance of findings

Completion of the cluster analysis revealed two main groups, cancer and pre-cancer type conditions and ‘healthy’ controls. Some of patients from the coeliac disease, rheumatoid arthritis and myocardial infarction group were outliers to the ‘healthy’ control group, with some even confined to the cancer group. There is potential AbSOD activity, catalase and CuZnSOD could be used to determine risk of cancer in rheumatoid arthritis and myocardial infarction. These findings also highlight the potential applications of PCA, CA and graph theory to relate slightly associated biochemical data to clinical risk, i.e., explores data without the requirement to meet assumptions, which is beyond the means of traditional parametric analyses.

CHAPTER 8: Summary and general discussion

8.1 Discussion

The first aim of this study was to investigate the superoxide dismutase activity of antibodies (AbSOD activity) from commercial and patient sources. This required optimisation and development of a method for the isolation and assaying of antibodies for superoxide dismutase activity. The second aim was to determine the effects pH associated with inflammatory environments would have on AbSOD activity. The third aim was to determine whether AbSOD activity would differ between patient groups with diseases associated with oxidative stress and immune dysfunction compared to 'healthy' controls. Finally, the fourth aim set out to understand the overall redox status of these patients.

The role of AbSOD activity in disease pathologies has received limited research interest, possibly owning to the unknown similarity of its structure to CuZnSOD (Richardson *et al.*, 1976). Furthermore, the research area has been dominated by researchers exploring the theory of the antibody catalysed water oxidation pathway in favour of AbSOD activity (Wentworth *et al.*, 2008).

8.1.1 Chapter 1 – 4

The experiments in this thesis were designed to provide an improved understanding of the effects of pH of AbSOD activity and CuZnSOD activity. The first findings of this project showed that CuZnSOD activity was independent of pH and AbSOD activity was optimal at acidic pH (5.5 – 6.5). It was also evident that upon prolonged exposure to superoxide radicals, the antioxidant activity of CuZnSOD was reduced, which was hypothesised to be due to the inhibitory effect of hydrogen peroxide. On the other hand, pro-oxidant activity was observed from antibodies (AbPro activity) upon prolonged exposure, which was optimal at pH 7.5. However, it was hypothesised this would only be relevant where peroxidase mechanisms (CAT and GPx) were at suboptimal pH, e.g., acidic environments associated with inflammation, or where their concentration or activity was significantly reduced. The findings in chapter 4 indicated a potential clinical application for antibodies that yield this AbSOD activity, where they could be used

therapeutically to provide antioxidant protection, injected directly to sites with inflammation and oxidative stress, e.g., rheumatic joints.

8.1.2 Chapter 5

Thus, the emphasis then moved to investigate the pH dependency of AbSOD activity in antibodies isolated from serum of patients with diseases associated with oxidative stress and immune dysfunction (coeliac disease, rheumatoid arthritis, myocardial infarction, breast cancer, multiple myeloma and MGUS).

The second set of findings showed AbSOD activity was increased at acidic pH (5.5) in rheumatoid arthritis and myocardial infarction. It was hypothesised that this may offer antioxidant protection at sites of inflammation in these pathologies, however, due to the associated reduction in peroxidase functionality at acidic pH, it could equally result in hydrogen peroxide formations, which may result in oxidative stress or recruitment of immune cells. The results from this study indicate that in rheumatoid arthritis and myocardial infarction, administration of chelation therapy could improve outcomes for patients, reduce oxidative stress by removal of metal ions, that along with the products of AbSOD activity may participate in Fenton chemistry.

The third set of findings showed AbSOD activity was increased in myeloma between pH 6.0 – 7.4, and upon prolonged exposure AbPro activity was decreased between pH 6.5 – 7.4. This finding suggested that even transient exposure to acidic environments, such as those in myeloma cells may increase SOD activity of antibodies. It was also hypothesised the monoclonal antibodies produced in myeloma may be more structurally unstable and susceptible to protein modifications conferring enhanced AbSOD activity. If AbSOD activity in the absence of sufficient hydrogen peroxide decomposition was a mechanism of nephrotoxicity in myeloma, urinary pH monitoring (approximate pH 7.0; Cancarini *et al.*, 2021) and subsequent corrective urine alkalinisation treatment to neutralise the pH, e.g., sodium bicarbonate treatment, would be recommended.

The work carried out in Chapter 5 demonstrated the first findings that AbSOD activity is decreased at pH 5.5 in rheumatoid arthritis and myocardial infarction, and was increased in myeloma between pH 6.0-7.4, compared to ‘healthy’ controls. Whether the increase or decrease in AbSOD activity

confers antioxidant protection or exacerbates oxidative stress requires more work, but it does provide novel evidence that antibodies with superoxide dismutase activity have a role in these pathologies.

8.1.3 Chapter 6

The work carried out in Chapter 6, was the first to demonstrate slightly increased lipid peroxidation (measured by hydroperoxide concentration in serum) in MGUS. This may encourage future studies into oxidation of lipids as a potential marker for MGUS to myeloma transformation. The data in chapter 6 also highlights the clinical potential of catalase activity as a prognostic tool in breast cancer and myeloma, where lower activity could be indicative of poorer outcomes. Comparably, the calculation of adjusted catalase activity (specific enzyme activity) may improve the detection of aberrant catalase functionality. The approach of assessing enzymatic efficiency through specific enzyme activity measurements (concentration and activity) could be applied to other categories of enzymes, e.g., liver enzymes, to better understand raised or low activity in asymptomatic patients.

8.1.4 Chapter 7

The work carried out in Chapter 7, was the first to demonstrate potential links between myeloma, breast cancer and MGUS in terms of their AbSOD activity, CuZnSOD and catalase response, using principal component and cluster analysis. The clustering of patient groups also highlighted the potential of this technique, and AbSOD activity, catalase and CuZnSOD as markers to be used to determine cancer risk in coeliac disease, rrheumatoid arthritis, and myocardial infarction.

8.2 Future work

This study set out to determine the superoxide dismutase activity (AbSOD) and pro-oxidant activity (AbPro) of antibodies isolated from the serum of patients with coeliac disease, rheumatoid arthritis, breast cancer, myeloma, MGUS and myocardial infarction, compared to 'healthy' controls. Firstly, experiments identified AbSOD activity was increased at acidic pH (5.5 – 6.0) and was increased in rheumatoid arthritis and myocardial infarction more than the other patient groups. The implication of this finding is not clear; however, it is hypothesised increased AbSOD activity at pH 5.5 may lead to the localised increase in hydrogen peroxide concentration at sites of inflammation and acute tissue damage, which due to the acidic pH is not decomposed by peroxidase / catalase enzymes. Further research could usefully explore the pH dependency of catalase and glutathione peroxidases in this context.

Secondly, it emerged that the SOD activity of antibodies decreases, and then transitions to pro-oxidant activity as pH increases from acidic (pH 6.5) to alkali (pH 7.4). Between these pH ranges, AbPro activity was in general increased the most in 'healthy' controls, whereas in myeloma it was decreased the most. The finding that antibodies from 'healthy' controls have pro-oxidant activity when exposed to a superoxide rich environment, offers some insight into the role of antibodies in redox homeostasis and the potential importance of pro-oxidant activity in physiology. In general, ROS produced in physiology have mostly been linked signalling pathways. A natural progression of this work would be to investigate the action of immunoglobulins in this setting.

Thirdly, the finding that antibodies from patients with multiple myeloma have increased AbSOD activity (pH 6.0) and reduced pro-oxidant activity (pH 6.5 – 7.4), brings new understanding about how pathological monoclonal antibodies may be involved with overall redox reactions and how this action could be implicated in renal injury. This may in turn lead to considerations for monitoring of urinary pH in monoclonal gammopathies but also in treatments with monoclonal antibody preparations such as breast cancer. The hypothesis that renal impairment associated with myeloma could result from cytotoxicity induced by monoclonal immunoglobulins and Bence Jones proteins (immunoglobulin light chains) with AbSOD activity, caused by increased accumulation of hydrogen peroxide, lends itself to further study.

This could be investigated using animal models, where FLCs with proven AbSOD activity could be injected into animals and alkalisation and chelation therapies versus no treatment assessed to determine efficacy.

Fourthly, it was found that breast cancer patients have decreased AbPro activity at pH 7.4. A limitation of this finding is the lack of information regarding treatment stage of the patients with breast cancer. However, whether the patients were or were not being treated still raises important questions about the redox activity of common monoclonal antibody treatments such as trastuzumab (Herceptin). Future work may determine the redox activity of trastuzumab directly and compare the redox activity of antibodies in untreated against treated patients, to determine whether redox activity of antibodies correlates with the efficacy of treatment. This work could be expanded to investigate the redox activity of monoclonal antibody therapies in other disease states, such as myeloma (Anti-CD38 and Anti-SLAMF7) and rheumatoid arthritis (Tocilizumab).

Fifthly, the results of this investigation have shown the antioxidant to pro-oxidant switch of immunoglobulins is time dependent. Initially, across the range of pH's studied, the exposure of antibodies to superoxide resulted in AbSOD activity (antioxidant). As the antibodies were exposed to superoxide for longer, the activity transitioned to AbPro activity (pro-oxidant). Finally, whilst Chapter 5 did not confirm the mechanism of AbPro activity, it did show differences between patients, which raises many questions about how this may contribute to overall 'health'. This may be a fruitful area for future work.

8.3 Concluding remarks

This thesis has provided deeper insight into the significance of pH on AbSOD activity and highlighted the potential challenges of interpreting data generated in experiments of *in vitro* redox environments. This is the first time the effects of pH on AbSOD activity of antibodies isolated from human serum has been investigated and compared in autoimmune disease, cardiovascular disease, and cancer to 'healthy' controls.

The investigations presented here also highlight the therapeutic potential of AbSOD activity in the treatment of rheumatoid arthritis, the potential to reduce oxidative stress via reduction of Fenton chemistry using chelation therapy in rheumatoid arthritis and myocardial infarction, a recommendation to monitor urinary pH in myeloma and use alkalinization treatment to correct aciduric patients to reduce risk of nephrotoxicity, the potential of catalase activity as a prognostic tool in breast cancer and myeloma, and the combined use of AbSOD activity, catalase and CuZnSOD to determine cancer risk in patients with coeliac disease, rheumatoid arthritis and myocardial infarction.

Despite its exploratory nature, the findings from this study indicate that antibodies of the immune system have a role to play in redox reactions *in vivo*, specifically in pathological and inflammatory environments. Whilst this study did not confirm whether AbSOD activity confers antioxidant protection, increases oxidative stress, or participates in redox signalling there are many questions raised about the function AbSOD activity may have across various oxidative stress-related pathologies that may inform future studies.

References

Aebi, H. E., 1984. Catalase in vitro. *Methods in Enzymology*. 105, p.121-126.

Akram, M., Iqbal, M., Daniyal, M. and Khan, A. U., 2017. Awareness and current knowledge of breast cancer. *Biological Research*. 50, article 33.

Alpha-Tocopherol, Beta Carotene Cancer Prevention Study Group, 1994. The effect of vitamin E and beta carotene on the incidence of lung cancer and other cancers in male smokers. *New England Journal of Medicine*. 330 (15), p.1029-1035.

Amachi, R., Hiasa, M., Teramachi, J., Harada, T., Oda, A., Nakamura, S., Hanson, D., Watanabe, K., Fujii, S., Miki, H., Kagawa, K., Iwasa, M., Endo, I., Kondo, T., Yoshida, S., Aihara, K. I., Kurahashi, K., Kuroda, Y., Horikawa, H., Tanaka, E., Matsumoto, T., and Abe, M., 2016. A vicious cycle between acid sensing and survival signaling in myeloma cells: acid-induced epigenetic alteration. *Oncotarget*. 7 (43), p.70447–70461.

Amici, A., Levine, R. L., Tsai, L. and Stadtman, E. R., 1989. Conversion of amino acid residues in proteins and amino acid homopolymers to carbonyl derivatives by metal-catalysed oxidation reactions. *Journal of Biological Chemistry*. 264 (6), p.3341-3346.

Anderson, M., Moshnikova, A., Engelman, D. M., Reshetnyak, Y. K. and Andreev, O. A. 2016. Probe for the measurement of cell surface pH in vivo and ex vivo. Proceedings of the *National Academy of Sciences of the United States of America*. 113 (29), pp8177-8181.

Andrade, B. B., Reis-Filho, A., Souza-Neto, S. M., Raffaele-Netto, I., Camargo, L. M., Barral, A. and Barral-Netto, M., 2010. Plasma superoxide dismutase-1 as a surrogate marker of vivax malaria severity. *PLoS Neglected Tropical Diseases*. 4 (4), e650.

Antonyuk, S. V., Strange, R. W., Marklund, S. L. and Hasnain, S. S., 2009. The structure of human extracellular copper-zinc superoxide dismutase at 1.7 A resolution: insights into heparin and collagen binding. *Journal of Molecular Biology*. 388 (2), p.310-326.

Argüelles, S., García, S., Maldonado, M., Machado, A., Ayala, A., 2004. Do the serum oxidative stress biomarkers provide a reasonable index of the general oxidative stress status?. *Biochimica et biophysica acta*. 1674 (3), p.251-259.

Auchere, F. and Rusnak, F., 2002. What is the ultimate fate of superoxide anion in vivo?. *Journal of Biological Inorganic Chemistry*. 7, p.664-667.

Babior, B. M., Takeuchi, C., Ruedi, J., Gutierrez, A., Wentworth, P., 2003. Investigating antibody-catalysed ozone generation by human neutrophils. Proceedings of the *National Academy of Sciences of the United States of America*. 100 (6), p.3031-3034.

Baecklund, E., Askling, J., Rosenquist, R., Ekbom, A. and Klareskog, L., 2004. Rheumatoid arthritis and malignant lymphomas. *Current Opinion in Rheumatology*. 16 (3), p.254-261.

Bagatini, M. D., Martins, C. C., Battisti, V., Gasparetto, D., da Rosa, C. S., Spanevello, R. M., Ahmed, M., Schmatz, R., Schetinger, M. R., and Morsch, V. M., 2011. Oxidative stress versus antioxidant defenses in patients with acute myocardial infarction. *Heart Vessels*. 26 (1), p.55-63.

Bamonti, F., Fulgenzi, A., Novembrino, C., and Ferrero, M. E., 2011. Metal chelation therapy in rheumatoid arthritis: a case report. Successful management of rheumatoid arthritis by metal chelation therapy. *Biometals: an international journal on the role of metal ions in biology, biochemistry, and medicine*. 24(6), p.1093-1098. https://doi.org/10.1007/s10534-011-9467-9

Bartesaghi, S. and Radi, R., 2018. Fundamentals on the biochemistry of peroxynitrite and protein tyrosine nitration. *Redox Biology*. 14, p.618–625.

Basnayake, K., Stringer, S. J., Hutchison, C. A., and Cockwell, P., 2011. The biology of immunoglobulin free light chains and kidney injury. *Kidney international*. 79(12), p.1289-1301. https://doi.org/10.1038/ki.2011.94

Basnayake, K., Ying, W. Z., Wang, P. X. and Sanders, P. W., 2010. Immunoglobulin light chains activate tubular epithelial cells through redox signaling. *Journal of the American Society of Nephrology*. 21 (7), p.1165-1173.

Bast, A., 1993. Oxidative stress and calcium homeostasis. In: Halliwell, B., Aruoma, O. I., *DNA and free radicals*, London: Ellis Horwood, p.95–108.

Battistoni, A. and Rotilio, G., 1995. Isolation of an active and heat-stable monomeric form of Cu,Zn superoxide dismutase from the periplasmic space of Escherichia coli. *FEBS Letters*. 374 (2), p.199-202.

Beck, R., Pedrosa, R. C., Dejeans, N., Glorieux, C., Levêque, P., Gallez, B., Taper, H., Eeckhoudt, S., Knoops, L., Calderon, P. B. and Verrax, J., 2011. Ascorbate/menadione-induced oxidative stress kills cancer cells that express normal or mutated forms of the oncogenic protein Bcr-Abl. An in vitro and in vivo mechanistic study. *Investigational New Drugs*. 29 (5) p.891-900.

Benedetti, A., Pompella, A., Fulceri, R., Romani, A., Comporti, M., 1986. 4-Hydroxynonenal and other aldehydes produced in the liver in vivo after bromobenzene intoxication. *Toxicologic Pathology*. 14 (4), p.457-461.

Bielski, B. H. J., Arudi, R. and Sutherland, M. W., 1983. A Study of the Reactivity of HO2/O2- with Unsaturated Fatty Acids*. *The Journal of Biological Chemistry*. 258 (8), p.4759-4761.

Bielski, B. H. J., Cabelli, D. E., Arudi, R. L., 1985. Reactivity of HO2/O2- Radicals in Aqueous Solution. *Journal of Physical and Chemical Reference Data*. 14, p.1041-1100.

Bienert, G. P., Møller, A. L., Kristiansen, K. A., Schulz, A., Møller, I. M., Schjoerring, J. K. and Jahn, T. P., 2007. Specific aquaporins facilitate the diffusion of hydrogen peroxide across membranes. *Journal of Biological Chemistry*. 282 (2), p.1183-1192.

BioTek Instruments Inc., 2017. *Electron structures of reactive oxygen curve (ROS) species, detectable using Synergy HTX*. Available: https://www.biotek.com/images/products/synergyht/ROS1.jpg. Last accessed 18th October 2017.

Bjelakovic, G., Nikolova, D., Gluud, L. L., Simonetti, R. G. and Gluud, C., 2012. Antioxidant supplements for prevention of mortality in healthy participants and patients with various diseases. *Cochrane Database of Systematic Reviews*. (3), article CD007176.

Bjelakovic, G., Nikolova, D., Simonetti, R. G. and Gluud, C., 2004. Antioxidant supplements for prevention of gastrointestinal cancers: a systematic review and meta-analysis. *Lancet.* 364 (9441), p.1219-1228.

Borchman, D., Lamba, O. P., Salmassi, S., Lou, M., Yappert, M. C., 1992. The dual effect of oxidation on lipid bilayer structure. *Lipids*. 27 (4), p.261-265.

Bouvet, J. P., Stahl, D., Rose, S., Quan, C. P., Kazatchkine, M. D. and Kaveri, S. V., 2001. Induction of natural autoantibody activity following treatment of human immunoglobulin with dissociating agents. *Journal of Autoimmunity*. 16 (2), p.163-172.

Briggs, R. G. and Fee, J. A., 1978 Further characterization of human erythrocyte superoxide dismutase. *Biochimica et Biophysica Acta*. 537 (1), p.86-99.

Bruno, R. S., Ramakrishnan, R., Montine, T. J., Bray, T. M., Traber, M. G., 2005. α-Tocopherol disappearance is faster in cigarette smokers and is inversely related to their ascorbic acid status. *American Journal of Clinical Nutrition.* 81 (1), p.95-103.

Case, A. J., 2017. On the Origin of Superoxide Dismutase: An Evolutionary Perspective of Superoxide-Mediated Redox Signaling. *Antioxidants (Basel, Switzerland).* 6 (4), article 82.

Chance, B., Sies, H. and Boveris, A., 1979. Hydroperoxide metabolism in mammalian organs. *Physiological Reviews*. 59, p.527–605.

Chicca, I. J., Heaney, J. L. J., Iqbal, G., Dunn, J. A., Bowcock, S., Pratt, G., Yong, K. L., Planche, T. D., Richter, A., and Drayson, M. T., 2020. Anti-bacterial antibodies in multiple myeloma patients at disease presentation, in response to therapy and in remission: implications for patient management. *Blood Cancer Journal*. 10 (11), 114.

Cohen, J., 1988a. Chapter 1: The concepts of power analysis. In: *Statistical Power Analysis for the Behavioural Sciences*. 2nd ed. New York: Lawrence Erlbaum Associates. p.1-18.

Cohen, J., 1988b. Chapter 2: The t Test for Means. In: *Statistical Power Analysis for the Behavioural Sciences.* 2nd ed. New York: Lawrence Erlbaum Associates. p.19-74

Cohen, J., 1992. A power primer. *Psychological Bulletin.* 112, p.155-159.

Cowley, P. M., Nair, D. R., DeRuisseau, L. R., Keslacy, S., Atalay, M. and DeRuisseau, K. C., 2017. Oxidant production and SOD1 protein expression in single skeletal myofibers from Down syndrome mice. *Redox Biology*. 13, p.421-425.

Crapo, J. D., Oury, T., Rabouille, C., Slot, J. W. and Chang, L. Y., 1992. Copper, zinc superoxide dismutase is primarily a cytosolic protein in human cells. Proceedings of the *National Academy of Sciences of the United States of America*. 89 (21), p.10405-10409.

Cummings, N. A. and Nordby, G. L., 1966. Measurement of synovial fluid pH in normal and arthritic knees. *Arthritis and Rheumatism*. 9 (1), p.47-56.

Dahlgren, C. and Karlsson, A., 1999. Respiratory burst in human neutrophils. *Journal of Immunological Methods.* 232 (1-2), p.3-14.

David, S., O'Shea, V. and Kundu, S., 2007. Base-excision repair of oxidative DNA damage. *Nature.* 447, p.941–950.

Day, R. W. and Quinn, G. P., 1989. Comparisons of Treatments After an Analysis of Variance in Ecology. *Ecological Monographs*. 59 (4), p.433-463.

De Grey, A. D. N. J., 2002. HO2*: the forgotten radical. *DNA Cell Biology*. 21 (4), p.251-257.

De Nooy, W., Mrvar, A., Batagelj, V., 2018. Exploratory Social Network Analysis with Pajek: Revised and Expanded Edition for Updated Software. In: *Structural Analysis in the Social Sciences 46.* 3rd ed. Cambridge: Cambridge University Press.

Debier, C. and Larondelle, Y., 2005. Vitamins A and E: Metabolism, roles and transfer to offspring. *British Journal of Nutrition*. 93 (2), p.153-174.

Delves, P. J., Martin, S. J., Burton, D. R., and Roitt, I. M., 2017a. Chapter 3: Antibodies. *Roitt's Essential Immunology*. 13th edition. New York: John Wiley & Sons, Incorporated. p.70-96.

Delves, P. J., Martin, S. J., Burton, D. R., and Roitt, I. M., 2017b. Chapter 2: Specific acquired immunity, In: *Roitt's Essential Immunology*. 13th ed. West Sussex: John Wiley and Sons, p.52-68.

Delves, P. J., Martin, S. J., Burton, D. R., and Roitt, I. M., 2017c. Chapter 17: Autoimmune diseases, In: *Roitt's Essential Immunology*. 13th ed. West Sussex: John Wiley and Sons, p.499-528.

Dimitrov, J. D., Ivanovska, N. D., Lacroix-Desmazes, S., Doltchinkova, V. R., Kaveri, S. V. and Vassilev, T. L., 2006. Ferrous ions and reactive oxygen species increase

antigen-binding and anti-inflammatory activities of immunoglobulin G. *Journal of Biological Chemistry.* 281 (1), p.439-446.

Dimitrov, J. D., Pashov, A. D. and Vassilev, T. L., 2012. Antibody polyspecificity: what does it matter? *Advances in Experimental Medicine and Biology*. 750, p.213-226.

Dinis, T. C., Almeida, L. M., Madeira, V. M., 1993. Lipid peroxidation in sarcoplasmic reticulum membranes: effect on functional and biophysical properties. *Archives of Biochemistry and Biophysics.* 301 (2), p.256-264.

Doesch, A. O., Mueller, S., Nelles, M., Konstandin, M., Celik, S., Frankenstein, L., Goeser, S., Kaya, Z., Koch, A., Zugck, C. and Katus, H. A., 2011. Impact of troponin I-autoantibodies in chronic dilated and ischemic cardiomyopathy. *Basic Research in Cardiology*. 106 (1), p.25-35.

Dröge, W., 2002. Free radicals in the physiological control of cell function. *Physiological Reviews.* 82 (1), p.47-95.

Dunnet, C. W.,1980. Pairwise Multiple Comparisons in the Homogeneous Variance, Unequal Sample Size Case. *Journal of the American Statistical Association*. 75 (372), p.789-795.

Dupuy, C., Ohayon, R., Valent, A., Noël-Hudson, M. S., Dème, D. and Virion, A., 1999. Purification of a novel flavoprotein involved in the thyroid NADPH oxidase. Cloning of the porcine and human cdnas. *Journal of Biological Chemistry.* 274 (52), p.37265-37269.

Ellerby, R.M., Cabelli, D. E., Graden, J. A. and Valentine, J. S., 1996. Copper−Zinc Superoxide Dismutase: Why not pH-Dependent?. *Journal of the American Chemical Society.* 118, p.6556-6561.

Erel, O., 2005. A new automated colorimetric method for measuring total oxidant status. *Clinical Biochemistry.* 38 (12), p.1103-1111.

Escolar, E., Lamas, G. A., Mark, D. B., Boineau, R., Goertz, C., Rosenberg, Y., Nahin, R. L., Ouyang, P., Rozema, T., Magaziner, A., Nahas, R., Lewis, E. F., Lindblad, L., and Lee, K. L., 2014. The effect of an EDTA-based chelation regimen on patients with diabetes mellitus and prior myocardial infarction in the Trial to Assess Chelation Therapy (TACT). *Circulation. Cardiovascular quality and outcomes*. 7 (1), p.15-24. https://doi.org/10.1161/CIRCOUTCOMES.113.000663

Fais, S., Venturi, G., and Gatenby, B., 2014. Microenvironmental acidosis in carcinogenesis and metastases: new strategies in prevention and therapy. *Cancer Metastasis Reviews.* 33 (4), p.1095-1108.

Firestein, G., 2003. Evolving concepts of rheumatoid arthritis. *Nature*. 423, p.356–361.

Flohe, L., Günzler, W. A. and Schock, H. H., 1973. Glutathione peroxidase: a selenoenzyme. *FEBS Letters*. 32 (1), p.132-134.

Franklin, J., Lunt, M., Bunn, D., Symmons, D. and Silman, A., 2006. Incidence of lymphoma in a large primary care derived cohort of cases of inflammatory polyarthritis. *Annals of the rheumatic diseases.* 65 (5), p.617-622.

Fried, R.,1975. Enzymatic and non-enzymatic assay of superoxide dismutase. *Biochimie.* 57 (5), p.657-660.

Fujita, Y., Mori, I., Kitano, S., 1983. Colour reaction between Pyrogallol Red – Molybdenum (VI) complex and protein. *Bunseki Kagaku*. 32, p.379-386.

Games, P. A. and Howell, J. F., 1976. Pairwise multiple comparison procedures with unequal n's and/or variances: A monte carlo study. *Journal of Education Statistics*. 1 (2), p.113-125.

Gangemi, S., Allegra, A., Alonci, A., Cristani, M., Russo, S., Speciale, A., Penna, G., Spatari, G., Cannavò, A., Bellomo, G., Musolino, C., 2012. Increase of novel biomarkers for oxidative stress in patients with plasma cell disorders and in multiple myeloma patients with bone lesions. *Inflammation Research*. 61 (10), p.1063-1067.

Garaud, S., Zayakin, P., Buisseret, L., Rulle, U., Silina, K., de Wind, A., Van den Eyden, G., Larsimont, D., Willard-Gallo, K., and Linē, A., 2018. Antigen Specificity and Clinical Significance of IgG and IgA Autoantibodies Produced in situ by Tumour-Infiltrating B Cells in Breast Cancer. *Frontiers in Immunology*. 9, 2660.

Garcia, P., 2018. *Report reveals the rising rates of autoimmune conditions*. Available: https://www.immunology.org/news/report-reveals-the-rising-rates-autoimmune-conditions. Last accessed 24.10.2020.

Garlick, P. B., Radda, G. K. and Seeley, P. J., 1979. Studies of Acidosis in the Ischaemic Heart by Phosphorus Nuclear Magnetic Resonance. *Biochemical Journal*. 184 (1), p.547-554.

Gebert, G., Benzing, H. and Strohm, M., 1971. Changes in the Interstitial pH of Dog Myocardium in Response to Local Ischemia, Hypoxia, Hyper- and Hypocapnia, Measured Continuously by Means of Glass Microelectrodes. *Pflügers Archiv - European Journal of Physiology.* 329 (1), p.72-81.

Gerling, I. C., 2009. Oxidative stress, altered-self and autoimmunity. *Open Autoimmunity Journal*. 1, p.33-36.

Getzoff, E. D., Tainer, J. A., Weiner, P. K., Kollman, P. A., Richardson, J. S. and Richardson, D. C., 1983. Electrostatic recognition between superoxide and copper, zinc superoxide dismutase. *Nature.* 306 (5940), p.287-290.

Cancarini, G., Terlizzi, V., Garatti, A., Zeni, L., Tonoli, M., Pezzini, E., Boni, F., Possenti, S., Viola, B. F. and Maggiotti, G., 2021. Supportive treatment for cast nephropathy in patients with multiple myeloma; a pilot study. *Journal of Nephropharmacology*. 10:e21.

Glorieux, C., Sandoval, J.M., Fattaccioli, A., Dejeans, N., Garbe, J.C., Dieu, M., Verrax, J., Renard, P., Huang, P. and Buc Calderon, P., 2016. Chromatin remodelling

regulates catalase expression during cancer cells adaptation to chronic oxidative stress. *Free Radicals in Biology and Medicine*. 99, p.436-450.

Gomez, W., Morales, R., Maracaja-Coutinho, V., Parra, V. and Nassif, M., 2020. Down syndrome and Alzheimer's disease: common molecular traits beyond the amyloid precursor protein. *Aging*. 12 (1), p.1011-1033.

Gómez-Marcos, M. A., Blázquez-Medela, A. M., Gamella-Pozuelo, L., Recio-Rodriguez, J. I., García-Ortiz, L. and Martínez-Salgado, C., 2015. Serum Superoxide Dismutase Is Associated with Vascular Structure and Function in Hypertensive and Diabetic Patients. *Oxidative Medicine and Cell Longevity*. 2016: article 9124676.

Góth, L. and Nagy, T., 2013. Inherited catalase deficiency: is it benign or a factor in various age-related disorders? *Mutation Research*. 753 (2), p.147-154.

Gottfredsen, R. H., Larsen, U. G., Enghild, J. J. and Petersen, S. V., 2013. Hydrogen peroxide induce modifications of human extracellular superoxide dismutase that results in enzyme inhibition. *Redox biology.* 1 (1), p.24-31.

Green, P. H. R. and Jabri, B., 2003. Coeliac disease. *The Lancet*. 362 (9381), p.383-391.

Gulesserian, T., Seidl, R., Hardmeier, R., Cairns, N. and Lubec, G., 2001. Superoxide dismutase SOD1, encoded on chromosome 21, but not SOD2 is overexpressed in brains of patients with Down syndrome. *Journal of Investigative Medicine.* 49 (1), p.41-46.

Guo, X., Yu, Y., Liu, X., Zhang, Y., Guan, T., Xie, G. and Wei, J. 2014. Heterologous expression and characterization of human cellular glutathione peroxidase mutants. *International Union of Biochemistry and Molecular Biology Life*. 66 (3), p.212-219.

Halliwell, B. and Gutteridge, J. M. C., 2015a. Oxidative stress and redox regulation: adaptation, damage, repair, senescence, and death. In: *Free radicals in biology and medicine*. 5th ed. New York: Oxford University Press. p.199-283.

Halliwell, B. and Gutteridge J.M.C., 2015b. Oxygen: boon yet bane—introducing oxygen toxicity and reactive species. In: *Free radicals in biology and medicine*. 5th Ed. New York: Oxford University Press. p.1-29.

Halliwell, B. and Gutteridge J.M.C., 2015c. Antioxidants from the diet. In: *Free radicals in biology and medicine.* 5th Ed. New York: Oxford University Press. p.153-198.

Halliwell, B. and Gutteridge J.M.C., 2015d. Antioxidant defences synthesized in vivo. In: *Free radicals in biology and medicine.* 5th Ed. New York: Oxford University Press. p.77-152.

Halliwell, B. and Gutteridge J.M.C., 2015e. Reactive species in disease: friends or foes?. In: *Free radicals in biology and medicine.* 5th ed. New York: Oxford University Press. p.511-638.

Halliwell, B. and Gutteridge, J. M. C., 1999. Antioxidant defences. In: *Free Radical in Biology and Medicine*. 3rd ed. New York: Oxford University Press. p.105-246.

Halliwell, B. and Whiteman, M., 2004. Measuring reactive species and oxidative damage in vivo and in cell culture: how should you do it and what do the results mean?. *British Journal of Pharmacology*. 142, p.231–255.

Halliwell, B., 1995. How to characterize an antioxidant: an update. *Biochemical Society Symposium.* 61, p.73-101.

Halliwell, B., 1997. Antioxidants and Human Disease: A General Introduction. *Nutrition Reviews*. 55 (1), p.S44–S49.

Handy, D.E. and Loscalzo, J., 2012. Redox Regulation of Mitochondrial Function. *Antioxidants and Redox Signaling.* 16 (11), p.1324-1349.

Harman, D., 1956. Aging: A theory based of free radical and radiation chemistry. *Journal of Gerontology.* 11 (3), p.298-300.

Harman, D., 1972. The biologic clock: the mitochondria? *Journal of the american geriatrics society*. 20 (4), p.145-147.

Hashmi, S. and Al-Salam, S., 2015. Acute myocardial infarction and myocardial ischemia-reperfusion injury: a comparison. *International journal of clinical and experimental pathology*. 8 (8), p.8786-8796.

Hayyan, M., Hashim, M. A. and AlNashef, I. M., 2016. Superoxide Ion: Generation and Chemical Implications. *American Chemical Society*. 116, p.3029−3085.

Hedges, L. V. and Olkin, I., 1985. *Statistical methods for meta-analysis*. 1st ed. Orlando: Academic Press.

Hodgson, E. K. and Fridovich, I., 1975. The interaction of bovine erythrocyte superoxide dismutase with hydrogen peroxide: inactivation of the enzyme. *Biochemistry.* 14 (24), p.5294-5299.

Holland, M. D., Galla, J. H., Sanders, P. W., and Luke, R. G, 1985. Effect of urinary pH and diatrizoate on Bence Jones protein nephrotoxicity in the rat. *Kidney International.* 27 (1), p.46-50.

Horsley, E. T., Burkitt, M. J., Jones, C. M., Patterson, R. A., Harris, L. K., Moss, N. J., del Rio, J. D., and Leake, D. S., 2007. Mechanism of the antioxidant to pro-oxidant switch in the behaviour of dehydroascorbate during LDL oxidation by copper (II) ions. *Archives in Biochemistry and Biophysics.* 465 (2), p.303-314.

Hozumi, N., Tonegawa, S., 1976. Evidence for somatic rearrangement of immunoglobulin genes coding for variable and constant regions. Proceedings of the *National Academy of Sciences of the United States of America*. 73 (10), p.3628-3632.

International Myeloma Working Group, 2003. Criteria for the classification of monoclonal gammopathies, multiple myeloma and related disorders: a report of the International Myeloma Working Group. *British Journal of Haematology*. 121 (5), p.749-757.

Jang, Y. C. and Remmen, H. V., 2009. The mitochondrial theory of aging: Insight from transgenic and knockout mouse models. *Experimental Gerontology*. 44 (4), p.256-260.

Jiang, Z. Y., Woollard, A. C. S. and Wolff, S.P., 1991. Lipid hydroperoxide measurement by oxidation of Fe2+ in the presence of xylenol orange. Comparison with the TBA assay and an iodometric method. *Lipids*. 26, p.853–856.

Jiang, Z., Woollard, A.C.S. and Wolff, S. P., 1990. Hydrogen peroxide production during experimental protein glycation. *The FEBS journal.* 268 (1), p.69-71.

Jolliffe, I. T. and Cadima, J., 2016. Principal component analysis: a review and recent developments. *Philosophical Transactions of the Royal Society A*. 374 (2065):20150202.

Jolliffe, I. T., 1972. Discarding Variables in a Principal Component Analysis. I: Artificial Data. *Journal of the Royal Statistical Society. Series C (Applied Statistics).* 21 (2), pp. 160-172.

Jolliffe, I., 2002a. Introduction. In: *Principal Component Analysis*. 2nd ed. New York: Springer. p.1-9.

Jolliffe, I., 2002b. Graphical Representation of Data Using Principal Components. In: *Principal Component Analysis.* 2nd ed. New York: Springer. p.78-110.

Jomová, K., Hudecova, L., Lauro, P., Simunkova, M., Alwasel, S. H., Alhazza, I. M., and Valko, M., 2019. A Switch between Antioxidant and Prooxidant Properties of the Phenolic Compounds Myricetin, Morin, 3',4'-Dihydroxyflavone, Taxifolin and 4-Hydroxy-Coumarin in the Presence of Copper (II) Ions: A Spectroscopic, Absorption Titration and DNA Damage Study. *Molecules.* 24 (23), 4335.

Kalaga, R., Li, L., O'Dell, J. R. and Paul, S., 1995. Unexpected presence of polyreactive catalytic antibodies in IgG from unimmunized donors and decreased levels in rheumatoid arthritis. *Journal of Immunology*. 155 (5), p.2695-2702.

Kamada, T. and Kawai, S., 1981. An algorithm for drawing general undirected graphs. *Information Processing Letters.* 31, pp. 7-15.

Kamanli, A., Naziroğlu, M., Aydilek, N. and Hacievliyagil, C., 2004. Plasma lipid peroxidation and antioxidant levels in patients with rheumatoid arthritis. *Cell Biochemistry and Function*. 22 (1), p.53-57.

Kaple, M.N., Mahakalkar, C.C., Kale, A., Shambharkar, S., 2020. Correlation of Metal Ions in Diabetic Patients. *Journal of Clinical and Diagnostic Research*. 14 (5), BC14-BC16. https://www.doi.org/10.7860/JCDR/2020/43798/13730

Kasai, H. and Nishimura. S., 1984. Hydroxylation of deoxyguanosine at the C-8 position by ascorbic acid and other reducing agents. *Nucleic Acids Research.* 12 (4), p.2137-2145.

Kasapović, J., Pejić, S., Todorović, A., Stojiljković, V. and Pajović, S. B., 2008. Antioxidant status and lipid peroxidation in the blood of breast cancer patients of different ages. *Cell Biochemistry and Function*. 26 (6), p.723-730.

Kato, Y., Ozawa, S., Miyamoto, C., Maehata, Y., Suzuki, A., Maeda, T. and Baba, Y., 2013. Acidic extracellular microenvironment and cancer. *Cancer Cell International.* 13 (1), Article no. 89.

Kaufman, L. and Rousseeuw, P. J., 1990a. *Finding Groups in Data: An Introduction to Cluster Analysis*. New Jersey: John Wiley & Sons, Inc. p.1-67.

Kaufman, L. and Rousseeuw, P. J., 1990b. *Finding Groups in Data: An Introduction to Cluster Analysis.* New Jersey: John Wiley & Sons, Inc. p.199-231.

Kellum J. A., 2000. Determinants of blood pH in health and disease. *Critical care (London, England)*, 4 (1), p.6-14.

Kettle, A. J., Clark, B. M. and Winterbourn, C. C., 2004. Superoxide converts indigo carmine to isatin sulfonic acid: implications for the hypothesis that neutrophils produce ozone. *Journal of Biological Chemistry.* 279 (18), p.18521-18525.

Kivelä, L., Caminero, A., Leffler, D. A., Pinto-Sanchez, M. I., Tye-Din, J. A. and Lindfors, K., 2021. Current and emerging therapies for coeliac disease. *Nature Reviews Gastroenterology and Hepatology*. 18 (3), p.181-195.

Kiziltunc, A., Coğalgil, S. and Cerrahoğlu, L., 1998. Carnitine and antioxidants levels in patients with rheumatoid arthritis. *Scandinavian Journal of Rheumatology.* 27 (6), p.441-445.

Klaus, T. and Deshmukh, S., 2021. pH-responsive antibodies for therapeutic applications. *Journal of biomedical science.* 28 (1), article 11.

Koelwyn, G. J., Newman, A. A. C., Afonso, M. S., van Solingen, C., Corr, E. M., Brown, E. J., Albers, K. B., Yamaguchi, N., Narke, D., Schlegel, M., Sharma, M., Shanley, L. C., Barrett, T. J., Rahman, K., Mezzano, V., Fisher, E. A., Park, D. S., Newman, J. D., Quail, D. F., Nelson, E. R., Caan, B. J., Jones, L. W. and Moore, K. J., 2020. Myocardial infarction accelerates breast cancer via innate immune reprogramming. *Nature Medicine.* 26 (9), p.1452-1458.

Kohanski, M. A., Dwyer, D. J., Hayete, B., Lawrence, C. A. and Collins, J. J., 2007. A common mechanism of cellular death induced by bactericidal antibiotics. *Cell*. 130, p.797–810.

Köhler, G., Milstein, C., 1975. Continuous cultures of fused cells secreting antibody of predefined specificity. *Nature.* 256 (5517), p.495-497.

Kopaniak, M. M., Issekutz, A. C. and Movat, H. Z., 1980. Kinetics of acute inflammation induced by E coli in rabbits. Quantitation of blood flow, enhanced vascular permeability, haemorrhage, and leukocyte accumulation. *The American journal of pathology.* 98 (2), p.485-498.

Kouoh, F., Gressier, B., Luyckx, M., Brunet, C., Dine, T., Cazin, M., Cazin, J. C., 1999. Antioxidant properties of albumin: effect on oxidative metabolism of human neutrophil granulocytes. *Il Farmaco.* 54 (10), p.695-699.

Koziolek, M., Grimm, M., Becker, D., Iordanov, V., Zou, H., Shimizu, J., Wanke, C., Garbacz, G. and Weitschies, W.. 2015. Investigation of pH and Temperature Profiles in the GI Tract of Fasted Human Subjects Using the Intellicap (®) System. *Journal of Pharmaceutical Science*. 104 (9), p.2855-2863.

Kramer, C. Y., 1956. Extension of Multiple Range Tests to Group Means with Unequal Numbers of Replications. *Biometrics.* 12 (3), p.307-310.

Krumova, K. and Cosa, G., 2016. Overview of Reactive Oxygen Species. In: Nonell, S. and Flors, C. Singlet Oxygen: Applications in Biosciences and Nanosciences, Volume 1. Cambridge: *Cambridge: Royal Society of Chemistry*. p.1-21

Lacroix-Desmazes, S., Bayry, J., Kaveri, S.V., Hayon-Sonsino, D., Thorenoor, N., Charpentier, J., Luyt, CE., Mira, JP., Nagaraja, V., Kazatchkine, M.D., Dhainaut, JF. and Mallet, V.O., 2005. High levels of catalytic antibodies correlate with favourable outcome in sepsis. *Proceedings of the National Academy of Sciences.* 102 (11), p.4109-4113.

Lambeth, J. D., 2004. Nox enzymes and the biology of reactive oxygen. *Nature Immunology.* 4, p.181-189.

Landsteiner, K., 1947. The Specificity of Serological Reactions. *Harvard: Harvard University Press*.

Lardner, A., 2001. The effects of extracellular pH on immune function. *Journal of leukocyte biology*. 69 (4), p.522-530.

Leake, D. S., 1997. Does an acidic pH explain why low-density lipoprotein is oxidised in atherosclerotic lesions?. *Atherosclerosis*. 129 (2), p.149-157.

Lebwohl, B., Sanders, D. S. and Green, P. H. R., 2018. Coeliac disease. *The Lancet*, 391 (10115), p.70-81.

Leipzig, L. J., Boyle, A. J., and McCann, D. S., 1970. Case histories of rheumatoid arthritis treated with sodium or magnesium EDTA. *Journal of chronic diseases*. 22 (8), p.553-563. https://doi.org/10.1016/0021-9681(70)90032-9

Leuschner, F., Li, J., Göser, S., Reinhardt, L., Ottl, R., Bride, P., Zehelein, J., Pfitzer, G., Remppis, A., Giannitsis, E., Katus, H. A. and Kaya, Z., 2008. Absence of autoantibodies against cardiac troponin I predicts improvement of left ventricular function after acute myocardial infarction. *European Heart Journal*. 29 (16), p.1949-1955.

Levanon, D., Lieman-Hurwitz, J., Dafni, N., Wigderson, M., Sherman, L., Bernstein, Y., Laver-Rudich, Z., Danciger, E., Stein, O. and Groner, Y., 1985. Architecture and anatomy of the chromosomal locus in human chromosome 21 encoding the Cu/Zn superoxide dismutase. *The EMBO journal*. 4 (1), p.77-84.

Levine, R. L., Williams, J. A., Stadtman, E.R., Shacter, E., 1994. Carbonyl assays for determination of oxidatively modified proteins. *Methods in Enzymology*. 233, p.346-357.

Li, C., Uribe, D. and Daling, J., 2005. Clinical characteristics of different histologic types of breast cancer. *British Journal of Cancer*. 93, p.1046-1052.

Li, Y., Huang, T. T., Carlson, E. J., Melov, S., Ursell, P. C., Olson, J. L., Noble, L. J., Yoshimura, M. P., Berger, C., Chan, P. H., Wallace, D. C. and Epstein, C. J., 1995. Dilated cardiomyopathy and neonatal lethality in mutant mice lacking manganese superoxide dismutase. *Nature Genetics*. 11 (4), p.376-381

Liang, H., Vallarino, C., Joseph, G., Manne, S., Perez, A. and Zhang, S., 2014. Increased risk of subsequent myocardial infarction in patients with type 2 diabetes: a

retrospective cohort study using the U.K. *General Practice Research Database*. Diabetes Care. 37 (5), p.1329-1337.

Liddell, E., 2005. Antibodies. In: *The Immunoassay Handbook*. 3rd edition. Oxford: Elsevier. p.144-166.

Liochev, S. I. and Fridovich, I., 1999. Superoxide and iron: partners in crime. *IUBMB Life.* 48 (2), p.157-161.

Loew, O., 1900. A new enzyme of general occurrence in organisms. *Science.* 11 (279), p.701-702.

Los, M., Dröge, W., Stricker, K., Baeuerle, P. A., Schulze-Osthoff, K., 1995. Hydrogen peroxide as a potent activator of T lymphocyte functions. *European Journal of Immunology.* 25 (1), p.159-65.

Lü, J. M., Lin, P. H., Yao, Q. and Chen, C., 2010. Chemical and molecular mechanisms of antioxidants: experimental approaches and model systems. *Journal of Cellular and Molecular Medicine*. 14 (4), p.840-860.

MacMillan-Crow, L. A., Crow, J. P., Kerby, J. D., Beckman, J. S., Thompson, J. A., 1996. Nitration and inactivation of manganese superoxide dismutase in chronic rejection of human renal allografts. *Proceedings National Academy Sciences United States of America*. 93 (21), p.11853-11858.

Malmborg, M., Christiansen, C. B., Schmiegelow, M. D., Torp-Pedersen, C., Gislason, G. and Schou, M., 2018. Incidence of new onset cancer in patients with a myocardial infarction - a nationwide cohort study. *BioMed Central cardiovascular disorders.* 18 (1), 198.

Mann, T. and Keilin, D., 1938. Haemocuprein, a Copper-Protein Compound of Red Blood Corpuscles. *Nature.* 142, p.148.

Marafini, I., Monteleone, G. and Stolfi, C., 2020. Association Between Coeliac Disease and Cancer. *International journal of molecular sciences*. 21 (11), 4155.

Marciano, B. E., Zerbe, C. S., Falcone, E. L., Ding, L., DeRavin, S. S., Daub, J., Kreuzburg, S., Yockey, L., Hunsberger, S., Foruraghi, L., Barnhart, L. A., Matharu, K., Anderson, V., Darnell, D. N., Frein, C., Fink, D. L., Lau, K. P., Long Priel, D. A., Gallin, J. I., Malech, H. L., Uzel, G., Freeman, A. F., Kuhns, D. B., Rosenzweig, S. D., Holland, S. M., 2018. X-linked carriers of chronic granulomatous disease: Illness, lyonization, and stability. *Journal of Allergy and Clinical Immunology.* 141 (1), p365-371.

Marikovsky, M., Ziv, V., Nevo, N., Harris-Cerruti, C. and Mahler, O., 2003. Cu/Zn superoxide dismutase plays important role in immune response. *Journal of Immunology*. 170 (6), p.2993-3001.

Marklund, S. L., Holme, E., Hellner, L., 1982. Superoxide dismutase in extracellular fluids. *Clinical Chimica Acta.* 126 (1), p.41-51.

Marklund, S., 1976. Spectrophotometric Study of Spontaneous Disproportionation of Superoxide Anion Radical and Sensitive Direct Assay for Superoxide Dismutase. *Journal of Biological Chemistry*. 251 (23), p.7504-7507.

Markowitz, H., Cartwright, G. E. and Wintrobe, M. M., 1959. Studies on copper metabolism. XXVII. The isolation and properties of an erythrocyte cuproprotein (erythrocuprein). *Journal of Biological Chemistry.* 234 (1), p.40-45.

Martz, E. and Francoeur, E., 1997. *History of Visualization of Biological Macromolecules*. Available: http://www.umass.edu/microbio/rasmol/history.htm#bender. Last accessed 31.10.16.

Mateen, S., Moin, S., Khan, A. Q., Zafar, A. and Fatima, N., 2016. Increased Reactive Oxygen Species Formation and Oxidative Stress in Rheumatoid Arthritis. *PloS one*. 11 (4), e0152925.

Matsuura, K., Ohara, K., Munakata, H., Hifumi, E. and Uda, T, 2006. Pathogenicity of catalytic antibodies: catalytic activity of Bence Jones proteins from myeloma patients with renal impairment can elicit cytotoxic effects. *Biological Chemistry*. 387 (5), p.543-548.

Mazzio, E. A., Smith, B. and Soliman, K. F. A., 2010. Evaluation of endogenous acidic metabolic products associated with carbohydrate metabolism in tumour cells. *Cell Biology Toxicology.* 26, p.177-188.

McCord, J. M. and Fridovich, I., 1969. Superoxide dismutase. An enzymic function for erythrocuprein (haemocuprein). *Journal of Biological Chemistry*. 244 (22), p.6049-6055.

McEwan, G. T., Lucas, M. L., Denvir, M., Raj, M., McColl, K. E., Russell, R. I., Mathan, V. I., 1990. A combined TDDA-PVC pH and reference electrode for use in the upper small intestine. *Journal of Medical Engineering and Technology*. 14 (1), p.16-20.

McMahon, M. J. and O'Kennedy, R., 2000. Polyreactivity as an acquired artefact, rather than a physiologic property, of antibodies: evidence that monoreactive antibodies may gain the ability to bind to multiple antigens after exposure to low pH. *Journal of Immunological Methods*. 241 (1-2), p.1-10.

Menkin, V. and Warner, C. R., 1937. Studies on Inflammation: XIII. Carbohydrate Metabolism, Local Acidosis, and the Cytological Picture in Inflammation. *The American journal of pathology*. 13 (1), p.25-44.

Mihaylova, N. M., Dimitrov, J. D., Djoumerska-Alexieva, I. K. and Vassilev, T. L., 2008. Inflammation-induced enhancement of IgG immunoreactivity. *Inflammation Research.* 57 (1), p.1-3.

Mills, G. C., 1957. Haemoglobin catabolism. I. Glutathione peroxidase, an erythrocyte enzyme which protects haemoglobin from oxidative breakdown. *Journal of Biological Chemistry*. 229 (1), p.189-197.

Moretti, S., Mrakic-Sposta, S., Roncoroni, L., Vezzoli, A., Dellanoce, C., Monguzzi, E., Branchi, F., Ferretti, F., Lombardo, V., Doneda, L., Scricciolo, A. and Elli, L., 2018. Oxidative stress as a biomarker for monitoring treated celiac disease. *Clinical and translational gastroenterology*. 9(6), article 157.

Morrison, S. and Neuberger, M. S., 2001. Antigen Recognition by B-cell and T-cell Receptors. In: Janeway, C. A., Travers, P., Walport, M. and Shlomchi, M. J. *Immunobiology*. 5th ed. New York: Garland Science. Chapter 3.

Nagano, Y., Matsui, H., Shimokawa, O., Hirayama, A., Nakamura, Y., Tamura, M., Rai, K., Kaneko, T. and Hyodo, I., 2012. Bisphosphonate-induced gastrointestinal mucosal injury is mediated by mitochondrial superoxide production and lipid peroxidation. *Journal of Clinical Biochemistry and Nutrition*. 51 (3), p.196-203.

Naghavi, M., John, R., Naguib, S., Siadaty, M. S., Grasu, R., Kurian, K. C., van Winkle, W. B., Soller, B., Litovsky, S., Madjid, M., Willerson, J. T., Casscells, W., 2002. pH Heterogeneity of human and rabbit atherosclerotic plaques; a new insight into detection of vulnerable plaque. *Atherosclerosis*. 164, p.27-35.

Niethammer, P., Grabher, C., Look, A. T., and Mitchison, T. J., 2009. A tissue-scale gradient of hydrogen peroxide mediates rapid wound detection in zebrafish. *Nature*. 459 (7249), p.996-999.

Niki, E., 2016. Oxidative stress and antioxidants: Distress or eustress?. *Archives of Biochemistry and Biophysics*. 595, p.19-24

Nimse, S. B. and Pal, D., 2015. Free radicals, natural antioxidants, and their reaction mechanisms. *Royal Society of Chemistry: Advances*. 5 (23), p.27986–28006.

Noichri, Y., Chalghoum, A., Chkioua, L., Baudin, B., Ernez, S., Ferchichi, S., and Miled, A., 2013. Low erythrocyte catalase enzyme activity is correlated with high serum total homocysteine levels in Tunisian patients with acute myocardial infarction. *Diagnostic pathology*. 8, 68.

Office for National Statistics, 2019. *Cancer registration statistics, England: 2017.* Available: https://www.ons.gov.uk/peoplepopulationandcommunity/healthandsocialcare/conditionsanddiseases/bulletins/cancerregistrationstatisticsengland/2017. Last accessed 24.10.2020.

Office for National Statistics, 2019. *National population projections: 2018-based.* Available: https://www.ons.gov.uk/peoplepopulationandcommunity/populationandmigration/populationprojections/bulletins/nationalpopulationprojections/2018based. Last accessed 31.01.21

Omenn, G. S., Goodman, G. E., Thornquist, M. D., Balmes, J., Cullen, M. R., Glass, A., Keogh, J. P., Meyskens, F. L., Valanis, B., Williams, J. H., Barnhart, S., Cherniack, M. G., Brodkin, C. A. and Hammar S., 1996. Risk factors for lung cancer and for intervention effects in CARET, the Beta-Carotene and Retinol Efficacy Trial. *Journal of the National Cancer Institute*. 88 (21), p.1550-1559.

Pace, C. N., Vajdos, F., Fee, L., Grimsley, G. and Theronica, G., 1995. How to measure and predict the molar absorption coefficient of a protein. *Protein Science*. 4, p.2411-2423.

Padayatty, S. J., Katz, A., Wang, Y., Eck, P., Kwon, O., Lee, J. H., Chen, S., Corpe, C., Dutta, A., Dutta, S. K., Levine, M., 2003. Vitamin C as an antioxidant: evaluation of its role in disease prevention. *Journal of the American College of Nutrition.* 22 (1), p.18-35.

Palace, V. P., Khaper, N., Qin, Q. and Singal, P. K., 1999. Antioxidant potentials of vitamin A and carotenoids and their relevance to heart disease. *Free Radicals in Biology and Medicine.* 26 (5-6), p.746-761.

Palasubramaniam, J., Wang, X. and Peter, K., 2019. Myocardial Infarction-From Atherosclerosis to Thrombosis. *Arteriosclerosis, Thrombosis and Vascular Biology*. 39 (8), e176-e185.

Passwater, R. A., 1975. *Supernutrition: Megavitamin Revolution*. New York. USA. Dial Press.

Pastor, R., and Tur, J. A, 2020. Response to exercise in older adults who take supplements of antioxidants and/or omega-3 polyunsaturated fatty acids: A systematic review. Biochemical pharmacology. 173, article 113649. https://doi.org/10.1016/j.bcp.2019.113649

Patil, N., Chavan, V., and Karnik, N. D., 2007. Antioxidant status in patients with acute myocardial infarction. *Indian journal of clinical biochemistry: IJCB.* 22 (1), p.45–51.

Patterson, A. D., Gonzalez, F. J., Idle, J. R., 2010. Xenobiotic metabolism: a view through the metabolometer. *Chemical Research Toxicology*. 23 (5), p.851-860.

Paul, S., Li, L., Kalaga, R., Wilkins-Stevens, P., Stevens, F. J., and Solomon, A., 1995. Natural Catalytic Antibodies: Peptide-hydrolyzing Activities of Bence Jones Proteins and VL Fragment (∗). *Journal of Biological Chemistry*. 270 (25), p.15257-15261.

Paul, S., Volle, D. J., Beach, C. M., Johnson, D. R., Powell, M. J. and Massey, R. J., 1989. Catalytic hydrolysis of vasoactive intestinal peptide by human autoantibody. *Science*. 244 (4909), p.1158-1162.

Pauling, L., 1948. Chemical achievement and hope for the future. *American Scientist.* 36 (1), p51-58.

Perry, J. J., Shin, D. S., Getzoff, E. D. and Tainer, J. A., 2010. The structural biochemistry of the superoxide dismutases. *Biochimica et biophysica acta*. 1804 (2), p.245-262.

Petyaev, I. and Hunt, J. 1996. Apparent superoxide dismutase-like activity of immunoglobulin. *Redox Report*. 2 (6), p.365-372.

Petyaev, I., Mitchinson, M. M., Hunt, J. V. and Coussons, P.J., 1998. Superoxide Dismutase Activity of Antibodies Purified from the Human Arteries and Atherosclerotic Lesions. *Biochemical Society Transactions*. 26 (S43), p.110.

Poetsch, A. R., 2020. The genomics of oxidative DNA damage, repair, and resulting mutagenesis. *Computational and Structural Biotechnology Journal.* 18, p.207-219.

Poljak, R. J., Amzel, L. M., Avey, H. P., Chen, B. L., Phizackerley, R. P. and Saul, F., 1973. Three-dimensional structure of the Fab' fragment of a human immunoglobulin at 2,8-A resolution. *Proceedings of the National Academy of Sciences of the United States of America*. 70 (12), p.3305-3310.

Poole, L. B., 2015. The basics of thiols and cysteines in redox biology and chemistry. *Free Radicals Biology Medicine.* 80, p.148–157.

Poprac, P., Jomova, K., Simunkova, M., Kollar, V., Rhodes, C. J., Valko, M., 2017. Targeting Free Radicals in Oxidative Stress-Related Human Diseases. Trends in *Pharmacological Sciences.* 38 (7), p.592-607.

Porter, H. and Folch, J., 1957. Cerebrocuprein I. A copper-containing protein isolated from brain. *Journal of Neurochemistry.* 1 (3), p.260-271.

Radak, Z., Ishihara, K., Tekus, E., Varga, C., Posa, A., Balogh, L., Boldogh, I., and Koltai, E., 2017. Exercise, oxidants, and antioxidants change the shape of the bell-shaped hormesis curve. *Redox biology*. 12, p.285-290. https://doi.org/10.1016/j.redox.2017.02.015

Radenkovic, S., Milosevic, Z., Konjevic, G., Karadzic, K., Rovcanin, B., Buta, M., Gopcevic, K. and Jurisic, V., 2013. Lactate dehydrogenase, catalase, and superoxide dismutase in tumour tissue of breast cancer patients in respect to mammographic findings. *Cell Biochemistry and Biophysics.* 66 (2), p.287-95.

Rahman, K., 2007. Studies on free radicals, antioxidants, and co-factors. *Clinical Interventions in Aging.* 2 (2) p.219–236.

Rajamäki, K., Nordström, T., Nurmi, Åkerman, K. E. O., Kovanen, P. T., Öörni, K. and Eklund, K. K. 2013. Extracellular Acidosis Is a Novel Danger Signal Alerting Innate Immunity via the NLRP3 Inflammasome. *The Journal of Biological Chemistry.* 288 (19), p.13410-13419.

Rawlings, J. M., Lucas, M. L. and Russell, R. I., 1987. Measurement of jejunal surface pH in situ by plastic pH electrode in patients with coeliac disease. *Scandinavian Journal of Gastroenterology.* 22 (3), p.377-384.

Ray, S. C., Patel, B., Irsik, D. L., Sun, J., Ocasio, H., Crislip, G. R., Jin, C. H., Chen, J., Baban, B., Polichnowski, A. J., and O'Connor, P. M., 2018. Sodium bicarbonate loading limits tubular cast formation independent of glomerular injury and proteinuria in Dahl salt-sensitive rats. *Clinical science (London, England: 1979)*. 132 (11), p.1179-1197. https://doi.org/10.1042/CS20171630

Reeder, B. J., Sharpe, M. A., Kay, A. D., Kerr, M., Moore, K. and Wilson, M. T., 2002. Toxicity of myoglobin and haemoglobin: oxidative stress in patients with rhabdomyolysis and subarachnoid haemorrhage. *Biochemical Society Transactions*. 30 (4), p.745-748.

Renton, A. E., Chiò, A., Traynor, B. J., 2014. State of play in amyotrophic lateral sclerosis genetics. *Nature Neuroscience*. 17 (1), p.17-23.

Reverberi, R. and Reverberi, L., 2007. Factors affecting the antigen-antibody reaction. *Blood transfusion = Trasfusione del sangue*. 5 (4), p.227–240.

Ricciotti, E. and FitzGerald, G. A., 2011. Prostaglandins and inflammation. *Arteriosclerosis, thrombosis, and vascular biology.* 31 (5), p.986–1000.

Richardson, J. S., 1977. Beta-Sheet topology and the relatedness of proteins. *Nature.* 268 (5620), p.495-500.

Richardson, J. S., Richardson, D. C., Thomas, K. A., Silverton, E. W. and Davies, D. R., 1976. Similarity of three-dimensional structure between the immunoglobulin domain and the copper, zinc superoxide dismutase subunit. *Journal of Molecular Biology*. 102 (2), p.221-235.

Richardson, J., Thomas, K. A., Rubin, B. H. and Richardson, D. C., 1975. Crystal structure of bovine Cu, Zn superoxide dismutase at 3 A resolution: chain tracing and metal ligands. *Proceedings of the National Academy of Sciences of the United States of America.* 72 (4), p.1349-1353.

Riley, P. A., 1994. Free radicals in biology: oxidative stress and effects of ionizing radiation. *International Journal of Radiation Biology*. 65, p.27–33.

Ristow, M. and Schmeisser, K., 2014. Mitohormesis: Promoting Health and Lifespan by Increased Levels of Reactive Oxygen Species (ROS). *Dose Response*. 12 (2), p.288-341.

Ristow, M. and Zarse. K., 2010. How increased oxidative stress promotes longevity and metabolic health: The concept of mitochondrial hormesis (mitohormesis). *Experimental Gerontology.* 45 (6), p.410-418.

Ristow, M., Zarse, K., Oberbach, A., Klöting, N., Birringer, M., Kiehntopf, M., Stumvoll, M., Kahn, C. R., and Blüher, M., 2009. Antioxidants prevent health-promoting effects of physical exercise in humans. *Proceedings of the National Academy of Sciences of the United States of America.* 106 (21), p.8665–8670.

Roche, M., Rondeau, P., Singh, N. R., Tarnus, E. and Bourdon, E., 2008. The antioxidant properties of serum albumin. *FEBS Letters*. 582 (13), p.1783-1787.

Rotilio, G., Bray, R. C. and Fielden, E. M., 1972. A pulse radiolysis study of superoxide dismutase. *Biochimica et Biophysica Acta.* 268 (2), p.605-609.

Rotstein, O. D., Nasmith, P. E. and Grinstein, S., 1987. The Bacteroides by-product succinic acid inhibits neutrophil respiratory burst by reducing intracellular pH. *Infection and Immunity*. 55 (4), p.864-870.

Saccon, R. A., Bunton-Stasyshyn, R. K., Fisher, E. M. and Fratta, P., 2013. Is SOD1 loss of function involved in amyotrophic lateral sclerosis? *Brain.* 136 (8), p.2342-2358.

Sakellariou, G. K., McDonagh, B., Porter, H., Giakoumaki, I. I., Earl, K. E., Nye, G. A., Vasilaki, A., Brooks, S. V., Richardson, A., Van Remmen, H., McArdle, A. and Jackson, M. J., 2018. Comparison of Whole Body SOD1 Knockout with Muscle-Specific SOD1 Knockout Mice Reveals a Role for Nerve Redox Signaling in Regulation of Degenerative Pathways in Skeletal Muscle. *Antioxidants and redox signalling*. 28 (4), p.275–295.

Salem, K., McCormick, M. L., Wendlandt, E., Zhan, F. and Goel, A., 2015. Copper-zinc superoxide dismutase-mediated redox regulation of bortezomib resistance in multiple myeloma. *Redox Biology.* 4, p.23-33.

Sarsour, E. H., Kalen, A. L. and Goswami, P. C., 2014. Manganese superoxide dismutase regulates a redox cycle within the cell cycle. *Antioxidants and redox signalling*. 20 (10), p.1618-1627.

Scandroglio, F., Tórtora, V., Radi, R. and Castro, L., 2014. Metabolic control analysis of mitochondrial aconitase: influence over respiration and mitochondrial superoxide and hydrogen peroxide production, *Free Radical Research.* 48 (6), p.684-693.

Schafer, F. Q., Buettner, G. R., 2001. Redox environment of the cell as viewed through the redox state of the glutathione disulfide/glutathione couple. *Free Radicals Biology Medicine*. 30 (11), p.1191-1212.

Schaur, R. J., 2003. Basic aspects of the biochemical reactivity of 4-hydroxynonenal. *Molecular Aspects of Medicine.* 24 (4-5), p.149-159.

Schmider, E., Ziegler, M., Danay, E., Beyer, L. and Bühner, M., 2010. Is it really robust? Reinvestigating the robustness of ANOVA against violations of the normal distribution assumption. *Methodology: European Journal of Research Methods for the Behavioural and Social Sciences*. 6 (4), p.147-151.

Schroeder, H. W. and Cavacini, L., 2010. Structure and function of immunoglobulins. *The Journal of allergy and clinical immunology.* 125(2 Suppl 2), S41–S52.

Segal, D. M., Padlan, E. A., Cohen, G. H., Rudikoff, S., Potter, M. and Davies, D. R., 1974. The three-dimensional structure of a phosphorylcholine-binding mouse immunoglobulin Fab and the nature of the antigen binding site. *Proceedings of the National Academy of Sciences of the United States of America.* 71 (11), p.4298-4302.

Sener, D. E., Gönenç, A., Akinci, M. and Torun, M., 2007. Lipid peroxidation and total antioxidant status in patients with breast cancer. *Cell Biochemistry and Function*. 25 (4), p.377-382.

Shacter, E., 2000. Quantification and significance of protein oxidation in biological samples. *Drug Metabolism Reviews.* 32 (3-4), p.307-326.

Sharma, A., Tripathi, M., Satyam, A. and Kumar, L., 2009. Study of antioxidant levels in patients with multiple myeloma. *Leukaemia and Lymphoma.* 50 (5), p.809-815.

Sheikh, S. P., Irfan, S. M. and Sheikh, S. S., 2020. Types of paraproteinemia in patients with multiple myeloma: A cross-sectional study. *Journal Of Pakistan Medical Association.* 70 (2), p.264-267.

Shuster, A. M., Gololobov, G. V., Kvashuk, O. A., Bogomolova, A. E., Smirnov, I. V., Gabibov, A. G., 1992. DNA hydrolyzing autoantibodies. *Science*. 256 (5057), p.665-667.

Sies, H. and Jones, D.P., 2020. Reactive oxygen species (ROS) as pleiotropic physiological signalling agents. *Nature reviews molecular cell biology.* 21, p.363–383.

Sies, H., 1985. Oxidative Stress: Introductory Remarks. In: *Oxidative Stress.* London: Academic Press, p.1–507.

Sies, H., 1991. Oxidative stress: from basic research to clinical application. *American Journal of Medicine.* 91 (3), p.31–38.

Sies, H., 1993. Strategies of antioxidant defense. *European Journal of Biochemistry.* 215, p.213-219.

Sies, H., Jones, D.P., 2020. Reactive oxygen species (ROS) as pleiotropic physiological signalling agents. *Nature Reviews Molecular Cell Biology.* 21, p.363–383.

Smirnova, L. P., Mednova, I. A., Krotenko, N. M., Alifirova, V. M. and Ivanova, S. A., 2020. IgG-Dependent Dismutation of Superoxide in Patients with Different Types of Multiple Sclerosis and Healthy Subjects. *Hindawi: Oxidative Medicine and Cellular Longevity*. 2020, p.1-11.

Sokal, R. R. and Michener, C. D., 1958. A Statistical Methods for Evaluating Relationships. *University of Kansas Science Bulletin*. 38, pp. 1409-1448.

Song, Y., Ruf, J., Lothaire, P., Dequanter, D., Andry, G., Willemse, E., Dumont, J. E., Van Sande, J., De Deken, X., 2010. Association of duoxes with thyroid peroxidase and its regulation in thyrocytes. *Journal of Clinical Endocrinology and Metabolism*. 95 (1), p.375-382.

Steck, N. and Grassl, G. A., 2014. Free Radicals and Pathogens – Role for Reactive Intermediates in Innate Immunity. In: Laher, I., *Systems Biology of Free Radicals and Antioxidants.* Springer, Berlin, Heidelberg. https://doi.org/10.1007/978-3-642-30018-9_103

Steinman, H. M., Naik, V. R., Abernethy, J. L. and Hill, R. L., 1974. Bovine erythrocyte superoxide dismutase. Complete amino acid sequence. *Journal of Biology Chemistry*. 249 (22), p.7326-7338.

Stevens, F. J., and Argon, Y., 1999. Pathogenic light chains and the B-cell repertoire. *Immunology Today*. 20 (10), p.451-457.

Stojiljković, V., Todorović, A., Radlović, N., Pejić, S., Mladenović, M., Kasapović, J. and Pajović, S. B., 2007. Antioxidant enzymes, glutathione and lipid peroxidation in peripheral blood of children affected by coeliac disease. *Annals of Clinical Biochemistry*. 44 (Pt 6), p.537-543.

Stoline, M. R., 1981. The Status of Multiple Comparisons: Simultaneous Estimation of All Pairwise Comparisons in One-Way ANOVA Designs. *The American Statistician.* 35 (3), p.134-141.

Sugino, N., Shimamura, K., Takiguchi, S., Tamura, H., Ono, M., Nakata, M., Nakamura, Y., Ogino, K., Uda, T. and Kato, H., 1996. Changes in activity of superoxide dismutase in the human endometrium throughout the menstrual cycle and in early pregnancy. *Human Reproduction*. 11 (5), p.1073-1078.

Symonyan, M. A. and Nalbandyan, R. M., 1979. The effect of x-rays on properties of superoxide dismutase. *Biochemical and Biophysical Research Communications.* 90 (4), p.1207-1213.

Talley, K. and Alexov, E., 2010. On the pH-optimum of activity and stability of proteins. *Proteins*. 78 (12), p.2699-2706.

Tan, E. M., and Smolen, J. S., 2016. Historical observations contributing insights on etiopathogenesis of rheumatoid arthritis and role of rheumatoid factor. *The Journal of experimental medicine*. 213 (10), p.1937–1950. https://doi.org/10.1084/jem.20160792

Tapia, P. C., 2006. Sublethal mitochondrial stress with an attendant stoichiometric augmentation of reactive oxygen species may precipitate many of the beneficial

alterations in cellular physiology produced by caloric restriction, intermittent fasting, exercise and dietary phytonutrients: "Mitohormesis" for health and vitality. *Medical Hypotheses.* 66 (4), p.832-843.

Tas, F., Hansel, H., Belce, A., Ilvan, S., Argon, A., Camlica, H. and Topuz, E., 2005. Oxidative stress in breast cancer. *Medical Oncology*. 22 (1), p.11-15.

Taverna, M., Marie, A. L., Mira, J. P. and Guidet, B., 2013. Specific antioxidant properties of human serum albumin. *Annals of intensive care*. 3(1), article 4.

Tavill, A. S., 2014. *Wilson's Disease*. Available: https://www.clevelandclinicmeded.com/medicalpubs/diseasemanagement/hepatology/wilson-disease/. Last accessed 01.07.21.

Thénard, L. J., 1811. Observations sur des nouvelles combinaisons entre l'oxigène et divers acides. *Annales de chimie et de physique*. 8, p.306–312.

Thermo Fisher Scientific Inc., 2013. *Extinction Coefficients*. Available: https://assets.thermofisher.com/TFS-Assets/LSG/Application-Notes/TR0006-Extinction-coefficients.pdf. Last accessed 21.03.21.

Tolmacheva, A. S., Ermakov, E. A., Buneva, V. N. and Nevinsky, G. A., 2018. Substrate specificity of healthy human sera IgG antibodies with peroxidase and oxydoreductase activities. *Royal Society open science*. 5(1), article 171097.

Tomoda, H., Morimoto, K. and Aoki, N., 1996. Superoxide dismutase activity as a predictor of myocardial reperfusion and salvage in acute myocardial infarction. *American Heart Journal.* 131 (5), p.849-856.

Toothaker, L. E., 1993. Violations of assumptions and robustness. In: Multiple comparison procedures. *SAGE Publications,* Inc. p.58-66.

Traber, M. G. and Stevens, J. F., 2011. Vitamins C and E: beneficial effects from a mechanistic perspective. *Free radical biology and medicine.* 51 (5), p.1000–1013.

Uniprot, 2006. *UniProtKB - P08294 (SODE_HUMAN).* Available: https://www.uniprot.org/uniprot/P08294. Last accessed 01.07.21.

Uniprot, 2007. *UniProtKB - P00441 (SODC_HUMAN).* Available: https://www.uniprot.org/uniprot/P00441. Last accessed 01.07.21.

Uniprot, 2017. *UniProtKB - P04179 (SODM_HUMAN).* Available: https://www.uniprot.org/uniprot/P04179. Last accessed 01.07.21.

Van der Bliek, A. M., Sedensky, M. M. and Morgan, P. G., 2017. Cell Biology of the Mitochondrion. *Genetics.* 207, p. 843–871

van Tilburg, C. M., Bierings, M. B., Berbers, G. A., Wolfs, T. F., Pieters, R., Bloem, A. C. and Sanders, E. A., 2012. Impact of treatment reduction for childhood acute lymphoblastic leukaemia on serum immunoglobulins and antibodies against vaccine-preventable diseases. *Paediatric Blood and Cancer*. 58 (5), p.701-707.

Vidarsson, G., Dekkers, G., Rispens, T., 2014. IgG subclasses and allotypes: from structure to effector functions. *Frontiers in Immunology.* 5 (520), p.1-17.

von Behring, E., Kitasato, S., 1890. Ueber das Zustandekommen der Diphtherie-Immunität und der Tetanus-Immunität bei Thieren [On the development of immunity to diphtheria and tetanus in animals]. *Deutsche Medizinische Wochenschrift.* 49, p.1113-1114.

Wang, P. X. and Sanders, P. W., 2007. Immunoglobulin light chains generate hydrogen peroxide. *Journal of the American Society of Nephrology.* 18 (4), p.1239-1245.

Wang, X., Wang, Q. and Sun, Z., 2012. Normal IgG downregulates the intracellular superoxide level and attenuates migration and permeability in human aortic endothelial cells isolated from a hypertensive patient. *Hypertension,* 60 (3), p.818–826.

Wardman, P., 1989. Reduction Potentials of One-Electron Couples Involving Free Radicals in Aqueous Solution. *Journal of Physical and Chemical Reference Data*. 18, p.1637-1755.

Weisiger, R. A. and Fridovich, I., 1973. Mitochondrial superoxide dismutase. Site of synthesis and intramitochondrial localization. *Journal of Biological Chemistry.* 248 (13), p.4793-4796.

Wentworth, A. D., Jones, L. H., Wentworth, P., Janda, K. D. and Lerner, R. A., 2000. Antibodies have the intrinsic capacity to destroy antigens. *Proceedings of the National Academy of Sciences of the United States of America*. 97 (20), p.10930-10935.

Wentworth, P. and Witter, D. P., 2008. Antibody-catalysed water-oxidation pathway. *Pure and Applied Chemistry.* 80 (8), p.1849-1858.

Wentworth, P., Jones, L. H., Wentworth, A. D., Zhu, X., Larsen, N. A., Wilson, I. A., Xu, X., Goddard, W. A., Janda, K. D., Eschenmoser, A. and Lerner, R. A., 2001. Antibody catalysis of the oxidation of water. *Science.* 293 (5536), p.1806-1811.

Wentworth, P., McDunn, J. E., Wentworth, A. D., Takeuchi, C., Nieva, J., Jones, T., Bautista, C., Ruedi, J. M., Gutierrez, A., Janda, K. D., Babior, B. M., Eschenmoser, A. and Lerner, R. A., 2002. Evidence for antibody-catalysed ozone formation in bacterial killing and inflammation. *Science.* 298 (5601), p.2195-2199.

Weyand, C.M. and Goronzy, J.J., 2021. The immunology of rheumatoid arthritis. *Nature Immunology*. 22, p.10-18.

White, H. D. and Chew, D. P., 2008. Acute myocardial infarction. *Lancet*. 372 (9638) p.570-584.

Wilcox, R., 2012. One-Way and Higher Designs for Independent Groups. In: *Introduction to robust estimation and hypothesis testing*. 3rd ed. Massachusetts: Elsevier. p.291-377.

Winterbourn, C. C., Kettle, A. J., and Hampton, M. B., 2016. Reactive Oxygen Species and Neutrophil Function. *Annual Reviews of Biochemistry*. 85, p.765-792.

World Medical Association, 2000. *WMA Declaration of Helsinki – ethical principles for medical research involving human subjects*. Available: https://www.wma.net/policies-post/wma-declaration-of-helsinki-ethical-principles-for-medical-research-involving-human-subjects/. Last accessed 21.03.21.

Xu, R. and Hajdu, C. H., 2008. Wilson disease and hepatocellular carcinoma. *Gastroenterology and hepatology.* 4 (6), p.438–439.

Yadlapati, S. and Efthimiou, P., 2016. Autoimmune/Inflammatory Arthritis Associated Lymphomas: Who Is at Risk?. *BioMed research international*. 8631061, p.1-11.

Yan, L. J., Levine, R. L. and Sohal, R. S., 1997. Oxidative damage during aging targets mitochondrial aconitase. *Proceedings of the National Academy of Sciences of the United States of America*. 94 (21), p.11168-11172.

Yim, M. B., Yim, H. S., Boon Chock, P., and Stadtman, E. R., 1998. Pro-oxidant activity of Cu, Zn-superoxide dismutase. *Age*. 21 (2), p.91–93.

Yin, J. and Schultz, P. G., 2005. Immunological Evolution of Catalysis. In: Keinan, E. Catalytic Antibodies. *Weinheim: Wiley Verlag Chemie.* p.1-29.

Ylä-Herttuala, S., Palinski, W., Rosenfeld, M. E., Parthasarathy, S., Carew, T. E., Butler, S., Witztum, J. L. and Steinberg, D., 1989. Evidence for the presence of oxidatively modified low-density lipoprotein in atherosclerotic lesions of rabbit and man. *Journal of Clinical Investigation.* 84 (4), p.1086-1095.

Zabriskie, J. B., 2009. Basic Components of the Immune System. *Essential Clinical Immunology.* New York: Cambridge University Press. pp1-20.

Zhang, W., Hu, X., Shen, Q. and Xing, D., 2019. Mitochondria-specific drug release and reactive oxygen species burst induced by polyprodrug nanoreactors can enhance chemotherapy. *Nature Communications.* 10 (1704), p.1-14.

Zhang, Y., Unnikrishnan, A., Deepa, S. S., Liu, Y., Li, Y., Ikeno, Y., Sosnowska, D., Van Remmen, H. and Richardson, A., 2017. A new role for oxidative stress in aging: The accelerated aging phenotype in Sod1-/- mice is correlated to increased cellular senescence. *Redox Biology*. 11, p.30-37.

Zhang, Y., Wang, Y., Li, Y., 2019. Major cause of antibody artifact bands on non-reducing SDS-PAGE and methods for minimizing artifacts*. Protein Expression Purification*. 164 (105459), p1-5.

Zintzaras, E., Voulgarelis, M. and Moutsopoulos, H. M., 2005. The risk of lymphoma development in autoimmune diseases: a meta-analysis. *Archives of Internal Medicine.* 165 (20), p2337-2344.

Zorov, D. B., Juhaszova, M. and Sollott, S. J., 2014. Mitochondrial reactive oxygen species (ROS) and ROS-induced ROS release. *Physiological Reviews*. 94, p.909-950. doi:10.1152/physrev.00026.2013

Appendix

Appendix 2.1: Preparation of x1 PBS

x 10 phosphate-buffered saline (PBS), pH 7.4

$Na_2HPO_4.12H_2O$	29.36 g
NaH_2PO_4 (anhydrous)	2.16 g
NaCl	87.6 g
Sodium azide	2.0 g

Make up to 1 litre with deionised water. Check that pH is 7.4, adjust if necessary.

Dilute 1:10 with deionised water before use.

Appendix 2.2: BGG vs BSA calibration curves

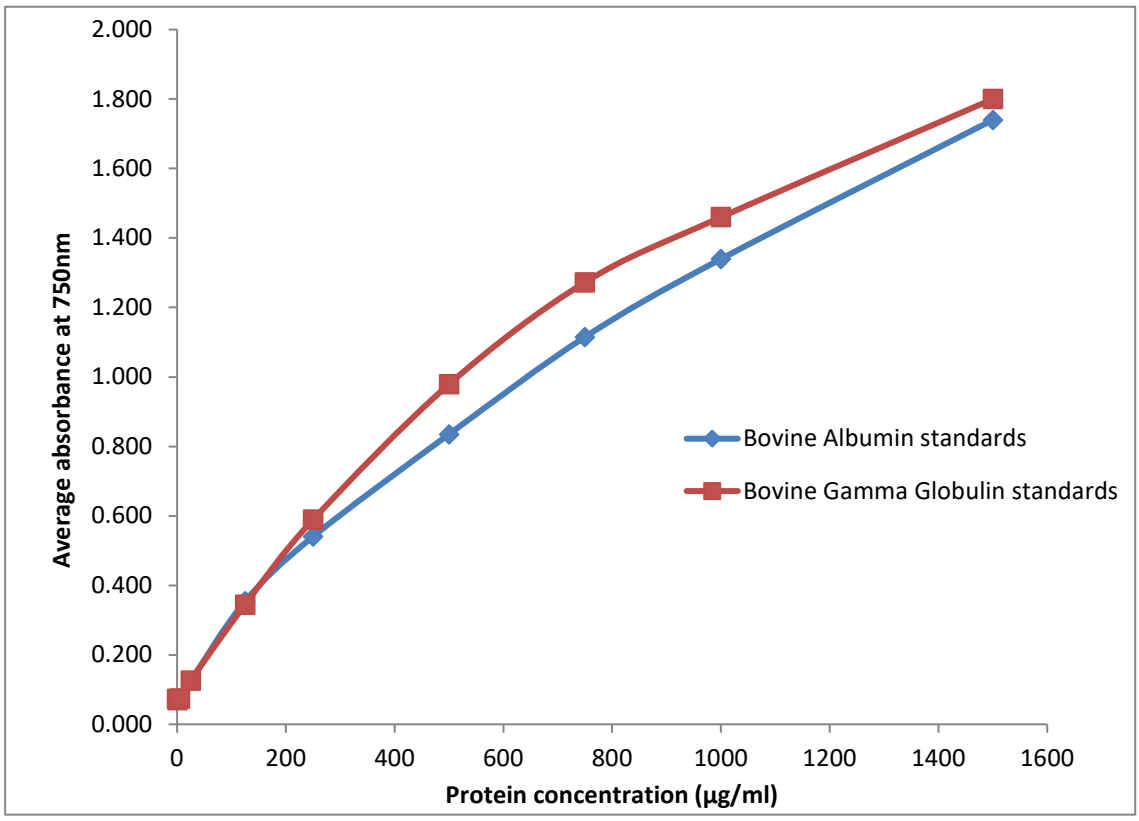

Modified Lowry protein assay: comparing the response of bovine serum albumin protein standard curve to bovine gamma globulin protein standard curve. The signal response from bovine gamma globulins is on average 6.2% greater than for bovine serum albumin calibrators.

Appendix 2.3: Biochemical inclusion criteria

Patients who have conditions potentially associated with altered immune function and oxidative imbalance will be identified through the pathology laboratory information system by a member of the hospital pathology laboratory. Examples of patient groups will include:

1) Cardiovascular disease (atherosclerosis)
2) Cancer (specifically breast cancer and myeloma)
3) Rheumatoid arthritis
4) Coeliac disease
5) Diabetes (type I and type II)

Data collection (retrospective):

Patients with ≥1.0ml serum or plasma remaining after diagnostic testing has been completed and meet one of the following biochemical criteria:

- Fasting total cholesterol >8.0 mmol/L compared to a group of individuals with levels <5.0 mmol/L.
- Fasting low density lipoprotein (LDL) cholesterol >6.2 mmol/L compared to a group of individuals with LDL <3.0 mmol/L.
- Fasting triglycerides >11.0 mmol/L compared to a group of individuals with triglyceride levels <1.8 mmol/L.
- Brain natriuretic peptide (BNP) >400 pg/ml compared to a group of individuals with BNP <100 pg/ml or comparable values for N-terminal pro-brain natriuretic peptide (NT-proBNP >2000 pg/ml compared to <400 pg/ml).
- C-reactive protein (CRP) >150 mg/L compared to a group of individuals with CRP <6 mg/L.
- Cardiac troponin >300 ng/L compared to individuals with cardiac troponin <56 ng/L.

- Serum free kappa chains >25 mg/L compared to individuals with free kappa 3.3 - 19.4 mg/L.
- Serum free lambda chains >30 mg/L compared to individuals with free lambda 5.7 - 26.3 mg/L.
- Positive bence jones protein (BJP) compared to normal individuals with negative BJP.
- Immunoglobulin G (IgG) >20g/L with a paraprotein (myeloma) monoclonal band visible on serum electrophoresis.

- Carcinoembryonic antigen (CAE) >5 µg/L compared to a group of individuals with CAE <5 µg/L.
- CA125 (Ovarian cancer) >100 kU/L compared to a group of individuals with CA125 <30 kU/L.
- CA153 (Breast cancer) >100 kU/L compared to a group of individuals with CA153 <35 kU/L.
- CA199 (Pancreatic cancer) >100 kU/L compared to a group of individuals with CA199 <35 kU/L.
- AFP (tumour marker) >100 kU/L compared to a group of individuals with AFP <10 kU/L

- Rheumatoid factor >100 U/ml compared to a group of individuals with rheumatoid factor <14 U/ml.
- Anti-cyclic citrullinated peptide antibody (anti-CCP) >100 U/ml compared to a group of individuals with anti-CCP <7 U/ml.

- Complement C3 <0.30 g/L compared to a group of individuals with complement C3 between 0.75-1.65 g/L.
- Complement C4 <0.05 g/L compared to a group of individuals with complement C4 between 0.14-0.54 g/L.
- Positive endomysial autoantibody IgA and/or IgG compared to a group of individuals with negative endomysial autoantibody IgA and IgG.
- Tissue transglutaminase autoantibody >10 U/ml compared to a group of individuals with tissue transglutaminase autoantibody <7 U/ml.
- Immunoglobulin A (IgA) >5 g/L compared to a group of individuals with IgA <4 g/L.

- Positive islet cell autoantibody compared to a group of individuals with negative islet cell autoantibody.
- Anti-GAD 65 autoantibodies >6 IU/ml compared to individuals with anti-GAD 65 autoantibody <5 IU/ml.
- Anti-IA-2 autoantibodies >10 IU/ml compared to individuals with anti-IA-2 autoantibodies <10 IU/ml.
- Fasting glucose of >8.0 mmol/L compared to a group of individuals with fasting glucose <6.0 mmol/L.
- HbA1c IFCC >64 mmol/mol (DCCT 8.0%) compared to a group of individuals with HbA1c <40 mmol/mol (DCCT 5.8%).

- C-peptide <30 pmol/L compared to a group of individuals with c-peptide 174-960 pmol/L.
- Fasting insulin >2000 pmol/L indicating severe insulin resistance compared to a group of individuals with insulin <80 pmol/L.

Statement of use

The biochemical data obtained from running searches using the inclusion criteria will be passed on from the 'gatekeeper. This information will be archived for future multivariant and network analysis. This looks for relationships between different parameters and can give insight (graphical and statistical) into relationships that have not previously been suspected.

Appendix 2.4: Removal of patients from data analysis

Removal of patients from the data analysis due to missing data points, analytical interference, and group sizes less than 6

Based on group sizes <6

- Patient 48 was removed as there was only 1 case in this group (Glioblastoma)
- Patient 76 was removed as there was only 1 case in this group (Churg-Strauss)
- Patients 13 and 42 as there were only 2 cases in this group (ischemic heart disease)
- Patients 15, 16, 44, 54 and 55 as there were only 5 cases in this group (Ovarian Cancer)
- Patients 24, 25, 83 and 88 as there were only 4 cases in this group (Waldenström macroglobulinemia)
- Patients 45, 46, 47, 66 and 68 as there were only 5 cases in this group (Gastro-intestinal cancer)
- Patients 49, 92, 93 and 94 as there were only 4 cases in this group (Diabetes)

Based on measurement error

Removed based on haemolysis and lipaemia – which are known to interfere with the accurate quantification of catalase and SOD (haemolysis) and hydroperoxides (lipaemia).

- Patient 4 (coeliac disease) was removed as the sample was slightly haemolysed
- Patient 17 (MGUS) was removed as the sample was slightly lipaemic
- Patient 18 (MGUS) was removed as the sample was slightly lipaemic
- Patient 19 (myeloma) was removed as the sample was slightly haemolysed
- Patient 33 (myeloma) was removed as the sample was slightly haemolysed
- Patient 56 (coeliac disease) was removed as the sample was slightly haemolysed
- Patient 58 (coeliac disease) was removed as the sample was slightly haemolysed
- Patient 61 (breast cancer) was removed as the sample was slightly haemolysed
- Patient 65 (coeliac disease) was removed as the sample was slightly haemolysed
- Patient 87 (MGUS) was removed as the sample was slightly haemolysed
- Patient 89 (myeloma) was removed as the sample was slightly haemolysed

- Patient 108 (‘Healthy’ control) was removed as the sample was slightly haemolysed
- Patient 111 (‘Healthy’ control) was removed as the sample was slightly haemolysed

Based on missing values

For hydroperoxides measurement – will not be included in analysis so were removed.

- Patient 26 (myeloma)
- Patient 75 (myeloma)

Appendix 2.5: Gender frequency table

The gender frequency and age range across disease and control groups

Patient group	Male (frequency)	Age mean (Years)	Age range (Years)	Female (Frequency)	Age mean (Years)	Age range (Years)	Cumulative no. per group	Cumulative age range (Years)
'Healthy' Control	10	43.3	27 - 61	9	48.6	28 - 71	19	27 - 71
Rheumatoid Arthritis	1	n/a	n/a	6	66.3	39 - 85	7	25 - 85
Coeliac Disease	3	51.0	22 - 77	8	42.1	18 - 65	11	18 - 77
Myocardial Infarction	5	75.4	64 - 87	1	n/a	n/a	6	64 - 87
Breast Cancer	0	n/a	n/a	7	60.7	42 - 74	7	42 - 74
Monoclonal Gammopathy of Unknown Significance	5	74.2	59 - 95	2	62.0	61 - 63	7	59 - 95
Myeloma	11	68.7	55 - 83	10	70.7	37 - 90	21	37 - 90

Appendix 2.6: Ethics approval from ARU

Anglia Ruskin University

Cambridge | Chelmsford
London | Peterborough

Chelmsford Campus
Bishop Hall Lane
Chelmsford
CM1 1SQ

T: +44 (0) 1245 493131

www.anglia.ac.uk
@angliaruskin
facebook.com/angliaruskin

Ashley Clarke
55 Victoria Street
Braintree
Essex
CM7 3HL

02nd January 2018

Dear Ashley

Principal Investigator: Ashley Clarke
FREP/DREP number: FST/FREP/17/705
Project Title: Antibodies with superoxide dismutase-like activity in human diseases associated with oxidative stress (Stage 1 – form 2)

I am pleased to inform you that your ethics application has been approved by the Faculty Research Ethics Panel (FREP) under the terms of Anglia Ruskin University's Research Ethics Policy (Dated 8 September 2016, Version 1.7).

Ethical approval is given for a period of 3 years for doctorate students from 02/01/2018. If your research will extend beyond this period, it is your responsibility to apply for an extension before your approval expires.

It is your responsibility to ensure that you comply with Anglia Ruskin University's Research Ethics Policy and the Code of Practice for Applying for Ethical Approval at Anglia Ruskin University available at www.anglia.ac.uk/researchethics including the following.

- The procedure for submitting substantial amendments to the committee, should there be any changes to your research. You cannot implement these amendments until you have received approval from FREP for them.
- The procedure for reporting accidents, adverse events and incidents.
- The Data Protection Act (1998) and General Data Protection Requirement from 25 May 2018.
- Any other legislation relevant to your research. You must also ensure that you are aware of any emerging legislation relating to your research and make any changes to your study (which you will need to obtain ethical approval for) to comply with this.
- Obtaining any further ethical approval required from the organisation or country (if not carrying out research in the UK) where you will be carrying the research out. This includes other Higher Education Institutions if you intend to carry out any research involving their students, staff or premises. Please ensure that you send the FREP copies of this documentation if required, prior to starting your research.
- Any laws of the country where you are carrying the research and obtaining any other approvals or permissions that are required.
- Any professional codes of conduct relating to research or requirements from your funding body (please note that for externally funded research, where the funding has been obtained via Anglia Ruskin University, a Project Risk Assessment must have been carried out prior to starting the research).

Appendix 2.7: Ethics approval from Addenbrooke's

Cambridge University Hospitals NHS
NHS Foundation Trust

Research and Development Department

15th September 2017

R&D ref: A094438

Box 277
Addenbrooke's Hospital
Hills Road
Cambridge
CB2 0QQ

Direct Dial: 01223 256407
Switchboard: 01223 245151

E-mail:sonakshi.kadyan@addenbrookes.nhs.uk
r&denquiries@addenbrookes.nhs.uk
www.addenbrookes.org.uk

Mr Ashley Clarke
Box 232,
Core Biochemical Assay Laboratory
Addenbrookes Hospital

Dear Mr Clarke

IRAS ID: 163984

Are levels of antibodies with superoxide dismutase-like activity (AbSOD), antioxidants and oxidative stress markers altered in human diseases associated with oxidative stress?

Thank you for sending details of the above named study.

The R&D department has received and reviewed the study documents. The project has been allocated the internal R&D reference number of **A094438**. Please quote this in all future correspondence regarding this study.

Capacity and capability to conduct this study at Cambridge University Hospitals NHS Foundation Trust is confirmed.

We would like to take this opportunity to remind you of your responsibilities under the terms of the Research Governance Framework for Researchers, Chief Investigators, Principal Investigators and Research Sponsors and to also of the requirement to notify R&D of any amendments or changes made to this study.

I wish you every success with this study.

Yours sincerely

Stephen Kelleher
R&D/NIHR BRC Manager

Appendix 5.1: Immunoglobulins extracted from serum samples

Purification of polyclonal antibodies from serum preliminary results 18.06.19

Run ID	Sample ID	Diagnosis	Description	IgG g/L	IgM g/L	IgA g/L
1	1H	Control	Healthy'	0.96	0.01	0.00
2	6H	Control	Healthy'	0.95	0.00	0.00
3	11H	Control	Healthy'	0.71	0.00	0.00
4	16H	Control	Healthy'	1.16	0.01	0.01
5	26H	Control	Healthy'	1.04	0.02	0.00
6	18	MGUS	MGUS - Paraprotein IgG Kappa	1.54	0.01	0.01
7	27	Myeloma	Multiple myeloma, Paraprotein IgG Kappa with high Serum kappa light chains	2.65	0.00	0.00
8	29	Myeloma	Multiple myeloma, Paraprotein IgG Kappa with high Serum kappa light chains	2.04	0.00	0.00
9	30	Myeloma	Multiple myeloma, Paraprotein IgG Lambda with high Serum lambda light chains	2.58	0.00	0.00
10	37	Myeloma	Multiple myeloma, Paraprotein IgG Lambda with high serum lambda light chains	1.01	0.00	0.00
11	86	Myeloma	Multiple Myeloma, Paraprotein IgG Lambda	2.49	0.00	0.00
12	24	Waldenström	Waldenstrom Macroglobulinaemia Paraprotein IgM Kappa	0.86	0.35	0.00
13	25	Waldenström	Waldenstrom Macroglobulinaemia Paraprotein IgM Kappa	0.29	0.17	0.00
14	88	Waldenström	Waldenstrom Macroglobulinaemia Paraprotein IgM Kappa	0.52	0.16	0.00
15	32	MGUS	MGUS, IgM Kappa High Serum Kappa free light chains	0.97	0.01	0.00